THE SYNTHESIS OF NAPHTHALENE-CONTAINING COMPOUNDS AND MATERIALS USING BENZANNULATION REACTIONS

A Dissertation

Presented to the Faculty of the Graduate School

of Cornell University

In Partial Fulfillment of the Requirements for the Degree of

Doctor of Philosophy

by

Samuel Jay Hein

May 2017

THE SYNTHESIS OF NAPHTHALENE-CONTAINING COMPOUNDS AND MATERIALS USING BENZANNULATION REACTIONS

Samuel Jay Hein, Ph.D

Cornell University

This dissertation describes recent advances in methodology to access novel aromatic architectures using a benzannulation strategy (Chapter 1). Silyl protected acetylenes are readily reacted to yield the corresponding 2-naphthylsilane. These compounds serve as synthetically useful building blocks for further derivatization and iterative benzannulation to access sterically crowded substrates (Chapter 2). Despite the high efficiency of this reaction, phenylene ethynylene macrocycles prove to be too rigid to undergo complete benzannulation (Chapter 3). Finally, the scope of this transformation was expanded beyond aryl substituted acetylenes with the benzannulation of silyl-haloacetylenes (Chapter 4). These products readily generate 2-naphthynes with the addition of cesium fluoride and can be oligomerized or cyclized to isolate substituted *ortho*-naphthalenes. Through our fundamental studies into this transformation, we have shown it serves as a versatile reaction in the organic synthetic chemists toolbox to access novel aromatic architectures.

BIOGRAPHICAL SKETCH

Sam Hein was born in Green Bay, WI with an identical twin brother, Carl, and had resided in Allouez, WI. Growing up with an identical twin, many people assumed that we would have many similar interests and goals throughout life. Surprisingly, our interests diverged in high school as Sam developed a strong interest in the physical sciences while Carl, had devoted his studies to history and social science. The decision to focus on chemistry began in the classroom of the Green Bay East High School AP Chemistry teacher, Mr. Thomas Arts. It was here that Sam learned the fundamental chemical knowledge that all chemists rely on.

Upon graduating high school, Sam attended the University of Wisconsin: Eau Claire as a chemistry major where he joined the research group of Professor Michael Carney where he studied organometallic chromium catalysts for the selective oligomerization of ethylene. Sam attended two summer NSF REU programs. For the first he traveled to Hattiesburg, Mississippi and attended the University of Southern Mississippi. Here he joined the lab of Professor Daniel Savin and studied the phase separation behavior of model block copolymer systems for potential applications in polymer fuel cell membranes. The second was at Case Western Reserve University in Cleveland, Ohio. He joined the lab of Professor Liming Dai and gained experience preparing and characterizing gold nanorods in order to increase the efficiency of organic solar cells.

After graduating UW: Eau Claire, he joined Dichtel Research Group where he was advised throughout his graduate work by Professor William R. Dichtel. After 4 years, the group moved to Northwestern University where Sam has spent his final year

of graduate research. After graduating Sam will start work at Capacitor Sciences in Menlo Park, California. In his spare time Sam enjoys juggling, binge watching Law and Order SVU episodes, “tasting” a variety of beers, and cruising on his motorcycle.

DEDICATION

This dissertation is dedicated to my family and friends
for their unwavering support.

ACKNOWLEDGEMENTS

First I would like to acknowledge my entire committee, Prof. William R. Dichtel, Prof. Geoffrey W. Coates, and Prof. Christopher K. Ober for their support throughout my time at Cornell.

Financial support of this research was through the Beckman Young Investigator Program of the Arnold and Mabel Beckman Foundation. the NSF (CHE-1124754), the Doctoral New Investigator Program of the ACS Petroleum Research Fund (52019-DNI7), a Sloan Research Fellowship from the Alfred P. Sloan Foundation, and a Camille Dreyfus Teacher-Scholar Award from the Camille and Henry Dreyfus Foundation. This work made use of the Cornell Center for Materials Research Shared Facilities which are supported through the NSF MRSEC program (DMR-1120296) and the IMSERC at Northwestern University, which has received support from the NSF (CHE-0923236, CHE-1048773); Soft and Hybrid Nanotechnology Experimental (SHyNE) Resource (NSF NNCI-1542205); the State of Illinois and International Institute for Nanotechnology (IIN).

The Dichtel group has been more than a place to work and learn, it has also been a second home throughout my time in graduate school. Will has been an amazing advisor and the training I have received from him will continue to support me as I begin my own career. I would like to acknowledge Dr. Hasan Arslan who mentored and trained me as I started to learn the skills I would need to become the chemist I am today. I would also like to acknowledge Dr. Dan Lehnherr who joined the benzannulation team

as a Post Doc and who was an invaluable source of inspiration and knowledge as I transitioned from an early to a late stage graduate student.

The friends I've made in Ithaca from day one of the program will continue to be with me and I hope to remain in touch with them. My high school chemistry teacher, Mr. Thomas Arts is the reason I fell in love with chemistry and follow it with the passion I currently have. My parents and family had instilled a desire to learn into me at an early age and have constantly stood by my side with unwavering support. Finally I would like to acknowledge my girlfriend, Jessica Daughtry, who has remained patient and loving throughout every stage of this journey.

TABLE OF CONTENTS

Rapid access to substituted 2-Naphthyne Intermediates via the Benzannulation of Halogenated Silylacetylenes

TABLE OF FIGURES

TABLE OF TABLES

TABLE OF SCHEMES

LIST OF ABBREVIATIONS

1,2-DCE	1,2-Dichloroethane
2D	Two-Dimensional
3D	Three-Dimensional
AcOH	Acetic Acid
APPI	Atmospheric pressure photoionization
Ar	Aryl
CNT	Carbon nanotube
DART	Direct analysis in real time
DBA	Dehydrobenzoannulenes
DCM	Dichloromethane
DMPS	Dimethylphenylsilyl
EDG	Electron Donating Group
EI	Electron impact
ESI	Electrospray ionization
Et	Ethyl
EWG	Electron Withdrawing Group
GC	Gas chromatography
GPC	Gel permeation chromatography
LC	Liquid chromatography
MALDI	Matrix assisted laser desorption ionization
Me	Methyl
MS	Mass spectrometry

n-Bu	*n*-Butyl
OHxg	Hexaglyme
OTf	Trifluorosulfonate
Ph	Phenyl
p-Tol	*para*-Toluene
SEC	Size exclusion chromatography
SWCNT	Single walled carbon nanotube
TBDMS	*t*-Butyldimethylsilyl
t-Bu	*tert*-Butyl
TFA	Trifluoroacetic Acid
THP	Tetrahydropyranyl
TIPS	Triisopropylsilyl
TMS	Trimethylsilyl
TOF	Time of Flight

CHAPTER ONE

SYNTHESIS OF NANOGRAPHENES AND RELATED POLYCYCLIC AROMATIC ARCHITECTURES VIA BENZANNULATION REACTIONS OF ACETYLENES

2.1 Abstract

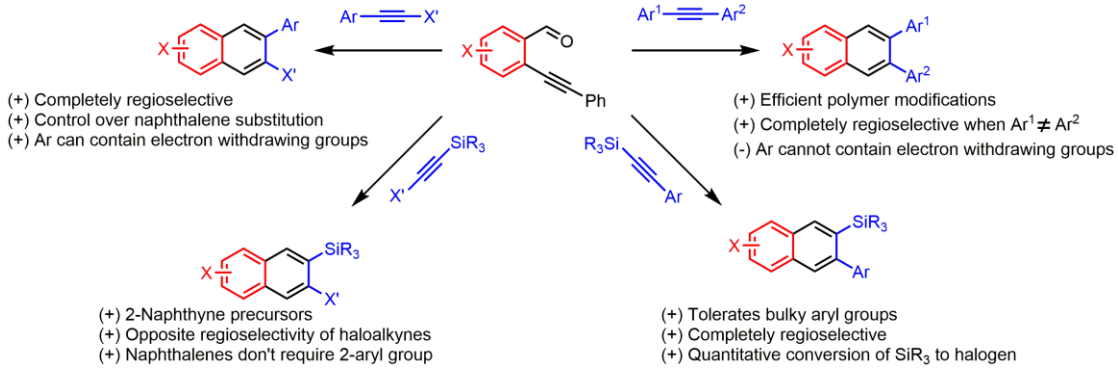

Aromatic compounds are integrated into organic field effect transistor (OFET), light emitting diode (OLED), and photovoltaic (OPV) devices. Available synthetic approaches have provided access to increasingly elaborate aromatic systems that exemplify the diverse structural landscape available for fundamental and applied studies. Substituents influence the energy levels, bandgaps, solution conformation, and crystal packing, all of which affect device performance. However, many substitution patterns are often outside the scope of current synthetic methods, especially for polycyclic systems. Most methods for functionalizing benzene are simply not applicable to naphthalene or larger systems, and convergent synthetic methods to novel aromatic structures that introduce multifunctional groups with excellent regiochemical control are underdeveloped. We have focused efforts to address these challenges and access novel aromatic molecules and materials with planar, helical or contorted π-systems.

In surveying cycloaddition reactions that might be used to modify the conjugated backbone of poly(phenylene ethynylene)s, we noted the exceptional activity of the Asao-Yamamoto benzannulation reaction. This transformation had been reported a decade earlier, but its scope and utility in synthesizing complex aromatic systems was mostly unrecognized. The benaznnulation of alkynes with various substituted 2-(phenylethynyl)benzaldehydes provides 2,3-substituted naphthalenes and and is highly efficient for sterically congested acetylenes, which opens new paths to poly- and oligo(o*rtho*-arylene)s and contorted hexabenzocoronenes. In most cases, the complete regioselectivity of the reaction is determined by the electronic character of the alkyne substrate. Upon recognizing these desireable features, we broadened the substrate scope to include silyl-, halo-, and aryl- substituted acetylenes. Collectively these methods access aromatic systems with extremely hindered bond rotations, heterocyclic aromatic compounds, functionalized 2-aryne precursors, polyheterohalogenated naphthalenes, diazatetracene derivatives, and graphene nanoribbons. As a result of these synthetic advancements, a broad range of fields are likely to directly benefit from newly accessible molecular and polymeric systems derived from polyfunctionalized naphthalenes.

2.2 Introduction

Substituted polycyclic aromatic hydrocarbons (PAHs) exhibit desirable electronic and optical properties for organic photovoltaic devices (OPVs), field effect transistors (OFETs), and light emitting diodes (OLEDs). However, efficient access to PAHs with complex substitution patterns remain a synthetic challenge. Transition-metal cross-coupling reactions between aryl halides and organometallic reagents are powerful and general, yet often lose efficiency for highly substituted substrates[1,2] and are generally conducted in linear sequences for polyfunctional targets. In contrast, cycloaddition reactions offer a convergent strategy to access highly substituted aromatic compounds and sometimes are more tolerant of steric hindrance. The most useful of these reactions are chemoselective, regioselective, tolerant of many functional groups, and provide substitution patterns that complement those available from electrophilic aromatic substitution or directed C-H activation strategies.

Scheme 1.1. Direct synthesis of polysubstituted aromatic rings through convergent cycloaddition reactions.

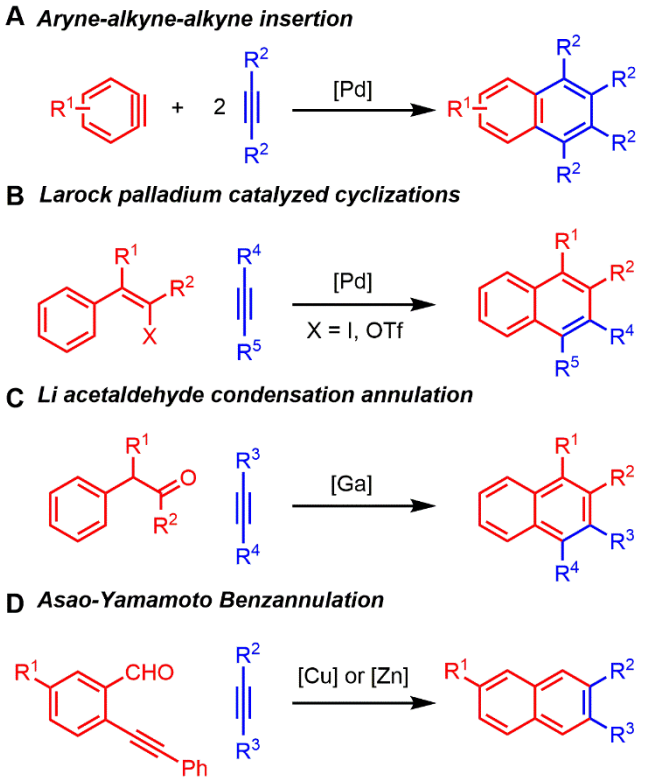

A [4+2] cycloaddition reaction between a terminal alkyne and a substituted cyclopentadienone or the cyclotrimerization of alkynes are versatile methods to prepare penta- and hexa- substituted benzene rings that have been used to synthesize *ortho*-phenylene dendrimers, fused polycyclic hydrocarbons, and graphene nanoribbons.[3–7] But despite the utility of these methods, many compounds derived from larger aromatic cores, such as naphthalenes, remain mostly outside their scope.[8,9] Cycloaddition reactions involving a formal [2+2+2] cycloaddition of a benzyne intermediate with access alkynes (Scheme 1.1a) provide substituted naphthalene systems, although mixtures of regioisomers are generally obtained when naphthalenes bearing asymmetric substitution patterns are targeted. Transition-metal mediated annulations of vinyl or aryl iodide/triflates, reported by Larock and coworkers produce substituted naphthalenes

(Scheme 1.1b) in which the regioselectivity is determined by the steric demands of the acetylene substituents.[10–12] A related transformation reported by Li[13] and Balamurugan[14] uses phenylacetaldehyde reactants (Scheme 1.1c).

In 2003, Asao and Yamamoto reported a $Cu(OTf)_2$ catalyzed benzannulation between *ortho*-phenylenebenzaldehyde and substituted acetylenes that produces a 2,3-disubstituted naphthalene ring in high yields (Scheme 1.1d).[15] While several metals are known to catalyze this reaction, the synthetic utility it exhibited was underappreciated in the scientific literature at the time.[16–18] This Account describes our fundamental studies on the reactivity, regioselectivity and mechanism of this transformation and how that understanding has been applied to access highly substituted naphthalene rings for the purposes of polymer modifications and novel PAH synthesis. The remarkable steric tolerance combined with the predictable regioselectivity afforded by this transformation will continue to enable the synthesis of novel PAHs with otherwise unavailable substitution patterns.

2.3 Benzannulation of Diarylacetylenes

In the mechanism first proposed by Yamamoto and coworkers, $Cu(OTf)_2$ acts as a Lewis-acid to coordinates to alkyne of the benzaldehyde reagent (**B)** to facilitate the nucleophilic attack by aldehyde oxygen to form Cu-bound benzopyrylium intermediate **C** (Figure 1.1). This intermediate undergoes a formal [4+2] cycloaddition with the diarylacetylene to give Cu-bound intermediate **D**. Under acidic conditions, the Cu-bound species is protonated and the conjugate base causes a retro [4+2] reaction, which yields 2,3-diarylnaphthalene **E** while naphthyl ketone derivative **F** is known to form in the absence of acid.

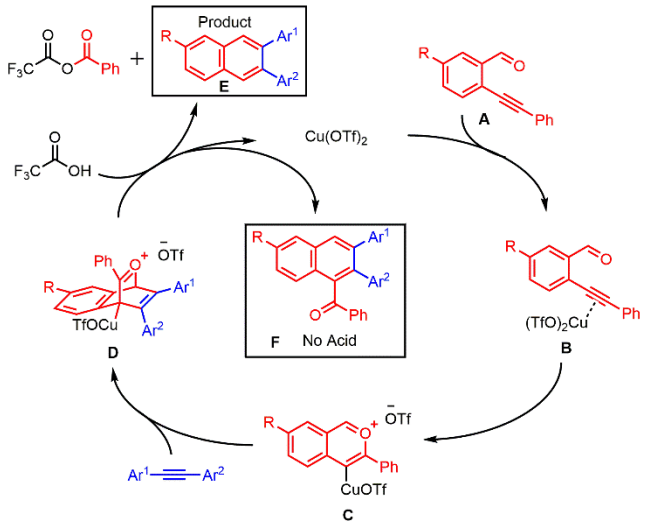

Figure 1.1. Proposed Mechanism by Yamamoto yielding naphthalene and naphthyl ketones. Adapted from Reference 19.

Despite the high efficiency of this reaction to synthesize substituted naphthalene products, the potential for mixtures of regioisomer derived from the benzannulation of asymmetric acetylenes and substituted benzaldehydes could render this transformation irrelevant for the construction of more complex aromatic compounds. In a related $AuCl_3$ catalyzed benzannulation of alkynes, naphthyl ketone derivatives (**F**) could be accessed with high regioselectivity in accordance with the electronic properties of the alkyne.[19] Until our work, it was not known whether naphthyl product **E** could be obtained regioselectively. We modified the $Cu(OTf)_2$ catalyzed conditions benzannulation conditions employing TFA instead of difluoroacetic acid and observed that similar electronic effects govern the benzannulation of diarylacetylenes under $Cu(OTf)_2$ catalyzed conditions compared to the $AuCl_3$ conditions, although their products are different.[20]

Table 1.1. Regioselective synthesis of diarylacetylenes from electronically different aryl substituents. Adapted from Reference 19.

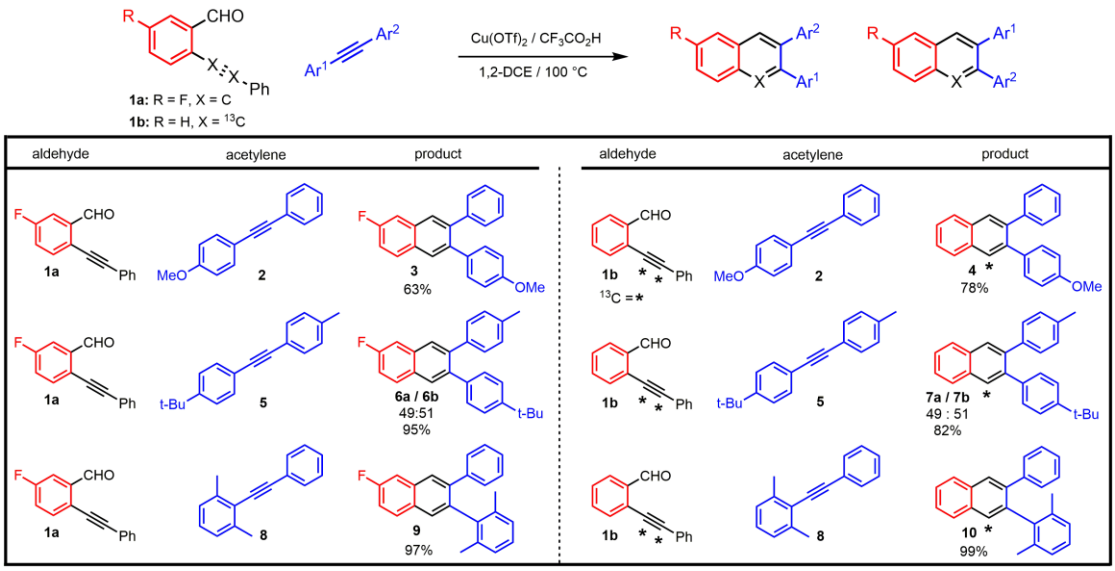

We first assessed the regioselectivity of this benzannulation with diarylacetylene **2** in order to determine the role of an electron donating methoxy group (Table 1.1). Using fluorinated and ^{13}C-labeled benzaldehydes (**1a–b**), we found the diarylacetylene yields nearly complete regioselectivity for products **3** and **4** respectively with >99:1 preference. The electron donating effects of **2** were further confirmed by analyzing the regioisomeric mixture produced when diarylacetylene **5,** bearing electronically similar 4-methyl and 4'-*t*-butyl phenyl substituents, was subjected to the same benzannulation conditions. The results of these reactions gave a near 1:1 regioisomeric mixture of the expected naphthalene products **6a–b** and **7a–b**. Substrate **8** was chosen to determine whether steric factors also influenced the regiochemical outcome. Rather than afford a scrambling of regioisomers, **8** was benzannulated efficiently to **9** and **10** with the same regiochemical outcome as observed for methoxy-substituted **1**. This is consistent that the electron donating ability of the methyl groups determines the regioselectivity rather than the steric demands of that substrate. This tolerance to phenylacetylenes bearing *ortho*- substituents is described in greater detail later in this chapter.

Scheme 1.2. Model for predicting the regiochemical outcome of alkyne benzannulation via relative stability of regioisomeric carbocations derived from the acetylene utilyzed in the benzannulation

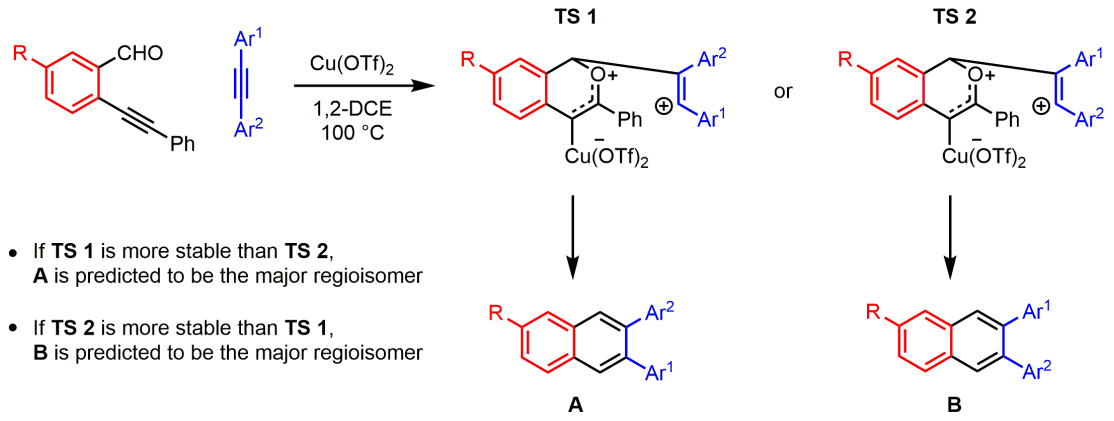

These studies gave useful insight into the mechanism first proposed by Yamamoto[15] and suggested that the [4+2] cycloaddition proceeds either asynchronously or through sequential bond formation resulting in a positive charge developing on one of the two acetylene carbons. The regioselectivity is therefore determined by the acetylene substituent that best stabilizes this developing charge (Scheme 1.2).[20] Density functional theory (DFT) calculations comparing the relative ground state energy using diarylacetylenes **1** and **8** supported this interpretation and showed a strong energetic preference (6.7–9.2 kcal/mol) for the transition state that best stabilized a developing positive charge. These results have developed into a simple predictive model that has enabled the synthesis of highly substituted naphthalenes controlled by the electronic interactions of the acetylene substrate.

Building upon the factors governing regiochemical outcomes and the capability to benzannulation sterically hindered alkynes, we leveraged this reaction to applications in ortho(arylene) synthesis. Poly(phenylene)s have attracted much interest in recent years for their applications in OLEDs, OFETs, and optoelectronic devices. Specifically,

poly(*ortho*-phenylene)s are of interest because they are known to adopt specific helical conformations in solution and solid states.[1,21,22] However, these structures are synthetically challenging to achieve due to low cross-coupling efficiencies caused by steric hindrances from *ortho*-substituted phenylenes. Poly(*para*-phenylene ethynylene)s (PPE), in contrast, are readily synthesized in high molecular weights from readily available starting materials. Given the remarkable steric tolerance and high reaction efficiencies of the Asao-Yamamoto benzannulation, we were interested in converting the embedded alkyne moieties along a PPE backbone into 2,3-naphthyl linkages for benzannulated polyphenylenes (**BPP**) containing alternating *para*- and *ortho*-phenylene linkages. This transformation was the first reported cycloaddition performed along a conjugated polymer backbone (Scheme 1.3).[23]

Scheme 1.3. Efficient Benzannulation of Poly(phenylene ethynylene)s. Adapted from Reference 19.

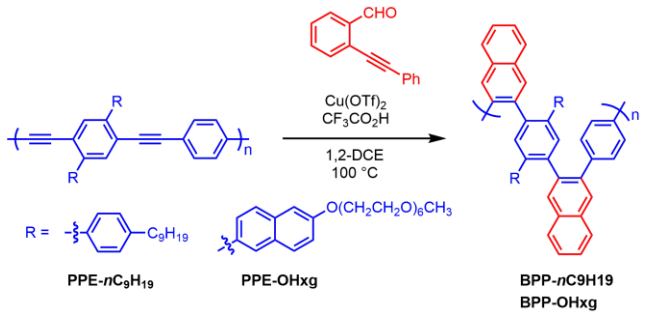

Due to the congested nature of the *ortho*-phenylene backbone, it is predicted the benzannulated polyphenylene (**12a**) should adopt a compact, non-planar conformation in organic solvents. UV-vis and photoemission spectroscopy provided the first indication that efficient benzannulation had occurred. The inability of adjacent aromatic rings to planarize prevents conjugation along the polymer backbone and blue shifts the UV-vis absorption λ_{max} by 140 nm after benzannulation. A similar trend is observed in

the photoemission spectrum where the λ_{em} are blue shifted by 22 nm and significantly broadened, a feature common to other *ortho*-phenylene linked polymers.[21] The most direct evidence for the efficient benzannulation along the polymer backbone was aquired by ^{13}C NMR on a polymer containing ^{13}C-enriched alkynes. Upon benzannulation, all the signals corresponding to ^{13}C-labeled alkynes were cleanly shifted to the aromatic region with no observable residual alkyne resonances remaining. This work demonstrated a new approach to synthesize high molecular weight polyphenylenes containing *ortho*-naphthyl linkages.

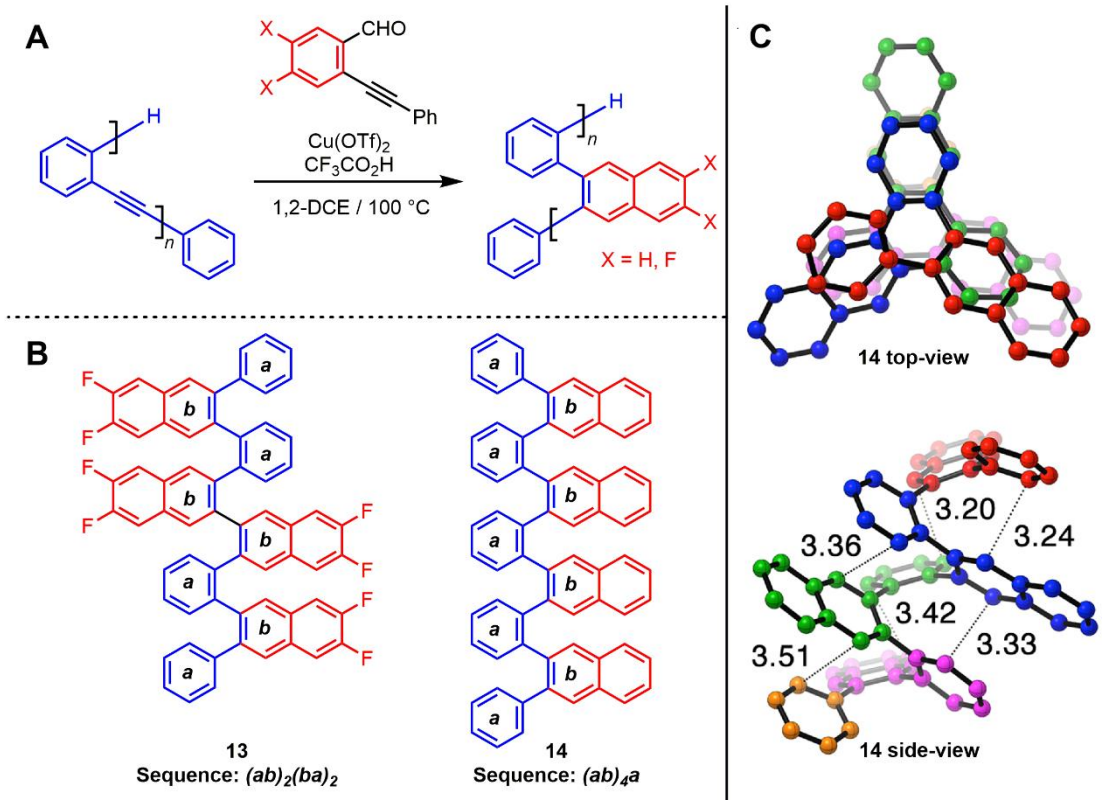

Figure 1.2. A) Synthetic approach to oligo(*ortho*-arylene)s from oligo(ortho-phenylene ethynylene)s. B) Sequences of *ortho*-arylene oligomers derived from the benzannulation of *ortho*-arylethynyl oligomers. C) X-ray crystallographic structures of alternating naphthalene-phenylene repeat units. Adapted from Reference 24. Reprinted with permission from The Royal Society of Chemistry.

The synthetic versatility available to poly(phenylene ethynylene)s allows for facile modification. As a result, *ortho*-arylene oligomers can be effectively made from *ortho*-phenylene ethynylene precursors containing mono- or diyne moieties (Figure 1.2a).[24] Through modulating the sequence of mono- and diynes, complex sequences, like **13** to more simple **14** patterns can be achieved via benzannulation cycloaddition reactions. Solid-state characterization of these materials was carried out through single crystal X-ray diffraction in which these compounds were observed to fold into a "closed" helical conformation (Figure 1.2c). Solution-state structures, elucidated through 1D and 2D NMR, confirmed 86% of the population took a completely folded conformation with the remainder possessing a partially unfolded conformation. The percentage of folded *ortho*-arylenes was increased to 88% or 94% when halogen substituents (X = Cl or F respectively) were introduced on the naphthalene linkages of the chain by changing the benzaldehyde used (Figure 1.2b) due to stronger π-stacking interactions between halogenated arenes and non-halogenated arene subunits. This method provided a direct synthetic approach to *ortho*-arylene oligomers through a modular benzannulation of *ortho*-phenylene ethynylenes. However, decreased reaction efficiencies at longer oligomer lengths prevented the benzannulation of higher order oligo- and poly(*ortho*-phenylene ethynylene)s to make poly(*ortho*-phenylene)s.

ortho-Arylene polymers and oligomers are of additional interest as precursors to well-defined nanographenes (NGs) and graphene nanoribbons (GNRs). These structures are obtained through an oxidative cyclodehydrogenation reaction which fuses neighboring aromatic rings to each other to yield a graphitized structure (Figure 1.3a). This bottom-up synthetic approach enables exceptional control over the width, length,

and edge structures of these materials. Thermal oxidation on *ortho*-arylene oligomers was attained through evaporation of **15** in ultra high vacuum on Au(111). Figure 1.3b shows scanning tunneling microscopy (STM) images of single molecules of **15** showing the non-planarity of these structures. Heating the substrate to 286 °C caused a change in the shape of the molecules consistent with the expected planar **17** (Figure 1.3c).[24] This approach carries with it the potential for one edge of a graphene nanoribbon to be selectively halogenated while the opposing edge structure contains only protons.

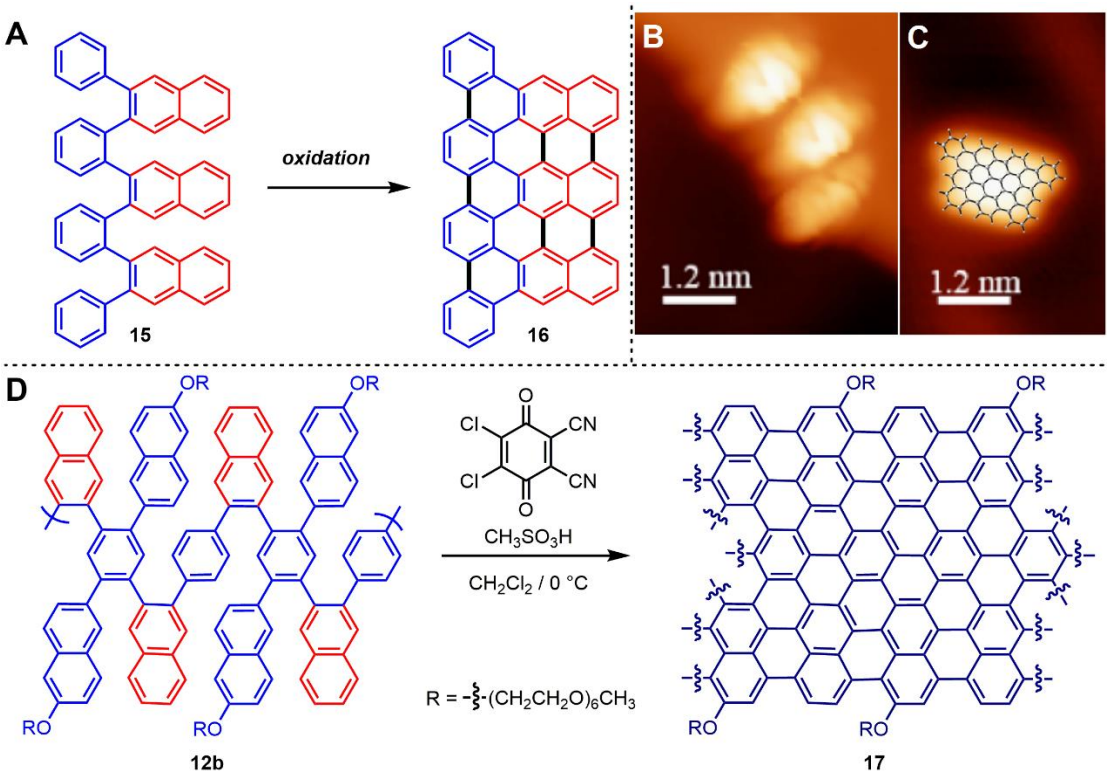

Figure 1.3. A) Scheme for the on-surface oxidation of *ortho*-phenylene oligomers for nanographene synthesis. B) Close-up of several *ortho*-arylene oligomers of **15** before annealing showing nonplanarity of the molecules. C) STM image of an individual 16 molecule obtained from annealing **15**, with its DFT optimized structure superimposed. Adapted from Reference 24. Reprinted with permission of The Royal Society of Chemistry. D) Chemical oxidation of BPP-OHxg into solution dispersible graphene nanoribbons. Adapted from Reference 25.

Oxidation of **PPE** with hexaethyleneglycol side chains **(12b)** using 2,3-dichloro-5,6-dicyanobenzoquinone (DDQ)/CH_3SO_3H yields a completely fused GNR **17** (Figure 1.3d) which can be easily dispersed in *N,N*-dimethylformamide and *N*-methyl-2-pyrrolidinone. The extent of oxidation was characterized through Raman spectroscopy, infrared spectroscopy, and solid state NMR of strategically ^{13}C-labeled derivatives. The bandgaps of individual GNRs was estimated through density functional theory (DFT) models to be 1.06 eV. Devices made from these materials were fabricated through aerosol-assisted chemical vapor deposition (AA-CVD) onto a copper foil substrate and transferred to SiO_2 using traditional graphene transfer techniques. Field-effect devices (FEDs) fabricated using this technique exhibited ambipolar charge transport. This was a significant development in the field of graphitic devices as, prior to this study, there had been no reports of solution synthesized GNRs that exhibit ambipolarity.[25]

Twisted and contorted PAHs exhibit interesting optical and electronic properties and form host-guest complexes with fullerenes with potential applications in photovoltaic devices.[26] Benzannulation strategies can provide rapid access to extended and contorted hexabenzocoronenes (HBCs) in just a few steps (Figure 1.4a).[27] Substituted diarylacetylenes **18a–d** were subjected to benzannulation conditions to afford their respective HBC precursors **19a–d**. Final oxidation of these materials using $FeCl_3$ proceeded efficiently with no evidence of rearrangement that often occurs in closely related systems.[28] Though all structures underwent rapid C-C bond formation to access **20a–d,** only **20a** and **20d** completely fused to products **21a** and **21d**, respectively. The steric hindrance associated with the *t*-butyl and extended naphthyl groups present in **20b** and **20c,** respectively, prevented these final C-C bonds from forming. DFT-optimized

structures of partially and fully fused compounds **20a** and **21a** further support the contorted conformations of these compounds (Figure 1.4b). This successful synthesis of extended and contorted HBCs demonstrates that a benzannulation strategy is an effective approach for the synthesis of increasingly complex PAHs.

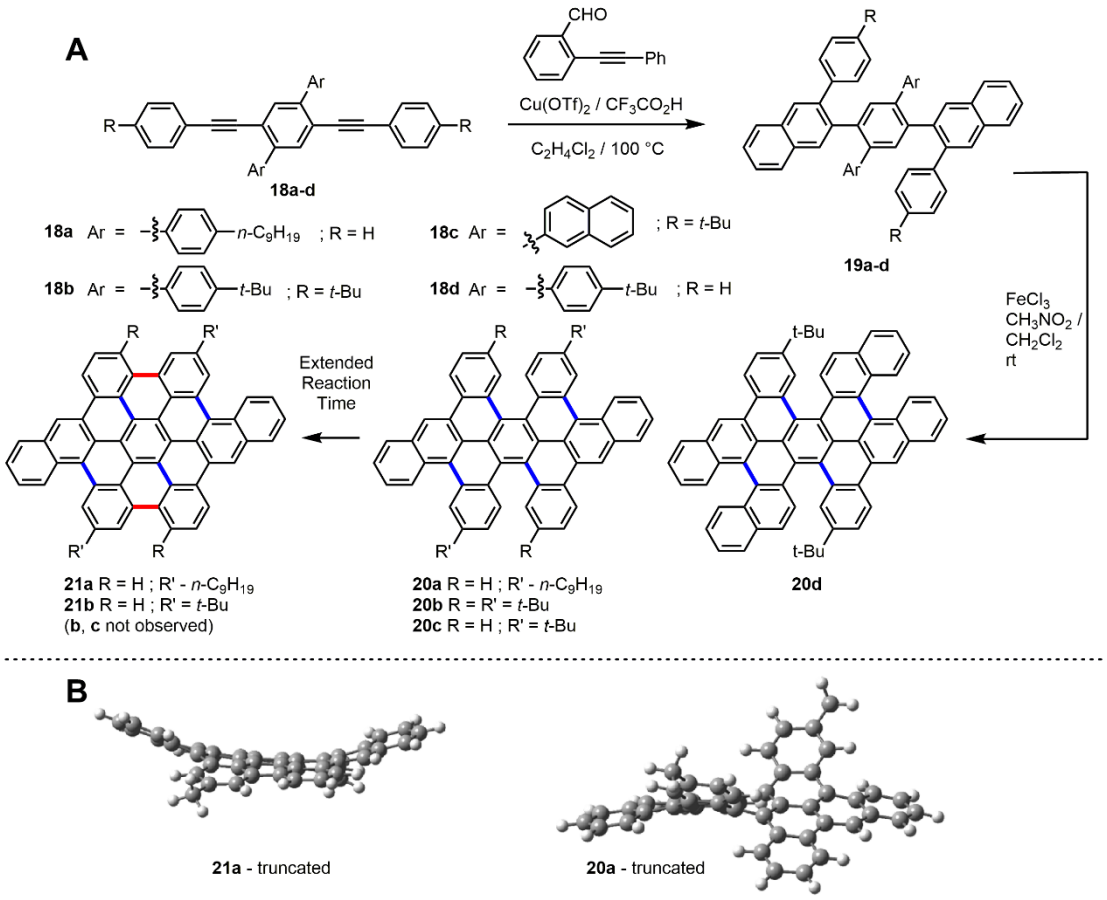

Figure 1.4. a) Synthetic scheme for partially fused HBC derivatives **20a-d** and fully fused HBC **21a-b** using a two-step benzannulation-cyclodehydrogenation strategy. b) DFT-optimized structures of partially and fused HBC compounds **20a** and **21a**. The *n*-C_9H_{19} were truncated to $–CH_3$ groups in the calculations. Adapted from Reference 25- Reproduced by permission of The Royal Society of Chemistry

2.3 Expanding Beyond Diarylacetylenes

Standard palladium cross-coupling techniques can quickly afford a variety of diarylacetylenes, but the sp^2-sp^2 naphthyl-phenyl bonds post benzannulation are very

stable and make further derivatization of the naphthalene ring at the 2 and 3 positions nearly impossible. Acetylenes bearing reactive functional groups would allow for further derivatization at the *ortho*- position inaccessable to diarylacetylenes. Silanes are a versatile functional group and are ubiquitous throughout organic chemistry as protecting groups for alcohols[29] and terminal alkynes.[30,31] Not only can new C-C bonds be formed directly through Hiyama cross-coupling conditions, but electrophilic cleavage of aryl silanes generally result in specific substituted aromatic compounds where the electrophile selectively occupies the position previously bonded to the silyl group.[32] We wanted to integrate this benzannulation reaction into a general strategy that could produce larger aromatic systems by expanding its utility into silyl-protected acetylenes.[33]

Scheme 1.4. Reaction scope for a variety of silyl-arylacetylenes

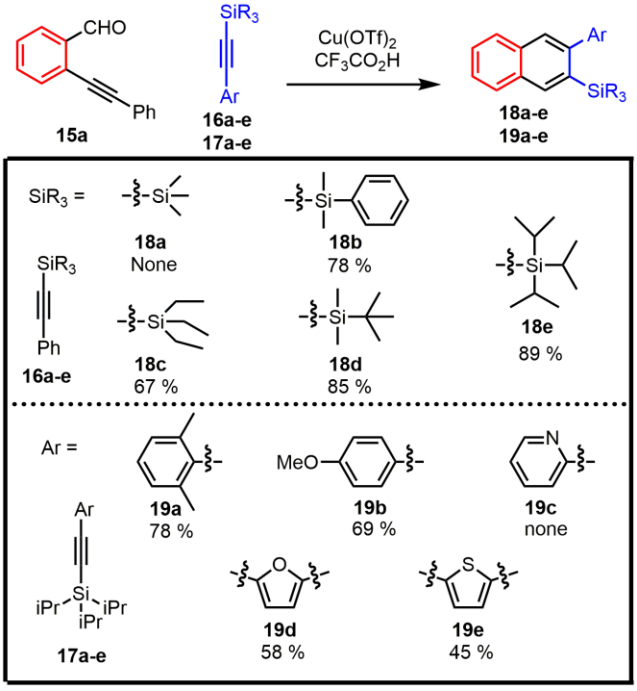

Only a small number of silylacetylenes had been known for benzannulation and did not include $Cu(OTf)_2$ or $ZnCl_2$ mediated reactions.[18] $Cu(OTf)_2$ mediated benzannulations require the presence of a strong Brønsted acid because its conjugate base suppresses unwanted naphthyl ketone side products (Figure 1.1). However, due to the sensitivity of most silicon groups towards strong acids, these conditions generated protodesilylated 2-phenylnaphthalene as the major or only benzannulation product. While this provides a one pot method to benzannulate and deprotect naphthylsilanes, in many cases it would be advantageous to retain the silicon group. By reducing the acid concentration to 1 equivalent, nearly all silicon protected acetylenes tested (**23b–e**), shown in Scheme 1.4, were preserved in the final naphthalene product (**25b–e**) in high yields. The only exception was the smallest, and most sensitive, trimethylsilyl (TMS) acetylene (**23a**) which was too labile to be retained upon benzannulation. Instead, **23a** was efficiently benzannulated in 75% yield using $ZnCl_2$ as a benzannulation catalyst without the presence of a strong acid.[16] Silylacetylenes also react with high regioselectivity, observed when **23a** was reacted with a bromo-benzaldehyde **22b** to afford **25f** in 50% yield (Scheme 1.5) as the major regioisomer.

Scheme 1.5. Regioselective Benzannulation of silyl-arylacetylenes

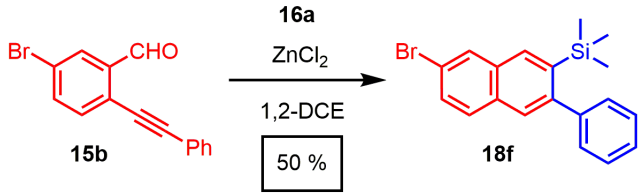

We studied the scope of this reaction beyond phenylacetylenes by evaluating a series of aromatic compounds containing tri(isopropyl)silyl protected acetylenes (**24a–e**). Impressively, the highly sterically hindered **24a** was well tolerated in the reaction,

yielding **26a** in 78% yield. Electron-donating moieties (**24b**, **24d**, and **24e**) were tolerated yielding the corresponding naphthalenes **26b, 26d**, and **26e**. However, electron withdrawing substituents, like the pyridine containing **24c** which was likely protonated during the reaction, had proved to be poor substrates for benzannulation yielding only benzaldehyde decomposition products and unreacted acetylene.

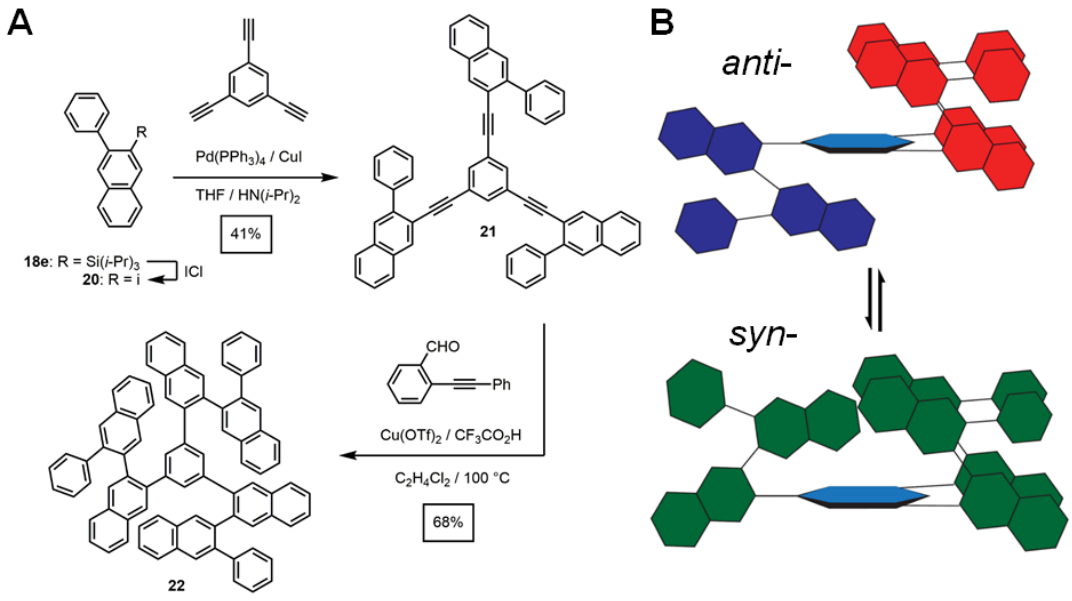

Figure 1.5. a) Reaction scheme for the synthesis of sterically congested oligo(*ortho*-arylene) **22**. b) Schematic depiction of the major *anti*- and *syn*- conformor of **22**. Adapted from Reference 31

The resulting 1-silyl-2-phenylnaphthalene **25e** were subjected to iodine monochloride to transform the aryl silane into the corresponding naphthyl iodide (**27**).[33] The outstanding efficiency and steric tolerance of the benzannulation reaction, combined with the synthetic versatility of halogenated naphthalenes derived from silylacetylenes, suggested to us a new strategy to access highly crowded aromatic architectures (Figure 1.5a). In order to explore this possibility, **27** was cross-coupled onto 1,3,5-triethynylbenzene to afford trialkyne **28** (Figure 1.5a). The internal alkynes

in this product were accessible for another benzannulation to give oligo(arylene) **29** in good yield. Full characterization of this compound was achieved via 2D NMR where it was found to exhibit primarily two conformations in solution at room temperature, assigned as the major *anti*- and minor *syn*- conformations in Figure 1.5b. These conformations are caused by the hindered bond rotations of each arm around the central benzene ring and persist even at elevated temperatures of 140 °C. The synthesis of this compound exemplified the tolerance this benzannulation reaction has towards highly congested environments.

The limited regioselectivity of diarylacetylenes with substituents lacking sufficient electronic difference, combined with the poor reactivity both diaryl and silyl protected acetylenes have for electron withdrawing groups, led us to investigate the benzannulation of halo-arylacetylenes (Table 1.2).[34] In contrast to previous diaryl- or silylacetylenes which tolerated only electron rich aryl substituents, haloacetylenes tolerated electronically deficient aryl groups with high efficiency. Arenes substituted with electron withdrawing methyl ester (**31a**), nitriles (**31b**), halogen (**31c-e**), groups underwent benzannulation in high yields to give the expected naphthalene products (**32a–e**). In contrast, the electron donating *para*-methoxyphenylbromoacetylene (**31f**) suffered from low conversion typical of inactive acetylenes. This work offered a complimentary method to access polyheterohalogentated naphthalenes derived from haloalkynes bearing electron deficient phenyl substituents. Expanding on our understanding of this reaction's mechanism, we proposed two mechanistic pathways are possible. For both proposed mechanisms, $Cu(OTf)_2$ readily coordinates to the alkyne of the benzaldehyde to form the Cu-bound benzopyrylium. Mechanism A features [4+2]

addition of the acetylene before demetalation and was first proposed by Yamamoto and co-workers. In mechanism B, the Cu-bound benzopyrylium is protonated before undergoing formal [4+2] addition of the acetylene (Table 1.2, bottom). To test the viability of this route, a ketal dimer of benzaldehyde **30a** was synthesized that decomposes into the free benzopyrylium with addition of CF_3CO_2H to simulate the copper-free route.

Table 1.2. Synthesis of heterohalogenated naphthalenes from halo-arylacetylenes. Adapted from Reference 32.

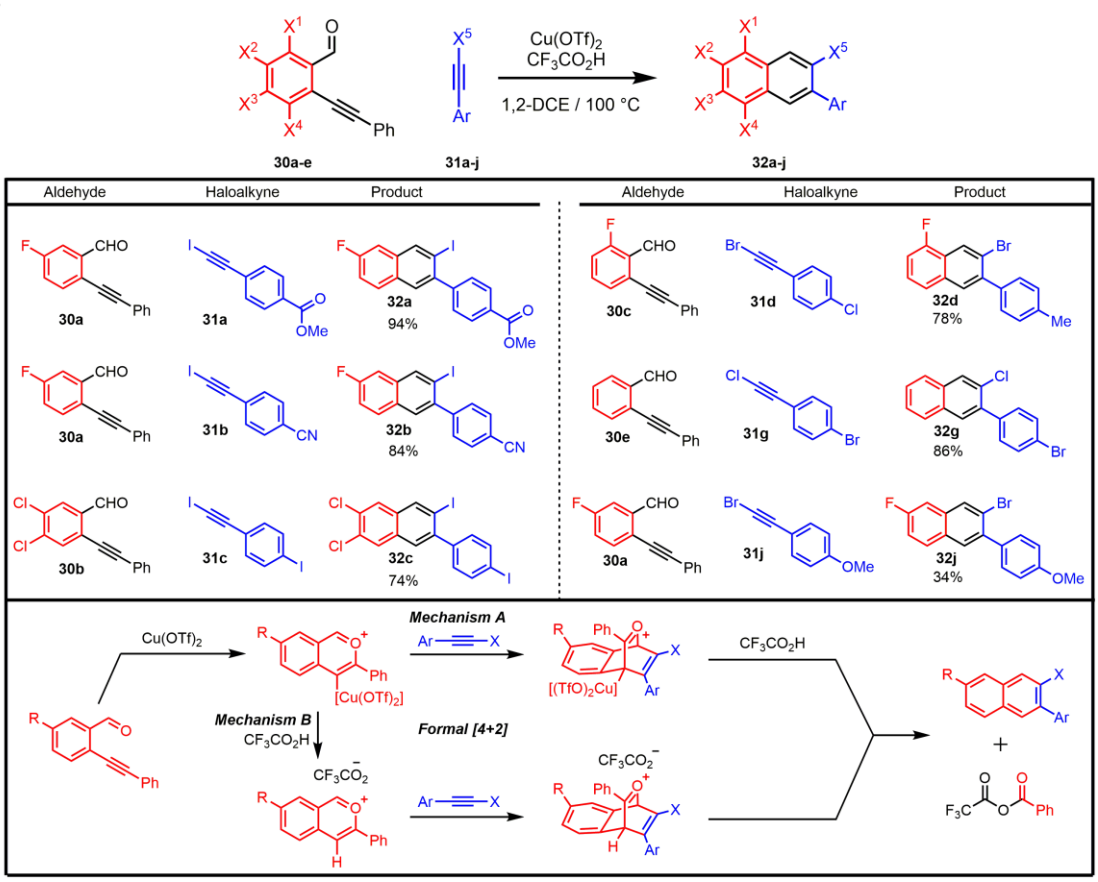

The free benzopyrylium reacts to afford a halogenated naphthalene with identical regioselectivity as the copper catalyzed route. DFT calculations of the proposed transitions states of either mechanism both predict the observed

regioselectivity in the reaction. On the premise that the mechanism includes a Cu-bound benzopyrylium, regardless of whether protonation occurs before or after C–C bond formation, a Cu-bound intermediate provides a means to install an additional halide.[18] With the addition of stoichiometric quantities of $CuCl_2$ or $CuBr_2$, we were able to install an additional halide to the position where copper is thought to bind to the pyrylium intermediate allowing well controlled substitution at 7 out of 8 positions of a naphthalene ring.

Using haloacetylenes, we were able to access fuctionalized and solution processable diazatetracenes in a 2 short steps (Scheme 1.6).[35] In the first step, dichloronaphthalenes **33**, **37–38** were constructed through the benzannulation of a dichlorobenzaldeyde, **30b**, with a substituted acetylene, **31c**, **35**–**36**. The second step featured a Buchwald-Hartwig amination of 1,2-diaminobenzene generating a diazatetracene core which naturally aromatizes to compounds **39**–**41**. The electronic-properties of these synthesized diazatetracenes can be tuned by modifying the substituents bound to the core.

Scheme 1.6. Synthesis of diazatetracenes. Adapted from Reference 33.

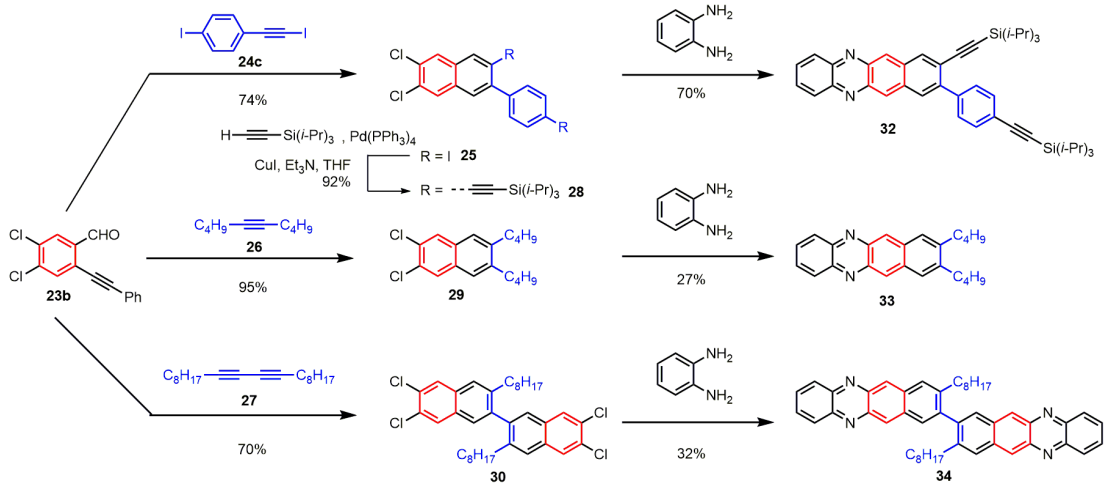

This is seen most clearly in the UV-vis absorption spectra of **39** and **40,** where the extended conjugation of **39** red-shifts due to its extended conjugation caused by the additional ethynyl and aryl groups. External influences, for example protonation of the embedded nitrogens, also have an effect on the optical and electronic properties of these substrates.

Unfortunately, haloacetylenes required one substituent on the alkyne to be substituted with an aryl substituent. When haloacetylenes substituted with *n*-butyl, triisopropylsilyl, or methylester groups were used, reaction efficiencies were reduced to below 5%. Through the use of a $ZnCl_2$ catalyst, we were able to demonstrate that halo-silylacetylenes undergo benzannulation with high efficiency and regioselectivity (Table 1.3). We observed this transformation to have a preference for iodo-silylacetylene (**43a**) over bromo-silylacetylene (**43b**), where the yield decreased dramatically from 93% to 18% for **44b** and **44c,** respectively. While this reaction occured with complete regioselectivity when halo-silylacetylenes (**43a–b**) were used, a 1:1 mixture of regioisomers (**44f–g)** was observed when proto-silylacetylene (**43c)** was used (Table 1.3).

Table 1.3. Synthesis of 2-naphthyne precursors from various substituted benzaldehydes

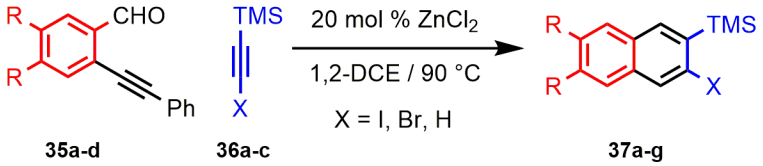

35a-d 36a-c 37a-g

Aldehyde	Acetylene	Product	Aldehyde	Acetylene	Product
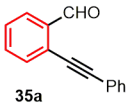 35a	 36a	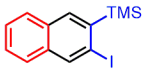 37a 75%	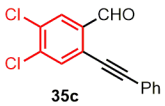 35c	 36a	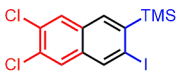 37d 70%
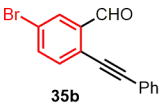 35b	 36a	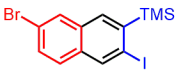 37b 93%	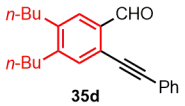 35d	 36a	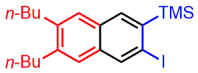 37e 59%
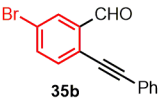 35b	 36b	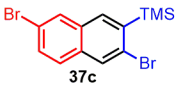 37c 18%	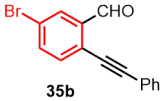 35b	 36c	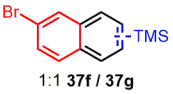 1:1 37f / 37g 61%

Interestingly, the regioselectivity for this substrate class was reversed from that observed for haloacetylenes (Figure 1.6a). We hypothesized this flip in selectivity was due to the stabilization of the *beta*-carbon by the silicon group, whereas the aromatic ring stabilized a developing positive charge on the carbon *alpha* to the aryl group for haloacetylenes (Figure 1.6b). This flip in regioselectivity is predicted through a DFT model of the proposed transition state between these two substrates. This model predicts a 2.0 kcal/ mol preference for the *anti*-regioisomer in the case of **44b** compared to 5.6 kcal/mol in favor of the *syn*-regioisomer for a bromophenylacetylene.

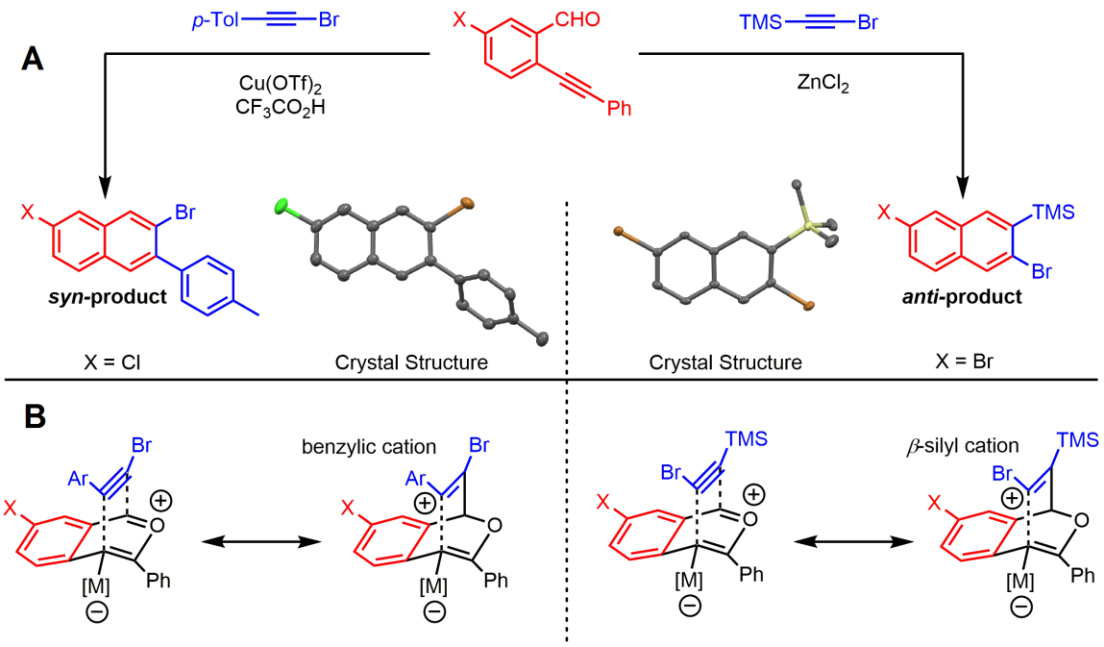

Figure 1.6. a) Haloarylacetylenes and halosilylacetylenes provide opposite regioselectivity in benzannulation reactions, as demonstrated by x-ray crystallography. Ellipsoids set to 50 % probability level for **44c**. b) Rationale for the regioselectivity of each reaction. The silicon substituent stabilizes developing positive charge on the carbon adjacent to the halogen, which makes the observed regioselectivity consistent with other benzannulation reactions.

While the aryl silane remains active for derivatization using iodine monochloride, structural comparisons can be made between **44a-e** and popular aryne precursors. Arynes are a reactive class of intermediate species that are most commonly generated through the desilylation/elimination of an *ortho*-silylaryl triflates/halides.[36–38] Transformations involving arynes have made them indespensible building blocks for the synthesis of natural products and PAHs.[39–45] While arynes derived from fused aromatic rings enable the synthesis of more complex structures, commercial and synthetic availability of these structures remains challenging. Substituted 2-naphthyne precursors had been reported by both Wong[46] and Maly,[47] but seven step syntheses limited general adaptation of these methods.

Scheme 1.7. Aryne generation and trapping with furan

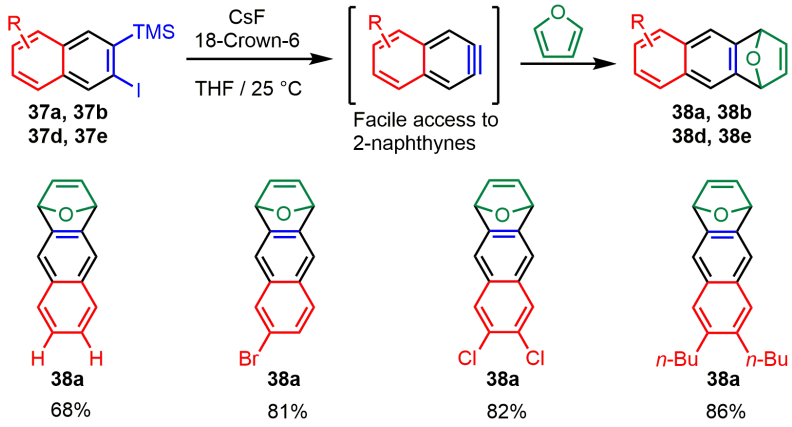

We proposed to use the naphthalene products afforded by the benzannulation of halo-silylacetylenes as a general method to access previously underrepresented 2-naphthynes. Compounds **44a**, **44b**, **44d**, and **44e** were sealed in a vial with cesium fluoride (2 equiv), 18-Crown-6 (4 equiv), and furan (15 equiv). After 12 hours, [2.2.1]oxabicyclic alkenes (**45a–d**) were isolated in high yields (68-86 %), confirming that these compounds are aryne precursors (Scheme 1.7). Given the availability of many substituted benzaldehyde cycloaddition partners, these findings demonstrated that benzannulation chemistry provides rapid entry to substituted 2-naphthyne intermediates. More details of this work are given in Chapter Four.

2.3 Conclusion

In this introductory chapter, we have reviewed a general method to access novel aromatic systems. Through our investigations into diarylacetylenes, we established that this reaction exhibits a high regioselectivity determined by which acetylene carbon best stabalized a positive charge on the metal-bound pyrylium ion intermediate. The steric tolerance of this transformation makes it an ideal strategy to access *ortho*-arylene and contorted PAHs. Through expanding the synthetic scope of acetylenes used, we found

silyl- and halo- substituted acetylenes are well tolerated and yield regioselective naphthalene products. These products are useful building blocks for the synthesis of highly crowded aromatic architectures and diazatetracenes. A benzannulation of silyl-haloacetylenes yield access to underrepresented 2-naphthyne precursors. These can be treated as monomers for polymerizations or used directly for the synthesis of substituted PAHs. The steric tolerance and regioselectivity of this reaction make it an indespensible synthetic tool for the construction of highly substituted polycyclic aromatic hydrocarbons.

REFERENCES

(1) Mathew, S. M.; Hartley, C. S. *Macromolecules* **2011**, *44*, 8425–8432.

(2) Ando, S.; Ohta, E.; Kosaka, A.; Hashizume, D.; Koshino, H.; Fukushima, T.; Aida, T. *J. Am. Chem. Soc.* **2012**, *134*, 11084–11087.

(3) Bronner, C.; Stremlau, S.; Gille, M.; Brauße, F.; Haase, A.; Hecht, S.; Tegeder, P. *Angew. Chem. Int. Ed.* **2013**, *52*, 4422–4425.

(4) Golling, F. E.; Quernheim, M.; Wagner, M.; Nishiuchi, T.; Müllen, K. *Angew. Chem. Int. Ed.* **2014**, *53*, 1525–1528.

(5) Müller, M.; Kübel, C.; Müllen, K. *Chem. – Eur. J.* **1998**, *4*, 2099–2109.

(6) Narita, A.; Verzhbitskiy, I. A.; Frederickx, W.; Mali, K. S.; Jensen, S. A.; Hansen, M. R.; Bonn, M.; De Feyter, S.; Casiraghi, C.; Feng, X.; Müllen, K. *ACS Nano* **2014**, *8*, 11622–11630.

(7) Feng, X.; Wu, J.; Ai, M.; Pisula, W.; Zhi, L.; Rabe, J. P.; Müllen, K. *Angew. Chem. Int. Ed.* **2007**, *46*, 3033–3036.

(8) Booth, G. In *Ullmann's Encyclopedia of Industrial Chemistry*; Wiley-VCH Verlag GmbH & Co. KGaA, 2000.

(9) de Koning, C. B.; Rousseau, A. L.; van Otterlo, W. A. L. *Tetrahedron* **2003**, *59*, 7–36.

(10) Liu, Z.; Larock, R. C. *Angew. Chem. Int. Ed.* **2007**, *46*, 2535–2538.

(11) Liu, Z.; Zhang, X.; Larock, R. C. *J. Am. Chem. Soc.* **2005**, *127*, 15716–15717.

(12) Huang, Q.; Larock, R. C. *Org. Lett.* **2002**, *4*, 2505–2508.

(13) Viswanathan, G. S.; Wang, M.; Li, C.-J. *Angew. Chem. Int. Ed.* **2002**, *41*, 2138–2141.

(14) Balamurugan, R.; Gudla, V. *Org. Lett.* **2009**, *11*, 3116–3119.

(15) Asao, N.; Nogami, T.; Lee, S.; Yamamoto, Y. *J. Am. Chem. Soc.* **2003**, *125*, 10921–10925.

(16) Fang, X.-L.; Tang, R.-Y.; Zhang, X.-G.; Zhong, P.; Deng, C.-L.; Li, J.-H. *J. Organomet. Chem.* **2011**, *696*, 352–356.

(17) Umeda, R.; Kaiba, K.; Morishita, S.; Nishiyama, Y. *ChemCatChem* **2011**, *3*, 1743–1746.

(18) Isogai, Y.; Menggenbateer; Nawaz Khan, F.; Asao, N. *Tetrahedron* **2009**, *65*, 9575–9582.

(19) Asao, N.; Takahashi, K.; Lee, S.; Kasahara, T.; Yamamoto, Y. *J. Am. Chem. Soc.* **2002**, *124*, 12650–12651.

(20) Arslan, H.; Walker, K. L.; Dichtel, W. R. *Org. Lett.* **2014**, *16*, 5926–5929.

(21) He, J.; Crase, J. L.; Wadumethrige, S. H.; Thakur, K.; Dai, L.; Zou, S.; Rathore, R.; Hartley, C. S. *J. Am. Chem. Soc.* **2010**, *132*, 13848–13857.

(22) Mathew, S. M.; Engle, J. T.; Ziegler, C. J.; Hartley, C. S. *J. Am. Chem. Soc.* **2013**, *135*, 6714–6722.

(23) Arslan, H.; Saathoff, J. D.; Bunck, D. N.; Clancy, P.; Dichtel, W. R. *Angew. Chem. Int. Ed.* **2012**, *51*, 12051–12054.

(24) Lehnherr, D.; Chen, C.; Pedramrazi, Z.; R. DeBlase, C.; M. Alzola, J.; Keresztes, I.; B. Lobkovsky, E.; F. Crommie, M.; R. Dichtel, W. *Chem. Sci.* **2016**, *7*, 6357–6364.

(25) Gao, J.; Uribe-Romo, F. J.; Saathoff, J. D.; Arslan, H.; Crick, C. R.; Hein, S. J.; Itin, B.; Clancy, P.; Dichtel, W. R.; Loo, Y.-L. *ACS Nano* **2016**, *10*, 4847–4856.

(26) Tremblay, N. J.; Gorodetsky, A. A.; Cox, M. P.; Schiros, T.; Kim, B.; Steiner, R.; Bullard, Z.; Sattler, A.; So, W.-Y.; Itoh, Y.; Toney, M. F.; Ogasawara, H.; Ramirez, A. P.; Kymissis, I.; Steigerwald, M. L.; Nuckolls, C. *ChemPhysChem* **2010**, *11*, 799–803.

(27) Arslan, H.; J. Uribe-Romo, F.; J. Smith, B.; R. Dichtel, W. *Chem. Sci.* **2013**, *4*, 3973–3978.

(28) Ormsby, J. L.; Black, T. D.; Hilton, C. L.; Bharat; King, B. T. *Tetrahedron* **2008**, *64*, 11370–11378.

(29) Wuts, P. G. M.; Greene, T. W. In *Greene's Protective Groups in Organic Synthesis*; John Wiley & Sons, Inc., 2006; 367–430.

(30) Weber, W. P. In *Silicon Reagents for Organic Synthesis*; Reactivity and Structure Concepts in Organic Chemistry; Springer Berlin Heidelberg, 1983; 129–158.

(31) Wuts, P. G. M.; Greene, T. W. In *Greene's Protective Groups in Organic Synthesis*; John Wiley & Sons, Inc., 2006; 927–933.

(32) Weber, W. P. In *Silicon Reagents for Organic Synthesis*; Reactivity and Structure Concepts in Organic Chemistry; Springer Berlin Heidelberg, 1983; 114–128.

(33) Hein, S. J.; Arslan, H.; Keresztes, I.; Dichtel, W. R. *Org. Lett.* **2014**, *16*, 4416–4419.

(34) Lehnherr, D.; Alzola, J. M.; Lobkovsky, E. B.; Dichtel, W. R. *Chem. – Eur. J.* **2015**, *21*, 18122–18127.

(35) Lehnherr, D.; Alzola, J. M.; Mulzer, C. R.; Hein, S. J.; Dichtel, W. R. *J. Org. Chem.* **2017**, *82*, 2004–2010.

(36) Himeshima, Y.; Sonoda, T.; Kobayashi, H. *Chem. Lett.* **1983**, *12*, 1211–1214.

(37) Crossley, J. A.; Kirkham, J. D.; Browne, D. L.; Harrity, J. P. A. *Tetrahedron Lett.* **2010**, *51*, 6608–6610.

(38) Mesgar, M.; Daugulis, O. *Org. Lett.* **2016**, *18*, 3910–3913.

(39) Tadross, P. M.; Stoltz, B. M. *Chem. Rev.* **2012**, *112*, 3550–3577.

(40) Bhojgude, S. S.; Bhunia, A.; Biju, A. T. *Acc. Chem. Res.* **2016**, *49*, 1658–1670.

(41) Wu, D.; Ge, H.; Hua Liu, S.; Yin, J. *RSC Adv.* **2013**, *3*, 22727–22738.

(42) Wenk, H. H.; Winkler, M.; Sander, W. *Angew. Chem. Int. Ed.* **2003**, *42*, 502–528.

(43) García-López, J.-A.; F. Greaney, M. *Chem. Soc. Rev.* **2016**, *45*, 6766–6798.

(44) Karmakar, R.; Lee, D. *Chem. Soc. Rev.* **2016**, *45*, 4459–4470.

(45) Hendrick, C. E.; Wang, Q. *J. Org. Chem.* **2017**, *82*, 839–847.

(46) Yick, C.-Y.; Chan, S.-H.; Wong, H. N. C. *Tetrahedron Lett.* **2000**, *41*, 5957–5961.

(47) Lynett, P. T.; Maly, K. E. *Org. Lett.* **2009**, *11*, 3726–3729.

CHAPTER TWO

RAPID SYNTHESIS OF CROWDED AROMATIC ARCHITECTURES FROM SILYL ACETYLENES

2.1 Abstract

Congested aromatic systems were prepared by benzannulating silyl-protected arylacetylenes. The silyl groups may be retained in the naphthalene products and transformed into iodides in high yield. The desirable attributes of this strategy, particularly its remarkable tolerance of sterically hindered alkynes, are showcased in the efficient synthesis of a congested, branched oligo(naphthalene). As such, benzannulations of diaryl and silyl-protected acetylenes show outstanding promise for constructing new aromatic systems.

The findings described in this chapter are adapted from Hein, S. J.; Arslan, H.; Keresztes, I.; Dichtel, W. R. *Org. Lett.* **2014**, *16* (17), 4416–4419.

2.2 Introduction

Extended aromatic architectures have attracted intense interest for organic optoelectronic devices, including photovoltaics[1] and field effect transistors,[2] as well as for accessing porous polymers.[3] Improved synthetic approaches have provided increasingly elaborate systems, such as poly(*o*-arylenes),[4] contorted hexabenzocorones (HBCs),[5] and cyclo(*p*-phenylenes).[6] These architectures exemplify the diverse structural landscape available for fundamental and applied studies. For example, oligo(*o*-phenylenes) exhibit specific helical conformations[7] and spectral properties that arise from either fully extended or coiled conformations,[8] but this structural motif was virtually unexplored[9] until cross-coupling conditions tolerant of their steric hindrance were identified. We recently adapted a benzannulation reaction first reported by Yamamoto[10] to prepare congested aromatic systems containing 2,3-diarylnaphthalene functionalities. This reaction is the first cycloaddition capable of modifying the relatively unreactive alkynes along the backbone of a poly(phenylene ethynylene) (PPE).[11] It also tolerates sterically demanding aryl substituents on the alkynes, as demonstrated by its use in recent syntheses of contorted HBCs[12] and a (6,6) carbon nanotube segment precursor.[13] Furthermore, ^{13}C-labeled and fluorine-substituted cycloaddition partners proved that the benzannulation reaction proceeds regioselectively for most diarylacetylene substrates.[11, 14] This feature will facilitate the synthesis of low-symmetry products as single regioisomers.

2.3 Results and Discussion

Here we integrate the benzannulation reaction into a general strategy to produce larger aromatic systems by expanding its utility to silyl-protected acetylenes. Only a

limited number of these substrates have been explored in benzannulation reactions[15] and are unreported as substrates for the $Cu(OTf)_2$ or $ZnCl_2$-mediated reactions described below. A broad range of silyl protecting groups is tolerated, including bulky triisopropyl (TIPS) and *t*-butyldimethyl silyl (TBS) acetylenes. Under typical benzannulation conditions, these groups are protodesilylated to provide the corresponding 2-arylnaphthalene. We modified the reaction conditions to retain the silyl group, such that they may be transformed to iodides and derivatized using cross-coupling reactions. We apply this method iteratively to access a branched oligo(naphthalene) product so hindered that it exhibits restricted bond rotations at 140 °C in tetrachloroethane. This compound demonstrates both the utility of silyl-substituted naphthalene synthons and the remarkable abilty of the benzannulation reaction to modify hindered alkynes.

Table 2.1. Benzannulation of silyl-protected phenylacetylenes using reduced equiv of CF_3CO_2H retains silyl groups larger than TMS in the naphthalene products 3b-3e.

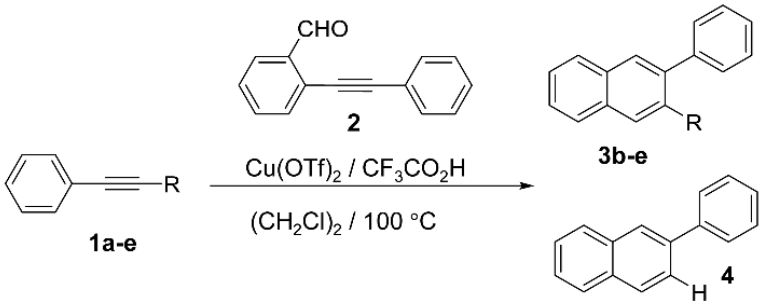

Conditions: **1** (0.100 g), **2** (2 equiv), $Cu(OTf)_2$ (0.05 equiv), CF_3CO_2H (1 equiv), $C_2H_4Cl_2$, 100 °C, 30 min

substrate	R	isolated yield (%)	
		3	**4**
1a	$Si(Me)_3$	none	40
1b	$Si(Et)_3$	67	none
1c	Si*t*-Bu$(Me)_2$	85	none
1d	Si(*i*-Pr)$_3$	89	none
1e	$SiPh(Me)_2$	78	none

We first evaluated the benzannulation of phenyl acetylenes protected by silyl groups that differ in size and relative stability. Typical reaction conditions include excess CF_3CO_2H (10 equiv per alkyne) because its conjugate base is thought to promote the formation of naphthalenes over naphthyl ketone side products.[10] These conditions provide desilylated 2-phenylnaphthalene **4** as the major or only benzannulation product for various silyl-protected phenylacetylenes, even for relatively robust TIPS, TBS, and dimethylphenylsilyl (DMPS) groups. In contrast, reducing the

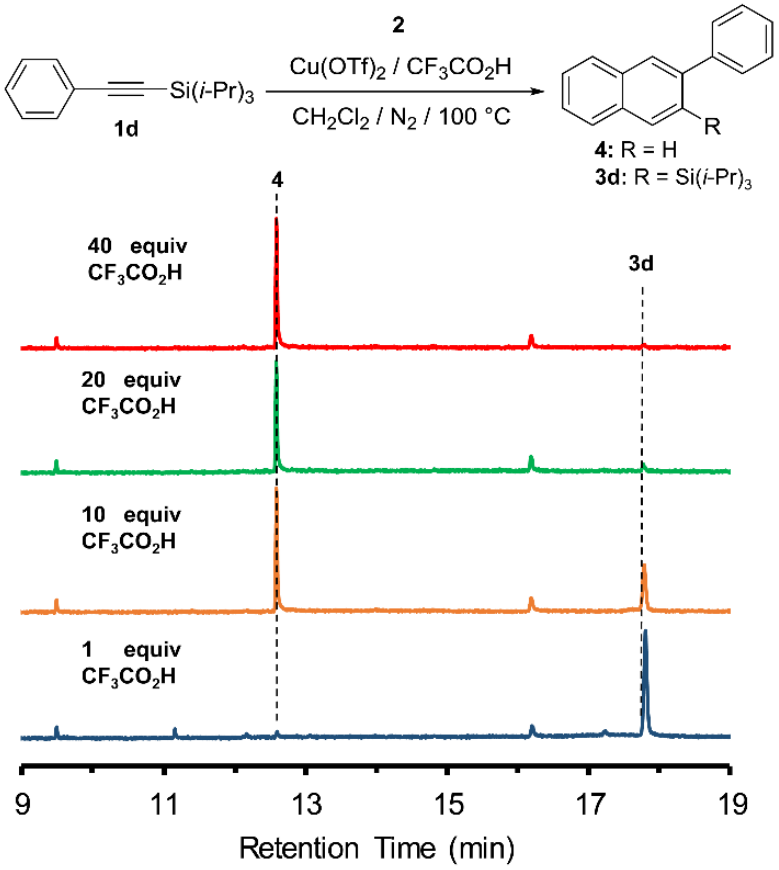

Figure 2.1. Partial GC/MS total ion count chromatograms of the crude reaction mixtures for the benzannulation of 1d in the presence of varying [CF3CO2H]. The TIPS group is retained in the presence of 1 equiv of CF3CO2H. Partial protodesilylation occurs with 10 equiv of CF3CO2H to provide 4, which is the dominant product with either 20 or 40 equiv of the acid are employed.

initial concentration of CF_3CO_2H (1 equiv per alkyne), provides nearly complete retention of the silyl eithers in naphthalene products **3b-e** (Table 2.1). After an aqueous workup and purification by flash chromatography, **3b-e** were isolated in good to excellent yields.

Substrates **1b** and **1c** provided only small amounts of protodesilylated product **4**, as observed by GC/MS, whose identity was confirmed by comparison to an independently prepared sample. No evidence for the formation of **4** was observed for larger substrates **1d** and **1e**. In contrast, the TMS group was unstable to even 1 equiv of CF_3CO_2H, and **4** was the only observed benzannulation product. Alternative benzannulation conditions[16] employ $ZnCl_2$ without added Brønsted acids, but are less active than the $Cu(OTf)_2$ / CF_3CO_2H conditions. **1a** was smoothly benzannulated in the presence of $ZnCl_2$ to provide **3a** in good isolated yield (75%), alongside trace protodesilylated side product **4**. Collectively, these experiments indicate that the Cu-catalyzed benzannulation reaction proceeds efficiently for silyl-protected alkynes and that silyl groups larger than TMS are stable to the modified reaction conditions. TMS groups are tolerated under alternative Zn-catalyzed conditions that do not employ stoichiometric CF_3CO_2H.

It will often be desirable to retain the silyl group to direct further functionalization at the 2-position of the naphthalene product (see below). However some synthetic routes will employ a silyl protecting group that should not be retained after benzannulation. Even the large TIPS group may be removed during the benzannulation reaction by using increased [CF_3CO_2H]. GC/MS analysis of crude

reaction mixtures of the benzannulation of **1d** that employed up to 20 equiv CF_3CO_2H provided mixtures of **3d** and **4** (Figure 2.1), whereas **4** was formed exclusively at higher [CF_3CO_2H] (40 equiv) without introducing additional side products. These experiments indicate that robust silyl protecting groups may be retained or removed *in situ* by adjusting the initial quantities of acid.

Table 2.2. Benzannulation of various TIPS-protected acetylenes.

alkyne	product	isolated yield (%)
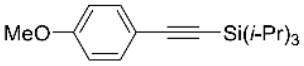 **5**	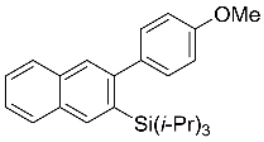 **6**	69%
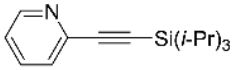 **7**	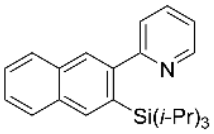 **8**	no conversion
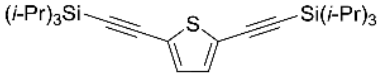 **9**	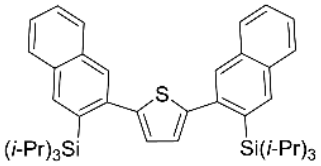 **10**	45%
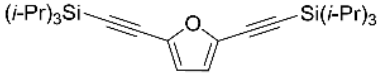 **11**	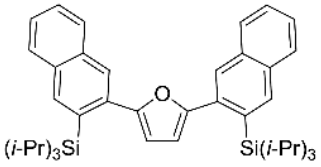 **12**	58%
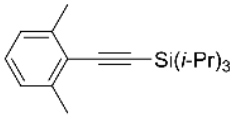 **13**	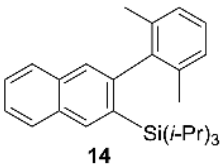 **14**	78%

Alkyne: (0.05 g) 2: (2 equiv), $Cu(OTf)_2$: (0.05 equiv), CF_3CO_2H: (1 equiv), 30 min, 100 °C

The substrate scope of the benzannulation reaction was expanded beyond phenylacetylene by evaluating a series of aromatic systems containing TIPS-protected acetylenes (Table 2.2). An alkyne with an electron-rich aromatic system, such as the methoxy substituted derivative **5**, is well tolerated. Electron-withdrawing aromatic systems, such as pyridine derivate **7**, which is likely to be protonated under the reaction conditions, are poor substrates. Common electron-rich heterocycles, such as thiophenes and furans are tolerated, as demonstrated by the acceptable isolated yields for the double benzannulation **9** and **11**, respectively. Naphthalene-substituted derivatives of thiophenes and furans are relatively unexplored, and naphthalene-substituted oligothiophenes were recently shown to form nanofibers on mica.[17] Finally, substrate **13**, which features an alkyne flanked by bulky 2,6-dimethylphenyl and TIPS substituents, is benzannulated in good yield, further highlighting the remarkable tolerance of this reaction to sterically crowded substrates.

The benzannulation of these model silyl-protected phenyl acetylene substrates provides naphthalene building blocks with variable silyl and aryl groups at the 2- and 3-positions, respectively. Although new C-C bonds may be formed at silyl sites directly under Hiyama cross-coupling conditions,[18] we explored converting the silyl group to a halide to take advantage of a full range of available transition metal-catalyzed C-C, C-N, C-O, and C-F bond-forming reactions. Silyl groups of each of the isolated naphthalenes **3b-d** underwent rapid and quantitative conversion to 2-iodo-3-phenylnaphthalene **15** upon treatment with ICl in CH_2Cl_2 (Table 2.3). The reaction proceeded to completion after only 5 min at rt, in contrast to previous reports that employed longer reaction times and elevated temperatures.[19] The DMPS naphthalene

3e is incompatible with this procedure, as desilylated product **4**, iodobenzene, and unidentified chlorinated products were observed by GC/MS instead of **15** (see Appendix Figure S2.43). These observations indicate that triethylsilyl (TES), TBS, and TIPS groups are readily converted to aryl iodide substrates, which readily undergo many C-C bond-forming reactions.

Table 2.3. The iodization/protodesilylation of each silyl naphthalane

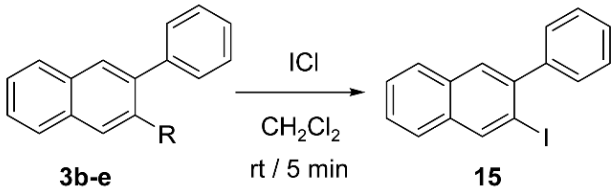

entry	3	R	isolated yield (%)
1	**3b**	$Si(Et)_3$	90
2	**3c**	$SitBu(Me)_2$	93
3	**3d**	$Si(iPr)_3$	92
4	**3e**	$SiPh(Me)_2$	none

1,2-diaryl linkages are quite sterically hindered, which made oligo-and poly(*o*-phenylenes) essentially unstudied prior to recent pioneering reports by Hartley[20] and Aida.[21] This substitution pattern also figures prominently in the bottom-up synthesis of graphene nanoribbons (GNRs) and other carbon nanostructures.[22] The outstanding efficiency and steric tolerance of the benzannulation reaction, combined with the synthetic versatility of halogenated naphthalenes derived from silyl acetylenes, suggests a new strategy to access highly crowded aromatic architectures. To explore this possibility, **15** was joined to 1,3,5-triethynyl benzene

Scheme 2.1 Synthesis of sterically crowded aromatic compound **17**

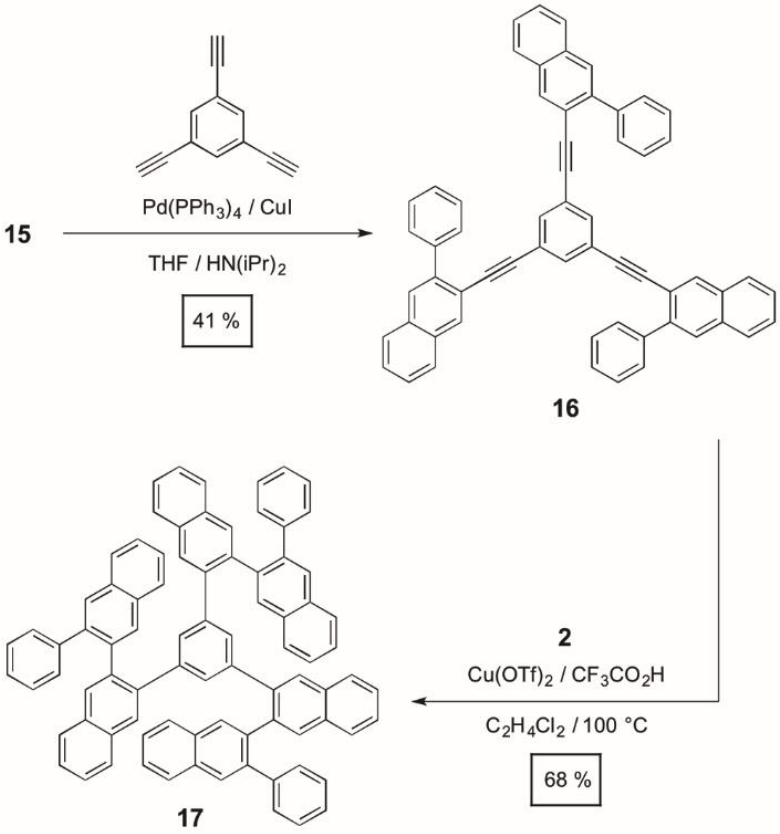

under Sonogashira cross-coupling conditions to provide the trialkyne **16**. Its internal alkynes remain accessible for another benzannulation reaction, providing oligo(arylene) **17,** in which each aromatic subunit is a part of at least one *o*-aryl linkage (Scheme 2.1). **17** was characterized using high resolution mass spectrometry, variable temperature 1D and 2D NMR spectroscopy, and UV/Vis and photoemission spectroscopies.

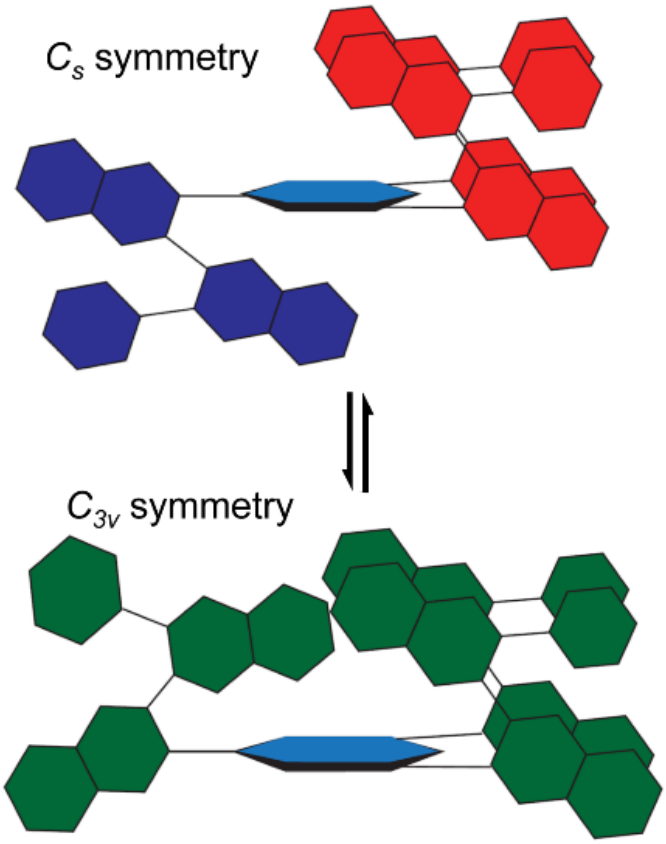

Figure 2.2. Schematic depiction of the major C_s symmetric conformer and minor C_{3v} conformer of compound 17. A more complete description of its conformational behavior is provided in the Appendix.

The ^{1}H and ^{13}C NMR spectra of **17** indicate that the *ortho*-aryl linkages of **17** restrict the C-C bond rotation around the central trisubstituted benzene ring, even at elevated temperature. At rt, its ^{1}H and ^{13}C NMR spectra exhibit 48 and 46 resonances, respectively, corresponding to a mixture of conformers undergoing slow exchange with respect to each measurement (See Supporting Information Figures S2.34-35). The major conformation exhibits C_S symmetry, in which one of the oligo(aryl) substituents on the central benzene ring is *anti* with respect to the other two (Figure 2.2). When rotation about the inner C-C bonds is slow on the NMR timescale, the hydrogens of the central benzene ring appear as two distinct singlets that integrate in a 2:1 ratio. A minor

conformation with C_{3v} symmetry, in which the three oligo(aryl) substituents are *syn*, is also observed. These hindered bond rotations that persist at elevated temperature demonstrate the extreme steric hindrance of **17** and highlight the ability of the benzannulation reaction to modify congested aromatic systems.

2.3 Conclusion

In conclusion, we have broadened the scope of the benzannulation reaction to silyl-protected phenylacetylenes. By varying the acid concentration, the silyl groups may either be removed or retained in the resulting phenylnaphthalene products. The reaction tolerates electron-donating substitutents and electron-rich heterocycles. When the silyl group is retained, it may be transformed to an iodide under mild conditions to enable further elaboration using various transition metal-catalyzed cross-coupling reactions. We demonstrate the utility of these transformations in the iterative synthesis of a highly congested aromatic system that exhibits restricted C-C bond rotations, even at elevated temperatures. These results, combined with the excellent regioselectivity of the benzannulation reaction, provide a powerful means to access sterically hindered aromatic architectures.

REFERENCES

(1) (a) Chang, Y. J.; Chow, T. J. *J. Mater. Chem.* **2011**, *21*, 9523. (b) Shin, R. Y. C.; Sonar, P.; Siew, P. S. Chen, Z. K. Sellinger, A. *J. Org. Chem.* **2009**, *74*, 3293–3298. (c) Liu, X.; Sun, Y.; Hsu, B. B. Y.; Lorbach, A.; Qi, L.; Heeger, A. J.; Bazan, G. C. *J. Am. Chem. Soc.* 2014, 5697–5708.; (d) Takimiya, K.; Osaka, I.; Mori, T.; Nakano, M. *Acc. Chem. Res.* **2014**, *47*, 1493–1502. (e) Schipper, D. J.; Moh, L. C. H.; Müller, P.; Swager, T. M. *Angew. Chem. Int. Ed.* **2014**, *126*, 5957–5961.

(2) (a) Xiao, S.; Kang, S. J.; Wu, Y.; Ahn, S.; Kim, J. B.; Loo, Y. L.; Siegrist, T.; Steigerwald, M. L.; Li, H.; Nuckolls, C. *Chem. Sci.* **2013**, *4*, 2018.; (b) Niimi, K.; Shinamura, S.; Osaka, I.; Miyazaki, E.; Takimiya, K. *J. Am. Chem. Soc.* **2011**, 8732–8739. (c) Jia, H. P.; Liu, S. X.; Sanguinet, L.; Levillain, E.; Decurtins, S. *J. Org. Chem.* **2009**, *74*, 5727–5729.

(3) (a) Vermeulen, N.; Karagiaridi, O.; Sarjeant, A. a; Stern, C. L.; Hupp, J. T.; Farha, O. K.; Stoddart, J. F. J. Am. Chem. Soc. **2013**, 135, 14916–14919.; (b) Modak, A.; Nandi, M.; Mondal, J.; Bhaumik, A. *Chem. Commun.*. **2012**, *48*, 248–250.; (b) Liu, J.; Yee, K.-K.; Lo, K. K. W.; Zhang, K. Y.; To, W. P.; Che, C.-M.; Xu, Z. *J. Am. Chem. Soc.* **2014**, *136*, 2818–2824. (c) Zhang, P.; Weng, Z.; Guo, J.; Wang, C. *Chem. Mater.* **2011**, *23*, 5243–5249.

(4) (a) Jones, T. V; Blatchly, R.; Tew, G. N. *Org. Lett.* **2003**, *5*, 3297–3299.; (b) Jones, T. V.; Slutsky, M. M.; Tew, G. N. *New J. Chem.* **2008**, *32*, 676.

(5) (a) Golling, F. E.; Quernheim, M.; Wagner, M.; Nishiuchi, T.; Müllen, K. *Angew. Chem. Int. Ed.* **2014**, *53*, 1525–1528.; (b) Zhang, Q.; Peng, H.; Zhang, G.; Lu,

Q.; Chang, J.; Dong, Y.; Shi, X.; Wei, J. *J. Am. Chem. Soc.* **2014**, *136*, 5057–5064.; (c) Dou, X.; Yang, X.; Bodwell, G. J.; Wagner, M.; Enkelmann, V.; Mu, K. *Org. Lett.* **2007**, *9*, 2485–2488. (d) Feng, X.; Wu, J.; Ai, M.; Pisula, W.; Zhi, L.; Rabe, J. P.; Müllen, K. *Angew. Chem. Int. Ed.* **2007**, *46*, 3033–3036.

(6) Jones, T. V; Slutsky, M. M.; Laos, R.; de Greef, T. F.; Tew, G. N. *J. Am. Chem. Soc.* **2005**, *127*, 17235–17240.

(7) Khan, A.; Hecht, S. *J. Polym. Sci. Polym. Chem.* **2006**, *44*, 1619–1627.

(8) Fuentes, N.; Martin-Lasanta, A.; Alvarez de Cienfuegos, L.; Robles, R.; Choquesillo-Lazarte, D.; García-Ruiz, J. M.; Martínez-Fernández, L.; Corral, I.; Ribagorda, M.; Mota, A. J.; Cárdenas, D. J.; Carreño, M. C.; Cuerva, J. M. *Angew. Chem. Int. Ed.* **2012**, *51*, 13036–13040.

(9) Poly(o-phenyelenes) had also been reported through oxidative polymerizations, but these materials were subsequently shown to contain a significant percentage of defects. See: (a) Kovacic, P.; Uchic, J. T.; Hsu, L.-C. *J. Polym. Sci. Part A-1 Polym. Chem.* **1967**, *5*, 945–964. (b) Kovacic, P.; Ramsey, J. *Polym. Sci. Polym. Chem* **1969**, *7*, 111–125. (c) Hsing, C.; Jones, M.; Kovacic, P. *J. Polym. Sci. Polym. Chem.* **1981**, *19*, 973–984.)

(10) Asao, N.; Nogami, T.; Lee, S.; Yamamoto, Y. *J. Am. Chem. Soc.* **2003**, *125*, 10921–10925.

(11) Arslan, H.; Saathoff, J. D.; Bunck, D. N.; Clancy, P.; Dichtel, W. R. *Angew. Chem. Int. Ed.* **2012**, *51*, 12051–12054.

(12) Arslan, H.; Uribe-Romo, F. J.; Smith, B. J.; Dichtel, W. R. *Chem. Sci.* **2013**, *4*, 3973.

(13) He, Z.; Xu, X.; Zheng, X.; Ming, T.; Miao, Q. *Chem. Sci.* **2013**, *4*, 4525.

(14) Arslan, H.; Walker, K. L.; Dichtel, W. R. *Org. Lett.* **2014**, *16*, 5926–5929.

(15) Isogai, Y.; Nawaz Khan, F.; Asao, N. *Tetrahedron* **2009**, *65*, 9575–9582.

(16) Fang, X. L.; Tang, R. Y.; Zhang, X. G.; Zhong, P.; Deng, C. L.; Li, J. H. *J. Organomet. Chem.* **2011**, *696*, 352–356.

(17) (a) Monguchi, Y.; Yanase, T.; Mori, S.; Sajiki, H. *Synthesis.* **2012**, *45*, 40–44. (b) Cheng, K.; Wang, C.; Ding, Y.; Song, Q.; Qi, C.; Zhang, X. M. *J. Org. Chem.* **2011**, *76*, 9261–9268.

(18) Mita, T.; Michigami, K.; Sato, Y. *Org. Lett.* **2012**, *14*, 3462–3465.

(19) (a) Hartley, C. S. *J. Org. Chem.* **2011**, *76*, 9188–9191. (b) He, J.; Mathew, S. M.; Cornett, S. D.; Grundy, S. C.; Hartley, C. S. *Org. Biomol. Chem.* **2012**, *10*, 3398–3405.

(20) (a) Ohta, E.; Sato, H.; Ando, S.; Kosaka, A.; Fukushima, T.; Hashizume, D.; Yamasaki, M.; Hasegawa, K.; Muraoka, A.; Ushiyama, H.; Yamashita, K.; Aida, T. *Nat. Chem.* **2011**, *3*, 68–73. (b) Ando, S.; Ohta, E.; Kosaka, A.; Hashizume, D.; Koshino, H.; Fukushima, T.; Aida, T. *J. Am. Chem. Soc.* **2012**, 11084–11087.

(21) (a) Narita, A.; Feng, X.; Hernandez, Y.; Jensen, S.; Bonn, M.; Yang, H.; Verzhbitskiy, I.; Casiraghi, C.; Hansen, M. R.; Koch, A. H. R.; Fytas, G.; Ivasenko, O.; Li, B.; Mali, K. S.; Balandina, T.; Mahesh, S.; De Feyter, S.; Müllen, K. *Nat. Chem.* **2014**, *6*, 126–132. (b) Schwab, M. G.; Narita, A.; Hernandez, Y.; Balandina, T.; Mali, K. S.; De Feyter, S.; Feng, X.; Müllen, K. *J. Am. Chem. Soc.* **2012**, *134*, 18169–18172.

CHAPTER 2 – APPENDIX

Table of Contents

A. **Materials.** All reagents were purchased from commercial sources and used without further purification. THF was purchased from commercial sources and purified using a custom-built alumina-based solvent purification system. HN(*i*Pr)$_2$ was purchased from commercial sources and purified by distillation. Other solvents were purchased from commercial sources and used without further purification. All reactions were monitored by TLC glass plates (silica gel 60 F_{254}) purchased from Merk Millipore and all flash chromatography was carried out using Silicycle silica gel (230-400 mesh).

Instrumentation. Infrared spectra were recorded on a Thermo Nicolet iS10 with a diamond ATR attachment and are uncorrected. UV/Vis absorbance spectra were recorded on a Cary 5000 UV-Vis-NIR spectrophotometer with an Hg lamp.

Photoemission spectra were recorded on a Horiba Jobin Yvon Fluorolog-3 fluorescence spectrophotometer equipped with a 450 W Xe lamp, double excitation and double emission monochromators, a digital photon-counting photomultiplier and a secondary InGaAs detector for the NIR range. Correction for variations in lamp intensity over time and wavelength was achieved with a solid-state silicon photodiode as the reference. The spectra were further corrected for variations in photomultiplier response over wavelength and for the path difference between the sample and the reference by multiplication with emission correction curves generated on the instrument.

Gas chromatography/electron impact mass spectrometry was performed on an Agilent 6890N Network GC System with a JEOL JMS-GCmate II Mass Spectrometer (magnetic sector). DART MS was performed on an Exactive Plus Orbitrap Mass Spectrometer with a DART SVP ion source from Ion Sense.

NMR spectra were recorded on a Varian 400 spectrometer with an ASW probe with a 20 MHz sample spin rate and on a Varian 500 spectrometer with a DBG probe. 2D NMR were recorded on a Varian 500 MHz spectrometer using a standard DBG probe. All spectra, unless otherwise stated, were recorded at ambient temperature.

B. Synthetic Procedures

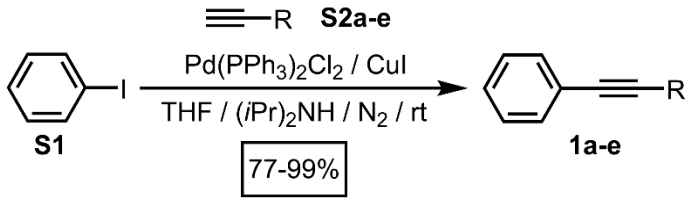

General procedure for the synthesis of 1a-1b: $Pd(PPh_3)_2Cl_2$ (0.0498 equiv) and CuI (0.115 equiv) were transferred to a round bottom flask and placed under a N_2 atmosphere. In a separate flask, a 1:1 THF/(iPr)$_2$NH mixture (25 mL) was sparged with N_2 for 30 min, after which it was transferred into a round bottom flask. In a separate flask, iodobenzene (1 equiv) and silyl acetylene (1.2 equiv) were dissolved in anhydrous THF (12 mL), degassed using three freeze-pump-thaw cycles, and finally added to the reaction mixture. The reaction mixture was stirred at rt for 3h, during which the reaction progress was monitored by TLC. After completion, the reaction mixture was washed with aqueous HCl (50 mL, 2 M) and extracted with CH_2Cl_2 (3 x 15 mL). The combined organic fractions were dried ($MgSO_4$), filtered, and the solvent was evaporated to provide each crude product. Products **1a**-**1e** were purified using column chromatography (SiO_2, hexanes) as colorless oils.

1a: **S1** (0.499 g, 2.44 mmol) was reacted with (trimethyl)silylacetylene **S2a** (0.38 mL, 2.7 mmol) following the general procedure outlined above. **1a** was isolated as a colorless oil (0.382 g, 89% Yield). Its ^{1}H and ^{13}C NMR spectra matched previously reported data.[1]

1b: S1 (0.306 g, 1.50 mmol) was reacted with (triethyl)silylacetylene **S2b** (0.256 g, 1.84 mmol) following the general procedure outlined above. **1b** was isolated as a colorless oil (0.244 g, 77% Yield). Its ^{1}H and ^{13}C NMR spectra matched previously reported data.[2]

1c: **S1** (0.304 g, 1.50 mmol) was reacted with (*tert*-butyldimethyl)silylacetylene **S2c** (0.258 g, 1.84 mmol) following the general procedure outlined above. **1c** was isolated as a colorless oil (0.321 g, 99% Yield). Its ^{1}H and ^{13}C NMR spectra matched previously reported data.[3]

1d: **S1** (2.991 g, 14.66 mmol) was reacted with (triisopropyl)silylacetylene **S2d** (3.258 g, 17.86 mmol) following the general procedure outlined above. **1d** was isolated as a colorless oil (3.736 g, 90% Yield). Its ^{1}H and ^{13}C NMR spectra matched previously reported data.[4]

1e: **S1** (0.494 g, 2.42 mmol) was reacted with (dimethylphenyl)silylacetylene **S2e** (0.52 mL, 2.9 mmol) following the general procedure outlined above. **1e** was isolated as a colorless oil (0.560 g, 97% Yield). Its ^{1}H and ^{13}C NMR spectra matched previously reported data.[5]

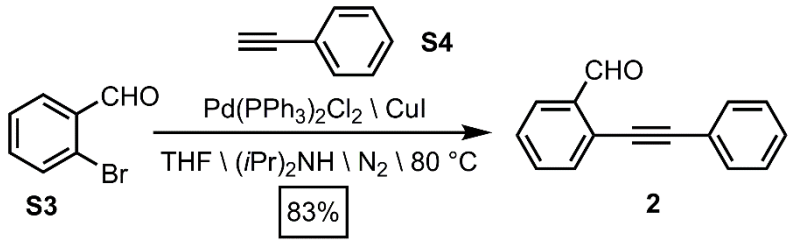

Synthesis of 2: $Pd(PPh_3)_2Cl_2$ (0.195 g, 0.270 mmol) and CuI (0.107 g, 0.541 mmol) were transferred to a round bottom flask and placed under a N_2 atmosphere. In a separate flask, anhydrous THF (250 mL) and $(i\text{Pr})_2\text{NH}$ (140 mL) were combined and sparged

with N_2 for 30 min. The THF/(iPr)$_2$NH mixture was transferred to the reaction flask under positive N_2 pressure using a cannula. In a separate flask, 2-bromobenzaldehyde (5.005 g, 27.03 mmol) and phenylacetylene (3.575 g, 32.43 mmol) were dissolved in anhydrous THF (20 mL), degassed through three freeze-pump-thaw cycles, and finally added to the reaction mixture. The reaction mixture was stirred for 3 h at 80 °C, after which it was washed with aqueous HCl (600 mL, 2 M) and extracted with CH_2Cl_2 (3 x 100 mL). The organic fractions were collected, dried with $MgSO_4$, and filtered. The solvent was removed under vacuum and the mixture was purified using column chromotography (SiO_2, 4:96 EtOAc : hexanes) to provide **2** (4.673 g, 83% Yield) as an orange oil. Its ^{1}H and ^{13}C NMR spectra matched a previous report.[6]

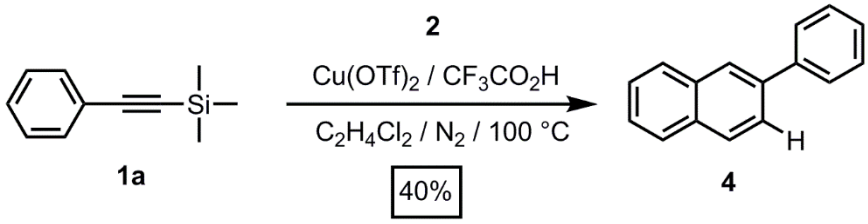

Synthesis of 4 under Cu-catalyzed benzannulation conditions: Cu(OTf)$_2$ (0.013 g, 0.036 mmol) was transferred to a round bottom flask and purged with N_2. In a separate vial, **1a** (0.106 g, 0.607 mmol) and **2** (0.420 g, 2.04 mmol) were dissolved in $C_2H_4Cl_2$ (5.7 mL). This solution was added transferred to the reaction flask and placed in a 100 °C oil bath. CF_3CO_2H (0.044 mL, 1 equiv) was added using a micro syringe and the solution was refluxed for 30 min. The crude reaction mixture was washed with saturated aqueous $NaHCO_3$ (5 mL) and extracted with CH_2Cl_2 (3 x 15 mL). The organic fractions were collected, dried ($MgSO_4$), and filtered to give a red solution. The solvent was removed and the product was purified using column chromatography (SiO_2, hexanes)

to yield a white powder (0.064 g, 40%). Its ^{1}H and ^{13}C NMR spectra matched a previous report.[7]

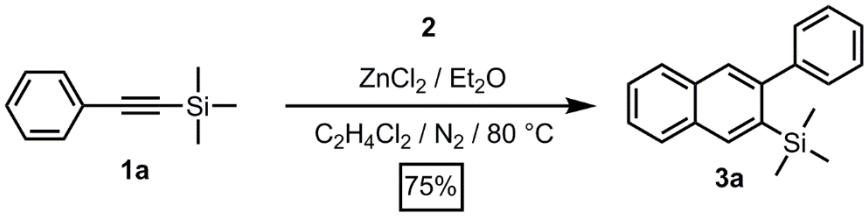

Synthesis of 3a under Zn-catalyzed conditions: 1a (0.052 g, 0.030 mmol) and **2** (0.233 g, 1.14 mmol) were dissolved in $C_2H_4Cl_2$ (3 mL) and placed in an oil bath heated to 80 °C. A solution of $ZnCl_2$ dissolved in Et_2O (1.0 M, 0.055 mL) was added to the reaction mixture, which was stirred at reflux for 1 h. The crude reaction mixture was washed with saturated aqueous $NaHCO_3$ (5.0 mL) and extracted with CH_2Cl_2 (3 x 15 mL). The organic fractions were collected, dried ($MgSO_4$), and filtered to give a red solution. The solvent was removed and the product was purified with column chromatography (SiO_2, hexanes) to yield a white powder (0.068 g, 75%). **3a:** ^{1}H NMR (500 MHz, $CDCl_3$): δ 8.05 (s, 1H), 7.89-7.79 (m, 3H), 7.77-7.72 (m, 3H), 7.53-7.47 (m, 4H), 7.39 (t, J = 7.8 Hz, 9H). ^{13}C NMR (125 MHz, $CDCl_3$) δ 145.88, 144.48, 137.40, 135.63, 133.27, 132.09, 131.86, 129.77, 128.02, 127.81, 127.65, 127.24, 126.93, 125.99, 0.83. IR (solid, ATR) 3052, 2951, 2158, 1739, 1576, 1485, 1442, 1309, 1246, 1136, 1074, 1017, 969, 951, 883, 833, 756, 745, 701, 688, 642 $cm^{-1.}$ HRMS (DART) calcd for $[C_{19}H_{20}Si]^{+}$ 276.1328, found 276.1325.

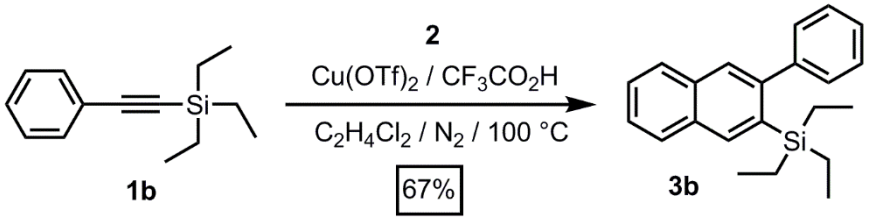

Synthesis of 3b: $Cu(OTf)_2$ (0.008 g, 0.02 mmol) was transferred to a round bottom flask and purged with N_2. In a separate vial, **1b** (0.101 g, 0.467 mmol) and **2** (0.190 g, 0.922 mmol) were dissolved in $C_2H_4Cl_2$ (4.5 mL). This solution was transferred to the reaction flask and placed in a 100 °C oil bath. CF_3CO_2H (0.035 mL, 1 equiv) was then added to the solution. The solution was refluxed and stirred for 30 min. The crude reaction mixture was washed with saturated aqueous $NaHCO_3$ (5 mL) and extracted with CH_2Cl_2 (3 x 15 mL). The organic fractions were collected, dried ($MgSO_4$), and filtered to give a red solution. The solvent was removed and the product was purified with column chromatography (SiO_2, hexanes) to yield **3b** as a colorless oil that slowly solidified (0.099 g, 67%). **3b:** ^{1}H NMR (400 MHz, $CDCl_3$): δ 8.05 (s, 1H), 7.89-7.79 (m, 2H), 7.67 (s, 1H), 7.53-7.47 (m, 2H), 7.42-7.34 (m, 5H), 0.84 (t, J = 7.8 Hz, 9H), 0.54 (q, J = 7.8 Hz, 6H). ^{13}C NMR (100 MHz, $CDCl_3$) δ 146.25, 144.55, 136.99, 133.90, 133.20, 131.81, 129.50, 128.04, 127.98, 127.73, 127.64, 127.27, 126.86, 125.88, 7.69, 4.36. IR (solid, ATR) 3052, 2950, 2871, 1578, 1484, 1442, 1416, 1376, 1279, 1308, 1237, 1136, 1072, 1001, 968, 951, 916, 888, 793, 761, 745, 721, 700 cm^{-1}. HRMS (EI) calcd for [$C_{22}H_{26}Si^+$] 318.1804, found 318.1802.

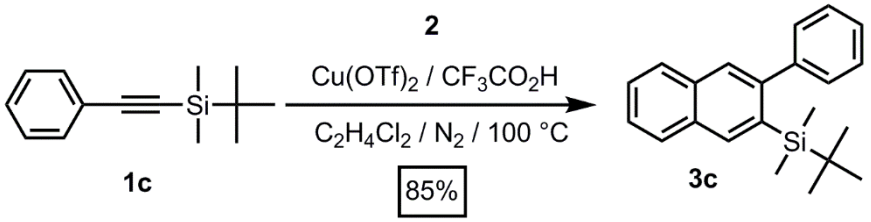

Synthesis of 3c: $Cu(OTf)_2$ (0.008 g, 0.02 mmol) was transferred to a round bottom flask and purged with N_2. In a separate vial, **1c** (0.111 g, 0.511 mmol) and **2** (0.190 g, 0.922 mmol) were dissolved in $C_2H_4Cl_2$ (4.6 mL). This solution was transferred to the reaction flask and placed in a 100 °C oil bath. CF_3CO_2H (0.035 mL, 1 equiv) was then added to the solution. The solution was refluxed and stirred for 30 min. The crude reaction mixture was washed with saturated aqueous $NaHCO_3$ (5 mL) and extracted with CH_2Cl_2 (3 x 15 mL). The organic fractions were collected, dried ($MgSO_4$), and filtered to give a red solution. The solvent was removed and the product was purified with column chromatography (SiO_2, hexanes) to yield **3c** as a colorless oil that slowly solidified (0.140 g, 85%) **3c:** ^{1}H NMR (500 MHz, $CDCl_3$): δ 8.11 (s, 1H), 7.89-7.87 (m, 1H) 7.79-7.77 (m, 1H), 7.63 (s, 1H), 7.52-7.48 (s, 2H), 7.38-7.34 (m, 5H), 0.84 (s, 9H), -0.04 (s, 6H). ^{13}C NMR (125 MHz, $CDCl_3$): δ 137.16, 130.15, 129.38, 129.01, 128.59, 128.30, 128.04, 127.80, 127.65, 127.55, 127.39, 127.06, 126.92, 125.92, 27.49, -3.08. IR (solid, ATR) 2953, 2925, 2881, 2853, 1484, 1470, 1461, 1442, 1404, 1388, 1359, 1306, 1250, 1136, 1073, 1007, 967, 951, 881, 819, 808, 795, 795, 759, 768, 744, 700, 673 cm^{-1}. HRMS (EI) calcd for [$C_{22}H_{26}Si^+$] 318.1804, found 318.1813.

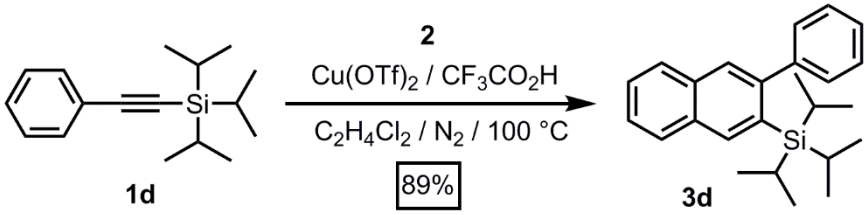

Synthesis of 3d: $Cu(OTf)_2$ (0.1694 g, 0.468 mmol) was transferred to a round bottom flask and purged with N_2. In a separate vial, **1d** (2.006 g, 9.269 mmol) and **2** (3.881 g, 18.82 mmol) were dissolved in $C_2H_4Cl_2$ (92 mL). This solution was transferred to the reaction flask and placed in a 100 °C oil bath. CF_3CO_2H (0.70 mL, 1 equiv) was then added to the solution, which was refluxed for 30 min. The crude reaction mixture was washed with saturated aqueous $NaHCO_3$ (30 mL) and extracted with CH_2Cl_2 (3 x 50 mL). The organic fractions were collected, dried ($MgSO_4$), and filtered to give a red solution. The solvent was removed and the product was purified with column chromatography (SiO_2, hexanes) to yield **3d** as a clear oil that slowly solidified (2.510 g, 89%). **3d:** ^{1}H NMR (500 MHz, $CDCl_3$): δ 8.05 (s, 1H), 7.89-7.79 (m, 2H), 7.67 (s, 1H), 7.53-7.47 (m, 2H), 7.42-7.34 (m, 5H), 0.84 (t, J = 7.8 Hz, 9H), 0.54 (q, J = 7.8 Hz, 6H) ^{13}C NMR (125 MHz, $CDCl_3$) δ 146.40, 144.95, 137.70, 132.81, 131.54, 129.85, 129.01, 128.07, 127.50, 127.32, 127.20, 126.85, 125.83, 19.51, 12.74 ppm. IR (solid, ATR) 2944, 2920, 2863, 2886, 1625, 1596, 1576, 1483, 1462, 1382, 1365, 1280, 1254, 1195, 1135, 1069, 1017, 999, 965, 950, 917, 880, 761, 744, 702, 669 cm^{-1}. HRMS (EI) calcd for [$C_{25}H_{32}Si^+$] 360.2273, found 360.2281.

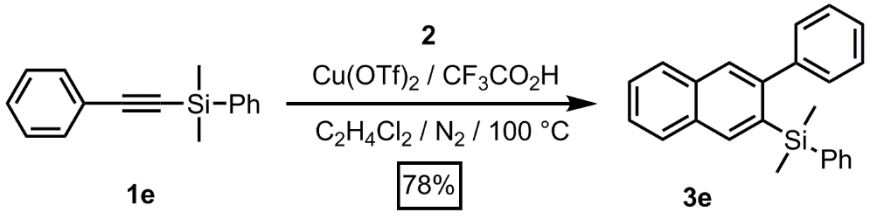

Synthesis of 3e: $Cu(OTf)_2$ (0.009 g, 0.03 mmol) was transferred to a round bottom flask under an atmosphere of N_2. In a separate vial, **1e** (0.107 g, 0.251 mmol) and **2** (0.174 g, 0.846 mmol) were dissolved in $C_2H_4Cl_2$ (4.2 mL). This solution was transferred to the reaction flask and placed in a 100 °C oil bath. CF_3CO_2H (0.048 mL, 1 equiv) was added to the solution. The solution was refluxed for 30 min. The crude reaction mixture was washed with saturated aqueous $NaHCO_3$ (10 mL) and extracted with CH_2Cl_2 (3 x 5 mL). The organic fractions were collected, dried ($MgSO_4$), and filtered to give a red solution. The solvent was removed and the product was purified using column chromatography (SiO_2, hexanes) to yield a white solid (0.111 g, 78%). **3e:** ^{1}H NMR (500 MHz, $CDCl_3$) δ 8.18 (s, 1H), 7.90 (d, 1H), 7.84 (d, 1H), 7.71 (s, 1H), 7.54 (m, 2H), 7.42 (d, 2H), 7.39-7.29 (m, 4H), 7.28 (d, 1H), 7.25 (d, 1H), 7.15 (d, 2H), 0.30 (s, 6H): ^{13}C NMR (125 MHz, $CDCl_3$) δ 146.04, 143.97, 140.02, 136.91, 135.29, 134.11, 133.55, 131.78, 129.80, 128.84, 128.16, 128.06, 127.78, 127.69, 127.67, 127.13, 127.11, 126.04, -0.94 ppm. IR (solid, ATR) 3049, 2950, 1582, 1485, 1494, 1448, 1426, 1406, 1245, 1135, 1110, 1074, 1027, 997, 969, 952, 923, 895, 882, 830, 808, 793, 771, 748, 699, 659 cm^{-1}. HRMS (DART) calcd for $[C_{24}H_{22}Si+H]^+$ 339.15635, found 339.15559.

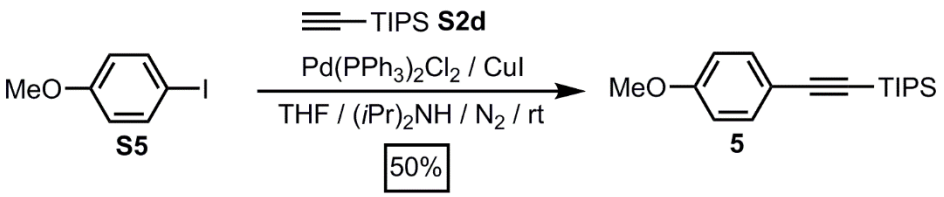

Synthesis of 5: S5 (0.250 g, 1.07 mmol) was reacted with **S2d** (0.30 mL, 1.3 mmol) following the general procedure outlined above for products **1a-e**. **5** was isolated as a colorless oil (0.154 g, 50% Yield). Its ^{1}H and ^{13}C NMR spectra matched previously reported data.[8]

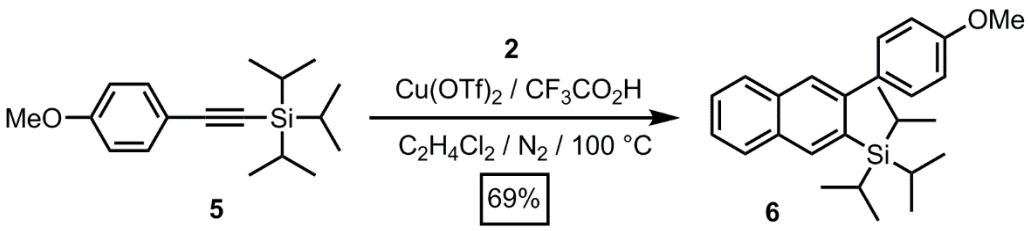

Synthesis of 6: $Cu(OTf)_2$ (0.004 g, 0.01 mmol) was transferred to a round bottom flask under an atmosphere of N_2. In a separate vial, **5** (0.050 g, 0.18 mmol) and **2** (0.071 g, 0.35 mmol) were dissolved in $C_2H_4Cl_2$ (1.7 mL). This solution was transferred to the reaction flask and placed in a 100 °C oil bath. CF_3CO_2H (0.013 mL, 1 equiv) was added to the solution. The solution was refluxed for 30 min. The crude reaction mixture was washed with saturated aqueous $NaHCO_3$ (5 mL) and extracted with CH_2Cl_2 (3 x 5 mL). The organic fractions were collected, dried ($MgSO_4$), and filtered to give a red solution. The solvent was removed and product **6** was purified using column chromatography (SiO_2, hexanes) to yield clear oil. (0.0472g, 69%) **6:** ^{1}H NMR (500 MHz, $CDCl_3$): δ 8.11 (s, 1H), 7.85 (m, 1H), 7.75 (m, 1H), 7.61 (s, 1H), 7.47 (m, 2H), 7.28 (d, 2H), 6.88 (d, 2H), 3.86 (s, 3H), 1.03 (d, 18H). ^{13}C NMR (125 MHz, $CDCl_3$) δ 158.93, 146.05, 137.66, 137.53, 133.19, 132.88, 131.49, 130.87, 129.32, 128.04, 127.45, 126.78, 125.73, 112.70, 55.48, 19.54, 12.79. IR (solid, ATR) 2944, 2863, 1609, 1513, 1483,

1462, 1437, 1283, 1242, 1173, 1068, 1035, 1017, 907, 881, 832, 786, 746, 732, 707, 672, 660 cm^{-1}. HRMS (DART) calcd for $[C_{26}H_{35}OSi + H]^+$ 391.2452, found 391.2450.

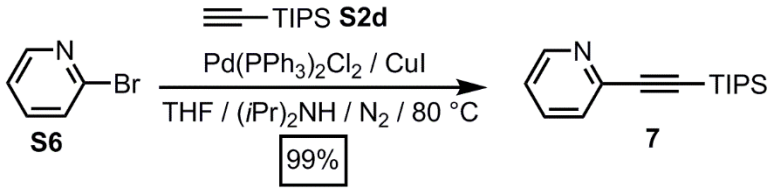

Synthesis of 7: $Pd(PPh_3)_2Cl_2$ (0.054 g, 0.079 mmol) and CuI (0.033 g, 0.16 mmol) were transferred to a round bottom flask and placed under a N_2 atmosphere. In a separate flask, a 1:1 THF/(iPr)$_2$NH mixture (25 mL) was sparged with N_2 for 30 min, after which it was transferred into a round bottom flask. In a separate flask, **S6** (0.248 g, 1.58 mmol) and **S2d** (0.5, 2.2 mmol) were dissolved in anhydrous THF (12 mL), degassed using three freeze-pump-thaw cycles, and finally added to the reaction mixture. The reaction mixture was stirred at 80 °C for 12h. After completion, the reaction mixture was washed with aqueous HCl (10 mL, 2 M) and extracted with CH_2Cl_2 (3 x 5 mL). The combined organic fractions were dried ($MgSO_4$), filtered, and the solvent was evaporated to provide each crude product. **7** was purified by column chromatography (1:1 EtOAc : hexanes) on deactivated silica (1:99 triethylamine : hexanes) as a yellow oil (0.401 g, 99% Yield). Its ^1H and ^{13}C NMR spectra matched previously reported data.[9]

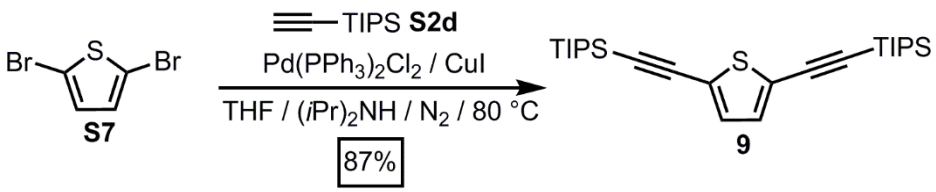

Synthesis of 9: $Pd(PPh_3)_2Cl_2$ (0.034 g, 0.048 mmol) and CuI (0.024 g, 0.10 mmol) were transferred to a round bottom flask and placed under a N_2 atmosphere. In a separate flask, a 1:1 THF/(iPr)$_2$NH mixture (25 mL) was sparged with N_2 for 30 min, after which it was transferred into a round bottom flask. In a separate flask, **S7** (0.254 g, 1.04 mmol) and **S2d** (0.55 mL g, 2.4 mmol) were dissolved in anhydrous THF (12 mL), degassed using three freeze-pump-thaw cycles, and finally added to the reaction mixture. The reaction mixture was stirred at 80 °C for 12h. After completion, the reaction mixture was washed with aqueous HCl (10 mL, 2 M) and extracted with CH_2Cl_2 (3 x 5 mL). The combined organic fractions were dried ($MgSO_4$), filtered, and the solvent was evaporated to provide each crude product. **9** was purified using column chromatography (SiO_2, hexanes) as a colorless oil (0.4023 g, 87%) **9:** ^{1}H NMR (500 MHz, $CDCl_3$): δ 7.03 (s, 2H), 1.11 (s, 21H).^{13}C NMR (125 MHz, $CDCl_3$) δ 131.99, 124.78, 98.95, 96.75, 18.77, 11.43. IR (solid, ATR) 2941, 2890, 2864, 2143, 1738, 1461, 1382, 1365, 1233, 1170, 1071, 1016, 995, 918, 881, 802, 757, 731, 675 cm^{-1}. HRMS (DART) calcd for $[C_{26}H_{44}Si_2S + H]^+$ 445.2775, found 445.2777.

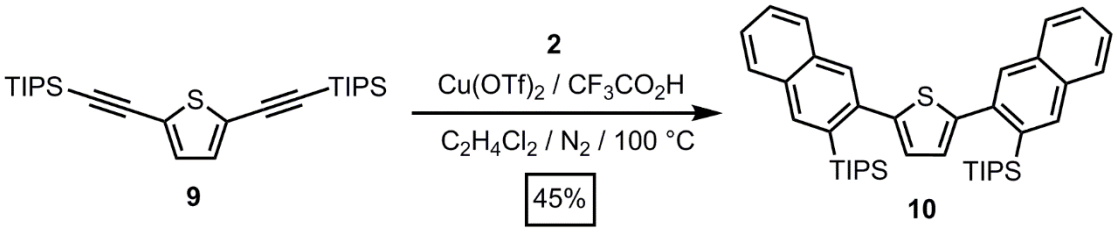

Synthesis of 10: $Cu(OTf)_2$ (0.002 g, 0.006 mmol) was transferred to a round bottom flask under an atmosphere of N_2. In a separate vial, **9** (0.051 g, 0.11 mmol) and **2** (0.095 g, 0.46 mmol) were dissolved in $C_2H_4Cl_2$ (1.1 mL). This solution was transferred to the

reaction flask and placed in a 100 °C oil bath. CF_3CO_2H (0.018 mL, 2 equiv) was added to the solution. The solution was refluxed for 30 min. The crude reaction mixture was washed with saturated aqueous $NaHCO_3$ (10 mL) and extracted with CH_2Cl_2 (3 x 5 mL). The organic fractions were collected, dried ($MgSO_4$), and filtered to give a red solution. The solvent was removed and the product was purified using column chromatography (SiO_2, hexanes) to yield a clear oil that slowly solidified to a white solid (0.0326 g, 45%). **10:** ^{1}H NMR (500 MHz, $CDCl_3$): 8.15 (s, 2H), 7.88 (m, 2H), 7.83 (s, 2H), 7.82 (m, 4H), 7.51 (s, 4H), 6.97 (s, 2H), 1.16 (s, 36H). δ ^{13}C NMR (125 MHz, $CDCl_3$) δ 145.57, 137.94, 137.68, 134.04, 132.68, 132.00, 131.88, 128.07, 127.67, 127.01, 126.89, 126.37, 19.76, 13.31. IR (solid, ATR) 2944, 2861, 1738, 1463, 1365, 1228,1216, 1017, 907, 881, 863, 812, 745, 709, 668, 649 cm^{-1}. HRMS (DART) calcd for $[C_{42}H_{56}Si_2S + H]^+$ 649.3714, found 649.3712.

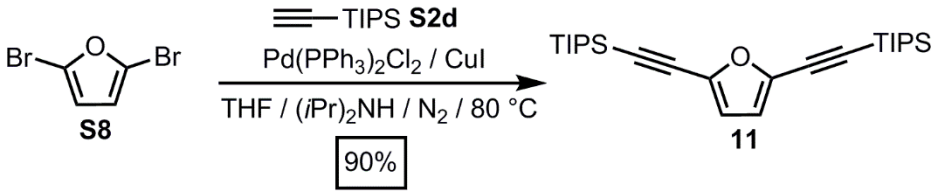

Synthesis of 11: $Pd(PPh_3)_2Cl_2$ (0.039 g, 0.055 mmol) and CuI (0.020 g, 0.10 mmol) were transferred to a round bottom flask and placed under a N_2 atmosphere. In a separate flask, a 1:1 THF/(iPr)$_2$NH mixture (25 mL) was sparged with N_2 for 30 min, after which it was transferred into a round bottom flask. In a separate flask, **S8** (0.254 g, 1.1 mmol) and **S2d** (0.55 mL g, 2.4 mmol) were dissolved in anhydrous THF (12 mL), degassed using three freeze-pump-thaw cycles, and finally added to the reaction mixture. The reaction mixture was stirred at 80 °C for 12h. After completion, the reaction mixture

was washed with aqueous HCl (10 mL, 2 M) and extracted with CH_2Cl_2 (3 x 5 mL). The combined organic fractions were dried ($MgSO_4$), filtered, and the solvent was evaporated to provide each crude product. **11** was purified using column chromatography (SiO_2, hexanes) as a colorless oil (0.425 g, 90%). **11:** ^{1}H NMR (500 MHz, $CDCl_3$): δ 6.54 (s, 2H), 1.12 (s, 21H). ^{13}C NMR (125 MHz, $CDCl_3$) δ 137.50, 116.59, 97.14, 95.86, 18.74, 11.37. IR (solid, ATR) 2942, 2891, 2865, 2151, 1738, 1567, 1498, 1462, 1382, 1366, 1217, 1195, 1071, 1017, 995, 968, 918, 881, 740, 675 cm^{-1}. HRMS (DART) calcd for $[C_{25}H_{44}OSi_2 + H]^+$, 429.3003 found 429.3002.

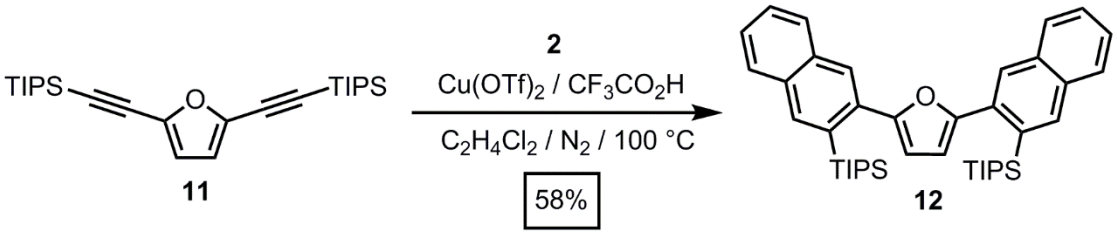

Synthesis of 12: $Cu(OTf)_2$ (0.004 g, 0.01 mmol) was transferred to a round bottom flask under an atmosphere of N_2. In a separate vial, **11** (0.051 g, x mmol) and **2** (0.098 g, 0.47 mmol) were dissolved in $C_2H_4Cl_2$ (4.2 mL). This solution was transferred to the reaction flask and placed in a 100 °C oil bath. CF_3CO_2H (0.018 mL, 2 equiv) was added to the solution. The solution was refluxed for 30 min. The crude reaction mixture was washed with saturated aqueous NaHCO3 (10 mL) and extracted with CH_2Cl_2 (3 x 5 mL). The organic fractions were collected, dried ($MgSO_4$), and filtered to give a red solution. The solvent was removed and product **14** was purified using column chromatography (SiO_2, hexanes) to yield a clear oil that slowly solidified to a white solid (0.0432 g, 58%). **14:** ^{1}H NMR (400 MHz, $CDCl_3$): δ 8.11, 7.89, 7.84, 7.53, 6.48, 1.05. ^{13}C NMR (100 MHz,

$CDCl_3$) δ 155.44, 137.66, 134.09, 132.83, 132.38, 130.68, 128.12, 127.78, 126.86, 126.50, 110.17, 110.03, 19.46, 12.55. IR (solid, ATR) 2944, 2888, 2864, 1739, 1484, 1463, 1382, 1365, 1280, 1225, 1191, 1075, 1017, 994, 951, 882, 862, 797, 633 cm^{-1}. HRMS (DART) calcd for $[C_{42}H_{56}OSi_2 + H]^+$ 633.3943, found 633.3937.

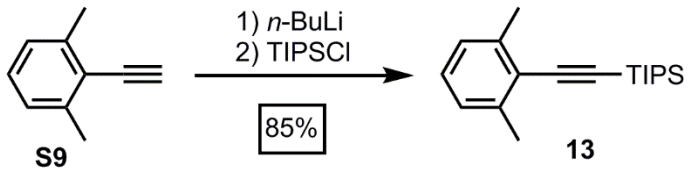

Synthesis of 13: A solution of **S9** (0.255g, 1.95 mmol) in anhydrous THF (10 mL) was transferred to a flame-dried flask under an N_2 environment. The reaction flask was cooled in a -78°C bath before adding *n*-BuLi (2.6 mL, 1.6 M in toluene) drop-wise over 10 min and allowed to stir for 1h at -78°C. The reaction mixture was quenched with TIPSCl (1.0 mL, 4.2 mmol) and the mixture was stirred for 30 min as it warmed to rt. The reaction mixture was washed with 2 M HCl (15 mL) and extracted with $CHCl_3$ (3x 5 mL). The organic layers were collected and dried ($MgSO_4$) and the solvent was removed under vacuum. **13** was purified using column chromatography (SiO_2, hexanes) as a colorless oil (0.469 g, 85%). **13:** ^{1}H NMR (500 MHz, $CDCl_3$): δ 7.10 (dd, 1H), 7.03 (d, 2H), 2.46 (s, 6H), 1.14 (s, 21H).^{13}C NMR (125 MHz, $CDCl_3$) δ 140.85, 127.80, 126.72, 123.57, 104.49, 99.34, 21.44, 18.87, 11.50. IR (solid, ATR) 2941, 2891, 2864, 2148, 1738, 1463, 1378, 1365, 1229, 1208, 1089, 1016, 995, 881, 838, 767, 733, 710, 675, 659 $cm^{-1.}$ HRMS (DART) calcd for $[C_{19}H_{30}Si + H]^+$ 287.2189, found 287.2188.

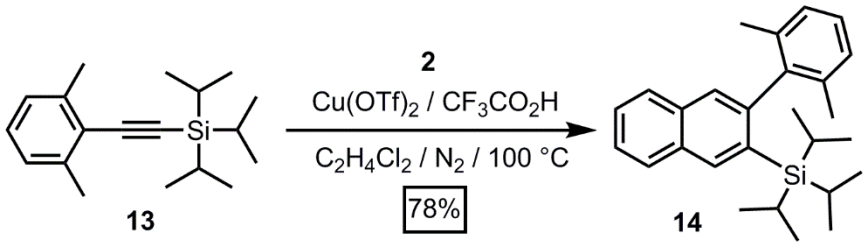

Synthesis of 14: $Cu(OTf)_2$ (0.005 g, 0.01 mmol) was transferred to a round bottom flask under an atmosphere of N2. In a separate vial, **13** (0.050 g, 0.18 mmol) and **2** (0.073 g, 0.35 mmol) were dissolved in $C_2H_4Cl_2$ (1.7 mL). This solution was transferred to the reaction flask and placed in a 100 °C oil bath. CF_3CO_2H (0.013 mL, 1 equiv) was added to the solution. The solution was refluxed for 30 min. The crude reaction mixture was washed with saturated aqueous $NaHCO_3$ (5 mL) and extracted with CH_2Cl_2 (3 x 5 mL). The organic fractions were collected, dried ($MgSO_4$), and filtered to give a red solution. The solvent was removed and product **14** was purified using column chromatography (SiO_2, hexanes) to yield a clear oil (0.053g, 78%). **14:** ^{1}H NMR (500 MHz, $CDCl_3$): δ 8.17 (s, 1H), 7.87 (m, 1H), 7.76 (m, 1H), 7.48 (m, 3H), 7.17 (t, 3H), 7.06 (d, 2H), 2.00 (s, 6H), 0.97 (d, 18H). ^{13}C NMR (125 MHz, $CDCl_3$) δ 144.75, 143.94, 137.88, 136.61, 135.05, 133.49, 131.20, 128.54, 128.11, 127.42, 127.30, 127.21, 126.55, 125.66, 21.64, 19.50, 12.91. IR (solid, ATR) 2942, 2864, 1738, 1463, 1377, 1217, 1061, 1016, 1000, 963, 951, 907, 885, 767, 745, 733, 707, 669, 646, 630 cm^{-1}. HRMS (DART) calcd for $[C_{27}H_{36}Si - i\text{Pr}]^+$ 345.2033, found 345.2032.

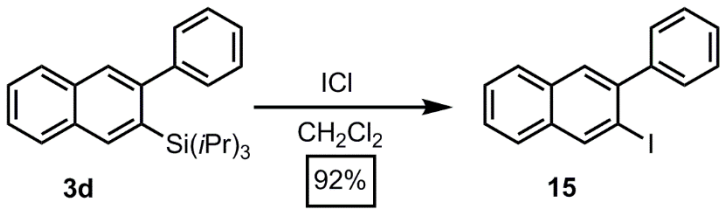

Preparative-scale synthesis of 15 from 3d: 3d (2.005 g, 5.546 mmol) and ICl (0.904 g, 5.546 mmol) were dissolved in separate CH_2Cl_2 solutions (40 mL and 10 mL respectively), which were combined. The resulting reaction mixture was stirred for 5 min, after which the solution was washed with saturated $Na_2S_2O_3$ (30 mL) and extracted with CH_2Cl_2 (3 x 15 mL). The organic fractions were combined, dried ($MgSO_4$), and filtered to provide a light yellow solution. The solvent was removed, and **15** was purified using column chromatography (SiO_2, hexanes) to provide a pale yellow oil that slowly solidified (1.694 g, 92%). **15:** ^{1}H NMR (500 MHz, $CDCl_3$): δ 8.51 (s, 1H), 7.78 (m, 3H), 7.53-7.44 (m, 7H). ^{13}C NMR (125 MHz, $CDCl_3$) δ 144.14, 143.34, 138.86, 134.04, 132.88, 129.77, 128.54, 128.01, 127.96, 127.82, 127.00, 126.85, 126.59, 96.77. IR (solid, ATR) 3051, 2920, 2849, 2204, 1949, 1578, 1486, 1443, 1417, 1319, 1270, 1219, 1191, 1131, 1072, 1054, 1025, 945, 915, 881, 867, 788, 758, 743, 969 cm^{-1}. HRMS (EI) calcd for [$C_{16}H_{11}I^+$] 329.9906, found 329.9896.

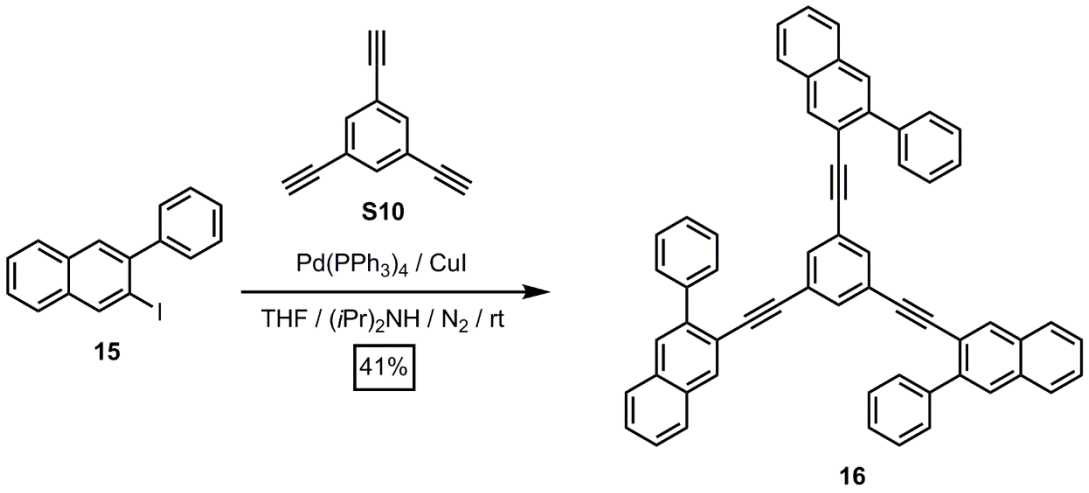

Synthesis of 16: S10 (0.100 g, 0.668 mmol), **15** (0.667 g, 2.020 mmol) and CuI (0.020 g, 0.11 mmol)) were dissolved in a mixture of THF (7 mL) and (iPr)$_2$NH (3 mL), which

was degassed using three freeze-pump-thaw cycles. $Pd(PPh_3)_4$ (0.040 g, 0.035 mmol) was quickly added to the surface of the still-frozen reaction mixture, and the flask was purged with three alternating N_2 and vacuum cycles and placed under a N_2 atmosphere. The reaction mixture was warmed to rt, stirred for 16 h, and finally quenched using aqueous HCl (2 M, 5 mL) and extracted with CH_2Cl_2 (3 x 15 mL). The organic fractions were collected, dried ($MgSO_4$), and filtered to give an orange solution. The solvent was removed, and the crude product was purified using column chromatography (SiO_2, 30:70, CH_2Cl_2 : hexanes) to provide 1**6** as a yellow solid (0.208 g, 41% yield). **16:** ^{1}H NMR (500 MHz, $CDCl_3$): δ 8.51 (s, 1H), 7.78 (m, 3H), 7.53-7.44 (m, 7H). ^{13}C NMR (125 MHz, $CDCl_3$) δ 140.73, 140.50, 133.62, 133.38, 133.33, 132.20, 129.72, 128.55, 128.14, 128.07, 127.76, 127.61, 127.40, 126.78, 124.14, 119.73, 91.24, 90.82. IR (solid, ATR) 3052, 2924, 2209, 1948, 1575, 1488, 1459, 1438, 1410, 1377, 1272, 1250, 1208, 1147, 1136, 1074, 1031, 1017, 1003, 949, 917, 886, 844, 794, 766, 743, 696, 677 cm^{-1}. HRMS (DART) calcd for [$C_{60}H_{37}^+$] 757.2890, found 757.2910.

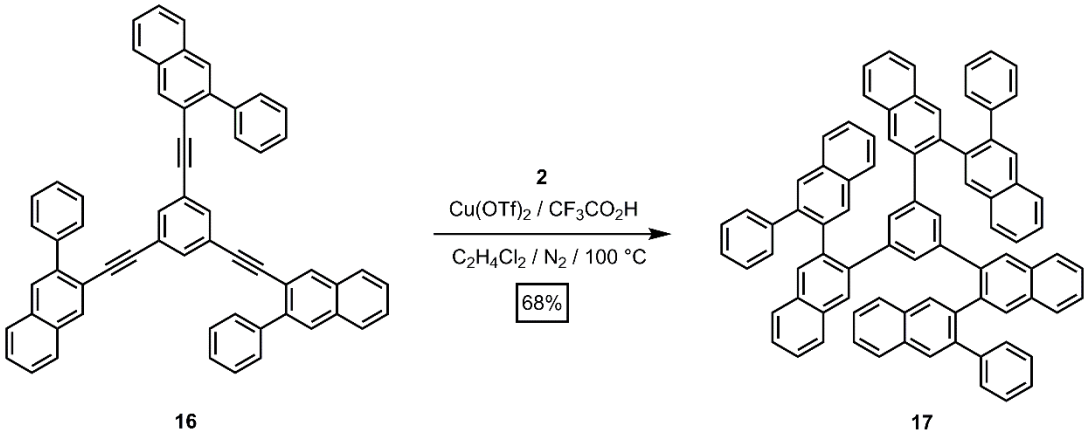

16 17

Synthesis of 17: 16 (0.101 g, 0.132 mmol) and $Cu(OTf)_2$ (0.006 g, 0.01 mmol) were added to a round-bottom flask under a N_2 atmosphere. In a separate vial, **2** (0.155 g, 0.753 mmol) was dissolved in $C_2H_4Cl_2$ (1.3 mL) and transferred to the reaction flask. CF_3CO_2H (0.030 mL, 3 equiv) was added to the reaction mixture, which was refluxed at 100 °C for 1 h. The reaction mixture was washed with saturated $NaHCO_3$ (15 mL) and extracted with $C_2H_4Cl_2$ (3 x 5 mL). The organic fractions were collected, dried ($MgSO_4$), and filtered to give a dark red solution. The solvent was removed, and the product was purified by column chromatography (SiO_2, 30:70 CH_2Cl_2 : hexane) to yield **17** as a pale yellow powder (0.096 g, 68% yield). **17:** ^{1}H NMR (500 MHz, $CDCl_3$): δ 8.15 (d, 2H), 8.13 (s, 1H,), 7.98 (s, 1H), 7.95 (s, 2H), 7.92 (d,2H), 7.88 (d, 1H), 7.87 (d, 1H), 7.84 (d, 1H), 7.80 (s, 1H), 7.69 (t, 2H), 7.64 (d, 2H), 7.57 (t, 2H), 7.56 (s, 2H), 7.54 (s, 2H), 7.54 (d, 2H), 7.45 (t, 1H), 7.44 (t, 2H), 7.40 (t, 2H), 7.39 (t, 1H), 7.38 (t, 1H), 7.34 (t, 1H), 6.88 (t, 4H), 6.88 (t, 2H), 6.80 (s, 2H), 6.77 (d, 4H), 6.70 (d, 1H), 6.50 (t, 1H), 6.39 (d, 2H), 6.24 (t, 2H), 6.22 (s, 1H), 6.11 (s, 2H), 6.04 (s, 1H). ^{13}C NMR (125 MHz, $CDCl_3$) δ 141.47, 141.10, 140.85, 140.42, 140.32, 140.20, 140.10, 139.60, 139.45, 139.37, 139.16, 139.03, 138.72, 138.28, 138.07, 133.28, 133.04, 132.96, 132.90, 132.64, 132.37, 131.60, 131.41, 131.19, 131.17, 130.72, 130.48, 130.28, 129.87, 129.85, 129.57, 129.30, 129.16, 129.11, 128.35, 128.21, 128.08, 128.04, 127.86, 127.72, 127.47, 126.85, 126.65, 126.50, 126.32, 126.25, 126.17, 126.08, 125.98, 125.84. IR (solid, ATR) 3051, 2925, 2131, 1947, 1590, 1488, 1444, 1415, 1318, 1274, 1180, 1133, 1074, 1018, 950, 882, 870, 809, 771, 743, 720, 697 cm^{-1}. HRMS (DART) calcd for [$C_{84}H_{56}^+$] 1064.4376, found 1064.4348.

C. 1D NMR Spectroscopy

Figure S2.1. ^{1}H NMR of **3a** (500 MHz, $CDCl_3$, 298 K)

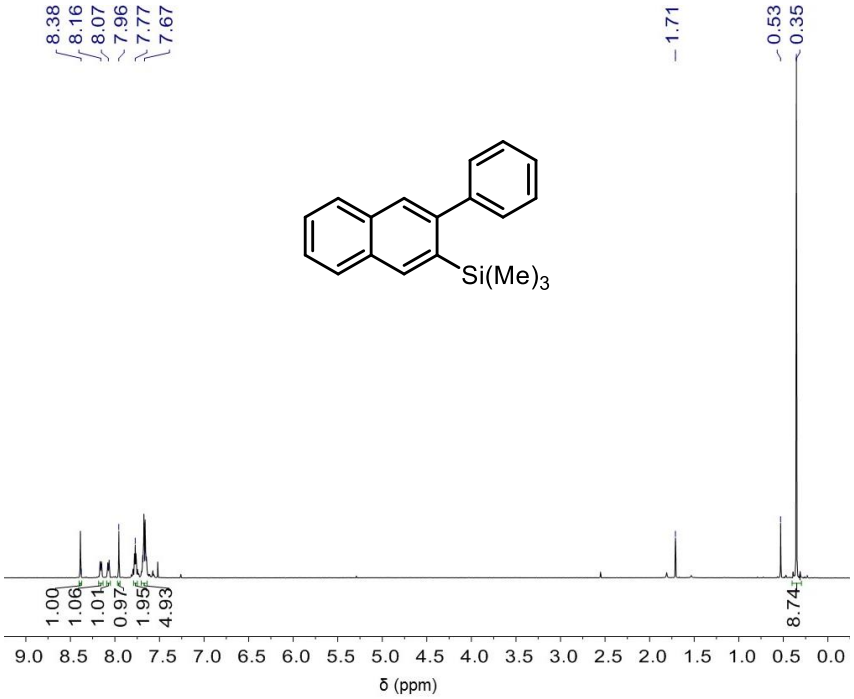

Figure S2.2. ^{13}C NMR of **3a** (125 MHz, $CDCl_3$, 298 K)

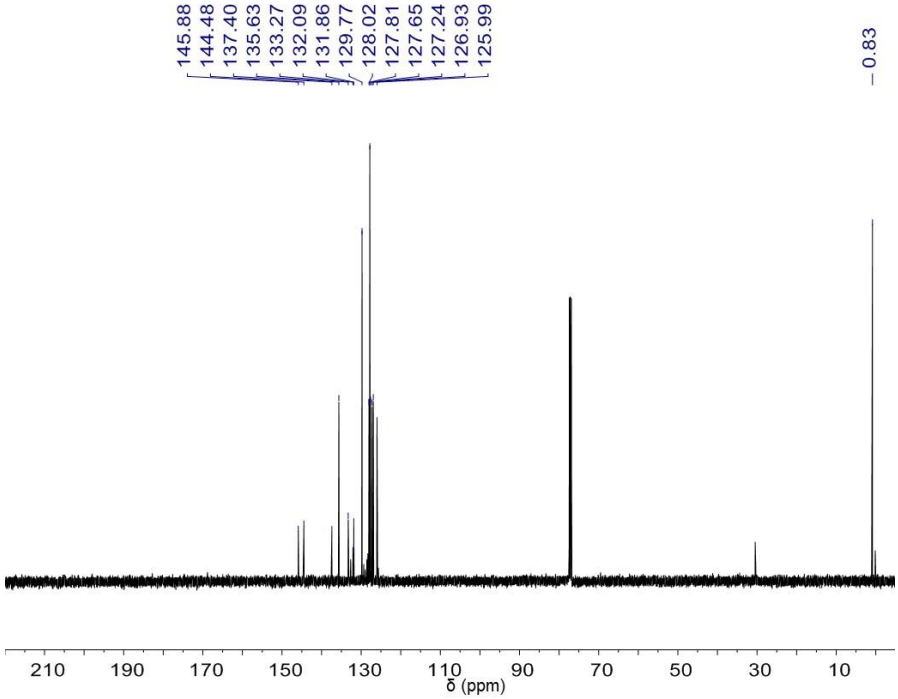

Figure S2.3. ^{1}H NMR of **3b** (400 MHz, $CDCl_3$, 298 K)

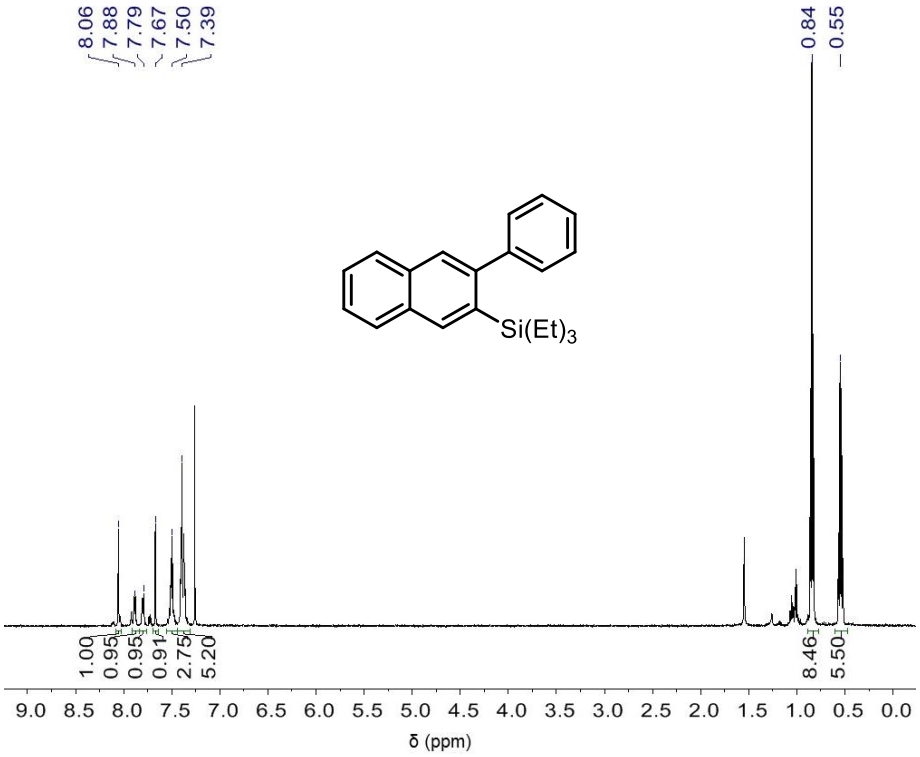

Figure S2.4. ^{13}C NMR of **3b** (100 MHz, $CDCl_3$, 298 K)

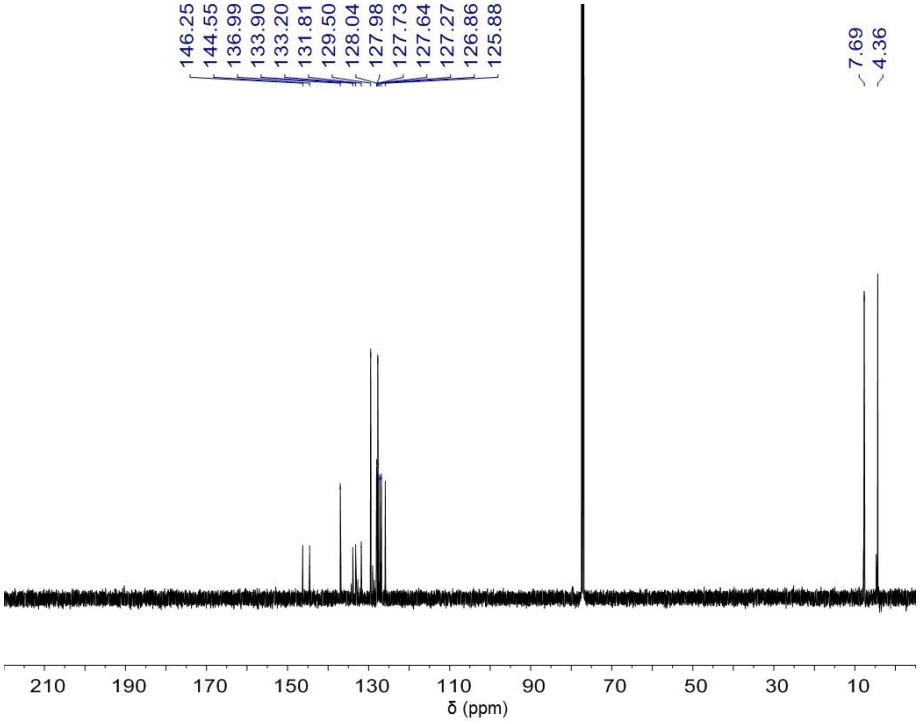

Figure S2.5. ^{1}H NMR of **3c** (500 MHz, $CDCl_3$, 298 K)

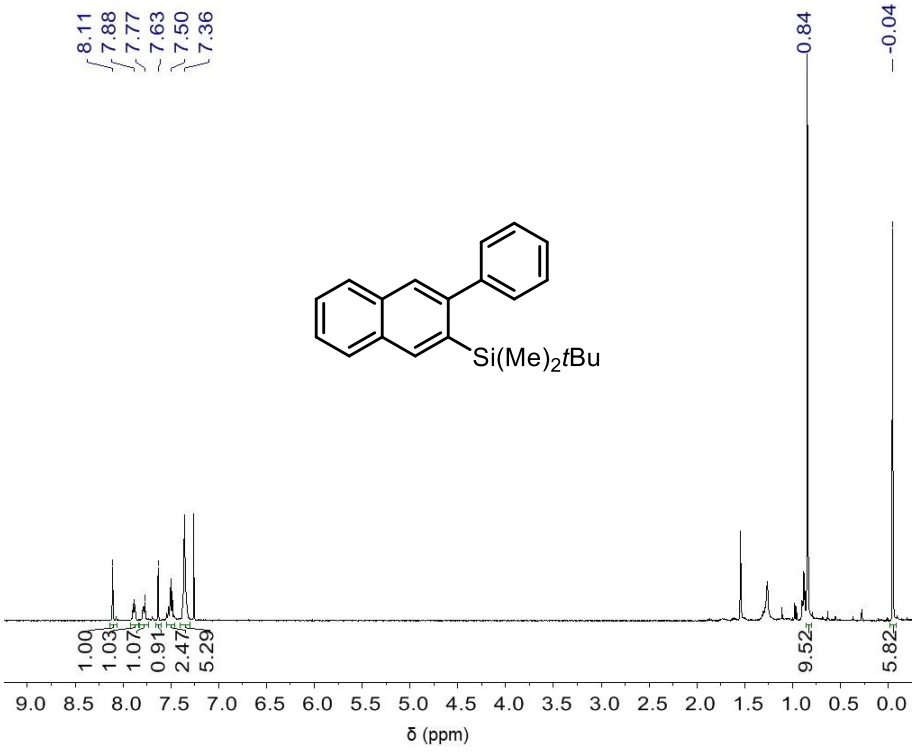

Figure S2.6. ^{13}C NMR of **3c** (125 MHz, $CDCl_3$, 298 K)

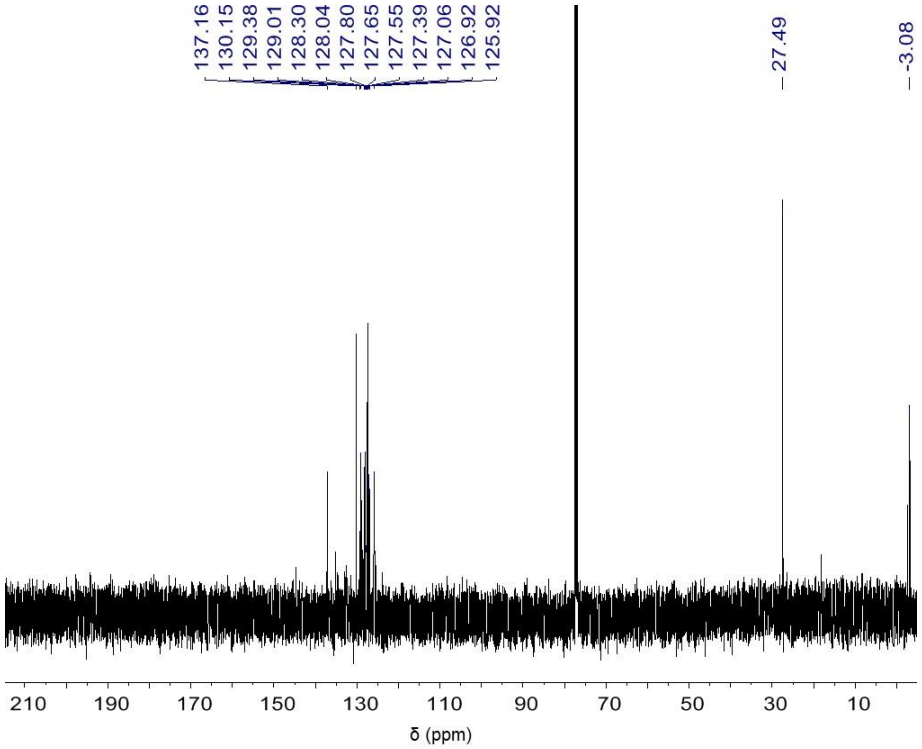

Figure S2.7. ^{1}H NMR of **3d** (500 MHz, $CDCl_3$, 298 K)

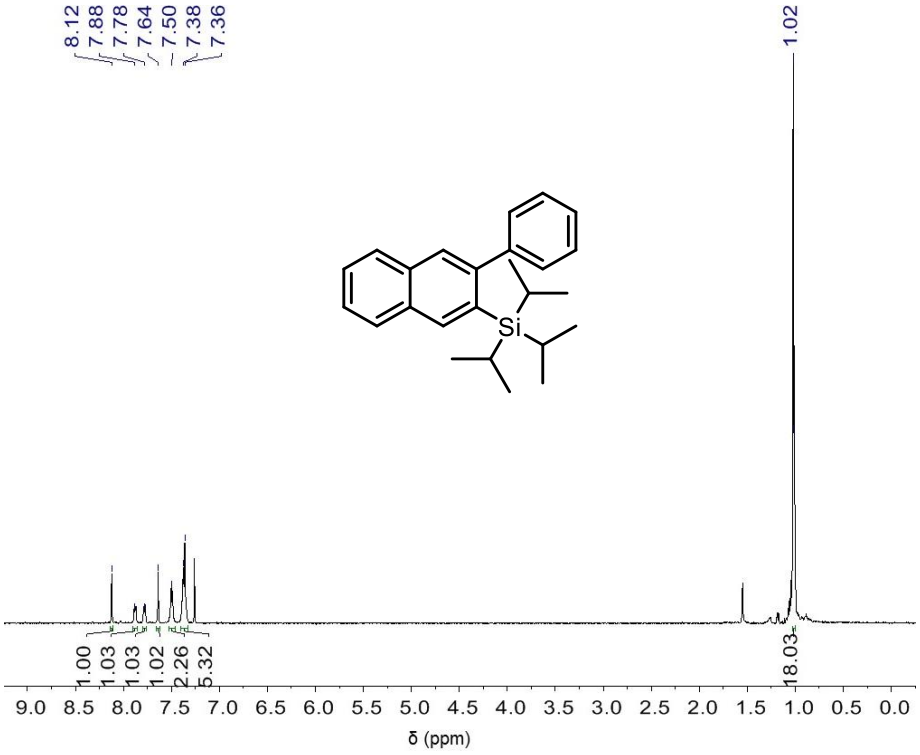

Figure S2.8. ^{13}C NMR of **3d** (125 MHz, $CDCl_3$, 298 K)

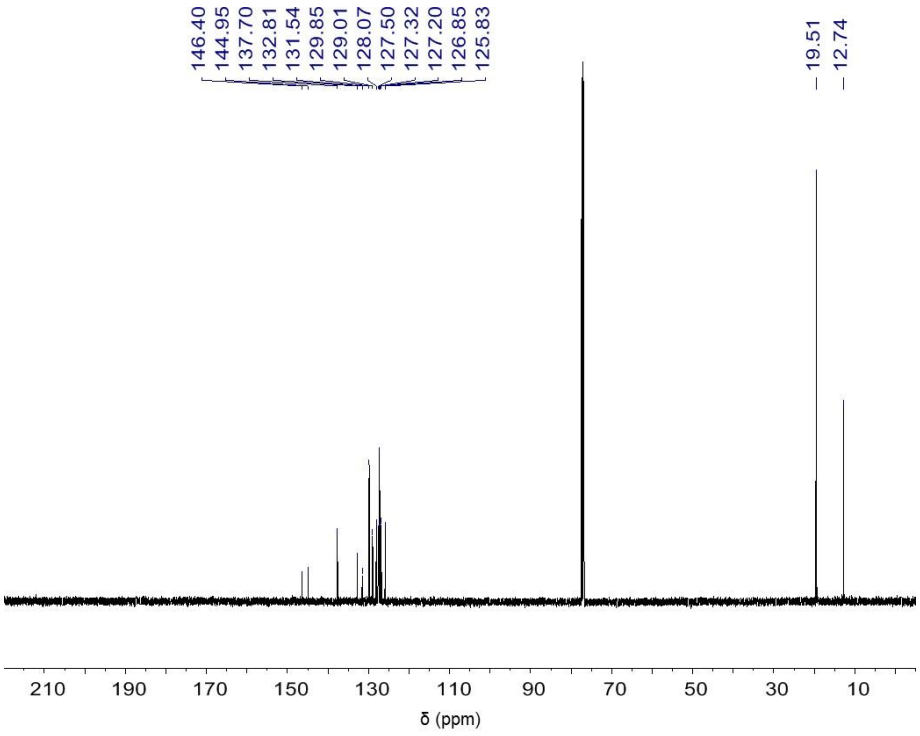

Figure S2.9. ^{1}H NMR of **3e** (500 MHz, $CDCl_3$, 298 K)

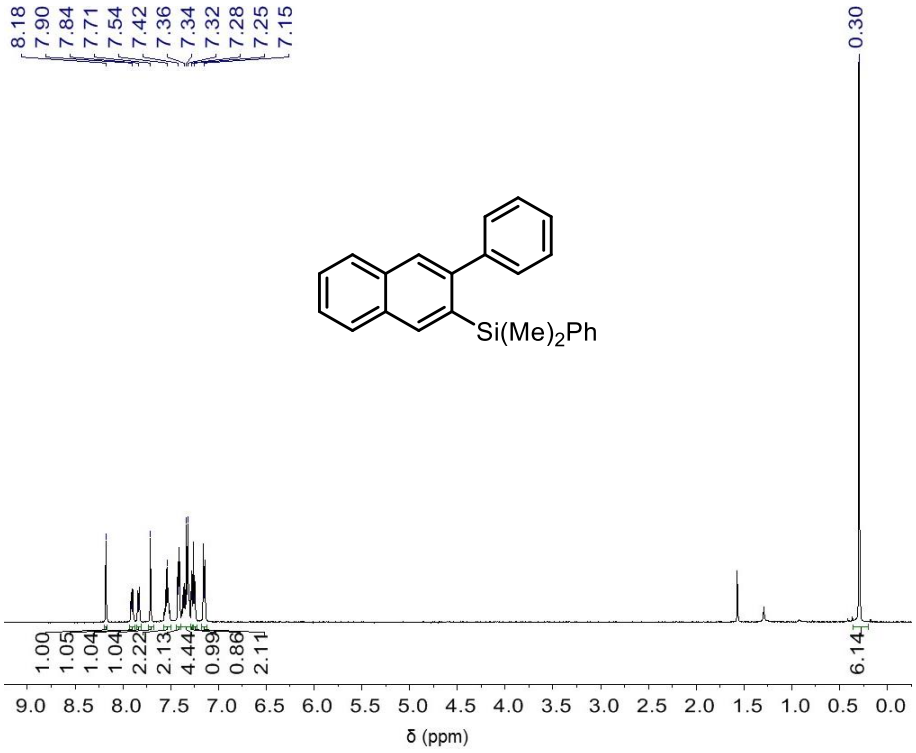

Figure S2.10. ^{13}C NMR of **3e** (125 MHz, $CDCl_3$, 298 K)

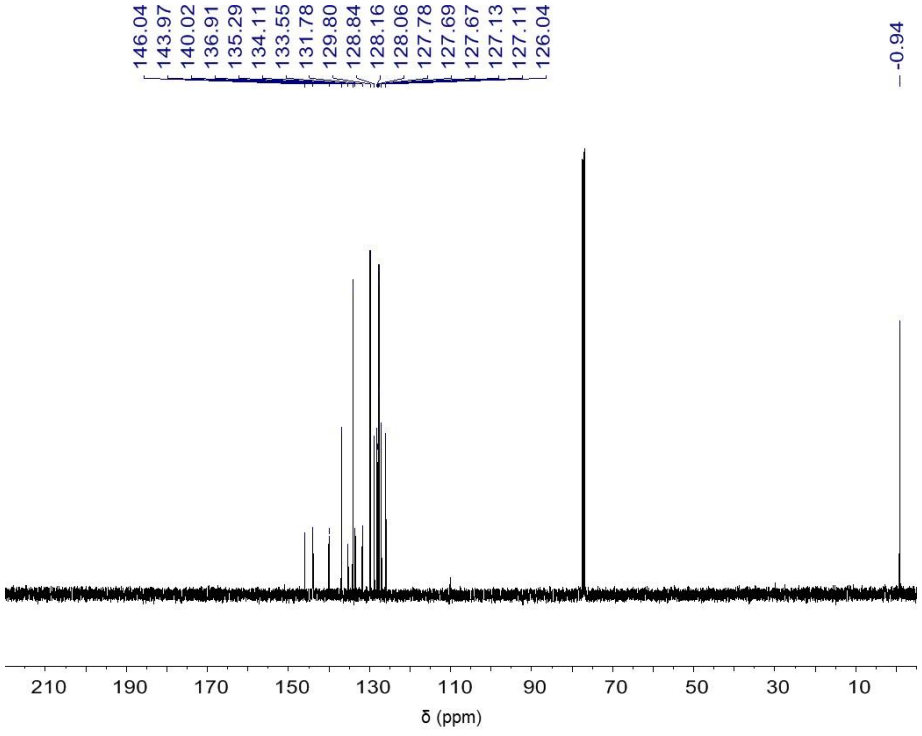

Figure S2.11. ^{1}H NMR of **6** (500 MHz, $CDCl_3$, 298 K)

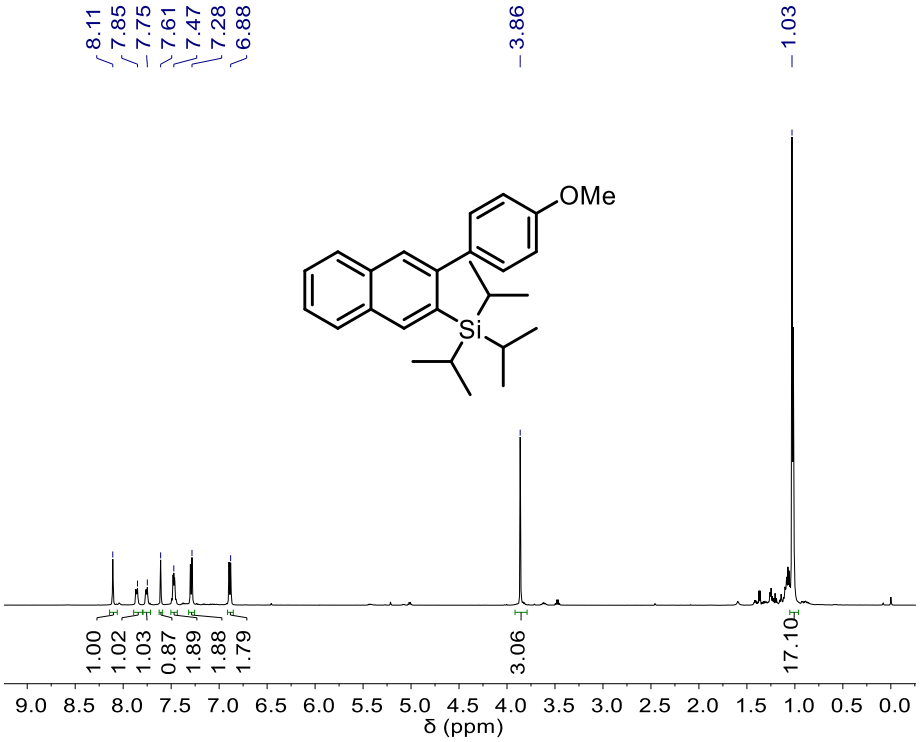

Figure S2.12. ^{13}C NMR of **6** (125 MHz, $CDCl_3$, 298 K)

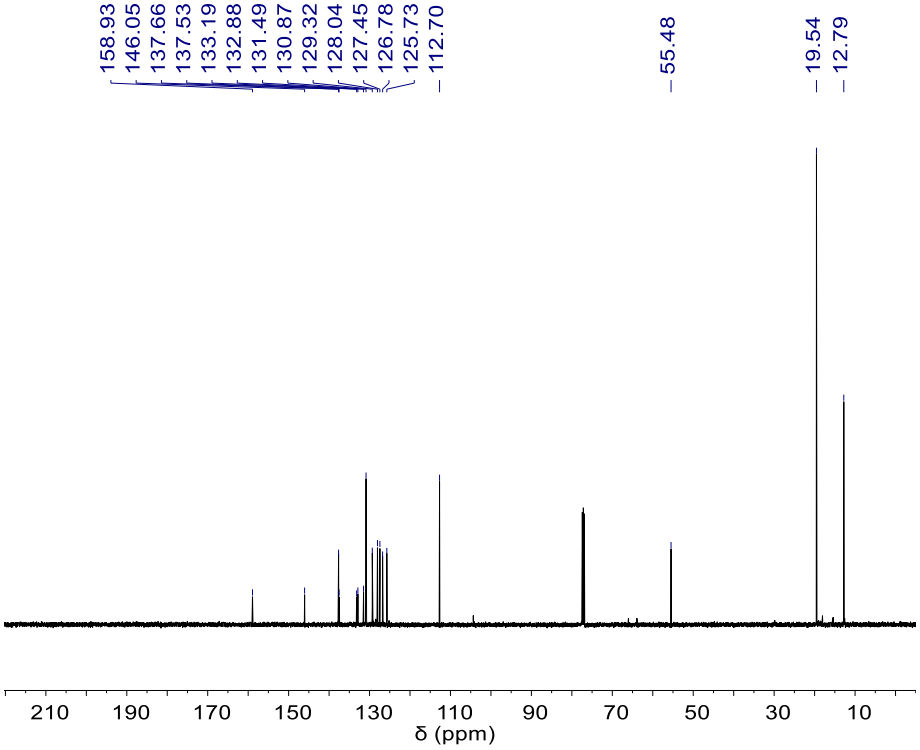

Figure S2.13. ^{1}H NMR of **9** (400 MHz, $CDCl_3$, 298 K)

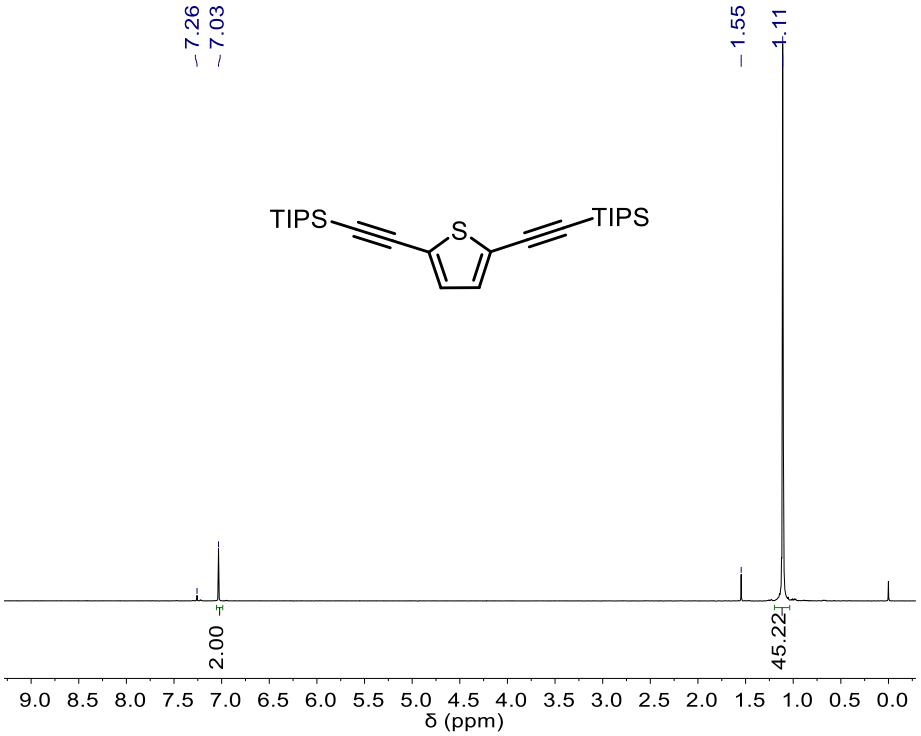

Figure S2.14. ^{13}C NMR of **9** (100 MHz, $CDCl_3$, 298 K)

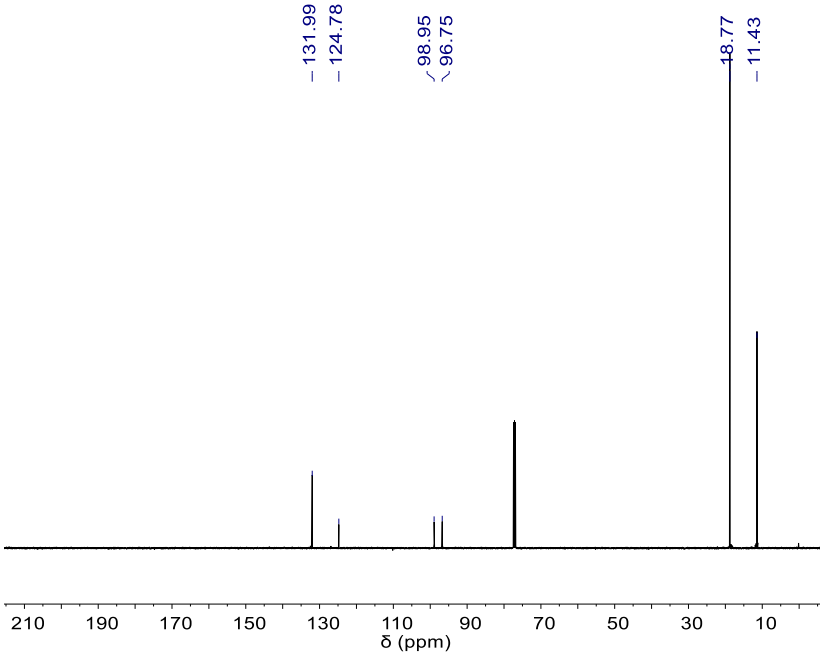

Figure S2.15. ^{1}H NMR of **10** (500 MHz, $CDCl_3$, 298 K)

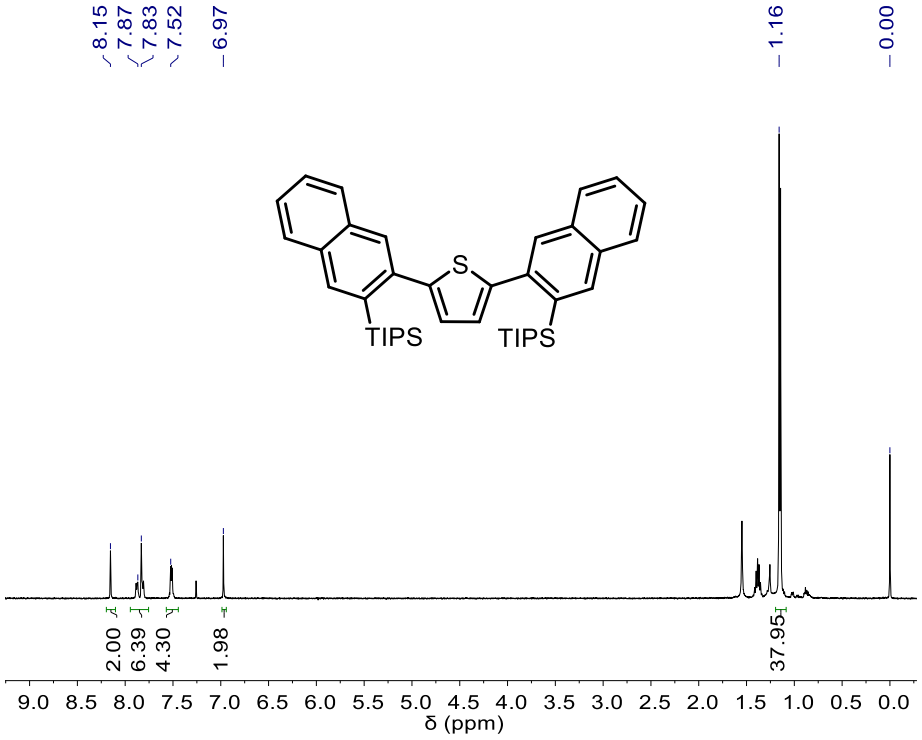

Figure S2.16. ^{13}C NMR of **10** (125 MHz, $CDCl_3$, 298 K)

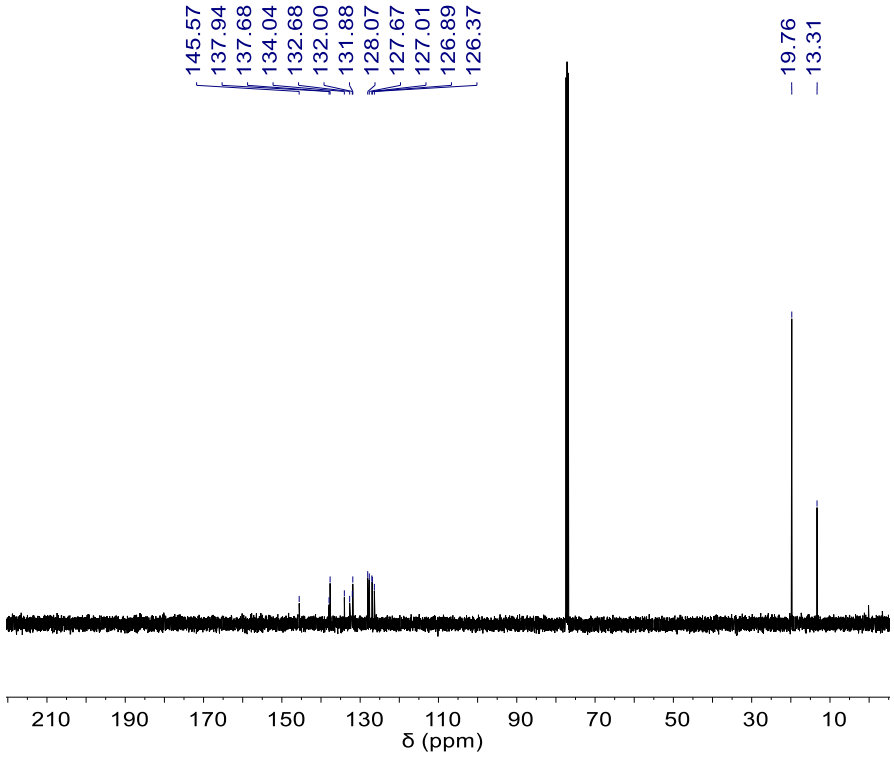

Figure S2.17. ^{1}H NMR of **11** (500 MHz, $CDCl_3$, 298 K)

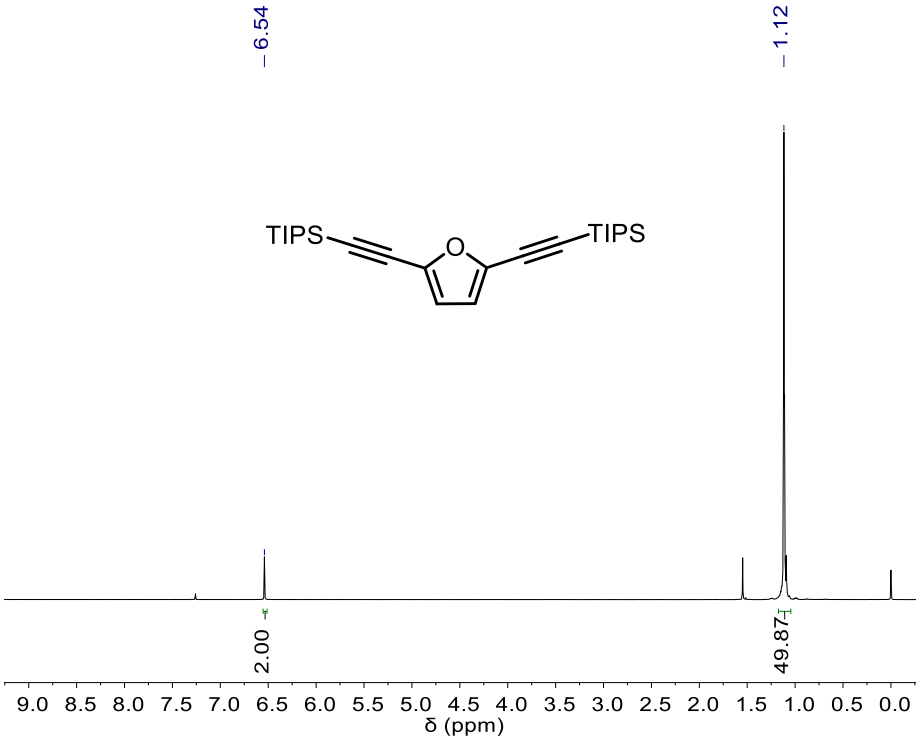

Figure S2.18. ^{13}C NMR of **11** (125 MHz, $CDCl_3$, 298 K)

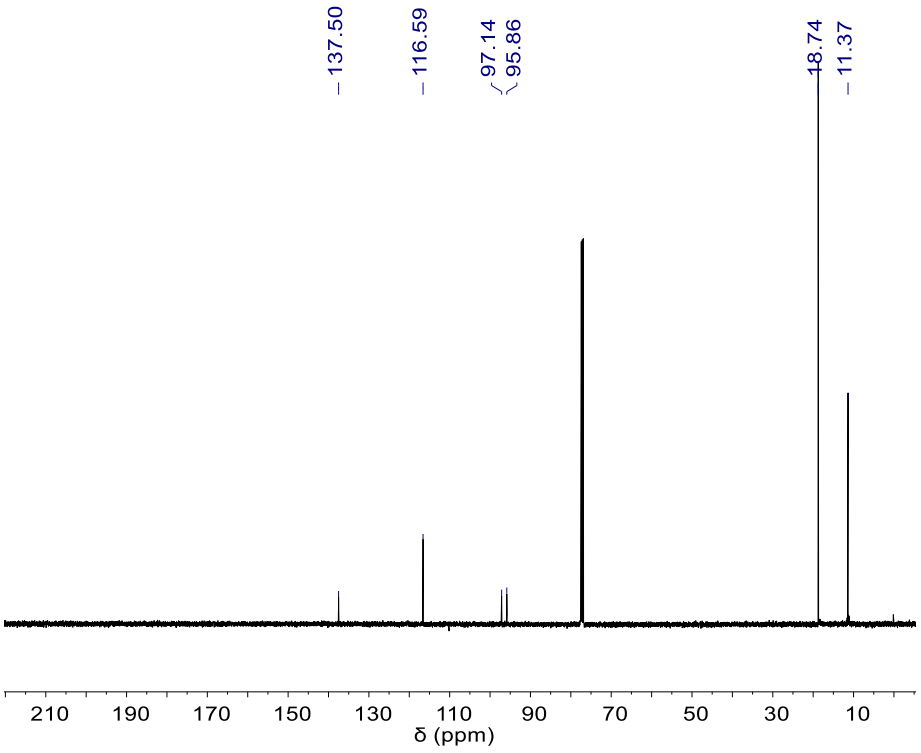

Figure S2.19. ^{1}H NMR of **12** (400 MHz, $CDCl_3$, 298 K)

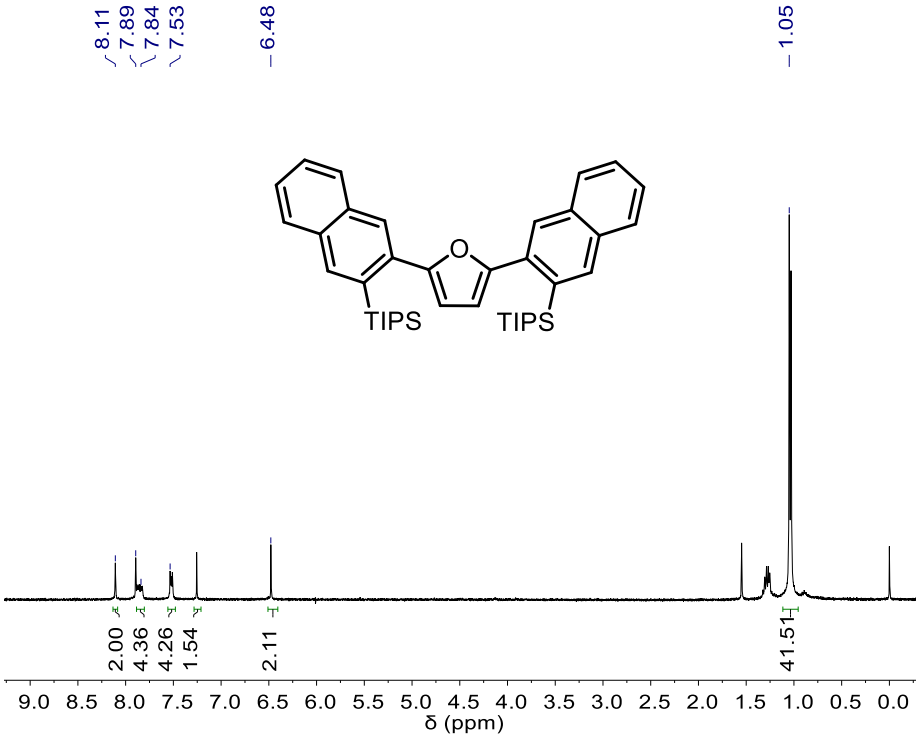

Figure S2.20. ^{13}C NMR of **12** (100 MHz, $CDCl_3$, 298 K)

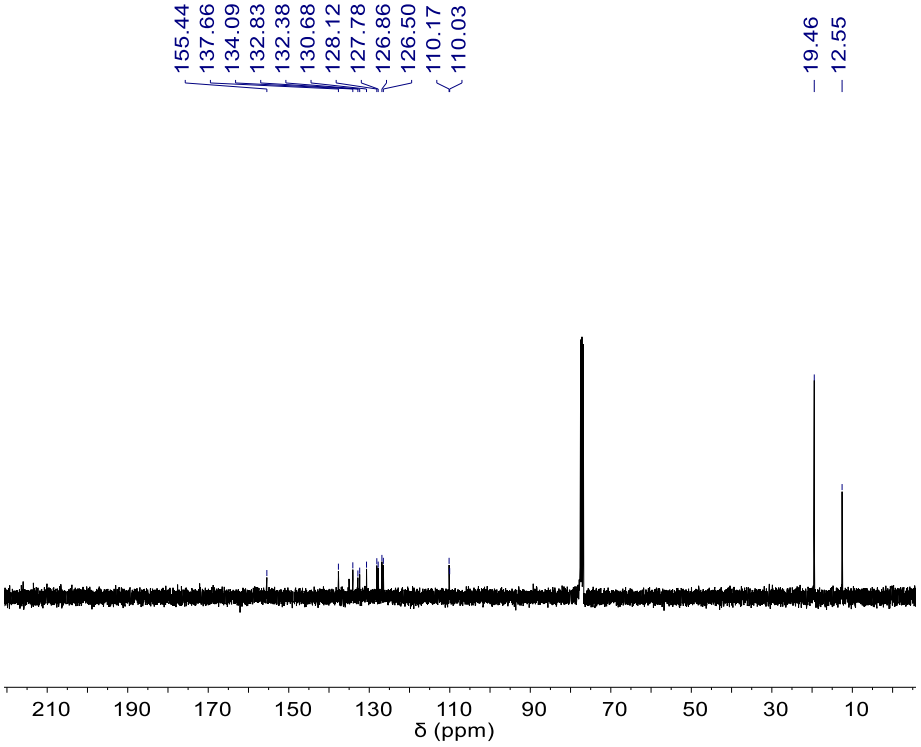

Figure S2.21. ^{1}H NMR of **13** (500 MHz, $CDCl_3$, 298 K)

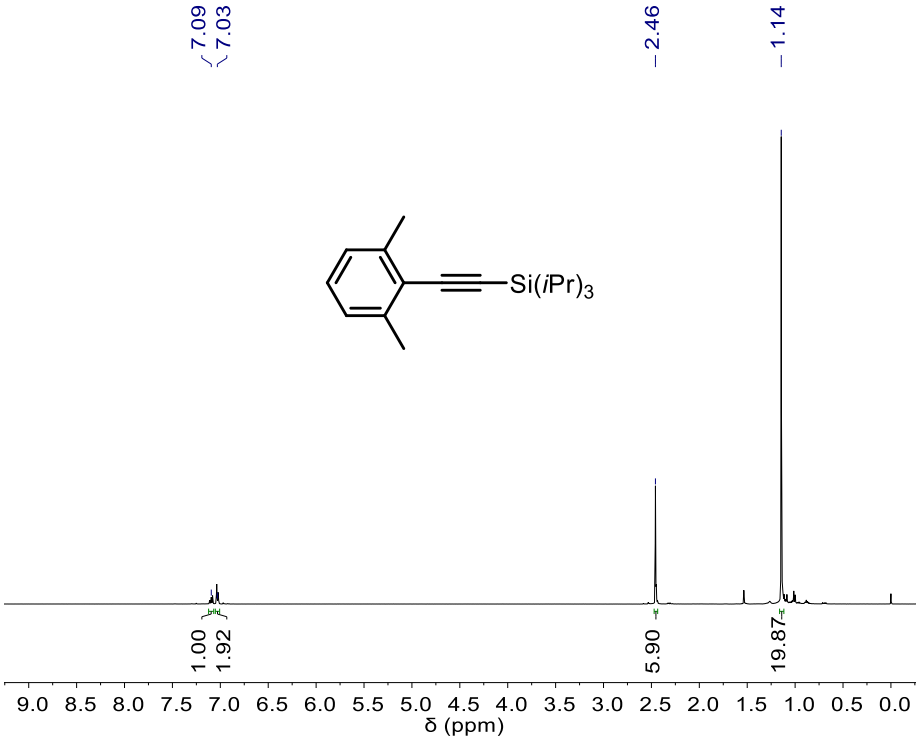

Figure S2.22. ^{13}C NMR of **13** (125 MHz, $CDCl_3$, 298 K)

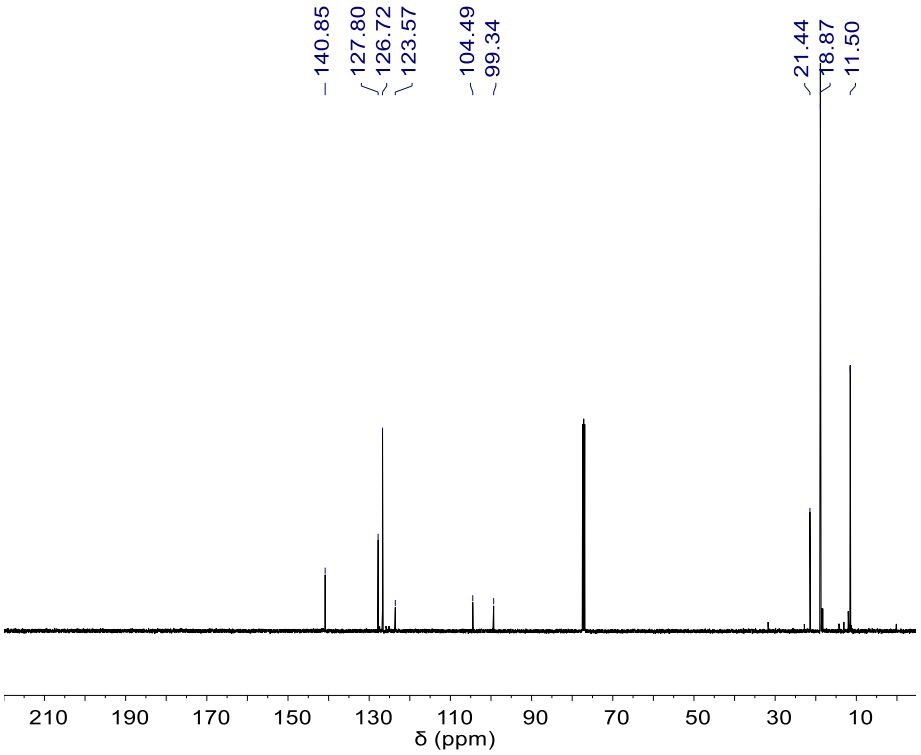

Figure S2.23. ^{1}H NMR of **14** (500 MHz, $CDCl_3$, 298 K)

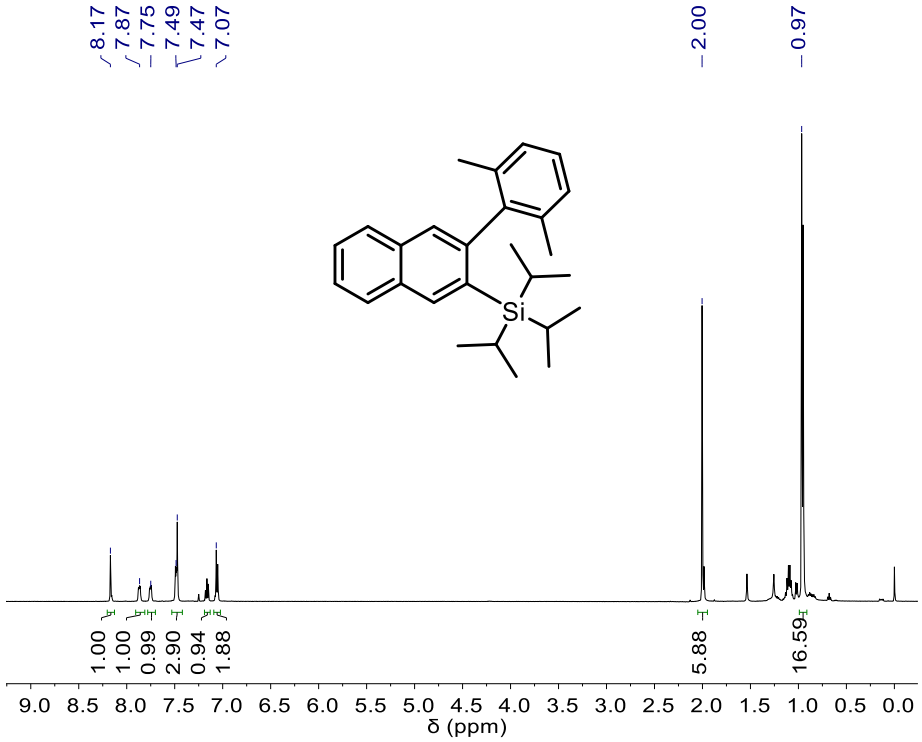

Figure S2.24. ^{13}C NMR of **14** (125 MHz, $CDCl_3$, 298 K)

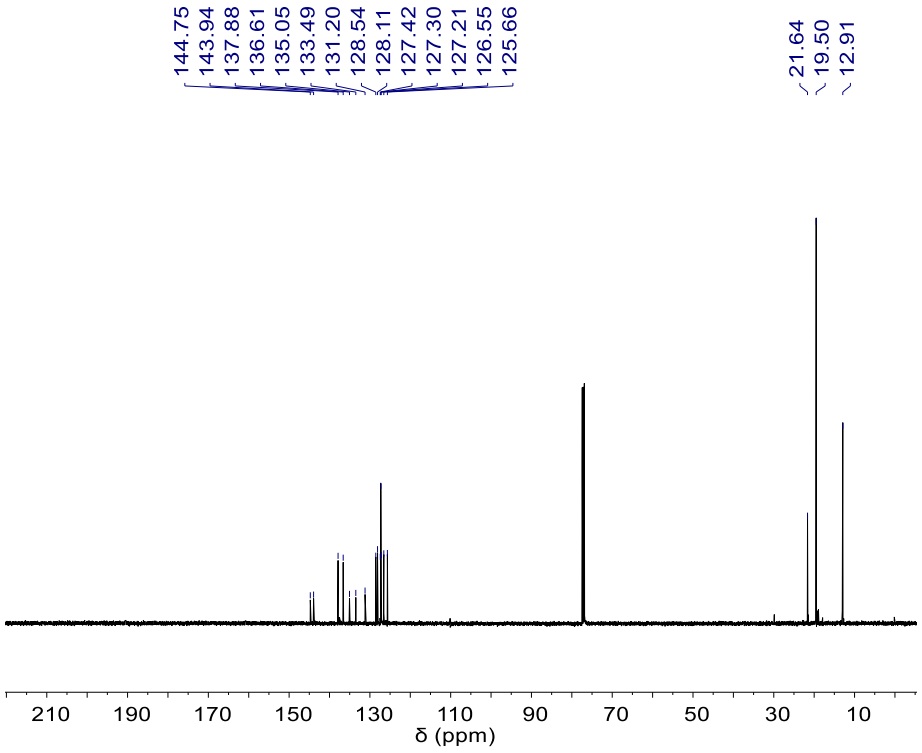

Figure S2.26. ^{1}H NMR of **15** (500 MHz, $CDCl_3$, 298 K)

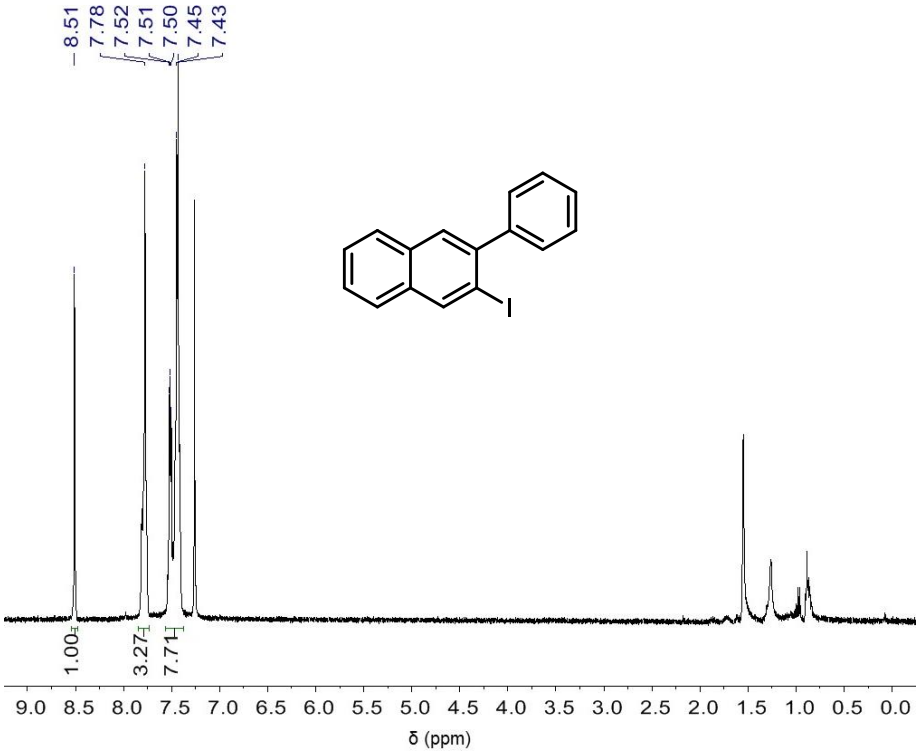

Figure S2.27. ^{13}C NMR of **15** (125 MHz, $CDCl_3$, 298 K)

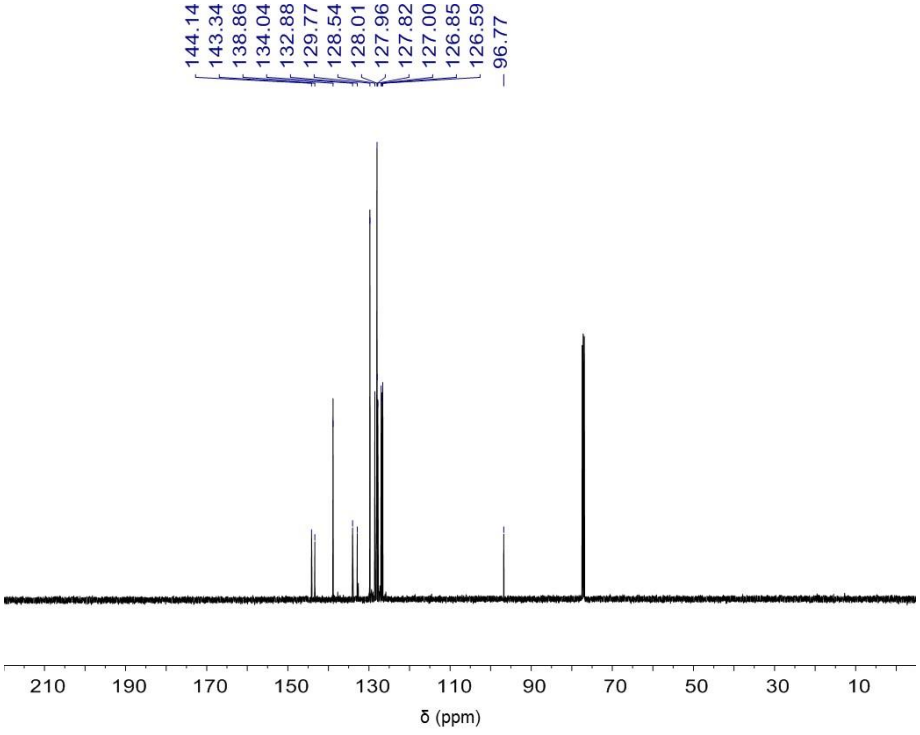

Figure S2.28. ^{1}H NMR of **16** (500 MHz, $CDCl_3$, 298 K)

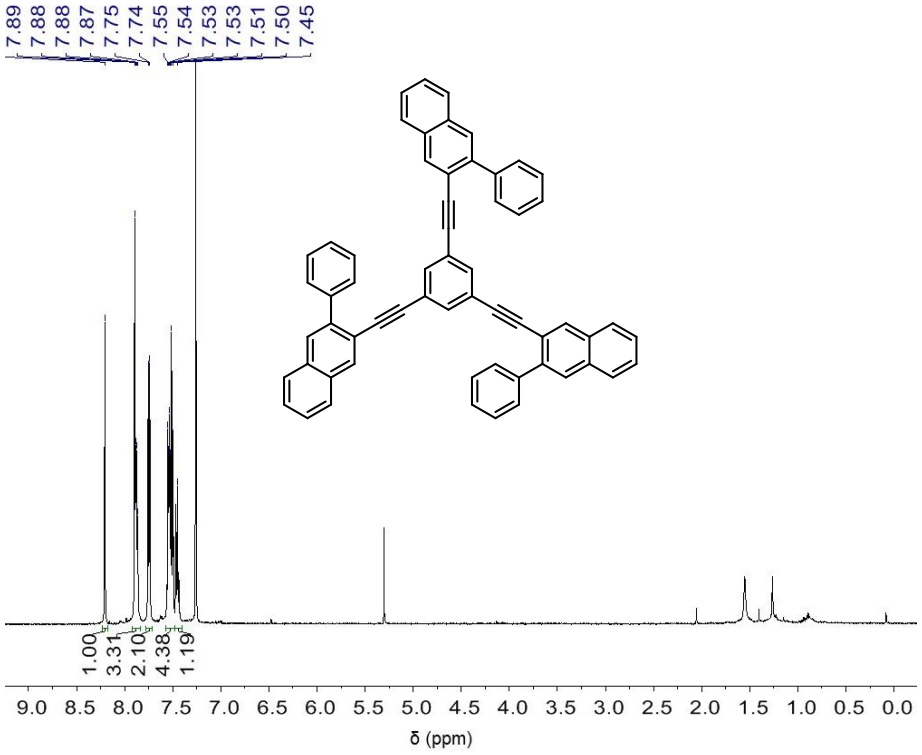

Figure S2.29. ^{13}C NMR of **16** (125 MHz, $CDCl_3$, 298 K)

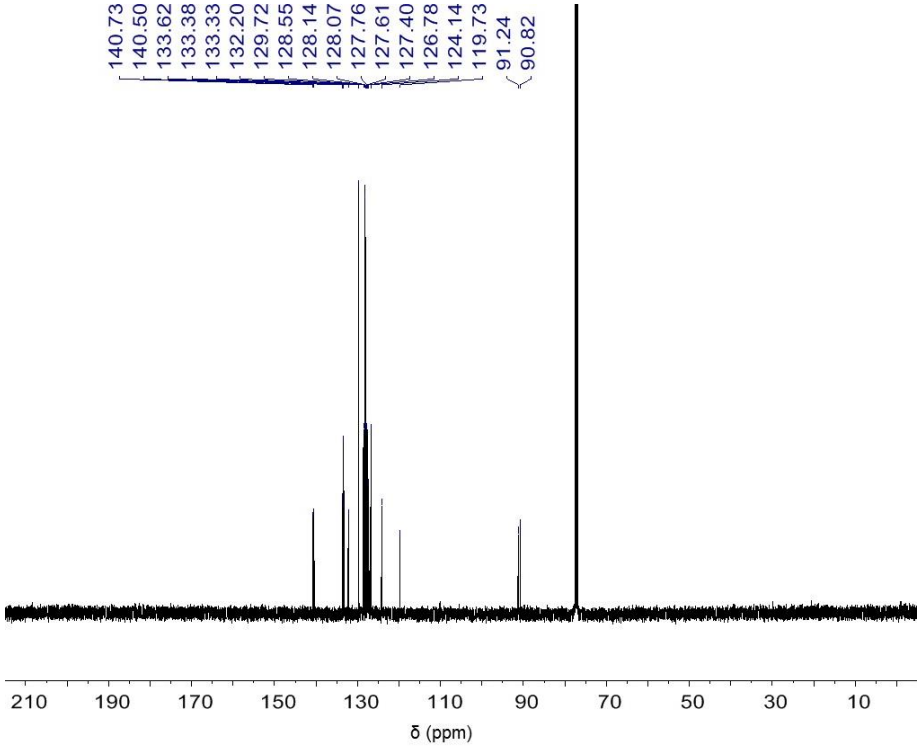

Figure S2.30. ^{1}H NMR of **17** (500 MHz, $CDCl_3$, 298 K)

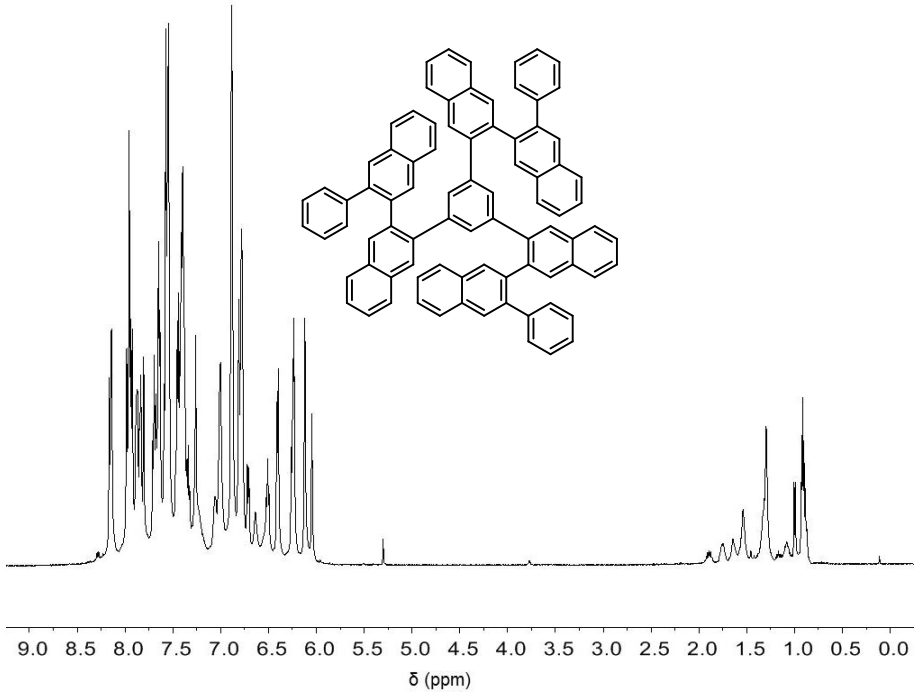

Figure S2.31. ^{13}C NMR of **17** (125 MHz, $CDCl_3$, 298 K)

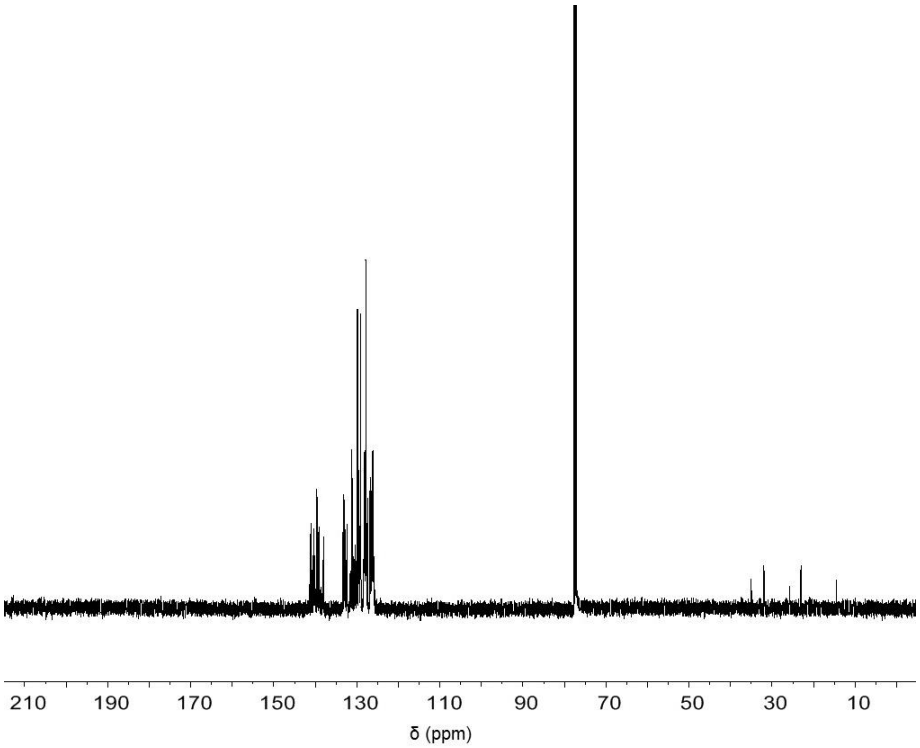

Figure S2.32. Partial 1H NMR spectra (500 MHz, $C_2D_2Cl_4$) of **17** obtained at a range of temperatures.

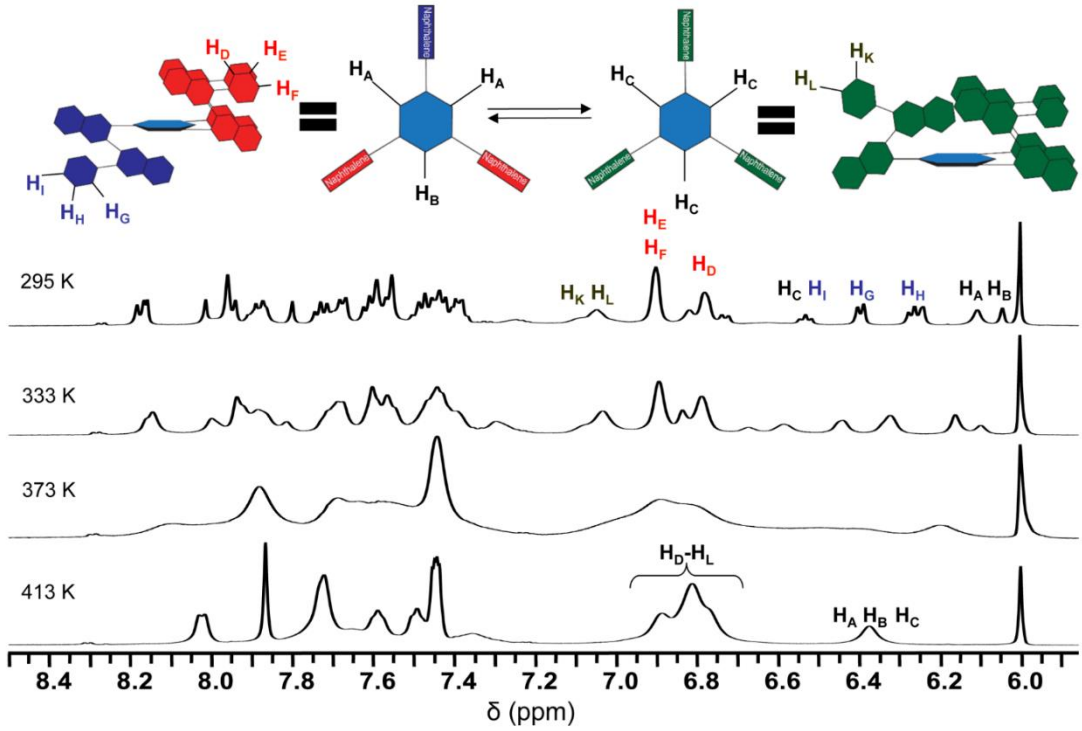

The *C*$_S$ confomation was fully assigned and the C_{3v} conformation was partially assigned in the rt ^{1}H NMR spectrum using a full complement of 2D NMR experiments. Hydrogens on the central benzene ring, H_a and H_b of the degenerate *C*$_S$ conformers, resonate at 6.04 and 6.10 ppm, respectively. The central protons of the *C*$_{3v}$ conformer (H_c) appear as a broad singlet centered at 6.52 ppm, which was identified by the exchange peak it shares with H_a and H_b. The relative integrations of the H_{ab} exchange peak and the H_{ac}/H_{bc} exchange peaks indicate that interconversion between degenerate C_S conformers is faster than interconversion between C_S and C_{3v} conformations. When the temperature is increased to 413 K, the ^{1}H and ^{13}C NMR spectra exhibit 14 and 24 signals, respectively, which are both consistent with the 16 proton and 26 carbon

chemical environments expected for **17**. Spectra obtained at 413 K simplify in a manner consistent with more rapid rotation about the exterior phenyl substituents, as well as coalescence of the H_a and H_b signals of the C_S conformer with the H_c signal of the C_{3v} conformer. These resonances remain broad, indicating slow rotation even at this elevated temperature.

Figure S2.33. Partial ^{1}H NMR spectra (500 MHz, $C_2D_2Cl_4$) of **17** obtained at other temperatures

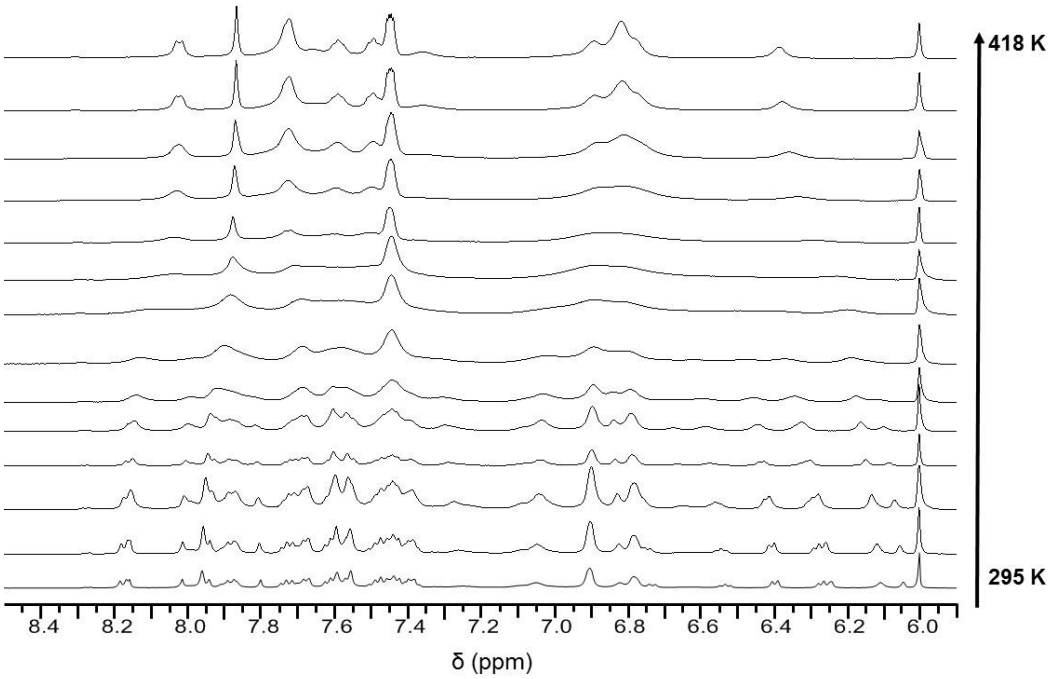

D. 2D NMR Spectroscopy

The peaks corresponding to H_1 for both C_S and C_{3v} conformations were assigned by analyzing cross-peaks observed in the COSY (full assignment below) and ROESY spectra (partial assignment below). The integration ratio of the two resonances that correspond to H_1 in the C_S conformation is 2:1 in the ^1H NMR, which is consistent with its assigned structure. ROESY exchange peaks between the two C_S H_1 and C_{3v} H_1 indicate that the two confirmations interconvert during the experiment. Once each ^1H and ^{13}C resonance of the C_S conformer was identified, these ROESY exchange peaks were used to assign several ^1H resonances of the C_{3v} conformer.

Figure S2.34. Partial ^{1}H NMR spectrum (500 MHz, $CDCl_3$, 295 K) of **17**, including assignments derived from the various 2D NMR experiments (see below).

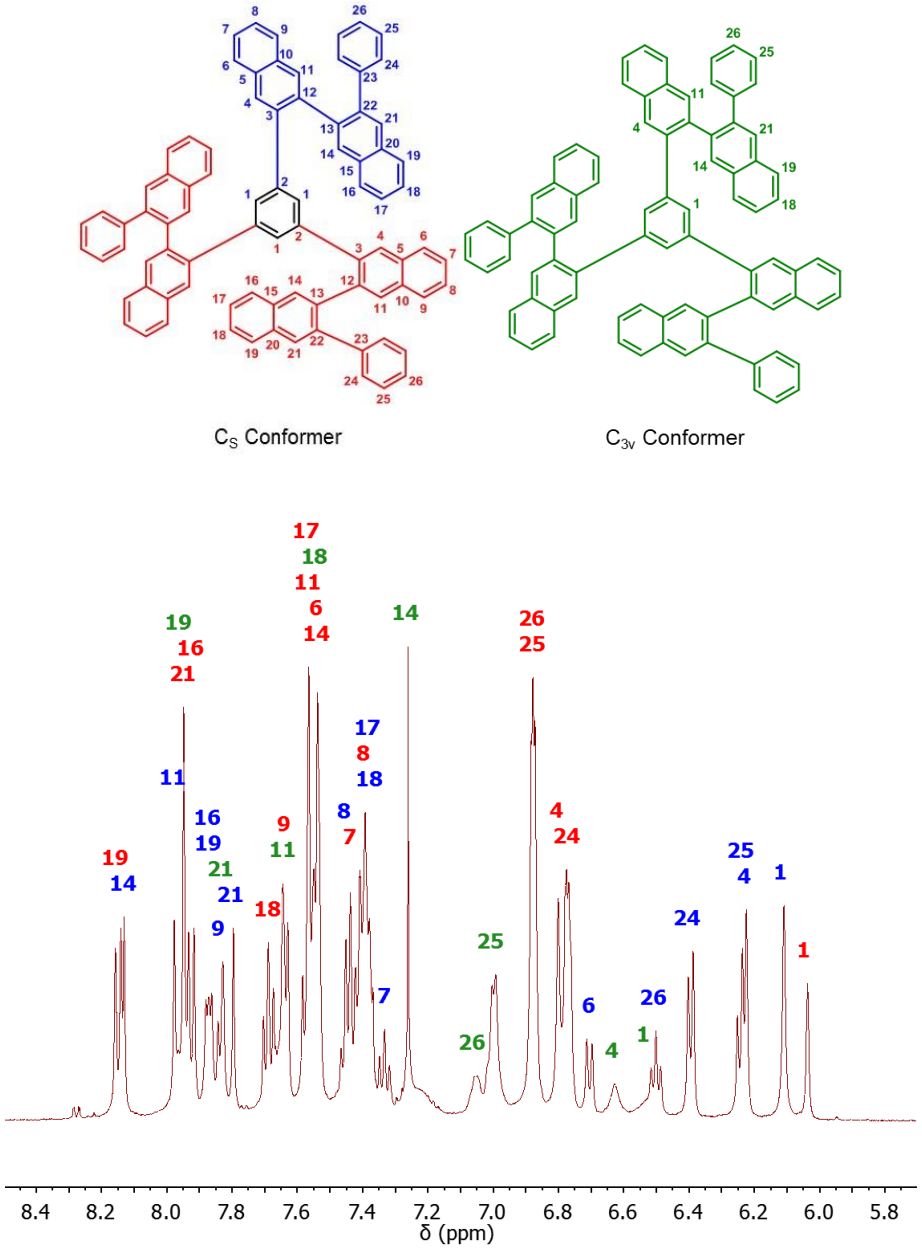

Figure S2.35. Partial ^{13}C NMR (125 MHz, $CDCl_3$, 295 K) of **17**, including assignments derived from various 2D NMR experiments (see below).

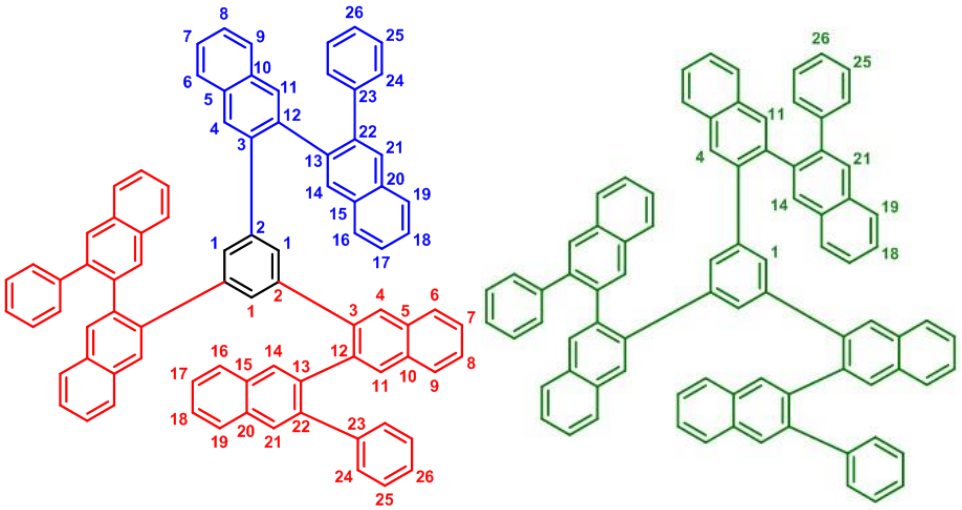

C_S Conformer

C_{3v} Conformer

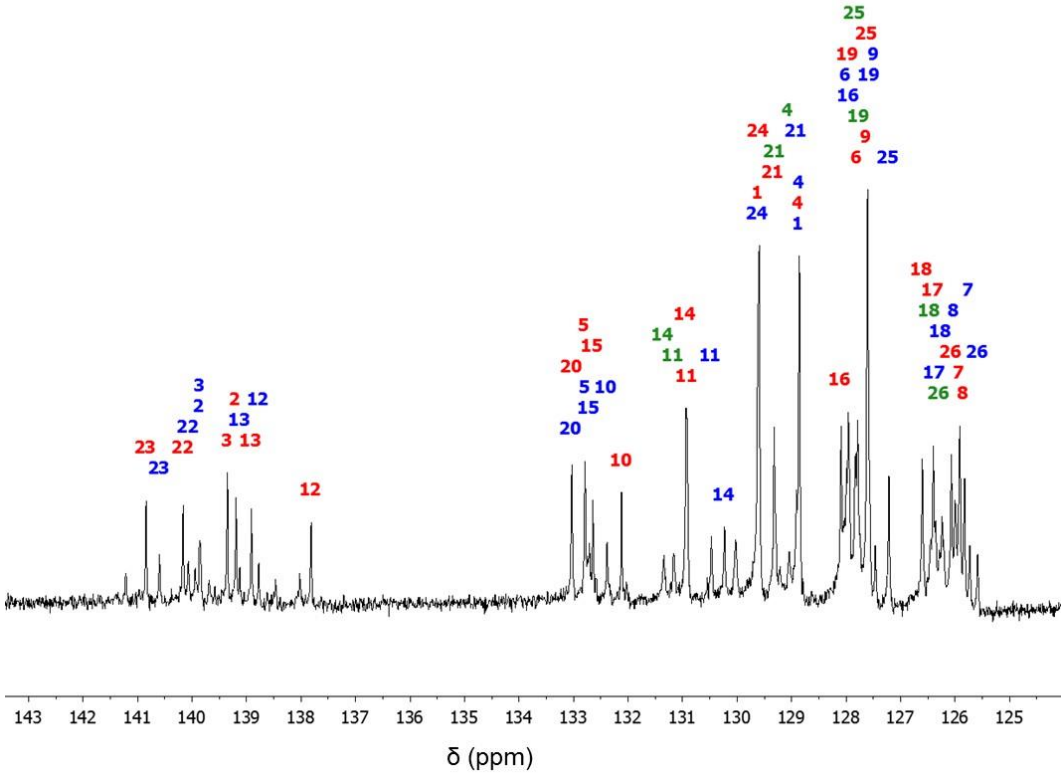

Figure S2.36. Partial COSY spectrum of the aromatic region of **17** (500 MHz, $CDCl_3$, 295 K)

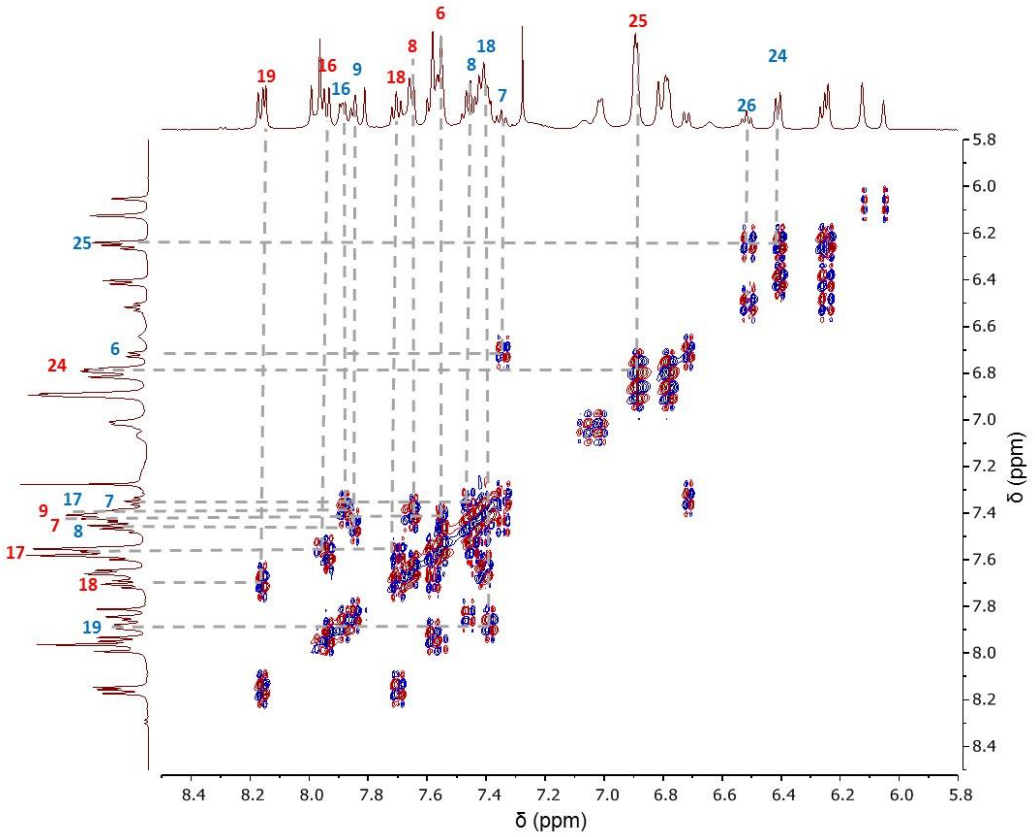

Figure S2.37. Partial ROESY spectrum of the aromatic region of **17** (500 MHz, $CDCl_3$, 295 K)

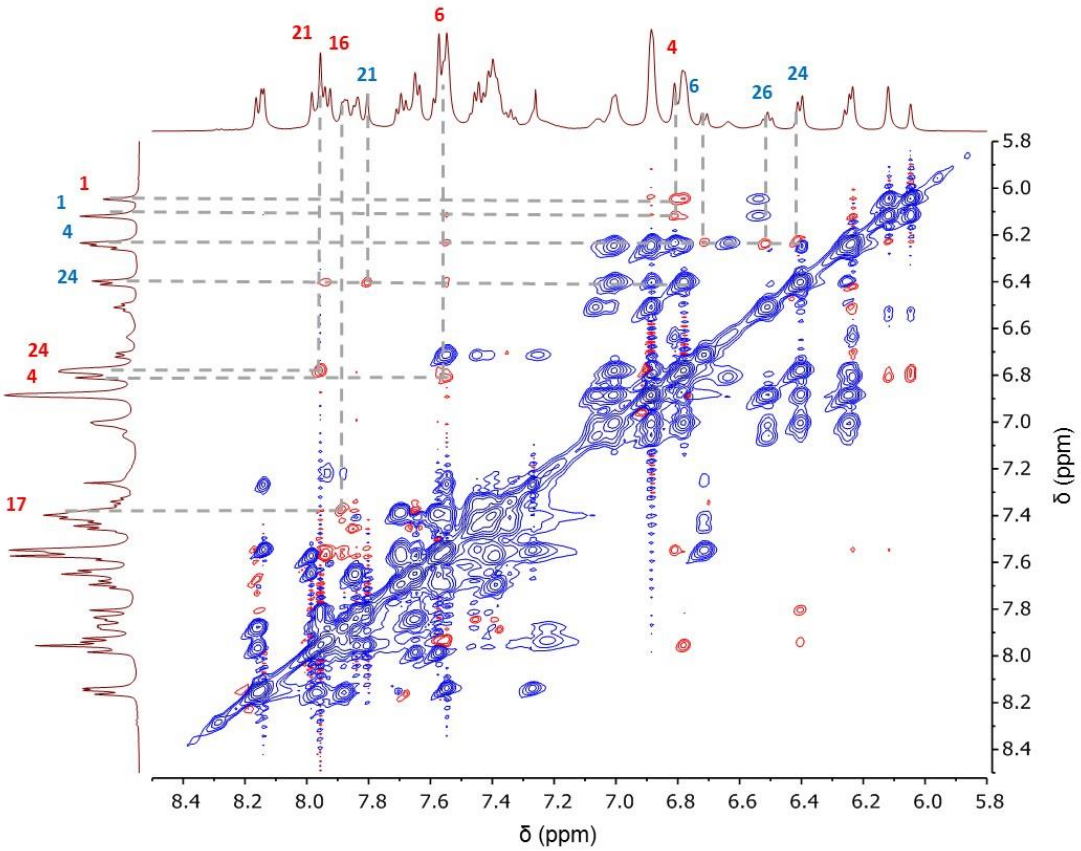

Figure S2.38. Band-selective HSQC spectrum of the aromatic region of **17** (500 MHz, 125 MHz, $CDCl_3$, 295 K)

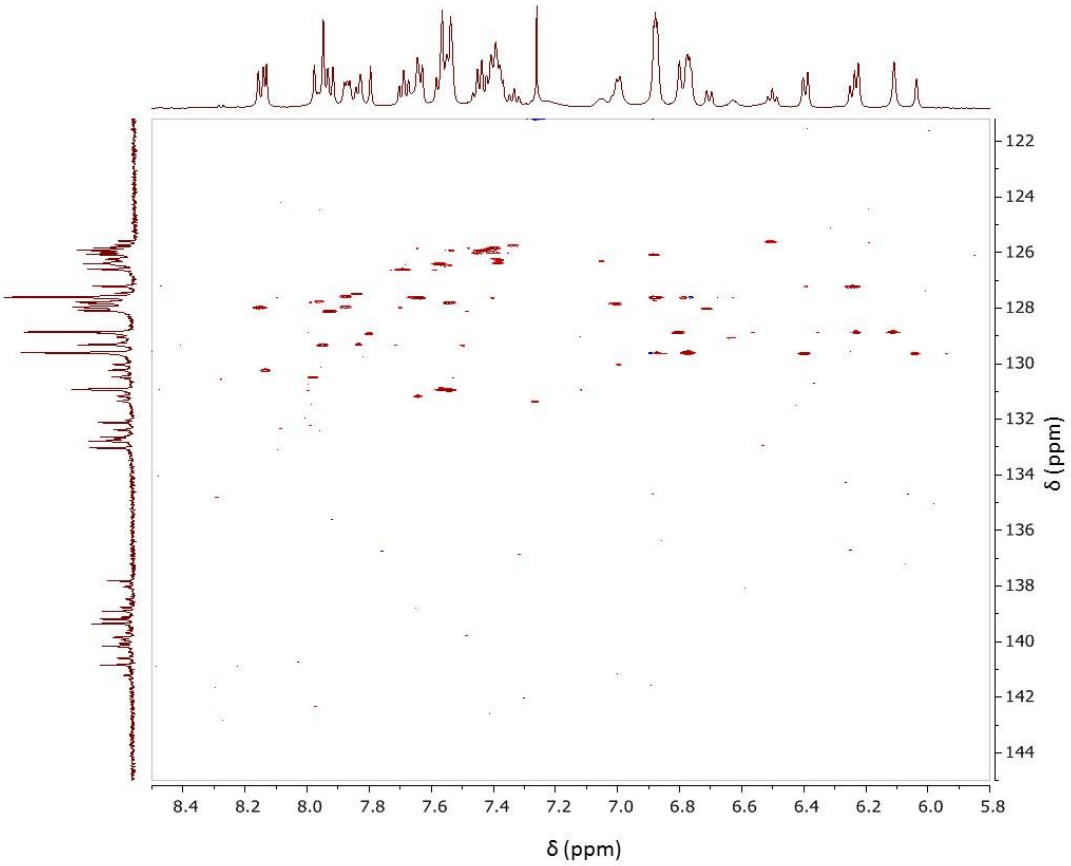

Figure S2.39. Band-selective HMBC spectrum of the aromatic region of **17** (500 MHz, 125 MHz, $CDCl_3$, 295 K)

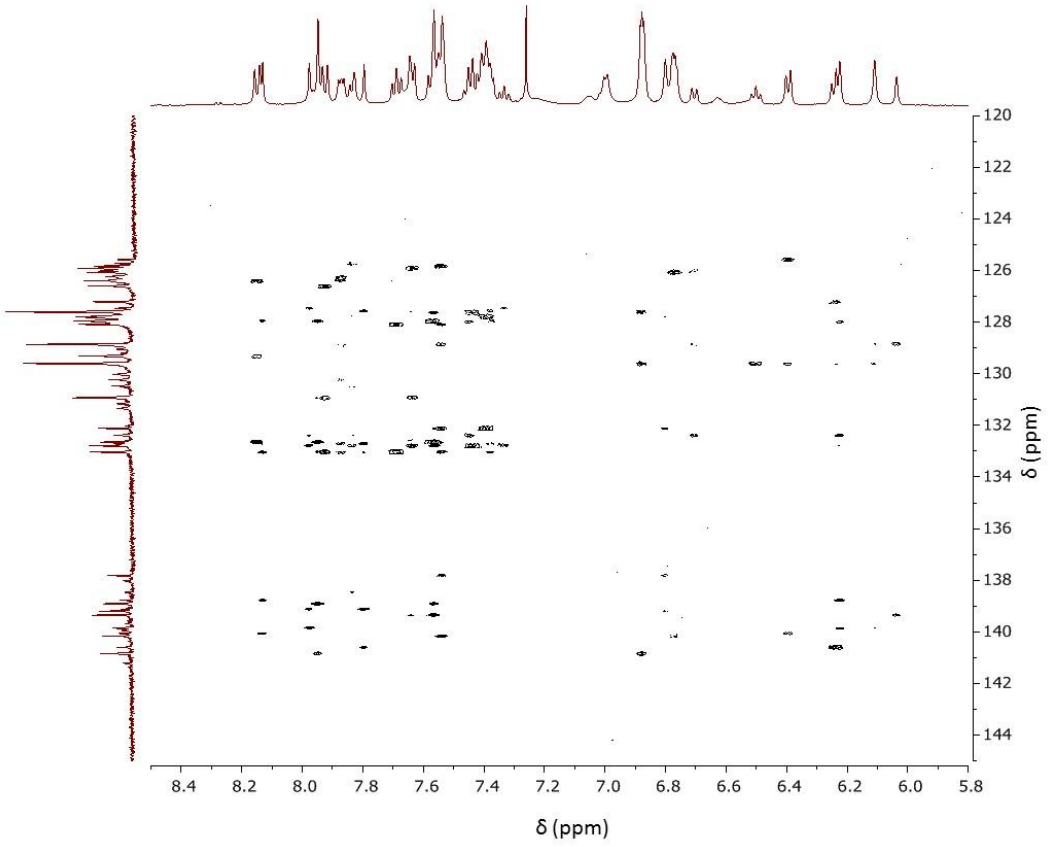

E. UV/Vis and Fluorescence Spectroscopy

Figure S2.40. UV/Vis absorption spectra (CH_2Cl_2, rt) of **16** (red) and **17** (blue). The spectra are normalized to the λ_{max} of each compound (λ_{max}= 261 nm for **16**; λ_{max}= 259 nm for **17**)

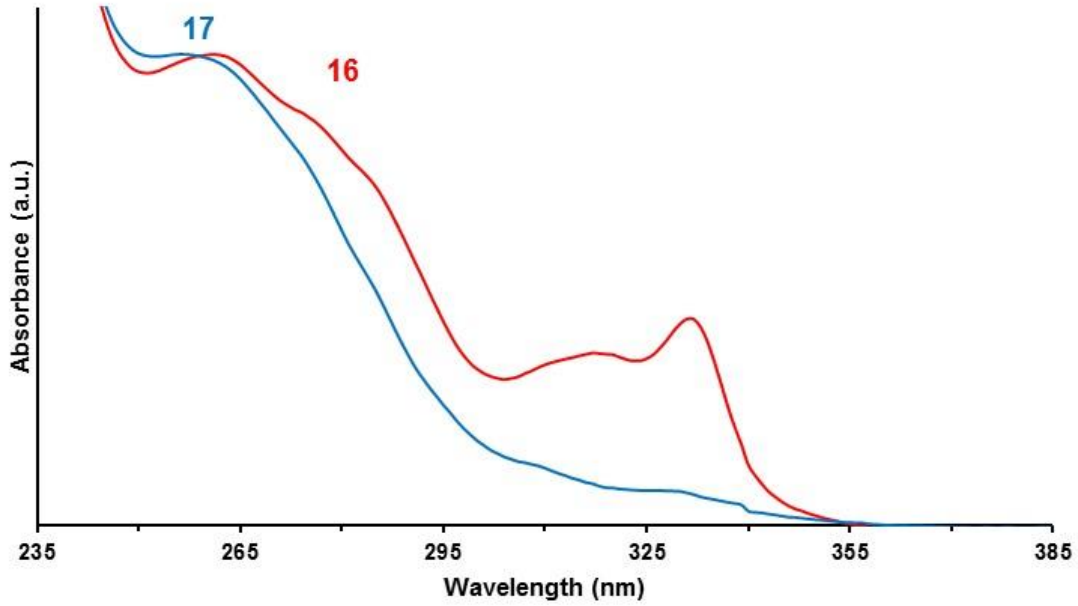

Figure S2.41. Photoemission spectra (CH_2Cl_2, rt) of **16** and **17** normalized to the optical density of each sample at its excitation wavelength (λ_{ex} = 250 nm for **16**; λ_{ex} = 250 nm for **17**).

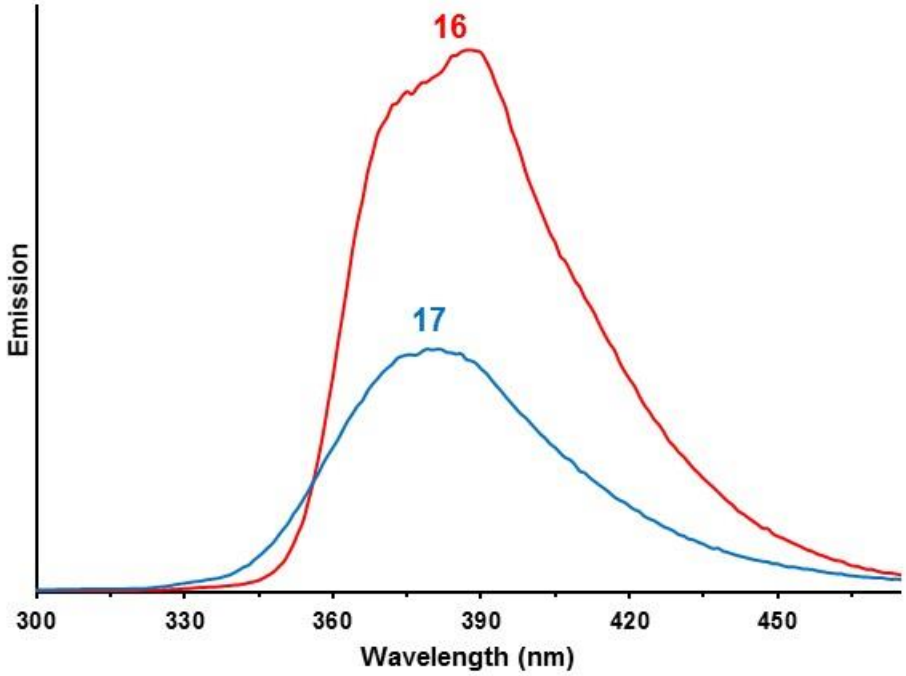

F. Gas Chromatography

Figure S2.42. Partial GC total ion chromatograms of crude reaction mixtures for the benzannulation of silyl acetylenes **1a-1e** using 1 equiv of CF_3CO_2H. The retention time of desilylated product **4** under these conditions is indicated by a vertical dashed line. Peaks corresponding to silyl naphthalene products **3a-3e** are labeled on each chromatogram, and the isolated yields of the silyl naphthalene product is also provided.

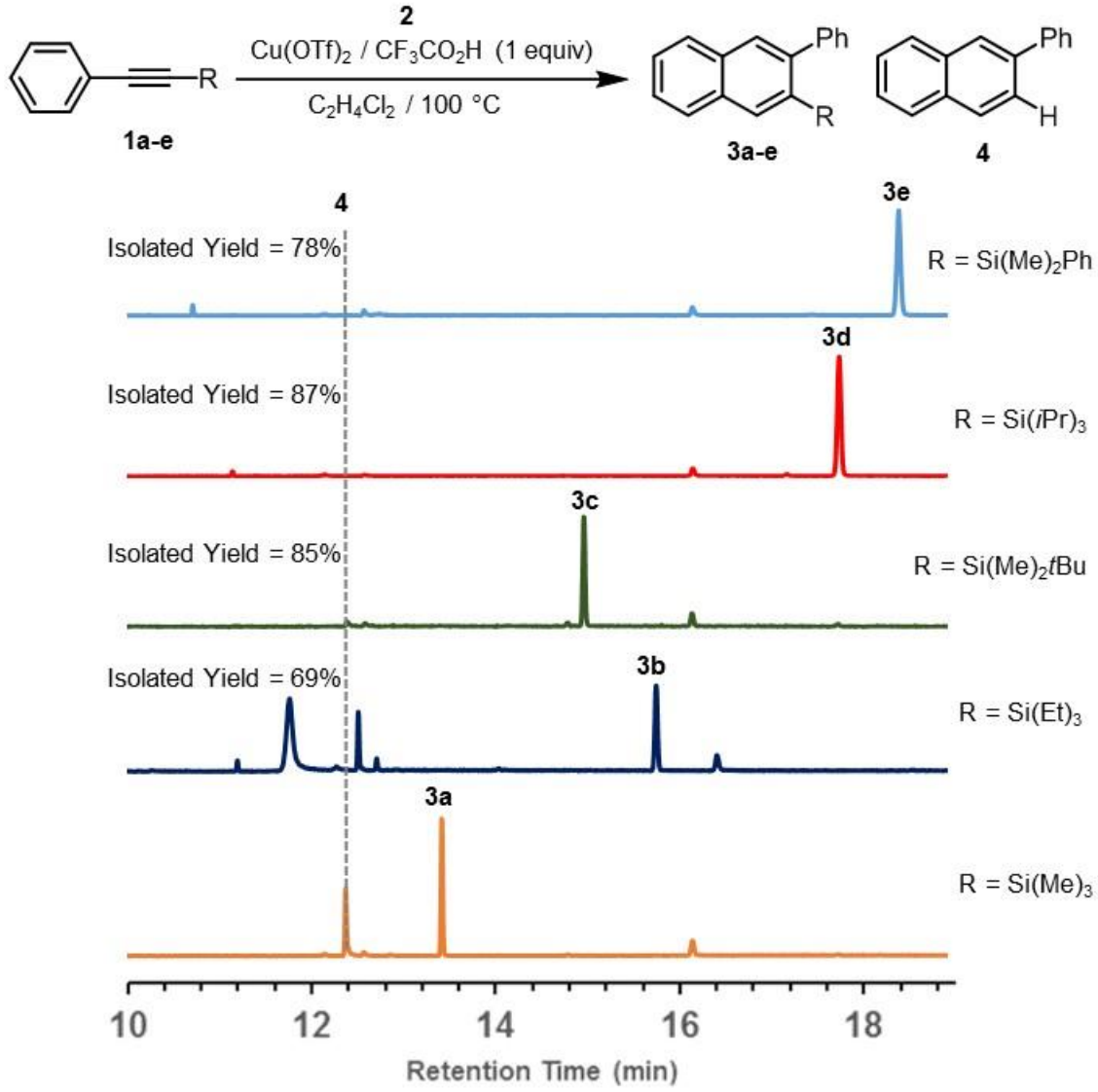

Figure S2.43. Partial GC total ion chromatograms obtained upon treating **3b**-**3e** with ICl. The retention time of desilylated product **4** and naphthyl iodide **15** under these conditions are indicated by vertical dashed lines, and the isolated yields of **15** are also provided.

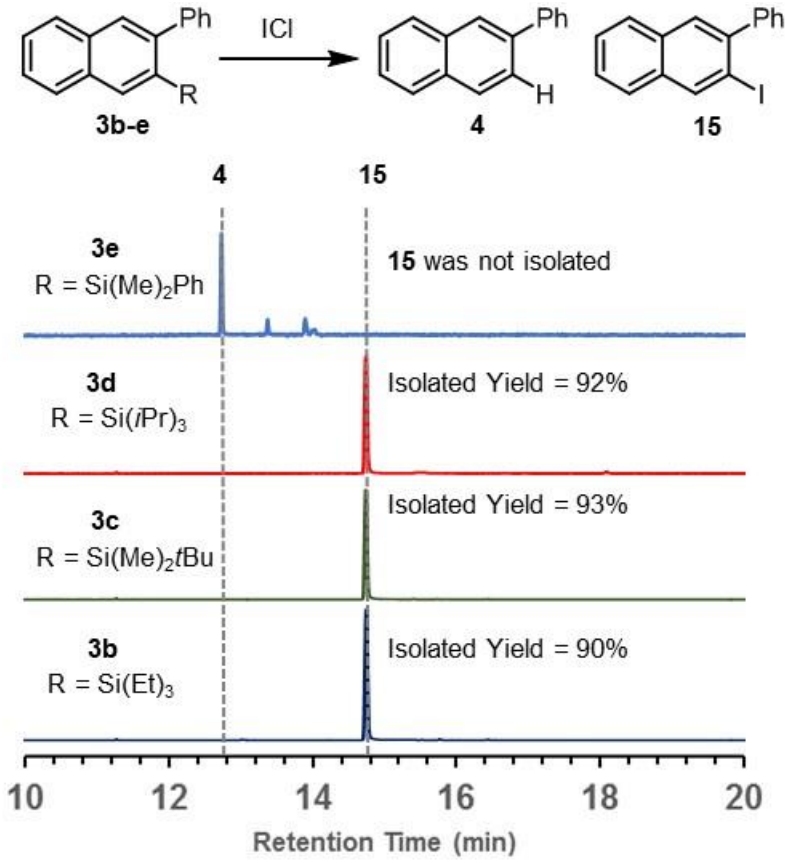

G. References

1. Zhang, Y.; Jamison, T. F.; Patel, S.; Mainolfi, N. *Org. Lett.* **2011**, *13*, 280–283.
2. Carril, M.; Correa, A.; Bolm, C. *Angew. Chem. Int. Ed.* **2008**, *47*, 4862–4865.
3. Creary, X.; Butchko, M. *J. Org. Chem.* **2002**, *67*, 112–118.
4. Yamaguchi, K.; Wang, Y.; Oishi, T.; Kuroda, Y; Mizuno, N. *Angew. Chem. Int. Ed.* **2013**, *52*, 5627–5630.
5. Nishihara, Y.; Saito, D.; Tanemura, K.; Noyori, S.; Takagi, K. *Org. Lett.* **2009**, *11*, 3546–3549.
6. Fairfax, D. J.; Austin, D. J.; Xu, S. L.; Padwa, A. *J. Chem. Soc., Perkin Trans. 1* **1992**, 2837-2844.
7. Asao, N.; Nogami, T.; Lee, S.; Yamamoto, Y. *J. Am. Chem. Soc.* **2003**, *125*, 10921–10925.
8. Castagnolo, D.; Botta, M. *Eur. J. Org. Chem.* **2010**, *2010*, 3224–3228.
9. Tuesuwan, B.; Kerwin, S. M. *Biochemistry* **2006**, *45*, 7265–7276.

CHAPTER THREE

BENZANNUALTION OF *ORTHO*-PHENYLENE ETHYNYLENE MACROCYCLES TOWARDS THE SYNTHESIS OF DISCRETE CARBON NANOTUBES SEGMENTS.

3.1 Abstract

Single walled carbon nanotubes (SWCNT) are of interest for applications in field effect transistors and transparent electrodes. The electronic character of these materials shifts drastically from metallic to semiconducting depending on the chirality and width of the SWCNT. Because of this, SWCNT have much promise for applications in field effect transistors and transparent electrodes. However, bulk SWCNT are currently made as a mixture of semiconducting and metallic CNTs of varying diameter and chirality. Separation of this mixture is possible but accessing monodisperse CNT through bottom-up synthetic approaches remains a goal for chemists. Previously, we had employed an Asao-Yamamoto benzannulation reaction to convert the embedded alkynes along a poly(phenylene ethynylene) into *ortho*-naphthyl linkages. We thought we could apply a similar strategy to phenylene ethynylene macrocycles to synthesize *ortho*-phenylene macrocycles which, upon cyclodehydrogenative oxidative conditions would yield carbon nanotube segments.

3.2 Introduction

Carbon nanotubes (CNT) are an allotrope of graphene that can be thought of as a sheet of carbon atoms rolled into a cylinder. Since their discovery in 1991,[1] CNTs have been found to have both metallic and semiconducting electronic properties.[2] Slight changes in the width and chirality of these materials drastically shifts the electronic conductivity of these materials from metallic to semiconducting. This level of variability in electronic character opens the doors for CNTs to be very precisely tuned for a specific application.

Though CNTs may currently be synthesized in kilogram quantities, the methods used to make them produce both metallic and semiconducting CNTs with varying widths and chiral vectors. Because of this, separation of this complex mixture is necessary if these materials are to be utilized as semiconductors in field effect transistors (FETs) or transparent electrodes for photovoltaic devices. Post-synthetic sorting of CNTs through electrophoresis,[3] chromatography,[4–7] and density-gradient centrifugation[8–11] have been developed and separate CNTs based on electronic type, diameter, affinity to a surfactant, and buoyant density. However, a long standing goal CNT growth is the direct synthesis of monodisperse CNT through selective growth. Selective CNT growth would combine the advantages of bulk CNT growth with the ease of patterning available to CVD growth conditions.

This type of selectivity has been a challenge in recent years. In order to accomplish this, inorganic catalyst supports have been developed that offer a specific crystal surface for CNTs to grow off of.[12–16] In recent years, increasing attention has been given towards the bottom up synthesis of CNTs without the use of a metal

catalyst.[17–19] This bottom-up synthesis of CNT segments allows for precise control over the width and chirality by synthetically changing the starting molecules.[20,21]

Benzannulation chemistry offers a general and rapid method to synthesize large complex aromatic architectures.[22–24] We were interested in applying an Asao-Yamamoto benzannulation reaction to convert a phenylene ethynylene macrocycle into an *ortho*-phenylene macrocycle that. These compounds would then be subjected to cyclodehydrogenative oxidative conditions to yield carbon nanotube segments that would be interesting for templated growth of precise carbon nanotubes. This approach would afford a general method for the synthesis of a variety CNT segments from materials that are simple to make using synthetic procedures, like alkyne metathesis.

3.3 Results and Discussion

Alkyne metathesis offers a unique method to achieve polyphenylene ethynylene macrocycles. A molybdenum alkyne metathesis catalyst was used to prepare phenylene ethynylene macrocycle **3** from monomer **1** (Scheme 3.1). Previously, these phenylene ethynylene macrocycles were synthesized using catalysts generated *in situ* from either **2**[25–29] or 1,10-phenanthroline-coordinated $(Ph_3SiO)_3Mo{\equiv}N$.[31,32] Typically, these reactions were performed in the presence of 5 Å molecular sieves to remove 2-butyne (>95%), which facilitates higher conversions and also prevents the undesired polymerization reaction of 2-butyne. In our experiments, a recrystallized sample of catalyst **2** provided **3** in 79% isolated yield (Scheme 3-1) after facile chromatography (SiO_2) to remove diphenylacetylene. This result suggests that alkyne metathesis, specifically catalyst **1**, is useful for complex macromolecule synthesis, and might be

useful for defect correction in the future synthesis of designed macromolecules, such as covalent organic frameworks, foldamers, and graphene nanoribbons.

Scheme 3.1. Synthesis and benzannulation of macrocycle **3**

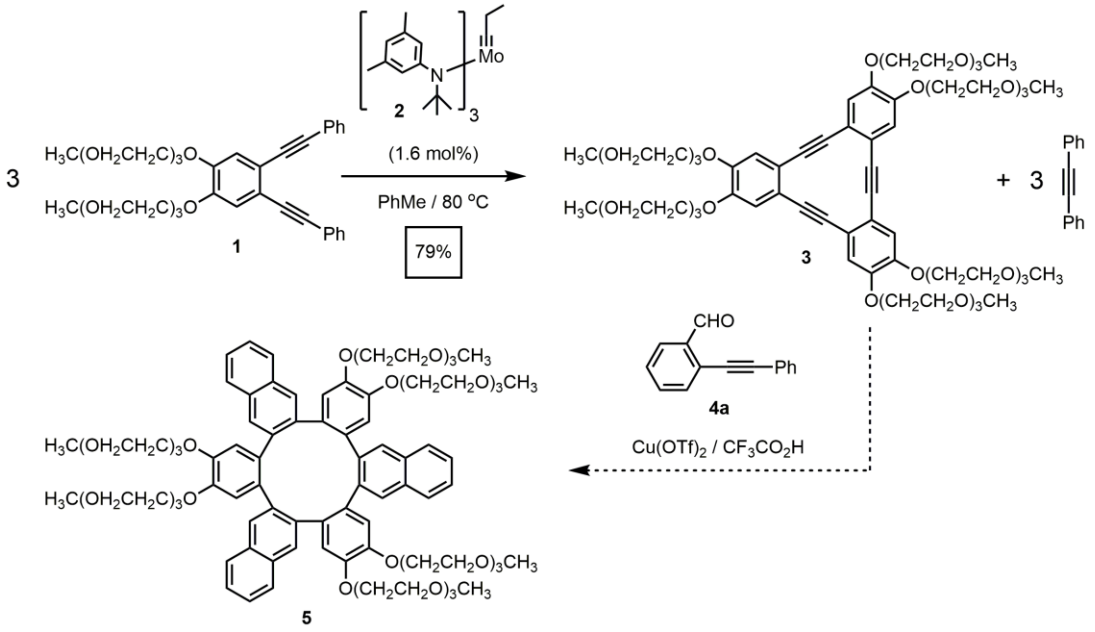

With this product in hand, we subjected it to benzannulation and observed whether the ortho-arylene macrocycle (**5**) was produced. Initial benzannulation attempts were done using typical conditions reported by Yamamoto[32] and monitored by MALDI-TOF-MS. The results are shown in Figure 3.1. In the MALDI-TOF mass spectra, multiple products (**5a-b**) are observable. Each of these products corresponding to a partially benzannulated macrocycle. Unexpectedly, a ketone side product appears to be a common occurrence in the reaction mixture. Using a different acid, in this case acetic acid, as a replacement additive in the benzannulation reaction yielded similar results.

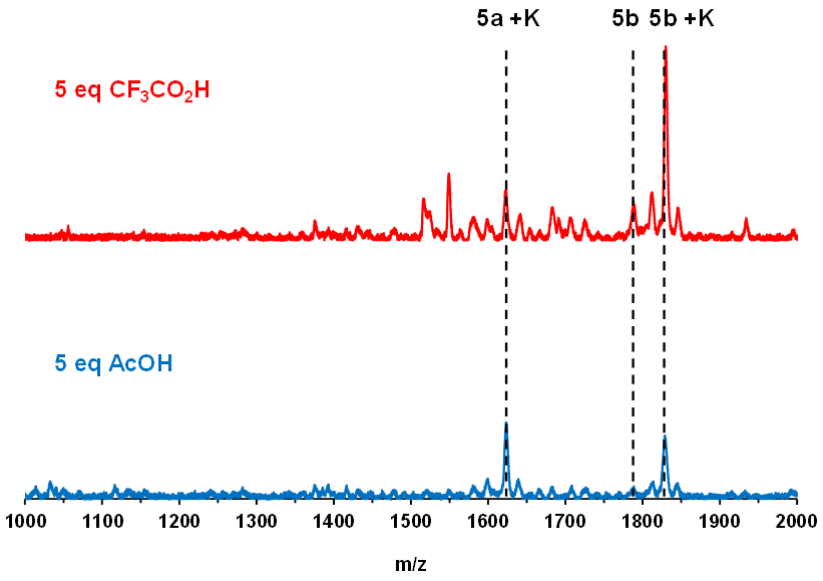

Figure 3.1. MALDI-TOF-MS of the crude reaction mixture after benzannulation of **3**.

Naphthyl ketones formation is known to be favorable when a strong acid is absent but should be suppressed with the addition of CF_3CO_2H. This would indicate the benzannulated ring may be too sterically congested to allow the CF_3CO_2H to protonate the copper bound intermediate species. Without this step the napthyl ketone product becomes a major product (Figure 1.1). Due to the steric demands of this system we thought these trimer monoyne macrocycles may have been too compact to efficiently benzannulate. We decided to synthesize an expanded alkyne macrocycle in hopes that the large ring would provide more space for the benzannulation to occur.

To this end, DBA[18]-OTHP macrocycle, obtained by the McGrier group, was deprotected using excess CF_3CO_2H to give the free hexahydroxy macrocycle **6** in high yields and then alkylated with **7** to give macrocycle **8** in 49 % yield. This macrocycle

was subjected to a variety of benzannulation conditions to explore the potential formation of the ortho-phenylene macrocycle **9** (Scheme 3.2).

Scheme 3.2. Synthesis and benzannulation of diyne macrocycle **8**.

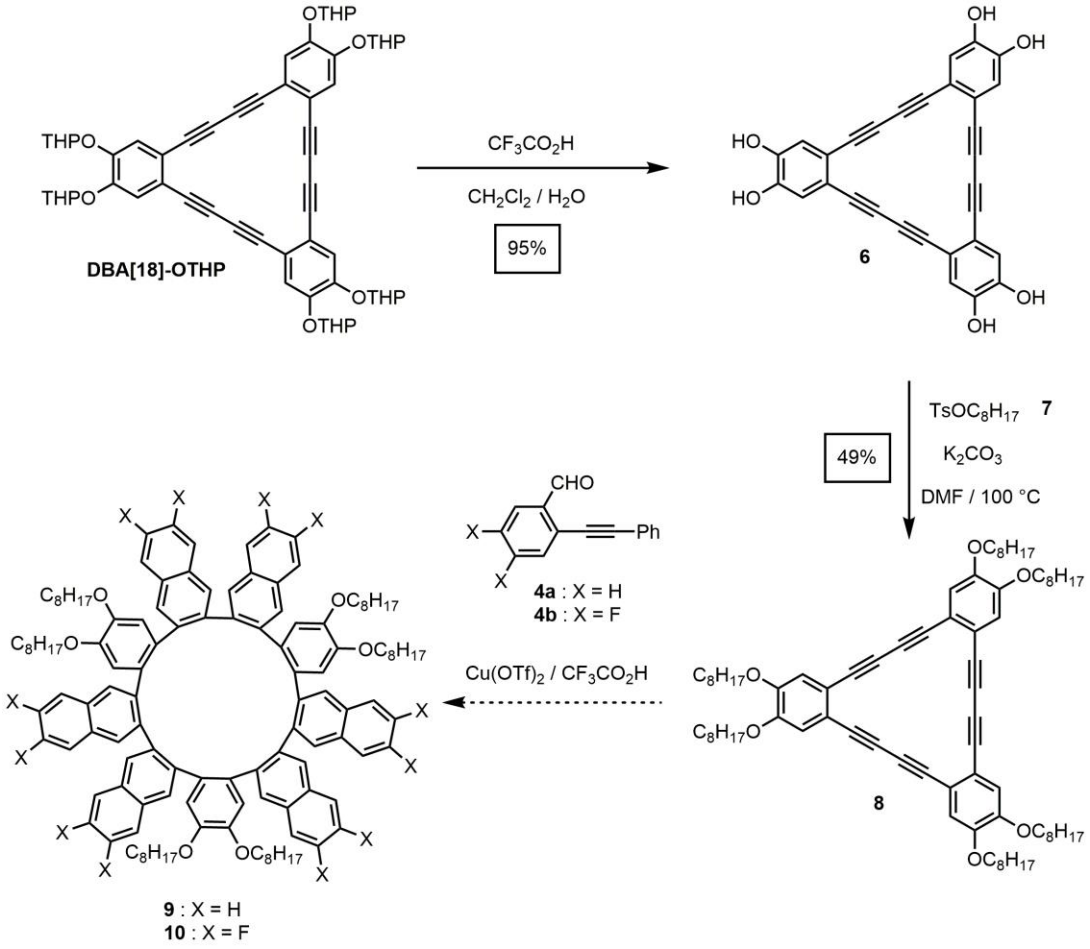

Upon benzannulation, we observe a complex mixture of products **9a-j** in the MALDI-TOF mass spectrometer (Figure 3.2), the list of molecular structures can be found in the appendix (**S3-18**). These structures are representative of compounds with similar molecular weights and do not represent the potential regioisomeric mixtures that are possible. The observable products were identified as incomplete benzannulation (**9a-c**) or benzannulated products bearing one or more naphthyl ketones (**9d-j**). By changing the reaction conditions we can change the product distribution observed in the MALDI-

TOF mass spectra. When the quantity of acid decreases from 5 equiv. to 1 equiv. fewer partially benzannulated products are observed in the mass spectra, however more naphthyl ketones are present as the benzannulation nears completion. $ZnCl_2$ is also a known benzannulation catalyst with the advantage of being much milder.[33] However, the mass spectra of the $ZnCl_2$ catalyzed benzannulation yields a similar product distribution.

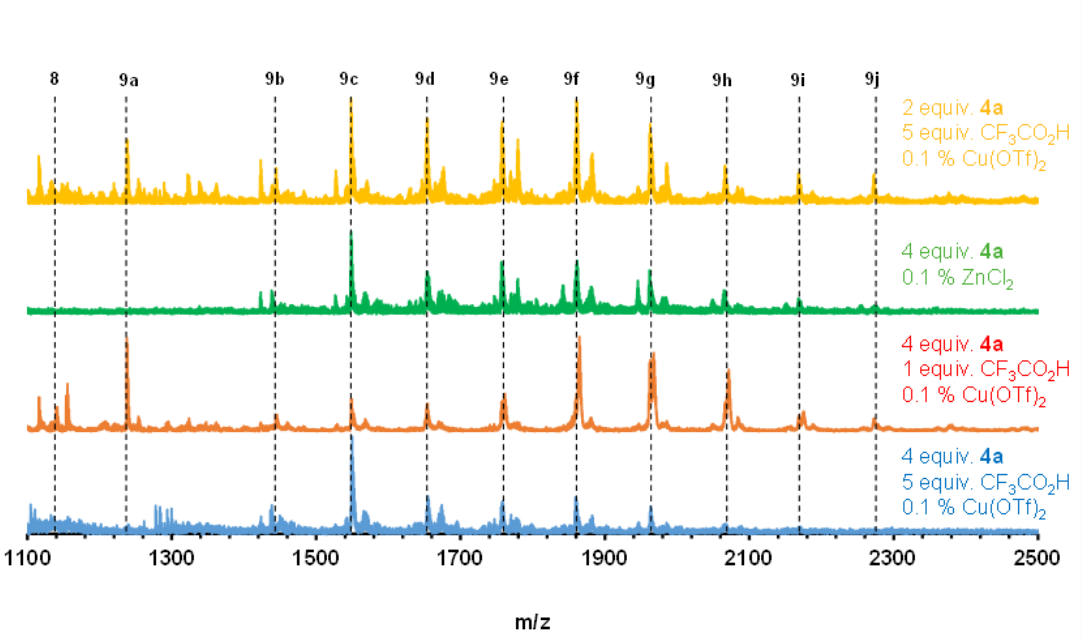

Figure 3.2. Stacked MALDI-TOF-MS of the crude reaction mixture upon benzannulation of **8**

Halogen substituted benzaldehydes tend to be more stable in the reaction conditions and can offer higher yields of the resulting benzannulated products. We chose difluorobenzaldehyde (**4b**) for these studies. The results can be seen in the MALDI-TOF mass spectra in Figure 3.3. Here again, we tested several benzannulation conditions including changing the catalyst to a $Zn(OTf)_2$, changing the acid to acetic acid, and CF_3CO_2Na. The mass spectra of each reaction upon completion showed a

complex mixture of partially benzannulated and products that contain one or more naphthyl ketones. The potential structures for the masses observed can be seen in the appendix of this chapter (**S3-24**). The more strongly acidic the reaction mixture is, the more likely we are to observe higher degrees of benzannulation. When the conjugate base of CF_3CO_2H is used, not only is partial benzannulation observed but even after 12 hours some starting material is still present in the reaction mixture.

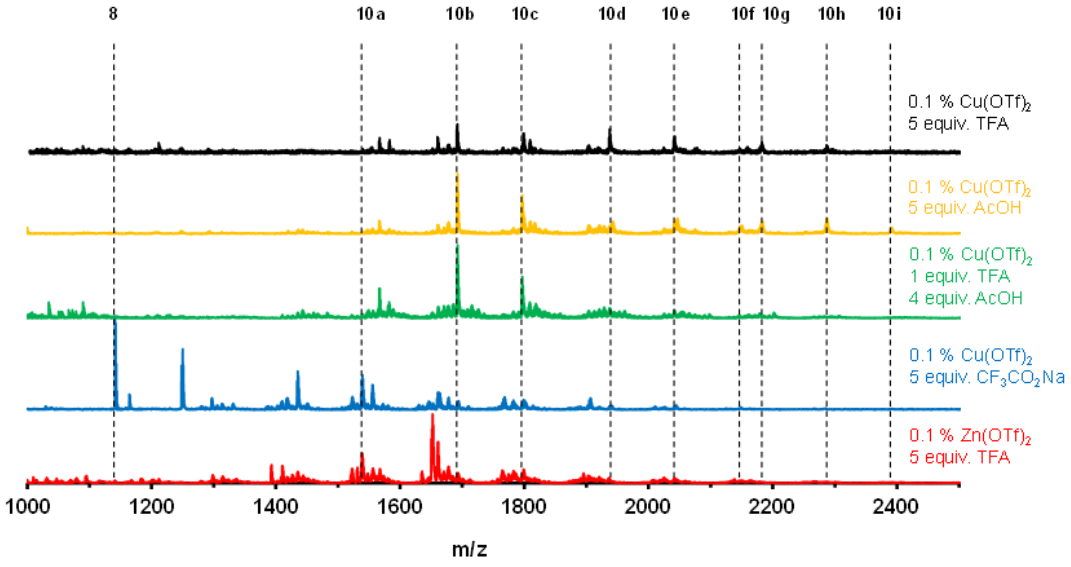

Figure 3.3. Stacked MALDI-TOF-MS of the crude benzannulation mixture of **8** after benzannulation with fluorinated benzaldehyde **4b** (2 equiv).

These results showed us that a benzannulation of macrocyclic phenylene ethynylenes is a very difficult goal to achieve with only one example reported.[34] Around this time there were reports of attempted synthesis of graphene nanohoops from π-expanded [*n*]cycloparaphenylenes (CPPs).[35] [*n*]CPPs consist of para-linked benzene rings connected in a ring. These materials are the smallest horizontal cross-section of an armchair CNT. While these rings have exhibited exciting host-guest complexes[36–38] and

interesting electronic properties[39–41], their potential application as seeds for homogeneous growth of armchair CNT has never been achieved to date. Common methods for CNT growth feature a Diels-Alder addition of acetylene into the bay regions of the CNT template,[17] however CPPs have not exhibited Diels-Alder reactivity. While chemical vapor deposition methods of [*n*]CPP have had an influence over the resulting CNT diameters, low yields limit the practical utility of this approach.[42] It is expected that CPPs with an extended π-system are crucial for high yielding CNTs. Mullen and coworkers reported the synthesis of π-extended CPP macrocycles which he subjected to an oxidative Scholl reaction.[43,44] These compounds, however, led to incomplete oxidation and rearrangements of the resulting fused nanotube segment. Independently, Jasti and coworkers reported their own synthesis of a π-extended CPP but again found rearrangements upon oxidation a common occurrence.[35]

3.4 Conclusion

In conclusion, Alkyne metathesis provided macrocycles to evaluate the benzannulation of alkyne-containing macrocycles. Though benzannulation of these structures were observed, the reaction did not exhibit characteristic efficiency or selectivity for 2,3-disubstituted naphthalene linkages that has been observed for other substrates. Meanwhile, literature reports of attempted Scholl-type oxidations of related cyclic phenylene-containing compounds showed undesirable rearrangements that do not provide expected carbon nanotube segments.

REFERENCES

(1) Iijima, S. *Nature* **1991**, *354*, 56–58.

(2) Saito, R.; Fujita, M.; Dresselhaus, G.; Dresselhaus, M. S.; *Appl. Phys. Lett.* **1992**, *60*, 2204–2206.

(3) Krupke, R.; Hennrich, F.; Löhneysen, H. v; Kappes, M. M. *Science* **2003**, *301*, 344–347.

(4) Moore, K. E.; Pfohl, M.; Tune, D. D.; Hennrich, F.; Dehm, S.; Chakradhanula, V. S. K.; Kübel, C.; Krupke, R.; Flavel, B. S. *ACS Nano* **2015**, *9*, 3849–3857.

(5) Knight, M.; Lazo-Portugal, R.; Ahn, S. N.; Stefansson, S. *J. Chromatogr. A* **2017**, *1483*, 93–100.

(6) Tanaka, T.; Urabe, Y.; Hirakawa, T.; Kataura, H. *Anal. Chem.* **2015**, *87*, 9467–9472.

(7) Liu, H.; Tanaka, T.; Urabe, Y.; Kataura, H. *Nano Lett.* **2013**, *13*, 1996–2003.

(8) Arnold, M. S.; Green, A. A.; Hulvat, J. F.; Stupp, S. I.; Hersam, M. C. *Nat. Nanotechnol.* **2006**, *1*, 60–65.

(9) Ghosh, S.; Bachilo, S. M.; Weisman, R. B. *Nat. Nanotechnol.* **2010**, *5*, 443–450.

(10) Antaris, A. L.; Seo, J.-W. T.; Green, A. A.; Hersam, M. C. *ACS Nano* **2010**, *4*, 4725–4732.

(11) Cambré, S.; Wenseleers, W. *Angew. Chem. Int. Ed.* **2011**, *50*, 2764–2768.

(12) Yang, F.; Wang, X.; Zhang, D.; Yang, J.; Luo, D.; Xu, Z.; Wei, J.; Wang, J.-Q.; Xu, Z.; Peng, F.; Li, X.; Li, R.; Li, Y.; Li, M.; Bai, X.; Ding, F.; Li, Y. *Nature* **2014**, *510*, 522–524.

(13) Azam, M. A.; Nawi, Z. M.; Azren, N. M.; Zulkapli, N. N. *Mater. Technol.* **2015**, *30*, A8–A13.

(14) Bachilo, S. M.; Balzano, L.; Herrera, J. E.; Pompeo, F.; Resasco, D. E.; Weisman, R. B. *J. Am. Chem. Soc.* **2003**, *125*, 11186–11187.

(15) An, L.; Owens, J. M.; McNeil, L. E.; Liu, J. *J. Am. Chem. Soc.* **2002**, *124*, 13688–13689.

(16) Zhang, F.; Hou, P.-X.; Liu, C.; Wang, B.-W.; Jiang, H.; Chen, M.-L.; Sun, D.-M.; Li, J.-C.; Cong, H.-T.; Kauppinen, E. I.; Cheng, H.-M. *Nat. Commun.* **2016**, *7*, 11160.

(17) Fort, E. H.; Donovan, P. M.; Scott, L. T. *J. Am. Chem. Soc.* **2009**, *131*, 16006–16007.

(18) Scott, L. T.; Jackson, E. A.; Zhang, Q.; Steinberg, B. D.; Bancu, M.; Li, B. *J. Am. Chem. Soc.* **2012**, *134*, 107–110.

(19) Yagi, A.; Segawa, Y.; Itami, K. *J. Am. Chem. Soc.* **2012**, *134*, 2962–2965.

(20) Sanchez-Valencia, J. R.; Dienel, T.; Gröning, O.; Shorubalko, I.; Mueller, A.; Jansen, M.; Amsharov, K.; Ruffieux, P.; Fasel, R. *Nature* **2014**, *512*, 61–64.

(21) Liu, B.; Liu, J.; Li, H.-B.; Bhola, R.; Jackson, E. A.; Scott, L. T.; Page, A.; Irle, S.; Morokuma, K.; Zhou, C. *Nano Lett.* **2015**, *15*, 586–595.

(22) Hein, S. J.; Arslan, H.; Keresztes, I.; Dichtel, W. R. *Org. Lett.* **2014**, *16*, 4416–4419.

(23) Arslan, H.; J. Uribe-Romo, F.; J. Smith, B.; R. Dichtel, W. *Chem. Sci.* **2013**, *4*, 3973–3978.

(24) Arslan, H.; Saathoff, J. D.; Bunck, D. N.; Clancy, P.; Dichtel, W. R. *Angew. Chem. Int. Ed.* **2012**, *51*, 12051–12054.

(25) Zhang, W.; Moore, J. S. *Angew. Chem. Int. Ed.* **2006**, *45*, 4416–4439.

(26) Zhang, W.; Brombosz, S. M.; Mendoza, J. L.; Moore, J. S. *J. Org. Chem.* **2005**, *70*, 10198–10201.

(27) Jyothish, K.; Wang, Q.; Zhang, W. *Adv. Synth. Catal.* **2012**, *354*, 2073–2078.

(28) Wang, Q.; Zhang, C.; Noll, B. C.; Long, H.; Jin, Y.; Zhang, W. *Angew. Chem. Int. Ed.* **2014**, *53*, 10663–10667.

(29) Yang, H.; Liu, Z.; Zhang, W. *Adv. Synth. Catal.* **2013**, *355*, 885–890.

(30) Fürstner, A.; Davies, P. W. *Chem. Commun.* **2005**, 18, 2307.

(31) Heppekausen, J.; Stade, R.; Goddard, R.; Fürstner, A. *J. Am. Chem. Soc.* **2010**, *132*, 11045–11057.

(32) Asao, N.; Nogami, T.; Lee, S.; Yamamoto, Y. *J. Am. Chem. Soc.* **2003**, *125*, 10921–10925.

(33) Fang, X.-L.; Tang, R.-Y.; Zhang, X.-G.; Zhong, P.; Deng, C.-L.; Li, J.-H. *J. Organomet. Chem.* **2011**, *696*, 352–356.

(34) He, Z.; Xu, X.; Zheng, X.; Ming, T.; Miao, Q. *Chem. Sci.* **2013**, *4*, 4525.

(35) J. Sisto, T.; N. Zakharov, L.; M. White, B.; Jasti, R. *Chem. Sci.* **2016**, *7*, 3681–3688.

(36) Bachrach, S. M.; Zayat, Z.-C. *J. Org. Chem.* **2016**, *81*, 4559–4565.

(37) Iwamoto, T.; Watanabe, Y.; Sadahiro, T.; Haino, T.; Yamago, S. *Angew. Chem. Int. Ed.* **2011**, *50*, 8342–8344.

(38) Wang, Y.; Jiao, M.; Wu, Z.; Irle, S. *J. Phys. Chem. C* **2017**, *121*, 2276–2284.

(39) Darzi, E. R.; Hirst, E. S.; Weber, C. D.; Zakharov, L. N.; Lonergan, M. C.; Jasti, R. *ACS Cent. Sci.* **2015**, *1*, 335–342.

(40) Taber, B. N.; Gervasi, C. F.; Mills, J. M.; Kislitsyn, D. A.; Darzi, E. R.; Crowley, W. G.; Jasti, R.; Nazin, G. V. *J. Phys. Chem. Lett.* **2016**, *7*, 3073–3077.

(41) Fujitsuka, M.; Lu, C.; Iwamoto, T.; Kayahara, E.; Yamago, S.; Majima, T. *J. Phys. Chem. A* **2014**, *118*, 4527–4532.

(42) Omachi, H.; Nakayama, T.; Takahashi, E.; Segawa, Y.; Itami, K. *Nat. Chem.* **2013**, *5*, 572–576.

(43) Nishiuchi, T.; Feng, X.; Enkelmann, V.; Wagner, M.; Müllen, K. *Chem. – Eur. J.* **2012**, *18*, 16621–16625.

(44) Golling, F. E.; Quernheim, M.; Wagner, M.; Nishiuchi, T.; Müllen, K. *Angew. Chem. Int. Ed.* **2014**, *53*, 1525–1528.

APPENDIX

Table of Contents

A. **Materials.** All reagents were purchased from commercial sources and used without further purification. Tetrahydrofuran was purchased from commercial sources and purified using a custom-built alumina-column based solvent purification system. HN(*i*Pr)$_2$ was purchased from commercial sources and purified by distillation. Other solvents were purchased from commercial sources and used without further purification.

Instrumentation. Infrared spectra were recorded on a Thermo Nicolet iS10 with a diamond ATR attachment and are uncorrected. UV/Vis absorbance spectra were recorded on a Cary 5000 UV-Vis-NIR spectrophotometer with an Hg lamp.

Gas chromatography/electron impact mass spectrometry was performed on an Agilent 6890N Network GC System with a JEOL JMS-GCmate II Mass Spectrometer (magnetic sector). DART MS was performed on an Exactive Plus Orbitrap Mass Spectrometer with a DART SVP ion source from Ion Sense.

NMR spectra of solutions were recorded on a Varian 400 spectrometer with an ASW probe with a 20 MHz sample spin rate. 2D NMR were recorded on a Varian 500 MHz spectrometer using a standard DBG probe. All spectra, unless otherwise stated, were recorded at ambient temperature.

B. Synthetic Procedures

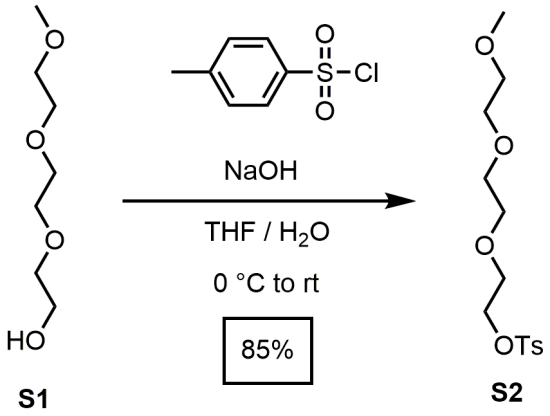

Synthesis of S2: Sodium Hydroxide (3.129g, 78.22 mmol) and triethylene glycol monomethyl ether (10.00 g, 60.90 mmol) was dissolved in 46 mL of a 4:1 THF/H_2O mixture and allowed to stir at rt. After 30 min the reaction mixture was placed in an ice water bath and 4-toluenesulfonyl chloride (11.61 g, 60.90 mmol) was slowly added. After 12 h, the reaction was washed with aqueous 2 M HCl (20 mL) and the product was extracted with CH_2Cl_2 (3 x 15 mL). The organic fractions were collected and dried with Na_2SO_4, filtered and the solvent was removed under vacuum to give **S2** as a clear oil (16.543 g, 85%). ^{1}H and ^{13}C spectra matched previously reported spectra.[1]

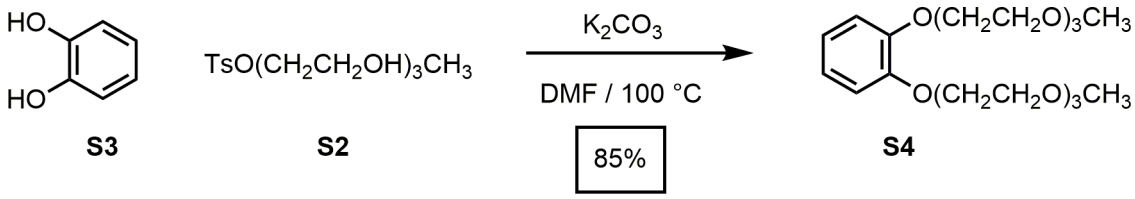

Synthesis of S4: Potassium carbonate (12.60 g, 91.19 mmol) and 1,2-dihydroxybenzene (2.497 g, 22.67 mmol) were transferred to a flame-dried flask and purged with nitrogen 3 times. Anhydrous DMF (50 mL) was transferred into the reaction flask and heated in

an 80 °C oil bath before **S2** (15.23 g, 47.84 mmol) was transferred to the reaction flask. After one hour, the reaction is washed with 2 M HCl (50 mL) and extracted with CH_2Cl_2 (3 x 20 mL) then with distilled H_2O (5 x 20 mL). The organic fractions were collected, dried (Na_2SO_4), and filtered, and the solvent was removed under vacuum. The crude mixture was purified by column chromatography (SiO_2) with CH_2Cl_2 then acetone to give **S4** as an orange oil (7.759 g, 85%). ^{1}H NMR (500 MHz, $CDCl_3$): δ 6.89 (m, 4 H), 4.15 (t, 4 H), 3.84 (t, 4H), 3.72 (m, 4 H), 3.65 (m, 8 H), 3.53 (m, 4 H), 3.36 (s, 6 H), ^{13}C NMR (125 MHz, $CDCl_3$) ^{13}C NMR (125 MHz, $CDCl_3$) δ 149.11, 121.73, 115.09, 72.03, 70.91, 70.78, 70.64, 69.87, 68.96, 59.12 ppm. IR (solid, ATR) 2871, 1738, 1592, 1502, 1452, 1351, 1328, 1254, 1217, 1199, 1104, 1053, 929, 850, 744 cm$^{-1.}$ HRMS (DART) calcd for $[C_{20}H_{34}O_8+H]^+$ 403.23319, found 403.23301.

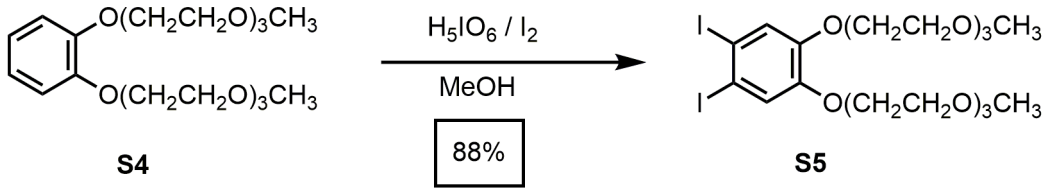

S4 **S5**

Synthesis of S5: H_5IO_6 (1.138 g, 4.992 mmol) and I_2 (2.536 g, 9.991 mmol) were transferred to a round bottom flask and dissolved in methanol (25 mL) at rt. After 20 min, **S4** (5.000 g, 12.42 mmol) was added via syringe and the reaction mixture was heated to 70 °C for 3 h. The reaction mixture was then washed with 2 M HCl (5 mL) and extracted with CH_2Cl_2 (3 x 15 mL). The organic fractions were combined, dried (Na_2SO_4), filtered, and the solvent removed under vacuum to give compound **S5** as a dark red oil (7.169 g, 88%). ^{1}H NMR (500 MHz, $CDCl_3$): δ 7.31 (s, 2 H), 4.10 (t, 4 H), 3.82 (t, 4H), 3.70 (m, 4 H), 3.64 (m, 8 H), 3.53 (m, 4 H), 3.36 (s, 6 H), ^{13}C NMR (125 MHz, $CDCl_3$) ^{13}C NMR (125 MHz, $CDCl_3$) δ 149.68, 130.57, 124.93, 72.05, 71.00,

70.81, 70.70, 69.77, 69.69, 69.28, 59.17.ppm. IR (solid, ATR) 2871, 1738, 1573, 1489, 1450, 1351, 1335, 1286, 1244, 1197, 1101, 1050, 941, 849, 636 $cm^{-1.}$ HRMS (DART) calcd for $[C_{20}H_{32}O_8I_2+H]^+$ 655.02648, found 655.02669.

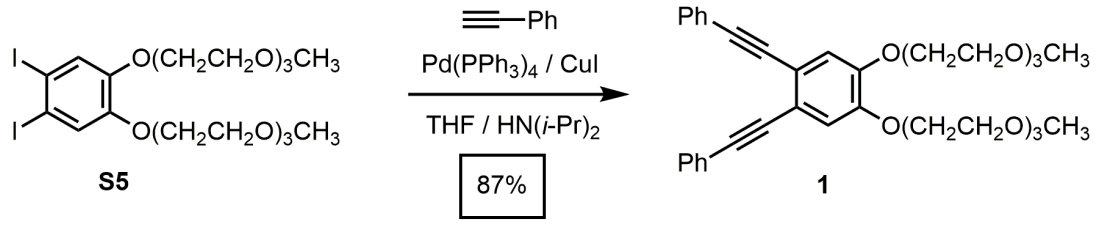

Synthesis of 1: $Pd(PPh_3)_2Cl_2$ (0.214 g, 0.305 mmol) and CuI (0.120 g, 0.630 mmol) were transferred to a flask and purged three times with nitrogen. **S5** (4.025g, 6.137 mmol) was dissolved in anhydrous THF (60 mL) and HN(*i*-Pr)$_2$ (30 mL) and sparged for 30 min with nitrogen before being transferred to the reaction mixture via cannula. Phenyl acetylene (1.3 mL, 12 mmol) was sparged for 30 min and added to the reaction mixture via syringe and the reaction was allowed to stir at rt. After 12 h the reaction was washed with 2 M HCl (30 mL) and extracted with CH_2Cl_2 (3 x 15 mL). The organic fractions were combined, dried (Na_2SO_4), filtered, and the solvent was removed under vacuum. The crude reaction mixture was purified by column chromatography (SiO_2) with CH_2Cl_2 then acetone to give **1** as a dark red oil (3.218 g, 87%). ^{1}H NMR (500 MHz, $CDCl_3$): δ 7.55 (m, 4 H), 7.32 (m, 6 H), 7.07 (s, 2 H), 4.20 (t, 4 H), 3.88 (t, 4H), 3.75 (m, 4 H), 3.67 (m, 8 H), 3.54 (m, 4 H), 3.37 (s, 6 H), ^{13}C NMR (125 MHz, $CDCl_3$) ^{13}C NMR (125 MHz, $CDCl_3$) δ 148.98, 131.60, 128.45, 128.29, 123.57, 119.32, 116.80, 92.39, 88.46, 72.04, 71.05, 70.82, 70.70, 69.69, 68.89, 59.14 ppm. IR (solid, ATR) 2872, 1738, 1592, 1510, 1451, 1412, 1351, 1245, 1201, 1103, 1026, 945, 852, 756, 722, 691 $cm^{-1.}$ HRMS (DART) calcd for $[C_{36}H_{43}O_8+H]^+$ 603.29579, found 603.29589.

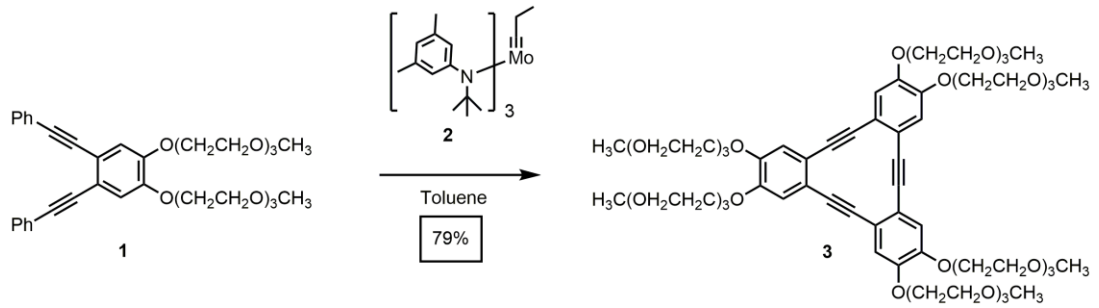

Synthesis of 3: In an N_2 glove box, **1** (0.100 g, 0.166 mmol) and 2 (0.003 mg, 4 µmol) were each dissolved in toluene (2.5 mL) with 1,3,5-tribromobenzene (0.052 g, 0.17 mmol) used as an internal standard and transferred to a Schlenk flask. The reactor was sealed, taken out of a glove box, and placed in an 80 °C oil bath for 24 h. The reaction was then washed with 2 M HCl (5 mL) and extracted with CH_2Cl_2 (3 x 5 mL). The organic fractions were combined, dried (Na_2SO_4), filtered and the solvent removed under vacuum. The crude reaction mixture was purified by preparatory TLC (SiO_2) with acetone : CH_2Cl_2 (7:3) to give **3** as a yellow oil (0.055 g, 79%). ^{1}H NMR (500 MHz, $CDCl_3$): δ 6.75 (s, 6 H), 4.13 (t, 12 H), 3.85 (t, 12 H), 3.74 (m, 12 H), 3.67 (m, 27 H), 3.55 (m, 12 H), 3.37 (s, 18 H), ^{13}C NMR (125 MHz, $CDCl_3$) δ 148.98, 120.23, 116.43, 91.93, 72.05, 71.03, 70.83, 70.70, 69.62, 68.69, 59.18 ppm. IR (solid, ATR) 2873, 1592, 1510, 1592, 1454, 1347, 1230, 1198, 1106, 1073, 947, 853, 721, 694, 668 cm^{-1}. HRMS (DART) for $[C_{66}H_{96}O_{24}+H]^+$ calculated: 1273.63643 measured 1273.63420

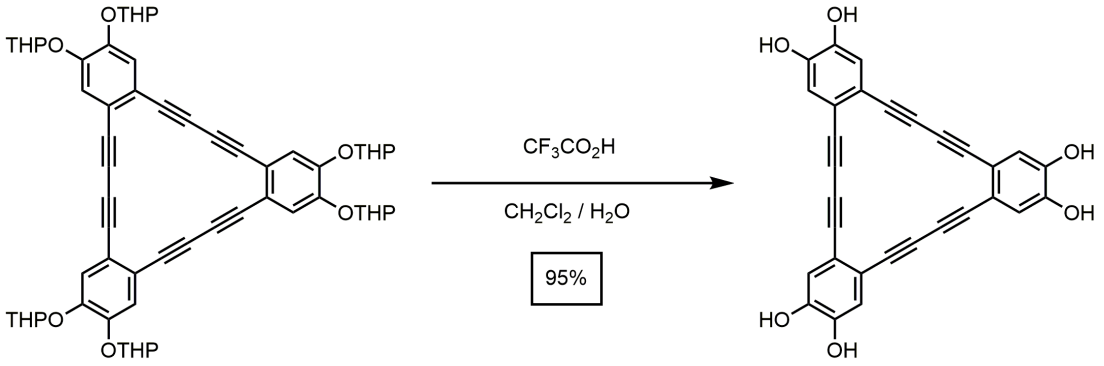

DBA[18]-OTHP **6**

Synthesis of 6: To a solution of DBA[18]-OTHP (0.101 g, 0.102 mmol) in 10:1 CH_2Cl_2 : H_2O (15 mL) was added dropwise trifluoroacetic acid (1 mL). The reaction mixture stirred for 1.5 hours at rt and then the product was filtered and washed with H2O, CH2Cl2, and hexanes to afford the title compound DBA[18]-OH (0.046 g, 95% yield) as a yellow-green solid. The ^{1}H and ^{13}C NMR correspond to the spectra reported by McGrier and coworkers.[2]

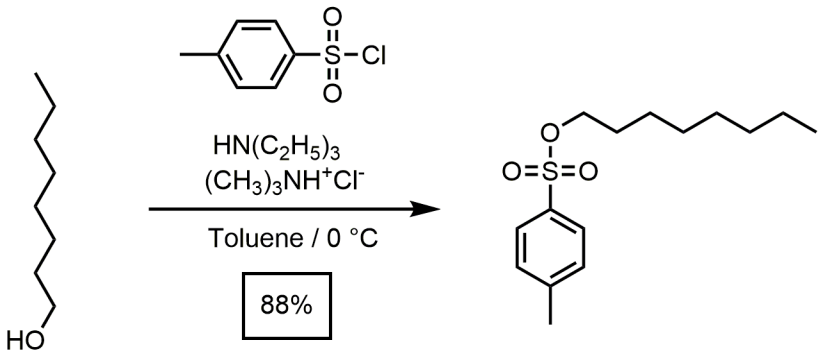

S6 **7**

Synthesis of 7: **S6** (5.005 g, 38.39 mmol), and toluenesulfonyl chloride (11.013 g, 57.77 mmol) were transferred to a roundbottom flask containing 75 mL of anhydrous toluene with trimethylamine (10 mL, 80 mmol) and N-trimethylamine hydrochloride (0.389 g, 4.07 mmol). This was stirred in an ice bath for 3 hours before water (50 mL was added to the reaction mixture, which was extracted with CH_2Cl_2 (3 x 50 mL). The organic

fractions were collected, dried with $MgSO_4$, filtered and concentrated. The crude product was purified by silica-gel chromatography (hexane/ether = 9:1) to give **7** as colorless oil. 1H and 13C NMR spectra matched previously reported values. [3]

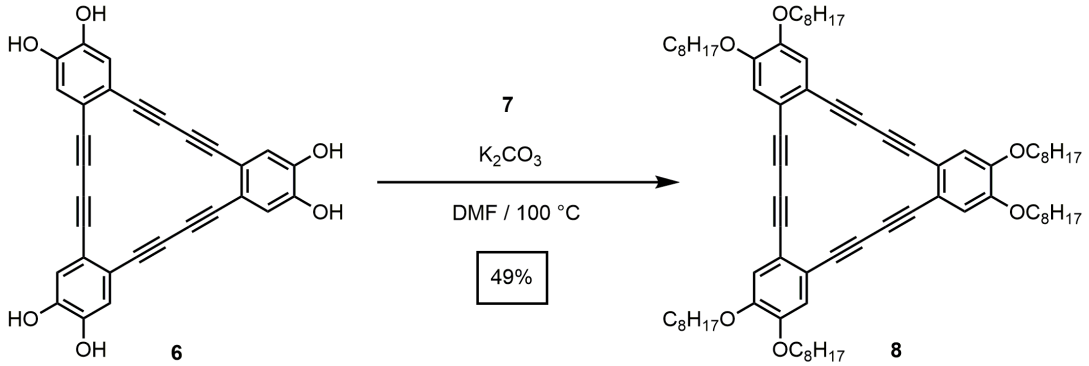

Synthesis of 8: 6 (0.040 g, 0.085 mmol), **7** (0.500 g, 1.75 mmol), and K_2CO_3 (0.145 g, 1.05 mmol) were transferred to a flame dried round bottom flask before being dissolved in anhydrous DMF (0.9 mL). The reaction mixture was placed in a 100 °C oil bath for 1 h until completion. Once the flask had cooled to rt, 2M HCl was added (10 mL) and the reaction was extracted with CH_2Cl_2 (3 x 5 mL). The organic fractions were collected and dried with $MgSO_4$ before removing the solvent under vacuum. The mixture was dissolved in a minimum amount of CH_2Cl_2 and precipitated into 5 mL of MeOH. **8** was isolated after filtration as a white solid (0.047g, 49 %). ^{1}H NMR (400 MHz, $CDCl_3$): δ 7.10 (s, 6 H), 4.04 (t, 12 H), 1.85 (p, 12H), 1.48 (p, 12 H), 1.40-1.28 (m, 48 H) ppm. ^{13}C NMR (125 MHz, $CDCl_3$) δ 149.9, 118.5, 116.1, 81.1, 69.4, 32.0, 29.5, 29.4, 29.3, 29.1, 26.1, 22.8, 14.26 ppm IR (solid, ATR) 2926, 2855, 2590, 1504, 1468, 1434, 1349, 1252, 1206, 1017, 905, 729 cm^{-1} HRMS (DART) for $[C_{78}H_{108}O_6+H]^+$ calculated: 1141.82187 measured 1141.81723 m/z

General Procedure for Benzannulation of Macrocycles

Benzaldehyde (2 eq) and $Cu(OTf)_2$ (0.1 eq) are transferred to a small test tube reaction flask capped with a rubber septa, evacuated, and backfilled with N_2. The macrocycle (0.020 mg) is dissolved in $C_2H_4Cl_2$ (0.25 mL) and is transferred to a reaction vessel. The reaction vessel was then heated to 100 °C over night and was monitored by thin layer chromatography and MALDI-TOF mass spectrometry.

C. 1D NMR Spectroscopy

Figure S3.1. ^{1}H NMR of **S4** (400 MHz, $CDCl_3$, 298 K)

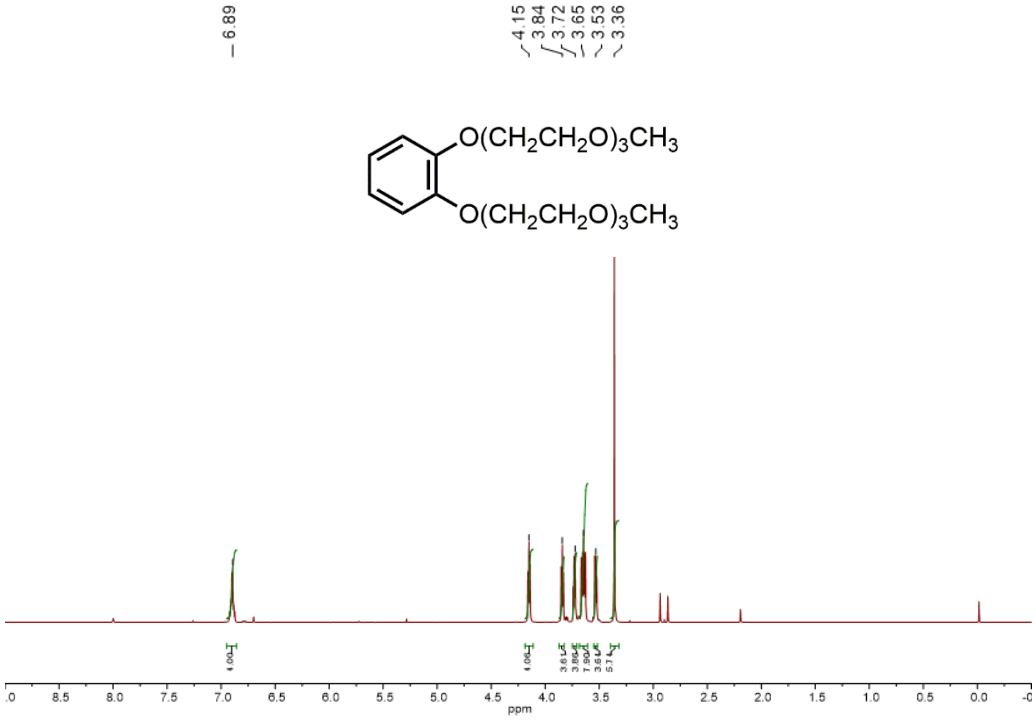

Figure S3.2. ^{13}C NMR of **S4** (100 MHz, $CDCl_3$, 298 K)

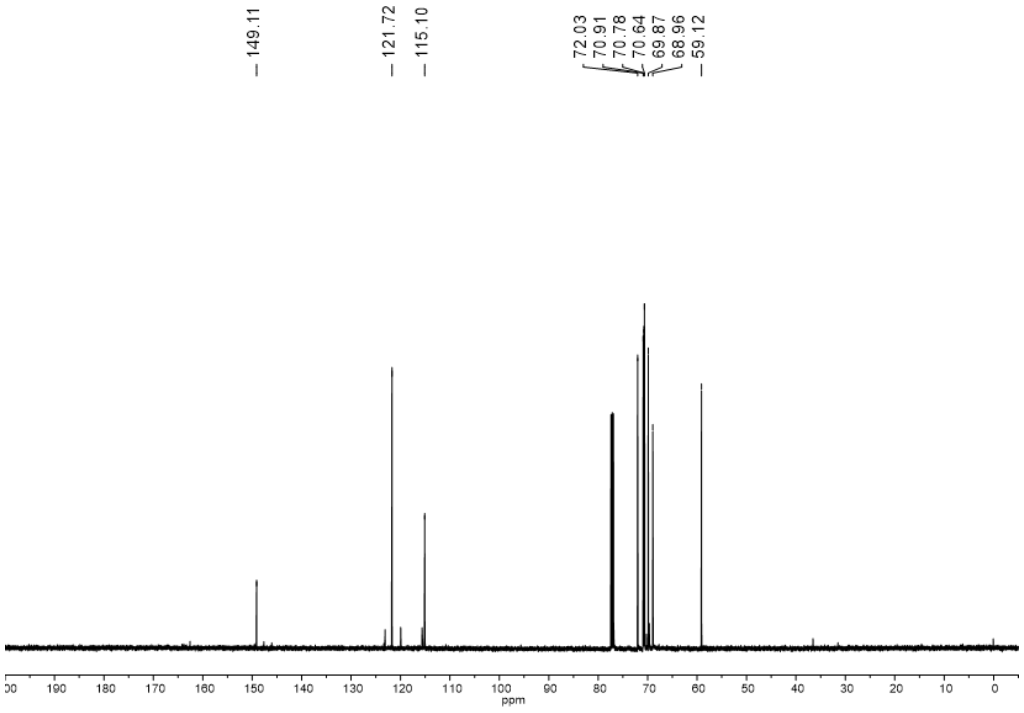

Figure S3.3. ^{1}H NMR of **S5** (500 MHz, $CDCl_3$, 298 K)

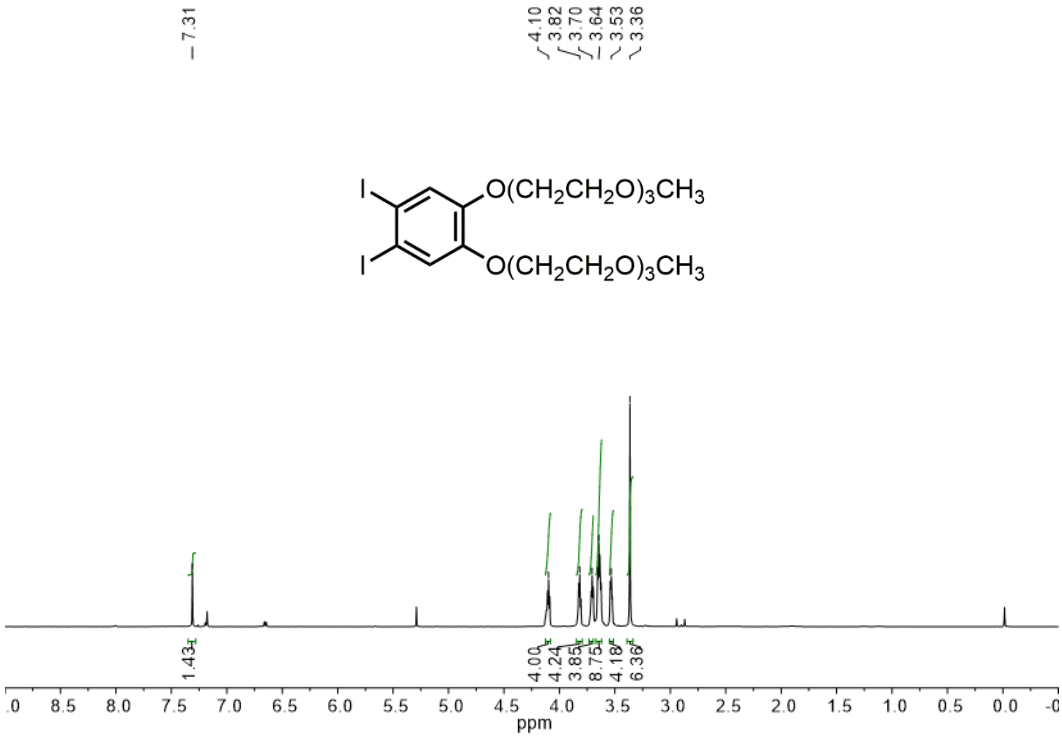

Figure S3.4. ^{13}C NMR of **S5** (125 MHz, $CDCl_3$, 298 K)

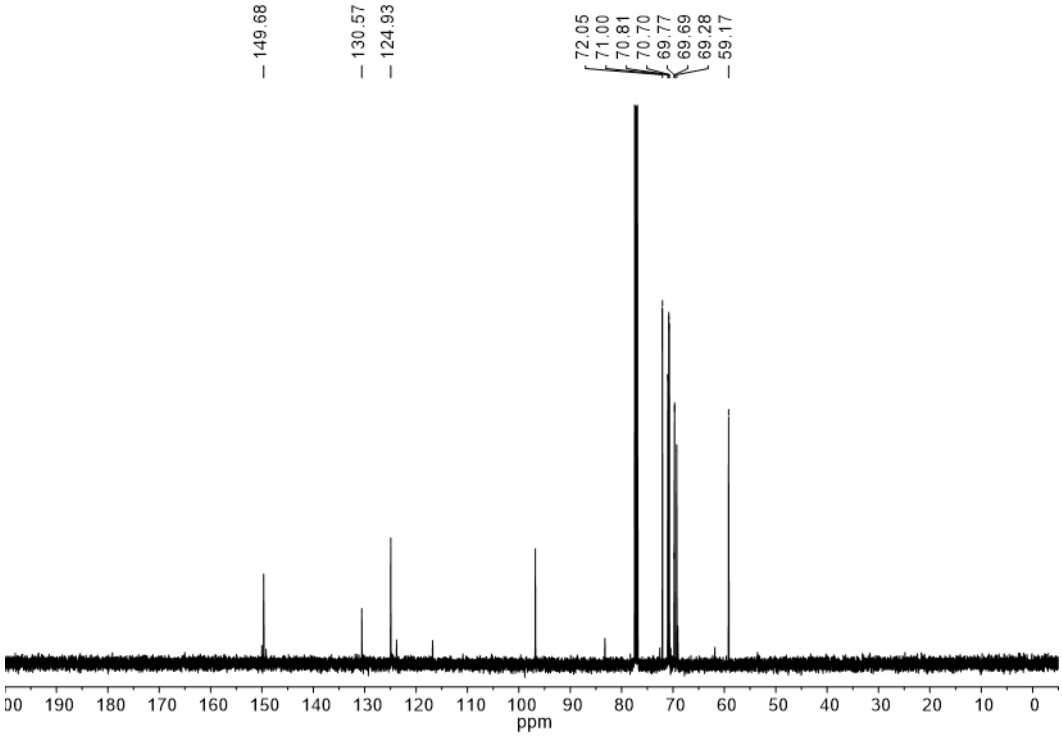

Figure S3.5. ^{1}H NMR of **1** (500 MHz, $CDCl_3$, 298 K)

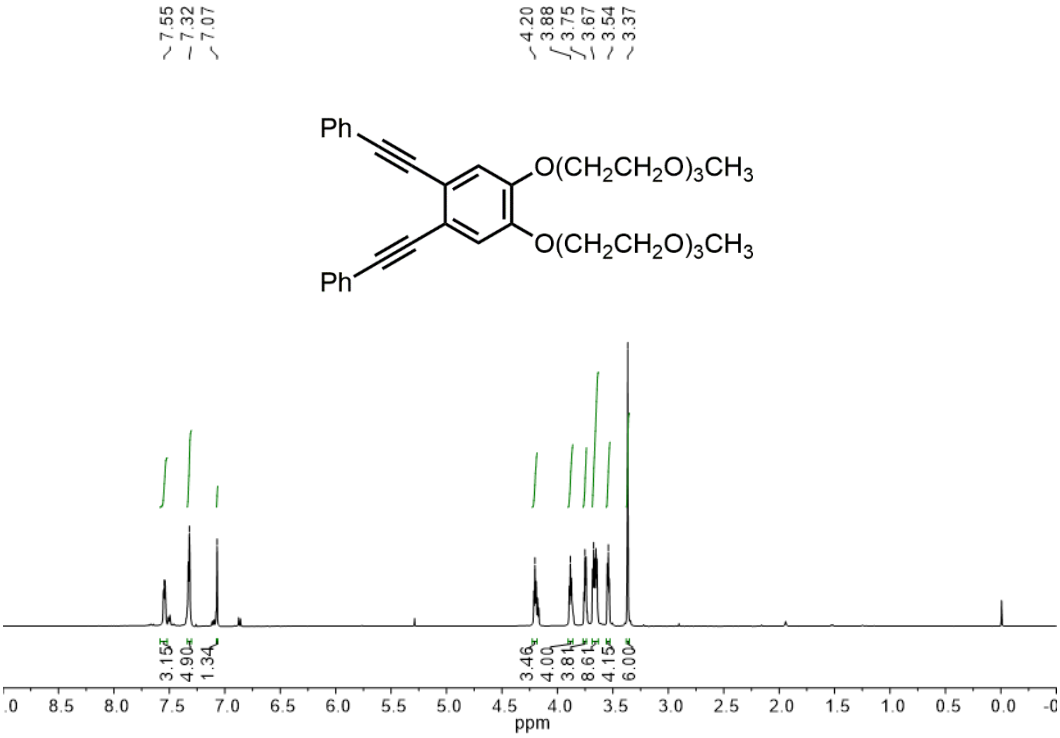

Figure S3.6. ^{13}C NMR of **1** (125 MHz, $CDCl_3$, 298 K)

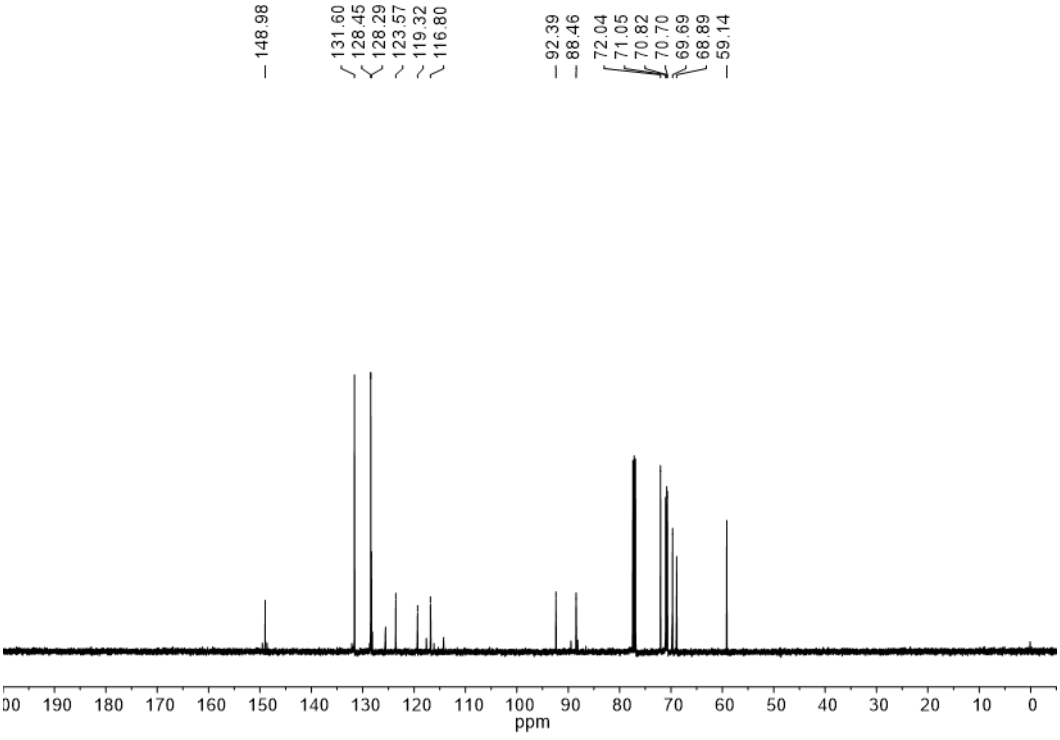

Figure S3.7. ^{1}H NMR of **3** (100 MHz, $CDCl_3$, 298 K)

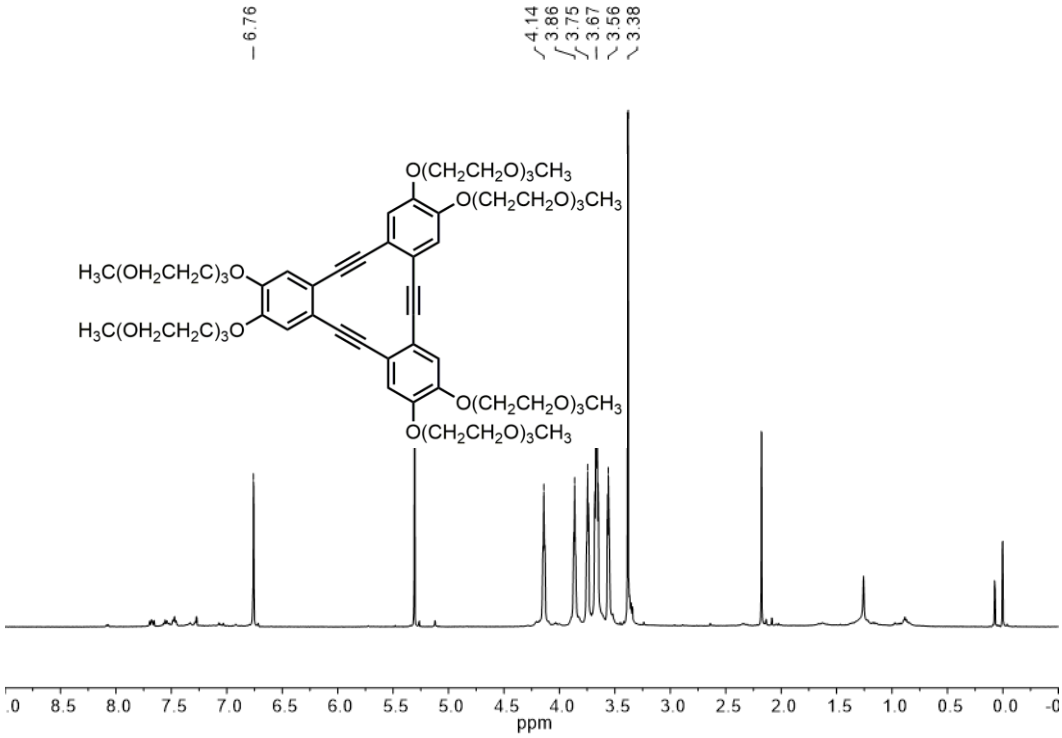

Figure S3.8. ^{13}C NMR of **3** (100 MHz, $CDCl_3$, 298 K)

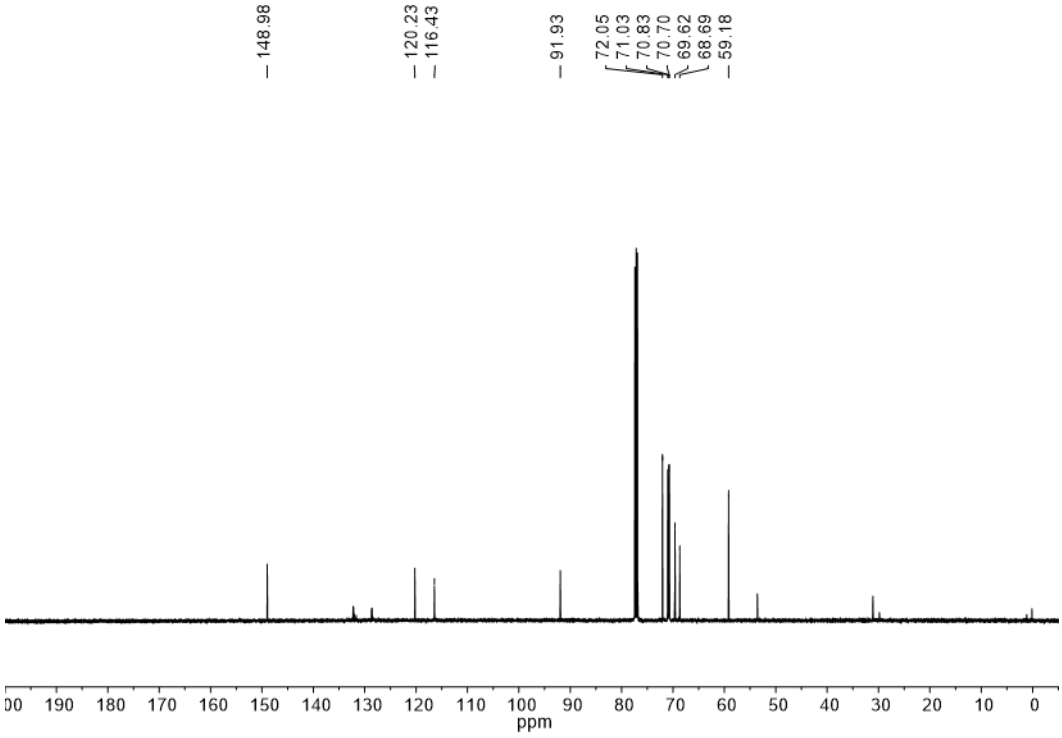

Figure S3.9. ^{13}H NMR of **8** (500 MHz, $CDCl_3$, 298 K)

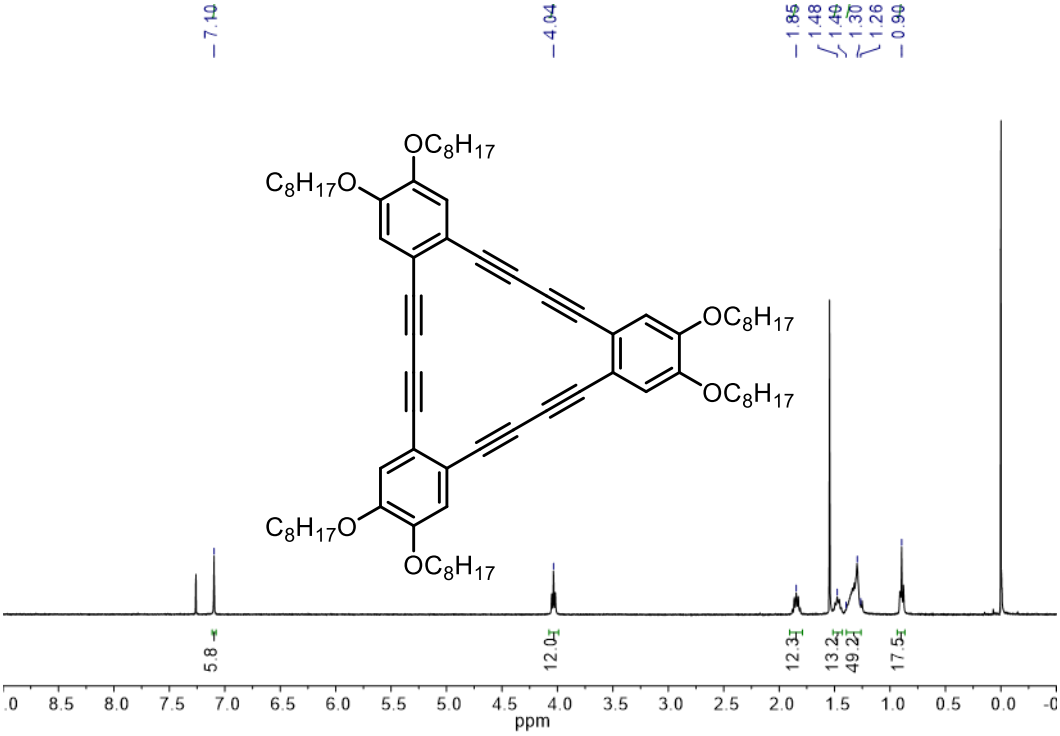

Figure S3.10. ^{13}C NMR of **8** (120 MHz, $CDCl_3$, 298 K)

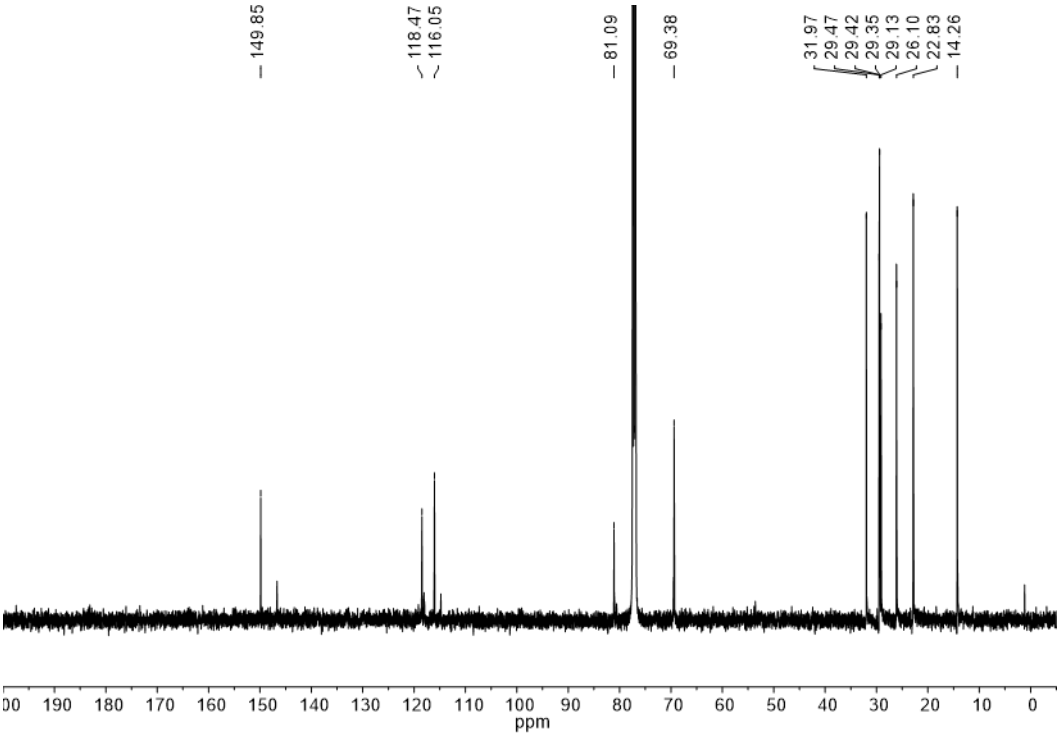

E. MALDI-TOF

Figure S3.11. MALDI-TOF-MS of crude benzannulation reaction mixture between **3** (1 equiv) **4a** (2 equiv), CF_3CO_2H (5 equiv), $Cu(OTf)_2$ (0.1 equiv).

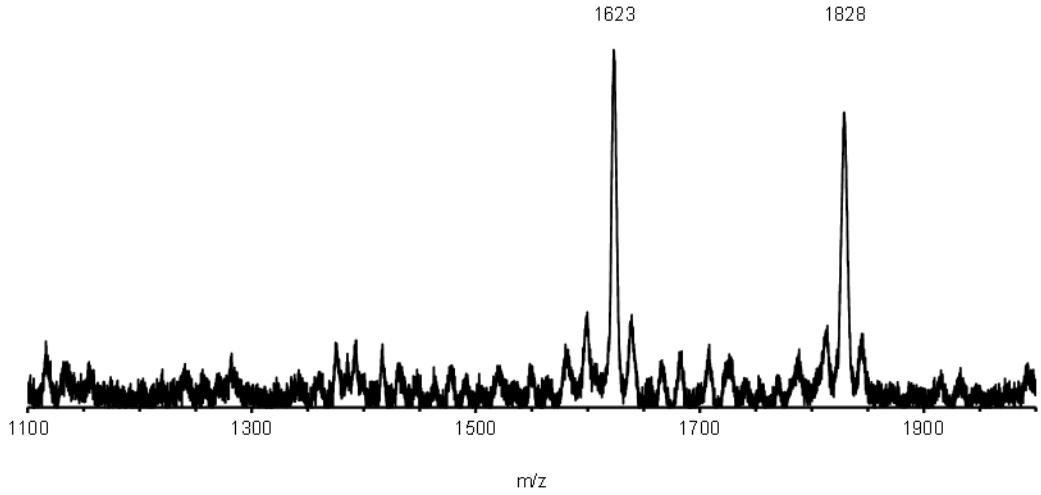

Figure S3.12: MALDI-TOF-MS of crude benzannulation reaction mixture between **3** (1 equiv) **4a** (2 equiv), AcOH (5 equiv), $Cu(OTf)_2$ (0.1 equiv).

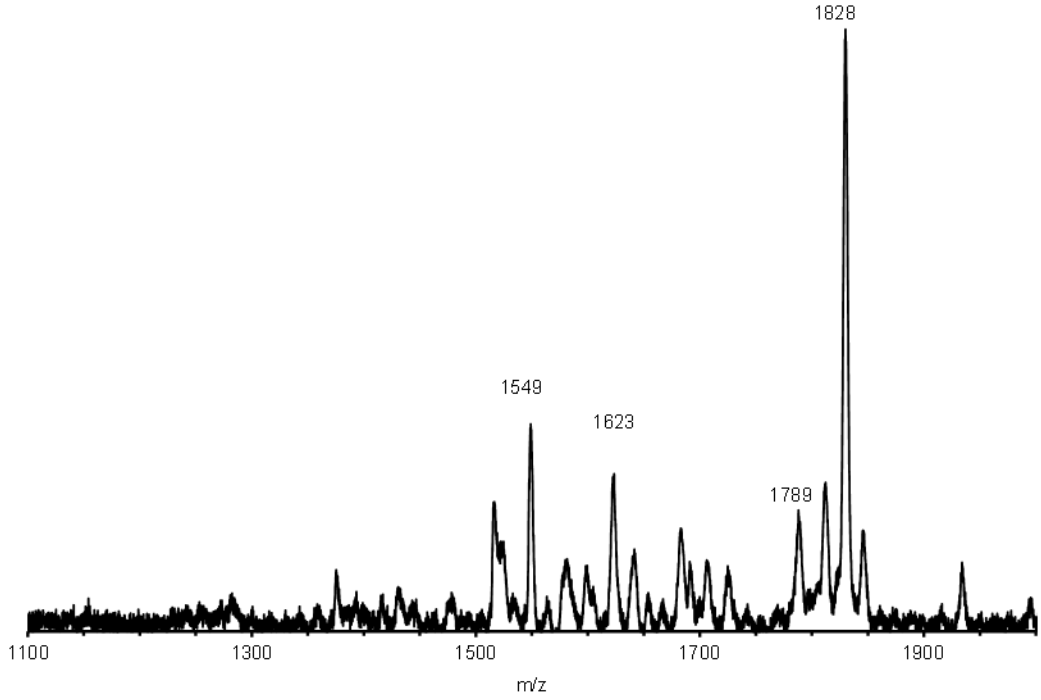

Figure S3.13. Potential structures for identifiable MALDI-TOF peaks when **3** undergoes benzannulation with **4a**.

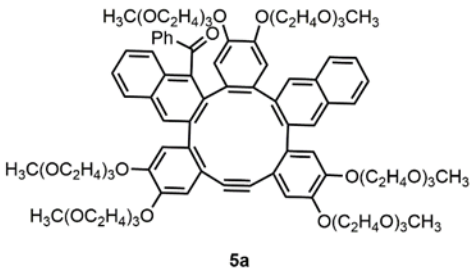

5a

Molecular Weight: 1581.85

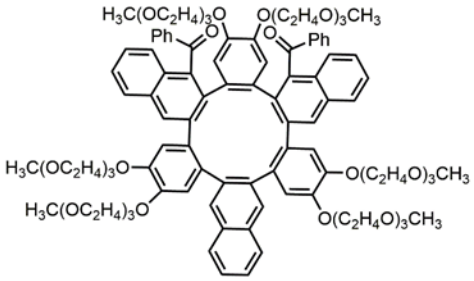

5b

Molecular Weight: 1788.09

Figure S3.14. MALDI-TOF-MS of crude benzannulation reaction mixture between **8** (1 equiv) **4a** (2 equiv), CF_3CO_2H (5 equiv), $Cu(OTf)_2$ (0.1 equiv).

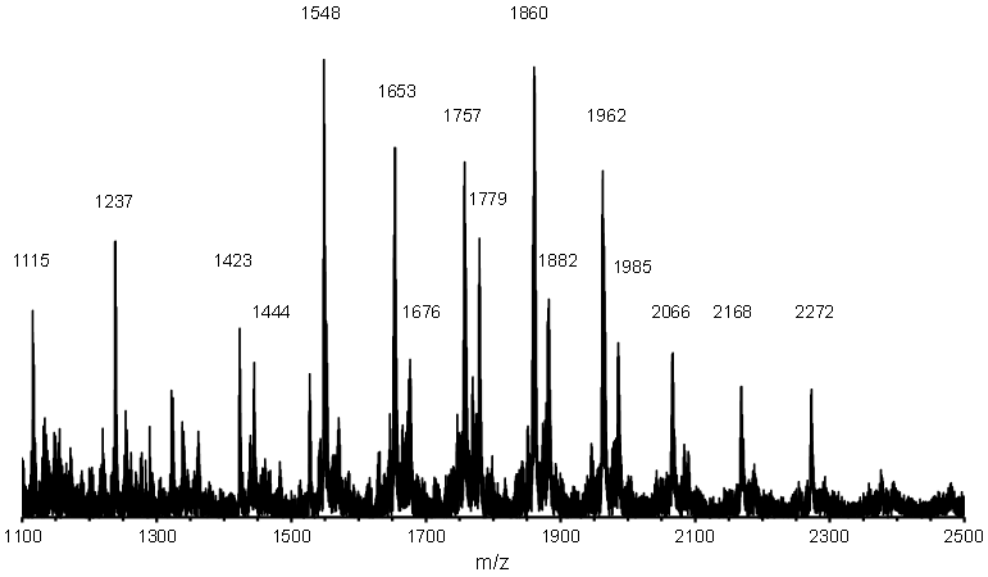

Figure S3.15. MALDI-TOF-MS of crude benzannulation reaction mixture between **8** (1 equiv) **4a** (4 equiv), $ZnCl_2$ (0.1 equiv).

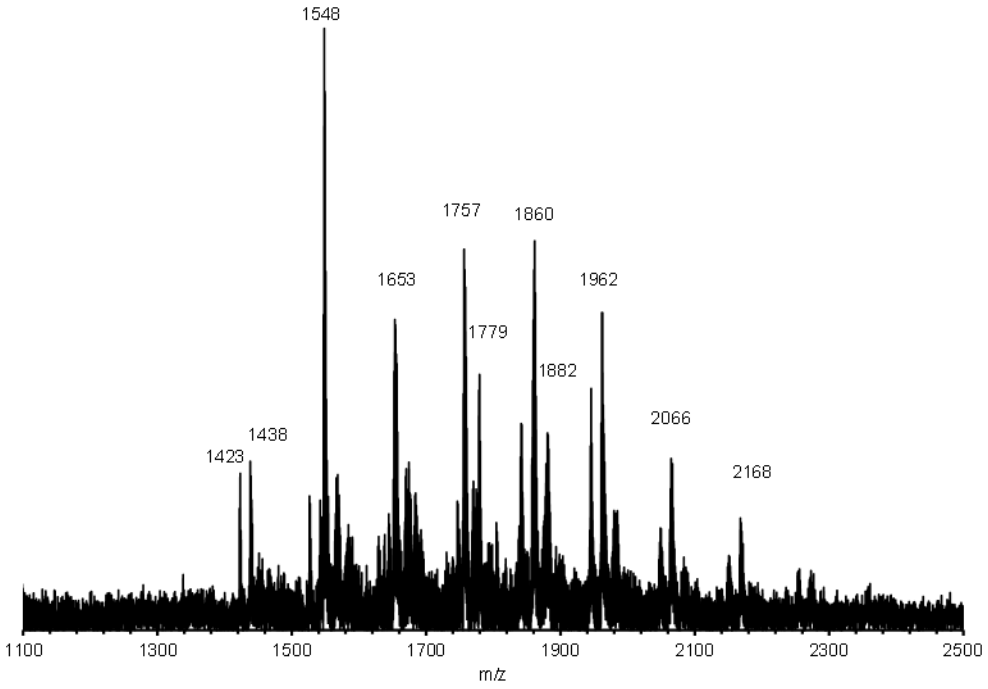

Figure S3.16. MALDI-TOF-MS of crude benzannulation reaction mixture between 8 (1 equiv) 4a (4 equiv), CF3CO2H (1 equiv), Cu(OTf)2 (0.1 equiv).

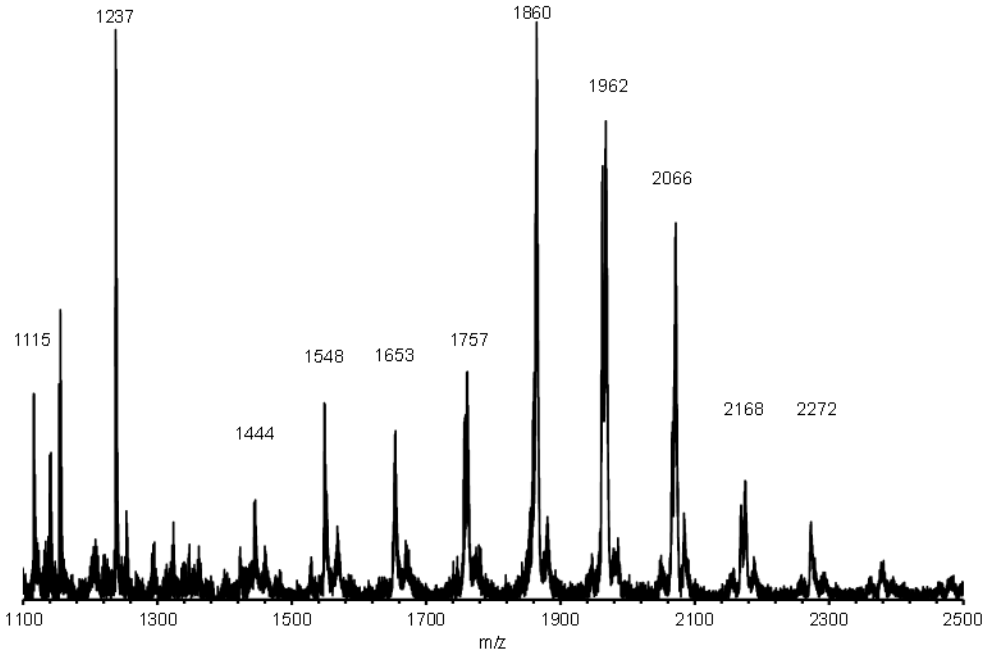

Figure S3.17. MALDI-TOF-MS of crude benzannulation reaction mixture between **8** (1 equiv) **4a** (4 equiv), CF_3CO_2H (5 equiv), $Cu(OTf)_2$ (0.1 equiv).

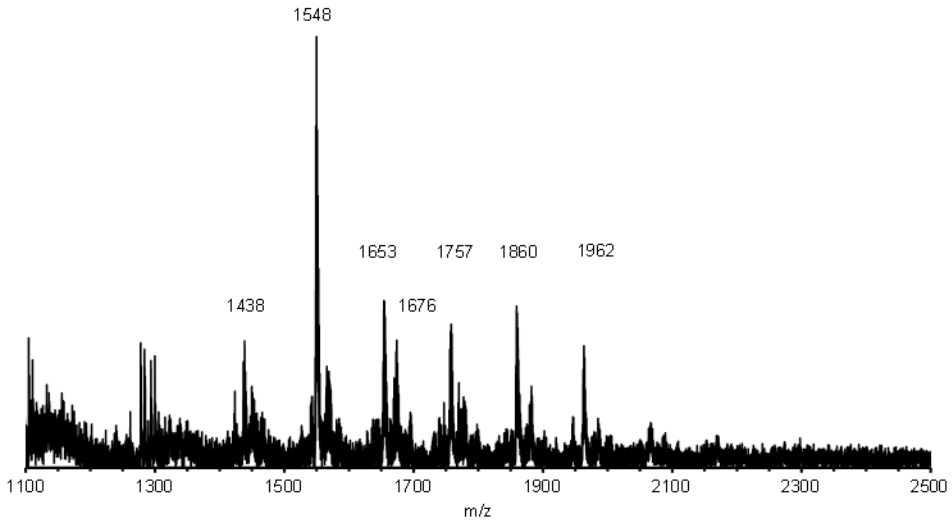

Figure S3.18. Potential structures for all identifiable MALDI-TOF peaks when **8** undergoes benzannulation with **4a**.

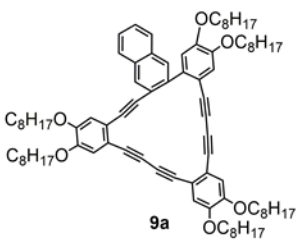

9a
Molecular Weight: 1243.85

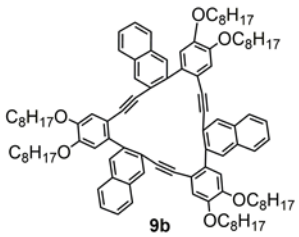

9b
Molecular Weight: 1448.12

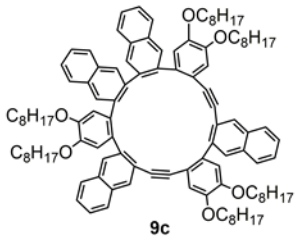

9c
Molecular Weight: 1550.26

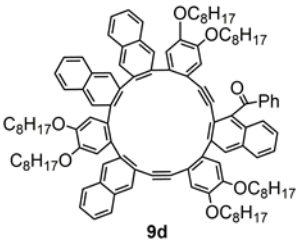

9d
Molecular Weight: 1654.37

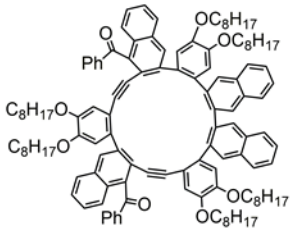

9e
Molecular Weight: 1758.48

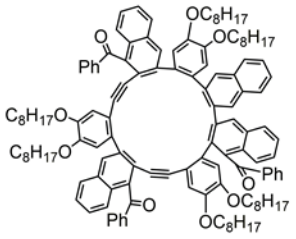

9f
Molecular Weight: 1862.58

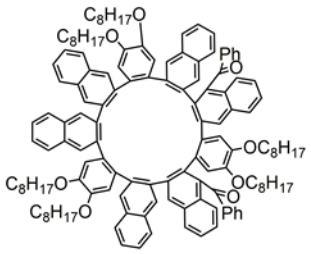

9g
Molecular Weight: 1962.75

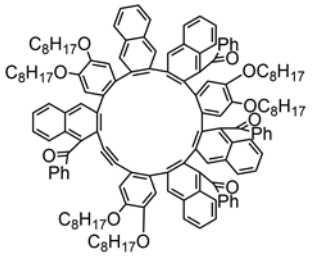

9h
Molecular Weight: 2068.83

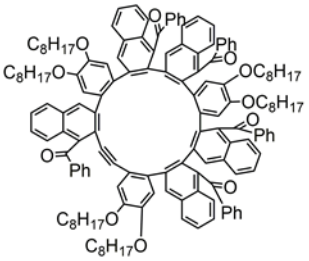

9i
Molecular Weight: 2172.94

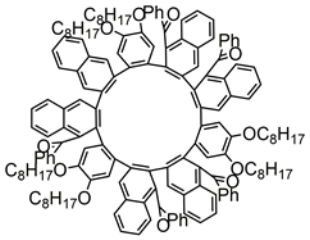

Molecular Weight: 2275.07
9j

Figure S3.19. MALDI-TOF-MS of crude benzannulation reaction mixture between **8** (1 equiv) **4b** (2 equiv), CF_3CO_2H (5 equiv), $Cu(OTf)_2$ (0.1 equiv).

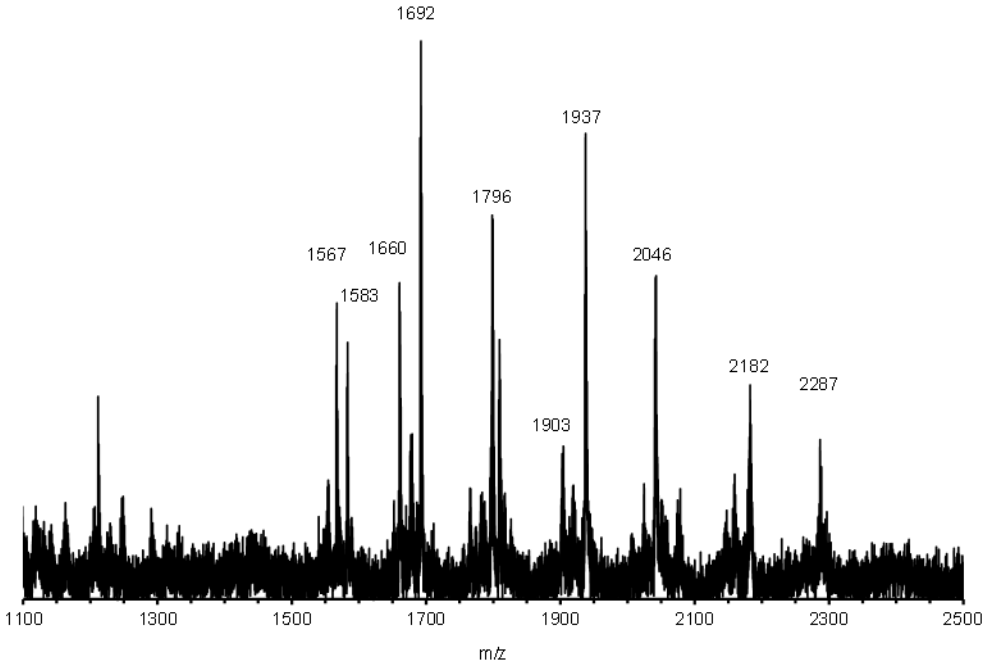

Figure S3.20. MALDI-TOF-MS of crude benzannulation reaction mixture between **8** (1 equiv) **4b** (2 equiv), AcOH (5 equiv), $Cu(OTf)_2$ (0.1 equiv).

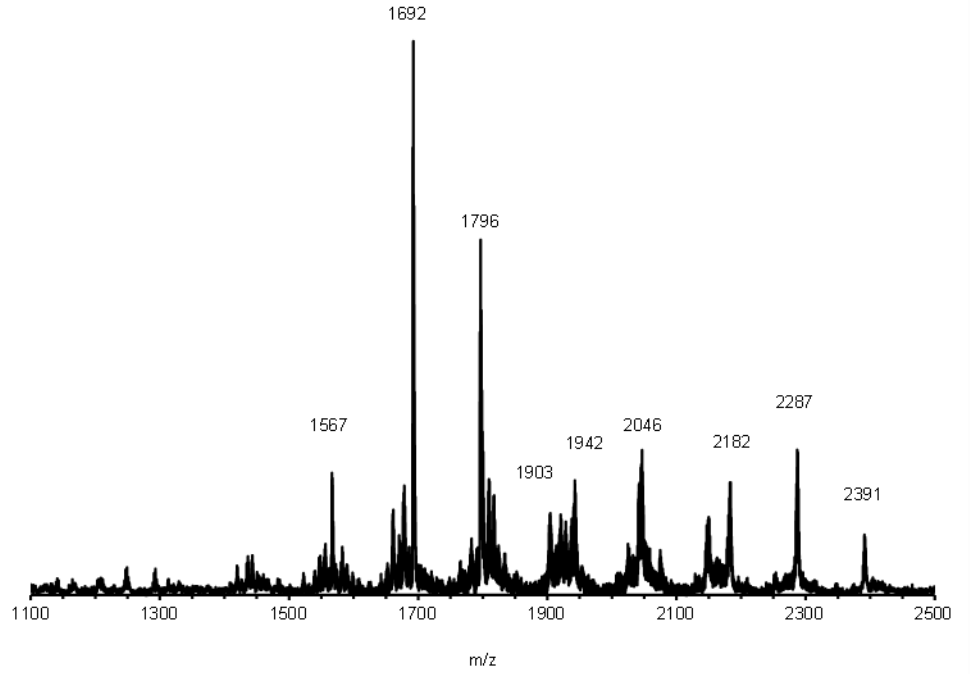

Figure S3.21. MALDI-TOF-MS of crude benzannulation reaction mixture between **8** (1 equiv) **4b** (4 equiv), CF_3CO_2H (1 equiv), AcOH (4 equiv), $Cu(OTf)_2$ (0.1 equiv).

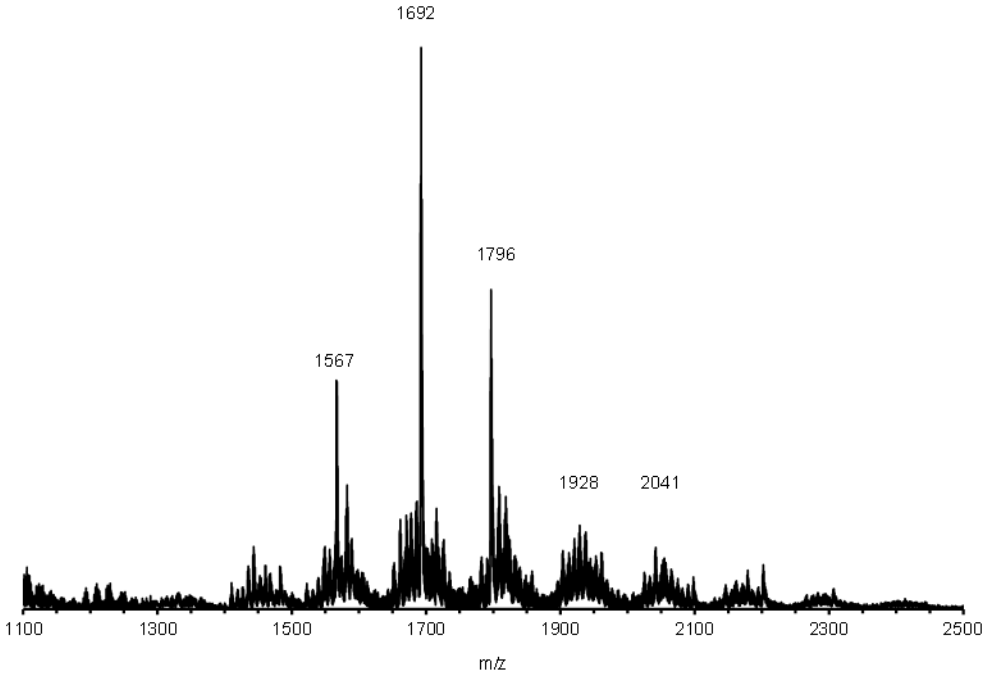

Figure S3.22. MALDI-TOF-MS of crude benzannulation reaction mixture between **8** (1 equiv) **4b** (2 equiv), CF_3CO_2H (5 equiv), CF_3CO_2Na (4 equiv), $Cu(OTf)_2$ (0.1 equiv).

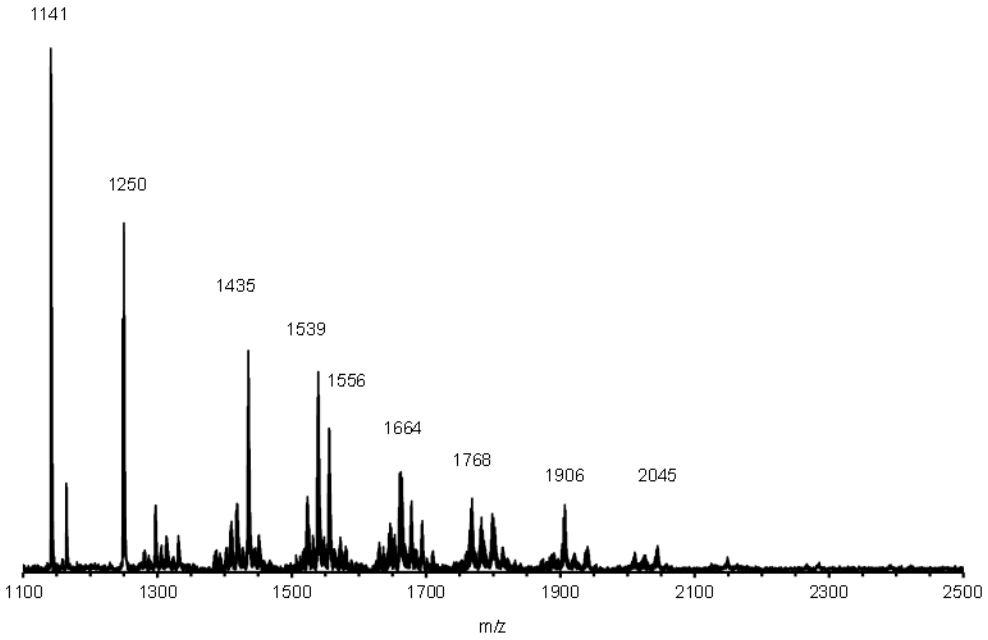

Figure S3.23. MALDI-TOF-MS of crude benzannulation reaction mixture between **8** (1 equiv) **4b** (2 equiv), CF_3CO_2H (5 equiv), $Zn(OTf)_2$ (0.1 equiv).

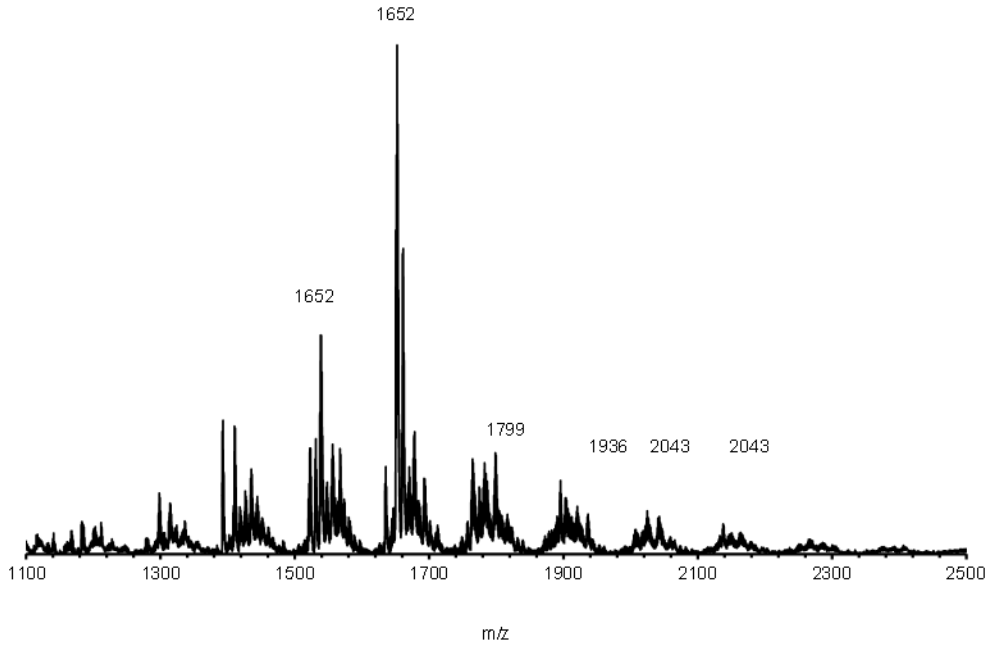

Figure S3.24. Potential structures for all identifiable MALDI-TOF peaks when **8** undergoes benzannulation with **4b**.

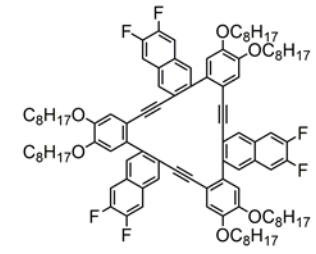

10a
Molecular Weight: 1556.07

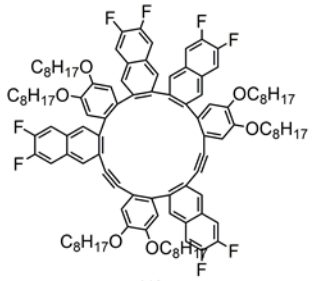

10b
Molecular Weight: 1694.18

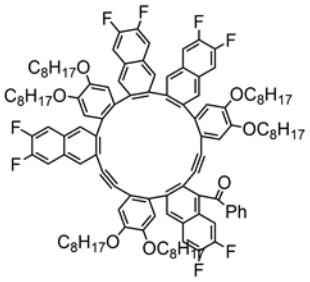

10c
Molecular Weight: 1798.29

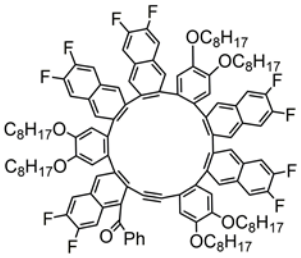

10d
Molecular Weight: 1936.41

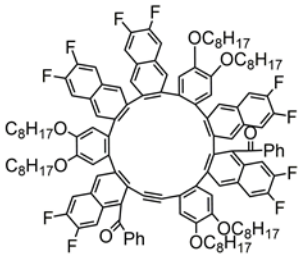

10e
Molecular Weight: 2040.52

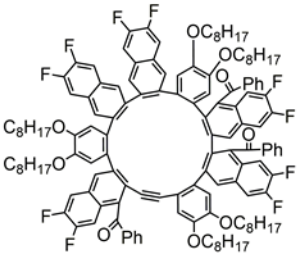

10f
Molecular Weight: 2144.62

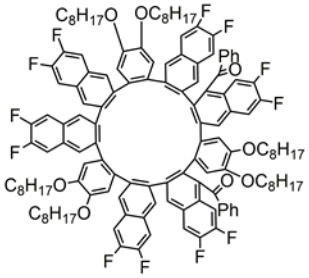

10g
Molecular Weight: 2178.63

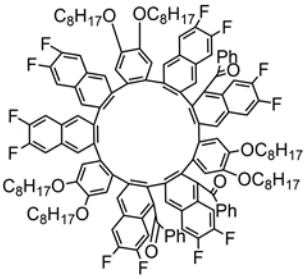

10h
Molecular Weight: 2282.74

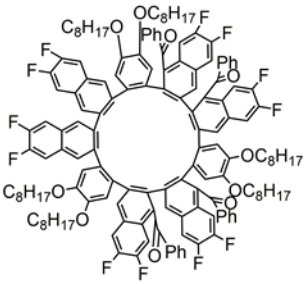

10i
Molecular Weight: 2386.85

G. References for Appendix

1) Kohmoto, S., Mori, E., Kishikawa, K., *J. Am. Chem. Soc.*, **2007**, *129,* 13364–13365

2) Baldwin L. A., Crowe J. W., Shannon M. D., Jaroniec C. P., McGrier P. L., *Chem. Mater.*, **2015**, *27,* 6169–6172

3) Yoshida Y., Sakakura Y., Aso N., Okada S., Tanabe Y., *Tetrahedron*, **1999,** *55*, 2183-2192

CHAPTER FOUR

RAPID ACCESS TO SUBSTITUTED 2-NAPHTHYNE INTERMEDIATES VIA THE BENZANNULATION OF HALOGENATED SILYLACETYLENES

4.1 Abstract

The versatility of aryne intermediates have made them indispensable building blocks for natural product and polymer synthesis. Because relatively few methods provide appropriately substituted precursors, 2-naphthynes, particularly those with other substituents, are relatively unexplored. Here we report a general synthetic strategy to access 2-naphthyne precursors through an Asao-Yamamoto benzannulation of ortho-(phenylethynyl)benzaldehydes with halo-silylacetylenes. This transformation provides 2-halo-3-silylnaphthalenes with high regioselectivity. These naphthalene products undergo desilylation/dehalogenation in the presence of F– to generate the corresponding 2-naphthyne intermediate, as evidenced by isolating its net [4+2] adduct with furan. When these 2-naphthynes are generated in the presence of a copper catalyst, ortho-naphthalene oligomers, trinaphthalene, and binaphthalene products can be selectively synthesized and isolated by controlling catalyst loading and reaction temperature. The efficiency, mild conditions, and versatility of the naphthalene products and naphthyne intermediates will provide efficient access to many new functional aromatic systems.

4.2 Introduction

Arynes represent a reactive class of intermediate species produced from the elimination of two functional groups on an *ortho*-substituted aromatic ring.[1] These compounds have a long, rich history in organic chemistry dating back to 1902 when Stoermer and Kalhert

first speculated their existence.[2] In 1927, Wittig and coworkers corroborated the existence of this intermediate[3] and in 1953 Roberts and coworkers published the first strong evidence to support the structure of *ortho*-benzyne.[4] Since this time, arynes have received much attention from the scientific community as their synthetic versatility continues to be explored. Transformations involving nucleophilic additions and multicomponent coupling reactions, bond insertions, and Diels-Alder pericyclic reactions have made arynes an indispensable intermediate in the synthesis of more than 75 natural products since their first use in 1967 in the synthesis of cryptaustoline and cryptowoline.[5–21] In the field of polycyclic aromatic hydrocarbons, Diels-Alder pericyclic reactions, alkyne trimerizations, and transition-metal mediated reactions have made arynes a useful synthetic tool for the construction of highly substituted aromatic systems. [22–37]

Due to the harsh conditions required to generate arynes, their synthetic scope was rather limited. Strong bases, such as sodium amide, organolithium compounds, or Grignard reagents, were required to eliminate an aryl halide through deprotonation of an *ortho*-proton. These conditions, while effective, limited the scope of potential synthetic applications due to the substrates intolerance to these harsh reagents. Benzenediazonium 2-carboxylates proved to be a more mild method for aryne generation that did not require the addition of a strong base but, the use of potentially explosive diazonium precursors was a serious drawback.[38] Alternative aryne generation methods needed to be developed before aryne chemistry could be widely used. In 1973, Dexheimer and Cunico reported *ortho*-silylaryl halides capable of generating benzynes with potassium *t*-butoxide, but, low yields of this transformation limited its synthetic

utility.[39] A turning point occurred in 1983 when Kobayashi *et. al.* reported efficient aryne generation from *ortho*-silylaryl triflates.[40] *ortho*-Silylaryl triflates are bench stable and easily generate arynes with the addition of a fluoride source. This method tolerates a wide range of previously incompatible functional groups and the rate of aryne generation can be simply controlled through the choice of fluoride and solvent.

However, many *ortho*-silylaryl triflates are not commercially available and the synthesis of substituted *ortho*-silylaryl triflates can be synthetically laborious. With the discovery of aryne generation from mild fluoride sources, interest in *ortho*-silylaryl halides has recently increased. In 2010, Harrity and coworkers showed *ortho*-silylaryl iodides were capable of efficiently generating arynes.[41] These *ortho*-silylaryl iodides were prepared through a [4+2] cycloaddition of (trimethylsilyl)iodoacetylene and substituted coumalates that afford *ortho*-silylaryl iodides as inseparable regioisomeric mixtures In 2016, Daugulis and Mesgar reported a one-step synthesis of ortho-silylaryl halides from commercially available starting materials.[42] The use of cryogenic temperatures, a glovebox, and highly water sensitive lithium reagents limits the large scale applicability.

While benzyne is the most commonly used aryne intermediate, 2-naphthynes remain underrepresented, presumably due to the synthetic challenges met with selectively substituting aromatic rings larger than benzene. Generally, 2-naphthynes can be generated from 2,3-dibromonaphthalene but the use of harsh organolithium reagents limits the number of functional groups available on these naphthalenes. The problem of functional group intolerance was solved for benzynes with the mild fluorine desilylation/elimination of *ortho*-silylaryl triflates, but to date, very few o*rtho*-

silylnaphthyl triflates are commercially available. In 1998, Fujiwara reported rapid synthesis of 2-naphthylsilanes bearing *ortho* hypervalent iodide leaving groups to efficiently generate 2-naphthynes, but the scope of substituted varieties has been limited and most examples have required lengthy synthetic procedures.[43,44] Wong[45] and Maly[46] reported substituted 2-naphthyne precursors, but the seven step syntheses of each method limit further adoption (Scheme 4.1a–b). Here we demonstrate a new variant of the Asao-Yamamoto benzannulation that provides 2-silyl-3-halonaphthalenes as single regioisomers (Scheme 4.1c). These compounds generate 2-naphthyne intermediates under mild conditions, which were trapped by furan, oligomerized, and found to undergo cyclodimerizaion or cyclotrimerization to bi- and tri naphthalenes, respectfully. Several examples featuring substituted *o*-phenylethynylbenzaldehydes are demonstrated, demonstrating the generality of this approach to access substituted 2-naphthyne intermediates

Scheme 4.1. Synthesis of substituted 2-naphthyne precursors

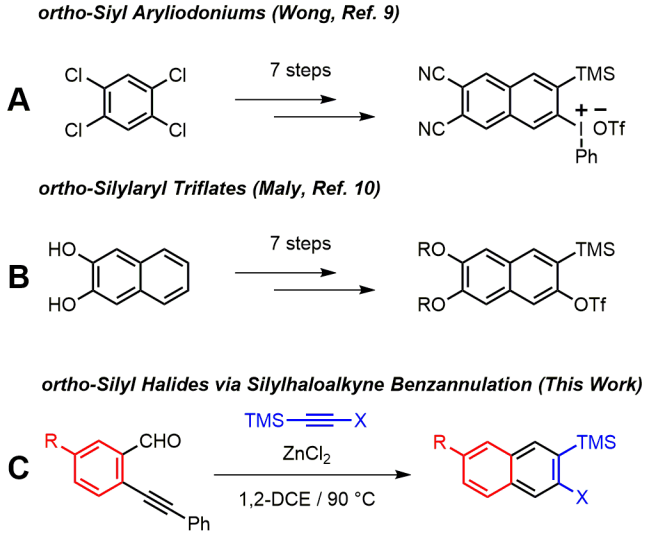

4.3 Results and Discussion

e first evaluated the scope and regioselectivity of the benzannulation reaction using substituted benzaldehydes and silylacetylenes (Table 4.1). Naphthalene products **3a-j** were obtained as single regioisomers, often in good to excellent yield. The reaction was more efficient for iodoacetylenes than bromoacetylenes, as shown for benzaldehyde

Table 4.1. Synthesis of 2-naphthyne precursors from substituted 2-(phenylethynyl)benzaldehydes

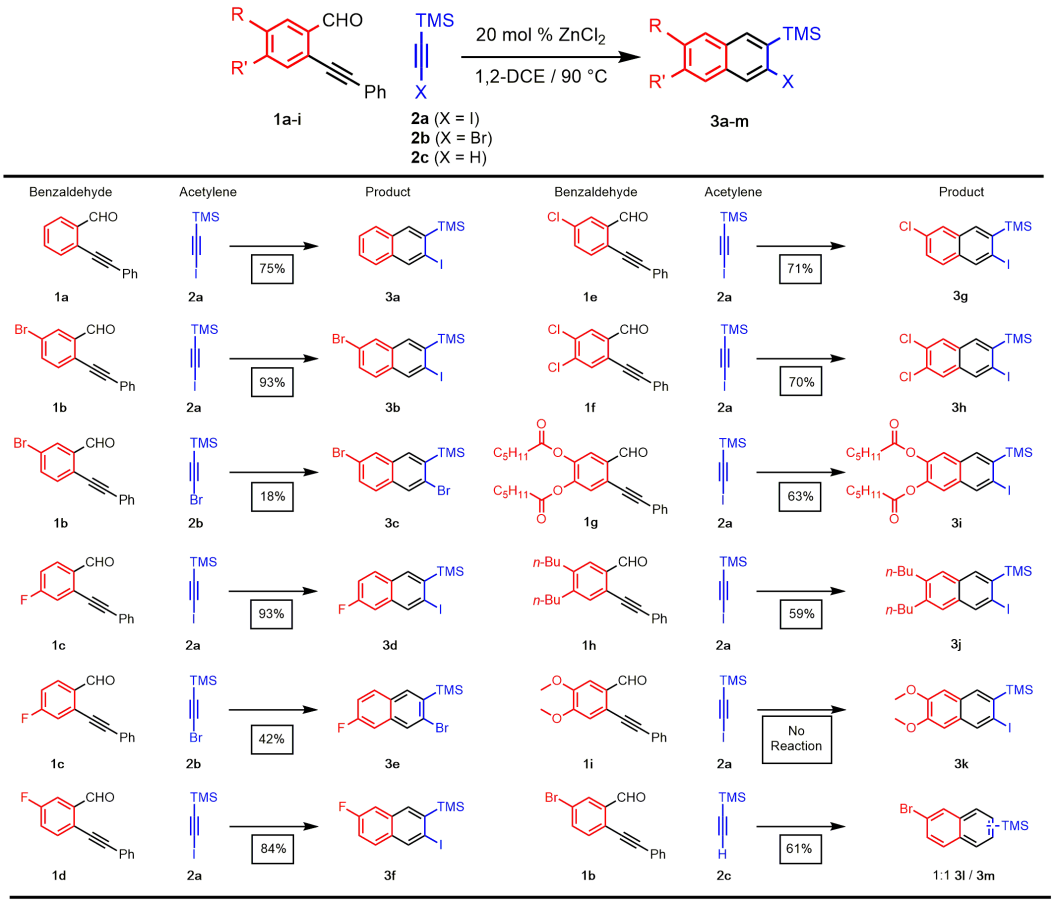

All yields are isolated yields. Reaction Conditions: Alkyne (**2a-c** , 0.10 M in 1,2-DCE); benzaldehyde (**1a**, 2.0 equiv or **1b-i**,1.3 equiv); $ZnCl_2$ (0.20 equiv).

1b with **2a** (X = I, 93% yield) and **2b** (X = Br, 18% yield). Likewise, the reaction of **1c** with **2a** and **2b** provided **3d** (93%) and **3e** (42%). Because of the higher yields generally observed for iodoacetylenes, we used **2a** for much of the rest of this study. Unsubstituted

and halogenated benzaldehydes (**1a–f**) performed well with yields ranging from 70–93% whereas those for benzaldehydes bearing phenolic ester **1g** and alkyl **1h** groups ranged from 59–63 %. Benzaldehydes bearing stronger electron donating groups, such as methoxy-substituted benzaldehyde **1i,** did not undergo benzannulation and instead formed a mixture of aldehyde decomposition products and unreacted alkyne.

The benzannulation reactions of **2a** and **2b** shown in Table 4.1 provide substituted naphthalene products as single regioisomers when non-pseudosymmetric benzaldehydes (e.g., **1c**, **1d**, but not **1f**) are employed. Our previous studies of diarylacetylenes and haloarylacetylenes indicated that regioselectivity arises from the ability of the acetylene substituents to preferentially stabilize developing positive charge at one of the acetylene carbons.[47] For example, when bromonated benzaldehyde **1b** undergoes benzannulation with a halo-arylacetylene, using either $Cu(OTf)_2$ or $ZnCl_2$ catalysts, the *syn*-regioisomer with respect to the iodine and bromine positions is obtained.[50] The opposite regioisomer is obtained for halosilylacetylene substrates; **1b** reacts with **2a** and **2b** to provide the corresponding *anti*-regioisomers **3b** and **3c**, respectively. These outcomes were confirmed by single crystal x-ray crystallography of **3c** (Figure 4.1a), compared to that obtained for a typical haloarylacetylene. The regiochemical outcome is insensitive to substitution patterns on the benzaldehyde, as demonstrated for the benzannulations of monofluorinated benzaldehyde regioisomers **1c** and **1d** with **2a**. Each reaction provides a single fluoronaphthalene regioisomer,

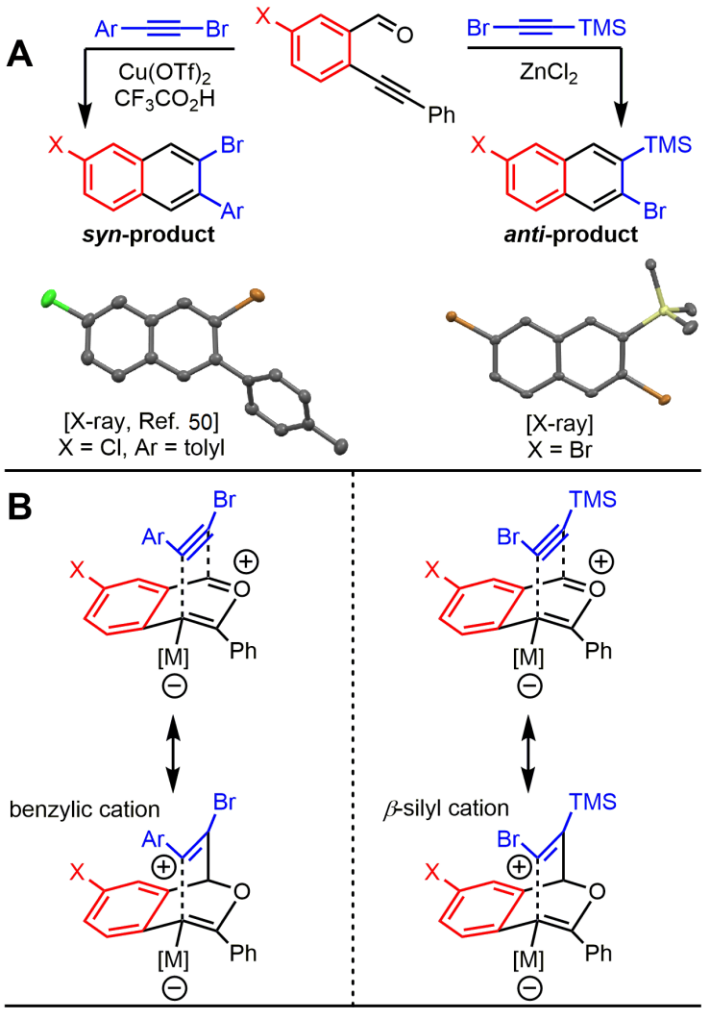

Figure 4.1. a) Haloarylacetylenes and halosilylacetylenes provide opposite regioselectivity in benzannulation reactions, as demonstrated by x-ray crystallography.[50] Ellipsoids set to 50 % probability level for 3c. b) Rationale for the regioselectivity of each reaction. The silicon substituent stabilizes developing positive charge on the carbon adjacent to the halogen, which makes the observed regioselectivity consistent with other benzannulation reactions.

whose structures were assigned by ^{19}F and 2D NMR spectroscopy (see Supporting Information). Finally, halogenation of the silylacetylene is also essential for regioselectivity, as the benzannulation reaction of trimethylsilylacetylene (**2c**) and **1b** provides a nearly 1:1 ratio of the two regioisomers.

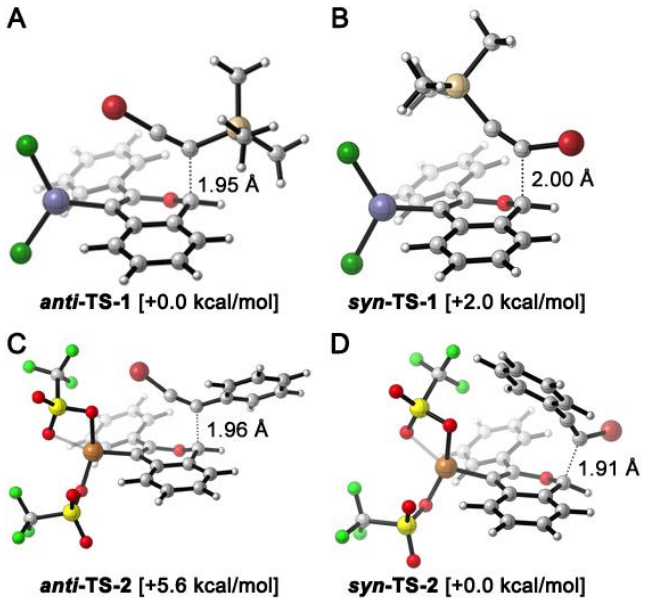

Figure 4.2. DFT calculated transition-states using B3LYP/6-31G(d) potentially responsible for the regioselectivity outcome in the benzannulation of: (A,B) silylhaloalkynes & (C,D) arylhaloalkynes, along with their relative electronic energies and bond forming interatomic distances. Element coloring scheme: C = silver, H = white, O = light red, Zn = blue, Cl = dark green, F = light green, S = yellow, Br = dark red, Cu = bronze.

The reversed regioselectivity of halosilylacetylene benzannulations likely originates from the combined ability of the silicon and halogen substituents to stabilize developing positive charge on the acetylene carbon *beta* to the silyl group.[51-53] In contrast, when halo-arylacetylenes are benzannulated, the aromatic ring stabilizes a developing positive charge on the carbon *alpha* to the ring (Figure 4.1b). A DFT model of the proposed transition states leading to either the *syn*- or *anti*-regioisomer correctly predicts the reversal in regioselectivity observed experimentally between silylhaloalkynes and arylhaloalkynes (Figure 4.2). The B3LYP/6-31G(d) calculated ZPE-corrected electronic energies of regioisomeric transition states predict a 2.0 kcal/mol preference for the *anti*-regioisomer in the case of silylhaloalkyne **2b** compared to 5.6 kcal/mol in favor of the *syn*-regioisomer for phenylbromoacetylene. An alternate

mechanism in which the metal is not bound to the benzopyrylium intermediate is also plausible and transition state energies of those structures also support a reversal of regioselectivity (see Supporting Information for details).

Scheme 4.2. Conversion of Aryl Silane to Aryl Iodide with ICl

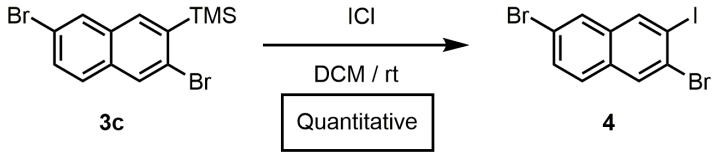

3c **4**

Furthermore, we had previously accessed a library of polyheterohalogenated naphthalenes through the benzannulation of arylhaloalkynes. Although this approach was used to prepare more than twenty polyheterohalogenated naphthalenes as single regioisomers, it was limited to 2-arylnaphthalene derivatives.[50] Silylhaloacetylene benzannulations eliminate this restriction, and instead provide 2-trimethylsilyl groups may be easily removed or further transformed. For example, treatment of **3c** with ICl afforded polyheterohalogenated naphthalene **4** in quantitative yield (Scheme 2). The TMS group incorporated into the naphthalene products serves as a versatile handle for further functionalization, as C(aryl)–Si bonds are readily transformed into I, Br, Cl, H, OH, CF_3, Me, and others, highlighting the vast chemical space available through this method.[54]

The 2-silyl-3-iodonaphthalenes serve as efficient precursors of 2-naphthyne intermediates in the presence of F^- at room temperature, as determined by furan trapping experiments .[55–57] Unsubstituted (**3a**), 6-bromo- (**3b)**, 6,7-dichloro- (**3h**), and 6,7-dibutyl-substituted (**3j**) 2-naphthynes provided [2.2.1]oxabicyclic alkenes (**5a-d**) in good to excellent isolated yields (68-86 %, Scheme 4.2). These structures are of interest

as monomers for aromatic polyketones,[58] poly(*ortho*-phenylene)s,[59] and polybenzonorbonadiene derivatives,[60] iptycene materials,[61–63] and precursors for acene derivatives.[31,64–66] Additionally, transition-metal catalyzed ring opening reactions of [2.2.1]oxabicyclic alkenes have proven to be powerful techniques for the construction of cyclic compounds containing multiple stereocenters, making them relevant synthons for drug and natural product synthesis.[67–75] Given the availability of many substituted benzaldehyde cycloaddition partners, these findings demonstrate that benzannulation chemistry provides rapid entry to substituted 2-naphthyne intermediates.

Scheme 4.3. Aryne generation and trapping with furan

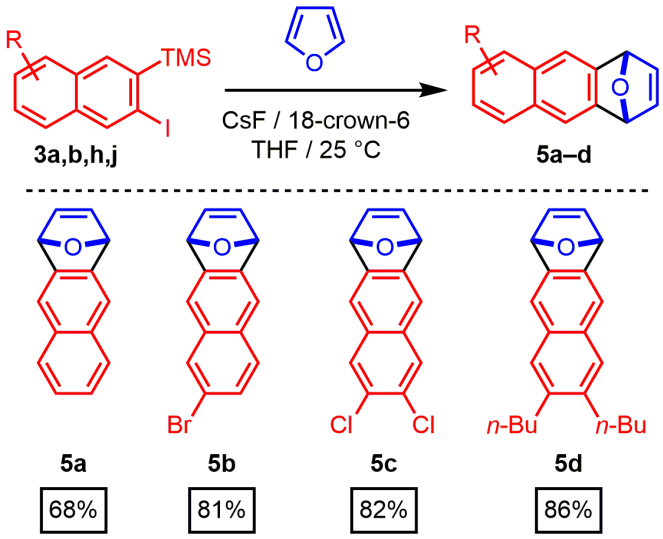

1,2-diaryl linkages are quite sterically hindered, which complicates the synthesis of oligo-and poly(*ortho*-phenylenes). Pioneering studies of oligomers were reported by Hartley[765,77] and Aida,[78] which demonstrated that *ortho*-phenylenes adopt specific helical conformations in the solid and solution phases. Our group also reported a synthesis of discrete oligo(*ortho*-arylene)s through a benzannulation of discrete oligo(*ortho*-phenylethynylene)s, however, decreased yields upon benzannulation of longer oligomers limits the size of these materials.[79] Poly(*ortho*-phenylene)s were

unknown until Nozaki *et. al.* published a formal aryne polymerization using trapped aryne equivalents to yield poly(*ortho*-phenylene)s.[59] Later Uchiyama *et. al.* developed a polymerization of benzyne using a copper(I) salt as an initiating species.[80] We therefore applied the polymerization conditions reported by Uchiyama to our 2-naphthyne precursors towards the synthesis of poly(ortho-naphthalene)s.

Poly(ortho-phenylene)s typically suffer from low solubility without assistance from solubilizing groups. To help enhance solubility, we chose dibutylnaphthyne precursor **3j** as our monomer. This polymerization was conducted with 0.5 mol % copper initiator in the presence of CsF (2 equiv) and 18-crown-6 (4 equiv) and the product was isolated by precipitation into methanol, which afforded oligo(ortho-naphthalene) **6** in 19 % yield (Scheme 4.4). ^{1}H and ^{13}C NMR experiments of the solid show broad peaks in the aromatic and alkyl regions that are characteristic of ortho-phenylene oligomers (**S4.38-39**). GPC of **6** revealed a distribution of oligomers with a *Mn* = 1800 g/mol and *Mw* = 1900 g/mol suggesting short oligomers with an average of **8** repeat units (Figure 4.3). This average molecular weight was further confirmed by MALDI-TOF mass spectrometry (**S4.63**). Analysis of the spectrum revealed a mass-to-charge ratio of each peak expressible as 238.2 × n + 1.0 (H) + 26.0 (CN) + 108.0 (Ag+) where n is the number of repeating units consistent with each chain containing a single cyano- group, which was transferred onto the growing oligomer chain during initiation. This polymerization is reported to occur through a chain growth mechanism with the length of the polymer determined by the ratio between the monomer and initiating copper catalyst.[80] At 0.5 mol % of CuCN we would expect a polymer with over 100 repeat units to form during this polymerization. Further study of the polymerization is

required to explain the observed low molecular weight and to optimize the polymerization.

During our attempts to optimize this polymerization we found the product distribution could be drastically changed by increasing the copper catalyst loading to 5 mol % at room temperature (Figure 4.3). Analysis of the GPC trace of the precipitated product revealed a significant shift in the retention time of the oligomeric peak reflective of shorter oligomers. Surprisingly a new peak emerged at significantly longer retention times suggesting a well-defined, low molecular weight compound. We hypothesized our polymerization terminated to give linear dimer or trimers. In this case, the ^{1}H and ^{13}C

Scheme 4.4. CuCN catalyzed polymerization of **3j**

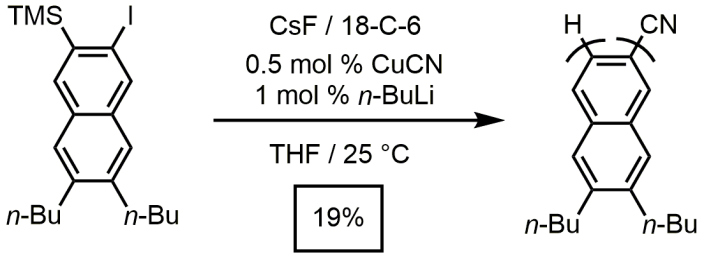

3j **6**

NMR spectra would show a complex mixture of ^{1}H and ^{13}C signals, however, examination of the ^{1}H and ^{13}C NMR spectra only two aromatic protons and five aromatic carbon shifts were found, suggesting a cyclic compound with a high degree of symmetry (**S4.40-41**). Finally, high-resolution mass spectrometry of the isolated product after purification by chromatography identified it as the cyclic hexabutyltrinaphthylene **7** in 49 % yield (Figure 4.3).

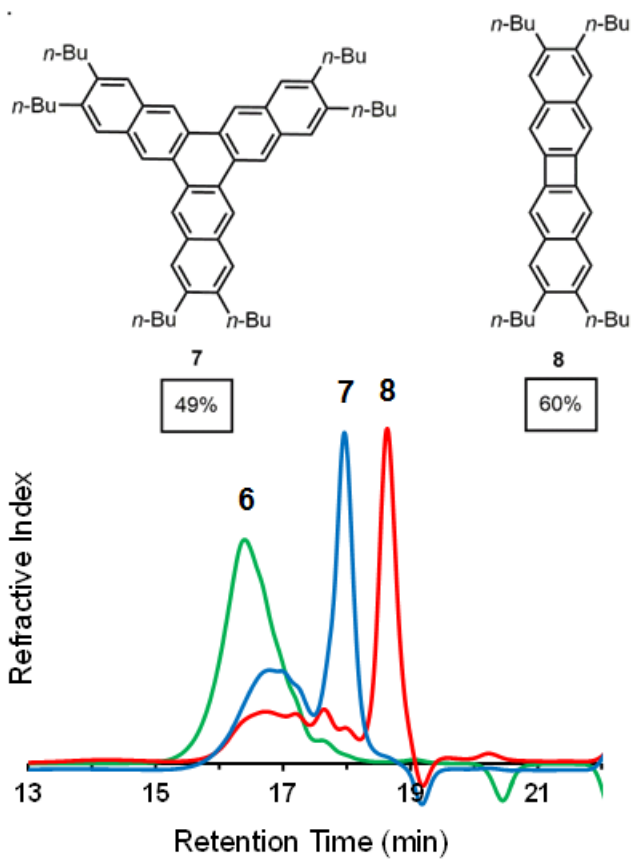

Figure 4.3. Gel Permeation Chromatography (GPC) data for the copper mediated cyclization with 0.5 mol % CuCN at room temperature (green), 5 mol % CuCN at room temperature (blue) and 5 mol % CuCN at 60 °C (red).

Interestingly, at elevated temperatures we again observed a significant change in product distribution in the GPC (Figure 4.3). Upon precipitation, this new reaction predominantly features a new peak in the GPC with an increased retention time indicating a smaller molecular weight compound forms that we identified as the tetrabutylbinaphthalene **8**. ^{1}H and ^{13}C NMR spectra suggest a symmetric cyclic naphthalene product with two proton and five carbon signals (**S4.42-43**) and high-resolution mass spectrometry data match the exact mass for **7**. X-ray crystallography of the purified compound unambiguously identified the structure as tetrabutylbinaphthalene product **8** (Figure 4.4).

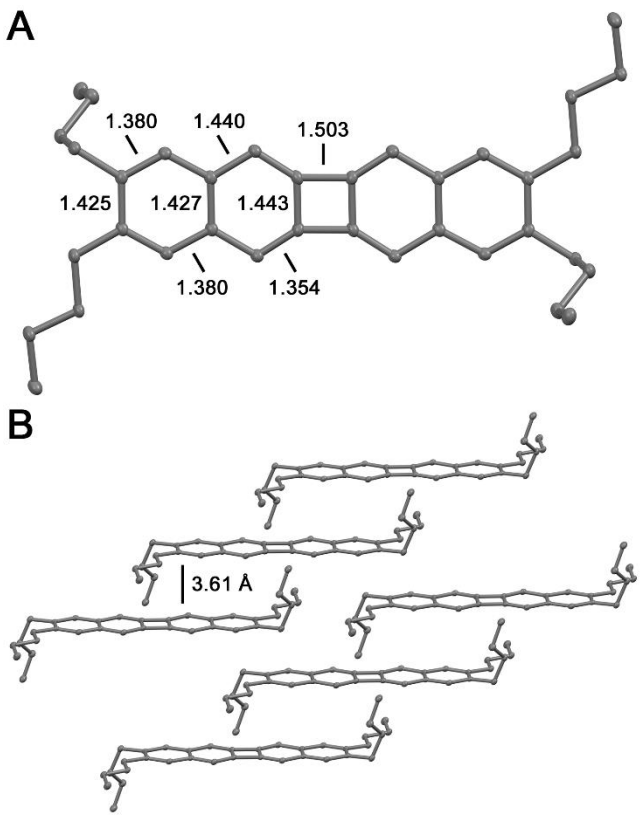

Figure 4.4. (A) Single crystal X-ray structure of **8** showing bond C-C distances around the aromatic rings in Å. Hydrogens are omitted for clarity, thermal ellipsoids shown at the 50% probability level. (B) Solid-state packing arrangement of **8** illustrating the interplanar distances between arenes.

[N]phenylenes are traditionally very difficult to access and their synthesis has been reported by only a few groups. Vollhardt and coworkers were the first to characterize these materials through a cobalt (2+2+2) cycloaddition of phenylene ethynylene substrates.[81–87] More recently, new synthetic strategies have been reported by Swager,[88] Xia,[89] and Bunz[90] These compounds consist of alternating aromatic rings fused cyclobutadienes with strong anti-aromatic character. The X-ray crystallographic structure showed a nearly planar geometry with torsion angles of 1.56° and 0.55° around the phenylene link. Analysis of the bond lengths confirms localization of the π-bonds around the 4-membered ring in order to offset the antiaromatic character of the

cyclobutadienoid with alternating 1.44 Å exocyclic and 1.35 Å endocyclic bond distances. (Fig. 4c). The solid-state arrangement of **8** features cofacial π-stacking with an unusually long interplanar distance of 3.61 Å, compared to the typical 3.4 Å distance of acenes.[91] This arrangement arises from the butyl side chains, whose conformation places their termini perpendicular to the arene plane, preventing closer cofacial packing. [92] Solid state packing exhbits a 3.6 Å interplanar distance between the arene rings (Figure 4.4b). UV-vis absorption and photoemission spectra of phenylenes **7** and **8** show distinct differences to naphthyne precursor **3j** and oligo(*ortho*-naphthalene) **6**.

4.4 Conclusion

The benzannulation of halosilylalcetylenes provides a general and rapid method to produce substituted 2-halo-3-silylnaphthalenes with high regioselectivity. The addition of a fluoride anion generates 2-naphthyne reactive intermediates, which were trapped as the [2.2.1]oxobicyclic alkene. These trapped arynes are themselves synthetically useful building blocks. A copper mediated aryne polymerization afforded low molecular weight oligomers, however when higher catalyst loadings are used the [2+2+2] and [2+2] cycloaddition products were observed in synthetically useful yields. These results show the utility of a copper-catalyzed benzannulation reaction for preparing to synthesize substituted tri- and binaphthalenes that are otherwise not easily prepared or derivatized. It has not escaped our imagination that the exquisite control of the halogenation pattern in conjunction with the diversity of aryne reactions available should enable rapid access to diverse and unique polycyclic conjugated aromatics architectures.

REFERENCES

(1) Wenk, H. H.; Winkler, M.; Sander, W. *Angew. Chem. Int. Ed.,* **2003**, *42*, 502–528.

(2) Stoermer, R.; Kahlert, B. *Berichte Dtsch. Chem. Ges.* **1902**, *35*, 1633–1640.

(3) Wittig, G. *Naturwissenschaften* **1942**, *30*, 696–703.

(4) Roberts, J. D.; Simmons, H. E.; Carlsmith, L. A.; Vaughan, C. W. *J. Am. Chem. Soc.* **1953**, *75*, 3290–3291.

(5) Kametani, T.; Ogasawara, K. *J. Chem. Soc. C* **1967**, 0, 2208–2212.

(6) Bhojgude, S. S.; Bhunia, A.; Biju, A. T. *Acc. Chem. Res.* **2016**, *49*, 1658–1670.

(7) Yoshida, H. In *Comprehensive Organic Synthesis II (Second Edition)*; Knochel, P., Ed.; Elsevier: Amsterdam, **2014**; 517–579.

(8) Tadross, P. M.; Stoltz, B. M. *Chem. Rev.* **2012**, *112*, 3550–3577.

(9) Samineni, R.; Srihari, P.; Mehta, G. *Org. Lett.* **2016**, *18*, 2832–2835.

(10) Shi, J.; Xu, H.; Qiu, D.; He, J.; Li, Y. *J. Am. Chem. Soc.* **2017**, *139*, 623–626.

(11) Gouthami, P.; Chegondi, R.; Chandrasekhar, S. *Org. Lett.* **2016**, *18*, 2044–2046.

(12) Karmakar, R.; Lee, D. *Org. Lett.* **2016**, *18*, 6105–6107.

(13) Vaidya, S. D.; Argade, N. P. *Org. Lett.* **2013**, *15*, 4006–4009.

(14) Chandrasoma, N.; Brown, N.; Brassfield, A.; Nerurkar, A.; Suarez, S.; Buszek, K. R. *Tetrahedron Lett.* **2013**, *54*, 913–917.

(15) Allan, K. M.; Stoltz, B. M. *J. Am. Chem. Soc.* **2008**, *130*, 17270–17271.

(16) Day, J. J.; McFadden, R. M.; Virgil, S. C.; Kolding, H.; Alleva, J. L.; Stoltz, B. M. *Angew. Chem. Int. Ed.* **2011**, *50*, 6814–6818.

(17) Sato, Y.; Tamura, T.; Mori, M. *Angew. Chem. Int. Ed.* **2004**, *43*, 2436–2440.

(18) Bronner, S. M.; Lee, D.; Bacauanu, V.; Cyr, P. *Synlett* **2017**.

(19) Buszek, K. R.; Brown, N.; Luo, D. *Org. Lett.* **2009**, *11*, 201–204.

(20) Bronner, S. M.; Goetz, A. E.; Garg, N. K. *J. Am. Chem. Soc.* **2011**, *133*, 3832–3835.

(21) Augros, D.; Yalcouye, B.; Choppin, S.; Chessé, M.; Panossian, A.; Leroux, F. R. *Eur. J. Org. Chem.* **2017**, *2017*, 497–503.

(22) Zhang, J.; Chen, Y.; Chen, X.; Zheng, X.; Cao, W.; Chen, J.; Zhang, M. *Tetrahedron* **2014**, *70*, 5820–5827.

(23) Guitián, E.; Pérez, D.; Peña, D. In *Palladium in Organic Synthesis*; Tsuji, J., Ed.; Topics in Organometallic Chemistry; Springer Berlin Heidelberg, **2005**; 109–146.

(24) Chen, Z.; Swager, T. M. *Org. Lett.* **2007**, *9*, 997–1000.

(25) Pei, B.-J.; Chan, W.-H.; Lee, A. W. M. *J. Org. Chem.* **2010**, *75*, 7332–7337.

(26) Suh, S.-E.; A. Barros, S.; M. Chenoweth, D. *Chem. Sci.* **2015**, *6*, 5128–5132.

(27) García-López, J.-A.; Greaney, M. F. *Org. Lett.* **2014**, *16*, 2338–2341.

(28) Wu, C.-Y.; Lin, Y.-C.; Chou, P.-T.; Wang, Y.; Liu, Y.-H. *Dalton Trans.* **2011**, *40*, 3748–3753.

(29) Alonso, J. M.; Díaz-Álvarez, A. E.; Criado, A.; Pérez, D.; Peña, D.; Guitián, E. *Angew. Chem. Int. Ed.* **2012**, *51*, 173–177.

(30) Konishi, A.; Hirao, Y.; Matsumoto, K.; Kurata, H.; Kubo, T. *Chem. Lett.* **2013**, *42*, 592–594.

(31) Romero, C.; Peña, D.; Pérez, D.; Guitián, E. *J. Org. Chem.* **2008**, *73*, 7996–8000.

(32) Liu, Y.-L.; Liang, Y.; Pi, S.-F.; Huang, X.-C.; Li, J.-H. *J. Org. Chem.* **2009**, *74*, 3199–3202.

(33) Criado, A.; Peña, D.; Cobas, A.; Guitián, E. *Chem. – Eur. J.* **2010**, *16*, 9736–9740.

(34) Hsieh, J.-C.; Cheng, C.-H. *Chem. Commun.* **2005**, *0*, 2459–2461.

(35) Ikadai, J.; Yoshida, H.; Ohshita, J.; Kunai, A. *Chem. Lett.* **2004**, *34*, 56–57.

(36) Liu, Z.; Zhang, X.; Larock, R. C. *J. Am. Chem. Soc.* **2005**, *127*, 15716–15717.

(37) Liu, Z.; Larock, R. C. *Angew. Chem. Int. Ed.* **2007**, *46*, 2535–2538.

(38) Friedman, L.; Logullo, F. M. *J. Am. Chem. Soc.* **1963**, *85*, 1549–1549.

(39) Cunico, R. F.; Dexheimer, E. M. *J. Organomet. Chem.* **1973**, *59*, 153–160.

(40) Himeshima, Y.; Sonoda, T.; Kobayashi, H. *Chem. Lett.* **1983**, *12*, 1211–1214.

(41) Crossley, J. A.; Kirkham, J. D.; Browne, D. L.; Harrity, J. P. A. *Tetrahedron Lett.* **2010**, *51*, 6608–6610.

(42) Mesgar, M.; Daugulis, O. *Org. Lett.* **2016**, *18*, 3910–3913.

(43) Kitamura, T.; Fukatsu, N.; Fujiwara, Y. *J. Org. Chem.* **1998**, *63*, 8579–8581.

(44) Gondo, K.; Kitamura, T. *Adv. Synth. Catal.* **2014**, *356*, 2107–2112.

(45) Yick, C.-Y.; Chan, S.-H.; Wong, H. N. C. *Tetrahedron Lett.* **2000**, *41*, 5957–5961.

(46) Lynett, P. T.; Maly, K. E. *Org. Lett.* **2009**, *11*, 3726–3729.

(47) Arslan, H.; Walker, K. L.; Dichtel, W. R. *Org. Lett.* **2014**, *16*, 5926–5929.

(48) Doddrell, D.; Jordan, D.; Riggs, N. V.; Wells, P. R. J. Chem. Soc., *Chem. Commun.* **1972**, *20*, 1158–1158.

(49) Doddrell, D.; Barfield, M.; Adcock, W.; Aurangzeb, M.; Jordan, D. *J. Chem. Soc., Perkin Trans.* **1976**, *4*, 402–412.

(50) Crystallographic data for 2-bromo-3-tosyl-7-chloronaphthalene was reported by Lehnherr and coworkers. Lehnherr, D.; Alzola, J. M.; Lobkovsky, E. B.; Dichtel, W. R. *Chem. – Eur. J.* **2015**, *21*, 18122–18127.

(51) Wierschke, S. G.; Chandrasekhar, J.; Jorgensen, W. L. *J. Am. Chem. Soc.* **1985**, *107*, 1496–1500.

(52) Lambert, J. B.; Wang, G. T.; Finzel, R. B.; Teramura, D. H. *J. Am. Chem. Soc.* **1987**, *109*, 7838–7845.

(53) Siehl, H.-U. *Pure and Applied Chemistry* **2009**, *67*, 769–775.

(54) (a) C. Zarate, M. Nakajima, R. Martin, *J. Am. Chem. Soc.* 2017, **139**, 1191–1197. (b) R. L. Funk, K. P. C. Vollhardt, *J. Am. Chem. Soc.* 1980, **102**, 5245–5253. (c) J. Morstein, H. Hou, C. Cheng, J. F. Hartwig, *Angew. Chem. Int. Ed.* 2016, **55**, 8054–8057. (d) B. Shao, A. L. Bagdasarian, S. Popov, H. M. Nelson, *Science* 2017, **355**, 1403–1407. (e) M. Tredwell, V. Gouverneur, *Org. Biomol. Chem.* 2006, **4**, 26–32.

(55) Chen, Q.; Yu, H.; Xu, Z.; Lin, L.; Jiang, X.; Wang, R. *J. Org. Chem.* **2015**, *80*, 6890–6896.

(56) Harrison, R.; Heaney, H.; Lees, P. *Tetrahedron* **1968**, *24*, 4589–4594.

(57) Masson, E.; Schlosser, M. *Eur. J. Org. Chem.* **2005**, *2005*, 4401–4405.

(58) Ito, S.; Wang, W.; Nishimura, K.; Nozaki, K. *Macromolecules* **2015**, *48*, 1959–1962.

(59) Ito, S.; Takahashi, K.; Nozaki, K. *J. Am. Chem. Soc.* **2014**, *136*, 7547–7550.

(60) Medina, J. M.; Ko, J. H.; Maynard, H. D.; Garg, N. K. *Macromolecules* **2017**, *50*, 580–586.

(61) Thomas, S. W.; Long, T. M.; Pate, B. D.; Kline, S. R.; Thomas, E. L.; Swager, T. M. *J. Am. Chem. Soc.* **2005**, *127*, 17976–17977.

(62) Chen, Z.; Amara, J. P.; Thomas, S. W.; Swager, T. M. *Macromolecules* **2006**, *39*, 3202–3209.

(63) Pei, B.-J.; Chan, W.-H.; Lee, A. W. M. *Org. Lett.* **2011**, *13*, 1774–1777.

(64) LeHoullier, C. S.; Gribble, G. W. *J. Org. Chem.* **1983**, *48*, 2364–2366.

(65) Morton, G. E.; Barrett, A. G. M. *J. Org. Chem.* **2005**, *70*, 3525–3529.

(66) Kitamura, C.; Abe, Y.; Ohara, T.; Yoneda, A.; Kawase, T.; Kobayashi, T.; Naito, H.; Komatsu, T. *Chem. – Eur. J.* **2010**, *16*, 890–898.

(67) Lautens, M.; Fagnou, K.; Hiebert, S. *Acc. Chem. Res.* **2003**, *36*, 48–58.

(68) Arrayás, R. G.; Cabrera, S.; Carretero, J. C. *Org. Lett.* **2003**, *5*, 1333–1336.

(69) Nishimura, T.; Kawamoto, T.; Sasaki, K.; Tsurumaki, E.; Hayashi, T. *J. Am. Chem. Soc.* **2007**, *129*, 1492–1493.

(70) Li, L.-P.; Rayabarapu, D. K.; Nandi, M.; Cheng, C.-H. *Org. Lett.* **2003**, *5*, 1621–1624.

(71) Mo, D.-L.; Chen, B.; Ding, C.-H.; Dai, L.-X.; Ge, G.-C.; Hou, X.-L. *Organometallics* **2013**, *32*, 4465–4468.

(72) Webster, R.; Boyer, A.; Fleming, M. J.; Lautens, M. *Org. Lett.* **2010**, *12*, 5418–5421.

(73) Endo, K.; Tanaka, K.; Ogawa, M.; Shibata, T. *Org. Lett.* **2011**, *13*, 868–871.

(74) Fan, B.-M.; Li, X.-J.; Peng, F.-Z.; Zhang, H.-B.; Chan, A. S. C.; Shao, Z.-H. *Org. Lett.* **2010**, *12*, 304–306.

(75) Zhang, W.; Zhu, S.-F.; Qiao, X.-C.; Zhou, Q.-L. *Chem. – Asian J.* **2008**, *3*, 2105–2111.

(76) Mathew, S. M.; Hartley, C. S. *Macromolecules* **2011**, *44*, 8425–8432.

(77) Mathew, S. M.; Engle, J. T.; Ziegler, C. J.; Hartley, C. S. *J. Am. Chem. Soc.* **2013**, *135*, 6714–6722.

(78) Ando, S.; Ohta, E.; Kosaka, A.; Hashizume, D.; Koshino, H.; Fukushima, T.; Aida, T. *J. Am. Chem. Soc.* **2012**, *134*, 11084–11087.

(79) Lehnherr, D.; Chen, C.; Pedramrazi, Z.; DeBlase, C. R.; M. Alzola, J.; Keresztes, I.; Lobkovsky, E. B. ; Crommie, M. F.; Dichtel, W. R. *Chem. Sci.* **2016**, *7*, 6357–6364.

(80) Mizukoshi, Y.; Mikami, K.; Uchiyama, M. *J. Am. Chem. Soc.* **2015**, *137*, 74–77.

(81) Miljanić, O. Š.; Holmes, D.; Vollhardt, K. P. C. *Org. Lett.* **2005**, *7*, 4001–4004.

(82) Holmes, D.; Kumaraswamy, S.; Matzger, A. J.; Vollhardt, K. P. C. *Chem. – Eur. J.* **1999**, *5*, 3399–3412.

(83) Fonari, A.; Röder, J. C.; Shen, H.; Timofeeva, T. V.; Vollhardt, K. P. C. *Synlett* **2014**, *25*, 2429–2433.

(84) Miljanić, O. Š.; Vollhardt, K. P. C. In *Carbon-Rich Compounds*; Haley, M. M., Tykwinski, R. R., Eds.; Wiley-VCH Verlag GmbH & Co. KGaA, 2006; 140–197.

(85) Han, S.; Anderson, D. R.; Bond, A. D.; Chu, H. V.; Disch, R. L.; Holmes, D.; Schulman, J. M.; Teat, S. J.; Vollhardt, K. P. C.; Whitener, G. D. *Angew. Chem. Int. Ed.* **2002**, *41*, 3227–3230.

(86) Bong, D. T.-Y.; Chan, E. W. L.; Diercks, R.; Dosa, P. I.; Haley, M. M.; Matzger, A. J.; Miljanić, O. Š.; Vollhardt, K. P. C.; Bond, A. D.; Teat, S. J.; Stanger, A. *Org. Lett.* **2004**, *6*, 2249–2252.

(87) Berris, B. C.; Hovakeemian, G. H.; Lai, Y. H.; Mestdagh, H.; Vollhardt, K. P. C. *J. Am. Chem. Soc.* **1985**, *107*, 5670–5687.

(88) Parkhurst, R. R.; Swager, T. M. *J. Am. Chem. Soc.* **2012**, *134*, 15351–15356.

(89) Jin, Z.; Teo, Y. C.; Zulaybar, N. G.; Smith, M. D.; Xia, Y. *J. Am. Chem. Soc.* **2017**, *139*, 1806–1809.

(90) Biegger, P.; Schaffroth, M.; Tverskoy, O.; Rominger, F.; Bunz, U. H. F. *Chem. Eur. J.* **2016**, *22*, 15896–15901.

(91) Bond distances and torsional angles are comparable to similar [N]phenylenes reported by Swager, Xia, Vollhardt, and Bunz

(92) (a) Bendikov, M.; Wudl, F.; Perepichka, D. F. *Chem. Rev.* **2004**, *104*, 4891–4946. (b) Anthony, J. E. *Chem. Rev.* **2006**, *106*, 5028–5048.

APPENDIX

Table of Contents

A. **Materials.** Benzaldehydes **1a**, **1b**, **1c**, **1d**, **1e**, **1f,** and **1i** were all synthesized according to a previous literature procedure.[1] 18-Crown-6 which was recrystallized from anhydrous acetonitrile and evacuated overnight until dryness. Tetrahydrofuran was purchased from commercial sources and purified using a custom-built alumina-column based solvent purification system. HN(iPr)$_2$ was purchased from commercial sources and purified by distillation. Other solvents were purchased from commercial sources and used without further purification.

Instrumentation. Infrared spectra were recorded on a Thermo Nicolet iS10 with a zinc selenide ATR attachment and are uncorrected. UV/Vis absorbance spectra were recorded on a Cary 5000 UV-Vis-NIR spectrophotometer with an Hg lamp. Photoemission spectra were recorded on a Horiba Jobin Yvon Fluorolog-3 fluorescence spectrophotometer equipped with a 450 W Xe lamp, double excitation and double emission monochromators, a digital photon-counting photomultiplier and a secondary InGaAs detector for the NIR range. Correction for variations in lamp intensity over time and wavelength was achieved with a solid-state silicon photodiode as the reference. The spectra were further corrected for variations in photomultiplier response over wavelength and for the path difference between the sample and the reference by multiplication with emission correction curves generated on the instrument.

High resolution mass spectroscopy were recorded on an Agilent 6210A LC/MS with either an electrostray ionization (ESI) or an Agilent 7890 GC with electron impact ionization time-of-flight (EI-TOF) or atmospheric pressure photoionization (APPI) sources. Matrix assisted laser desorption ionization time-of-flight (MALDI-TOF) mass spectra were recorded on a Bruker Autoflex III with a 2,5-dihydroxybenzoic acid matrix

and silver trifluoroacetate additive. Gel Permeation Chromatography traces were recorded using 2 PolyPore 300x7.5mm columns with 18 Angles Dawn Heleos Multi Angle Light Scattering and Optilab T-rex Differential Refractive Index detectors. Polystyrene standards (1KDa, 2KDa, 3KDa, 5KDa) were purchased from Agilent and used as is.

NMR spectra of solutions were recorded on a Varian 400 spectrometer with an ASW probe with a 20 MHz sample spin rate, 400 MHz Agilent DD MR-400 NMR equipped with AutoX probe, Bruker 500 MHz spectrometer with a DCH CryoProbe. 2D NMR were recorded on a 400 MHz Agilent DD MR-400 NMR with AutoX probe and a 600 MHz Bruker Avance III spectrometer with BBI probe. All spectra were recorded at ambient temperature.

B. Synthetic Procedures

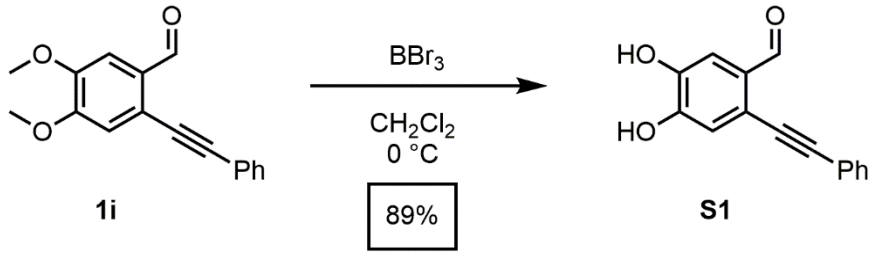

Synthesis of S1: **1i** (10.024 g, 37.645 mmol) was transferred to a flame dried round bottom flask and dissolved in 180 mL of anhydrous CH_2Cl_2 at 0 °C. Boron tribromide (56 mL, 1M in CH_2Cl_2) is slowly added to the reaction over 5 minutes. The mixture was removed from the ice bath and allowed to warm to rt. After 12 hours, the reaction was again placed in a 0 °C bath and methanol (50 mL) is slowly added to quench any unreacted boron tribromide. The mixture is washed with 2 M HCl (100 mL), extracted with CH_2Cl_2 (3 x 100 mL), dried with $MgSO_4$ and filtered. The solvent was concentrated to dryness before being redissolved in methanol (50 mL) and 1 mL CF_3CO_2H and stirred at room temperature for 1 hour. The solvent was removed under vacuum and purified by silica gel column chromatography (Hexanes/Ethyl Acetate, 1:1). **S1** was isolated as a white solid (8.011 g, 89 %). ^{1}H NMR (400 MHz, CD_3OD): δ 10.33 (s, 1 H), 7.53-7.50 (m, 2 H), 7.38-7.34 (m, 3 H), 7.31 (s, 1 H) ppm, ^{13}C NMR (125 MHz, CD_3OD) δ 191.7, 153.0, 148.0, 132.4, 132.2, 130.6, 129.7, 129.6, 129.5, 124.1, 121.5, 119.9, 113.9, 94.7, 85.9 ppm. IR (solid, ATR) 3271, 2481, 2393, 1634, 1598, 1562, 1507, 1440, 1424, 1353, 1316, 1261, 1213, 1189, 1165, 1088, 984, 955, 880, 754, 746, 684, 662 cm^{-1}. HRMS (APPI) calcd for $[C_{15}H_{10}O_3]^+$, 238.0624 found 238.0633.

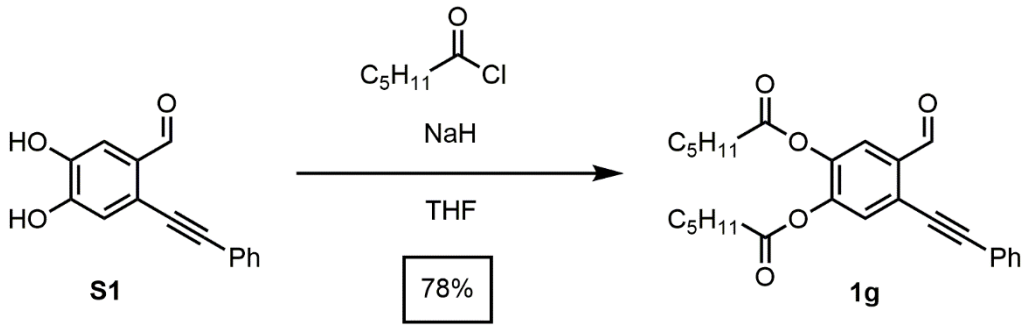

Synthesis of 1i: S1 (3.007 g, 12.62 mmol) and a 60 % dispersion of NaH in mineral oil (1.08 g, 26.9 mmol) were transferred to a flame dried flask. The reagents were dissolved in 130 mL of anhydrous THF and the reaction was allowed to stir at rt for 1 hour. Hexanoic acid chloride (3.746 g, 27.83 mmol) were then added to the mixture slowly and stirred for 1 hour at rt. The reaction was washed with 2 M HCl (50 mL) and extracted with CH_2Cl_2 (3 x 50 mL). The organic layer was dried using $MgSO_4$, filtered, and concentrated before being purified by silica gel column chromatography. Compound **1g** was isolated as a light orange oil (4.261 g, 78 %). ^{1}H NMR (400 MHz, $CDCl_3$): δ 10.55 (s, 1 H), 7.76 (s, 1 H), 7.58-7.53 (m, 2 H), 7.51 (s, 1 H), 7.42-7.37 (m, 3 H), 2.58 (t, *J* = 7.7 Hz, 4 H), 1.80-1.71 (m, 4 H), 1.43-1.35 (m 10 H), 0.96-0.94 (t, *J* = 6.90 Hz, 6 H) ppm, ^{13}C NMR (100 MHz, $CDCl_3$) δ 190.0, 170.8, 170.4, 146.8, 142.9, 134.3, 133.39 131.9, 130.3, 129.5, 128.7, 128.1, 125.5, 122.7, 122.1, 97.1, 83.6, 66.0, 34.2, 34.1, 31.4, 31.4, 24.7, 24.6, 22.5, 15.4, 14.0 ppm. IR (solid, ATR) 2957, 2931, 2871, 1770, 1694, 1603, 1496, 1482, 1467, 1443, 1411, 1379, 1319, 1237, 1130, 1085, 915, 852, 756, 689 cm^{-1}. HRMS (ESI) calcd for $[C_{27}H_{31}O_5]H^+$, 435.2166 found 435.2166.

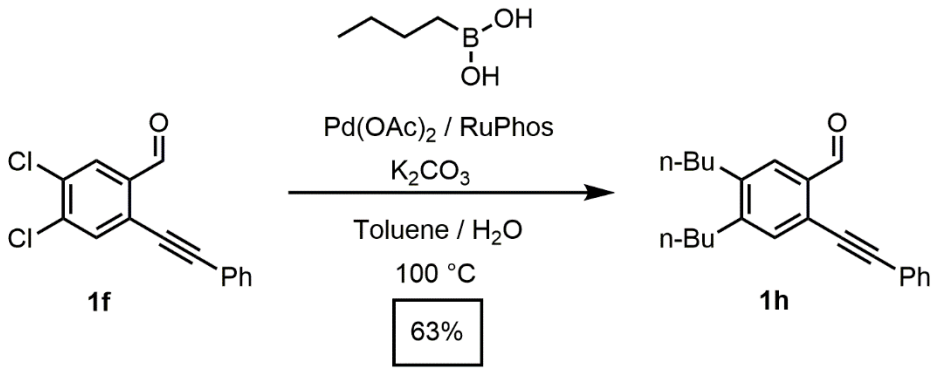

Synthesis of 1h: Palladium(II) Acetate (0.020 g, 0.089 mmol), RuPhos (0.074 g, 0.160 mmol), potassium carbonate (1.548 g, 11.20 mmol), n-butyl boronic acid (0.939 g, 9.21 mmol), and **1f** (1.003 g, 3.645 mmol) were added to a 250 mL round bottom flask before being evacuated and back filled with N_2. In a separate flask, 36 mL of a 10:1 mixture of toluene and water was sparged with nitrogen gas for one hour before being transferred to the reaction mixture. When all the solvent had been added, the reaction flask was placed in a 100 °C oil bath and allowed to stir at reflux for 6 hours. After the reaction was finished, it was cooled to rt, quenched with 20 mL of 2 M HCl, and extracted with CH_2Cl_2 (3 x 50 mL). The organic fractions were collected and dried using $MgSO_4$ before being purified by column chromatography (70% Hexanes : 30% CH_2Cl_2) to give **1h** as an orange solid (0.730 g, 63 %). ^{1}H NMR (500 MHz, $CDCl_3$): δ 8.28 (s, 1H), 7.78 (s, 1H), 7.54 (s, 1H), 7.43 (s, 1H), 2.78-2.73 (m, 4H), 1.71-1.60 (m, 4H), 1.50-1.37 (m, 4H), 1.00-0.95 (dt, *J* = 2.8, 7.2 Hz, 6H) ppm, ^{13}C NMR (125 MHz, $CDCl_3$) δ 191.7, 147.8, 142.0, 133.7, 131.6, 128.8, 128.5, 127.7, 124.2, 122.7, 95.1, 85.3, 32.9, 32.9, 32.5, 32.2, 22.8, 22.7, 14.0 ppm. IR (solid, ATR) 29.55, 2927, 2870, 1684, 1601, 1494, 1464, 1441, 1430, 1393, 1378, 1315, 1260, 1206, 1171, 1152, 1103, 1067, 1025, 937,

913, 879, 758, 733, 690, 667, 654 cm^{-1}. HRMS (ESI) calcd for $[C_{23}H_{26}O]H^+$, 319.2056 found 319.2056.

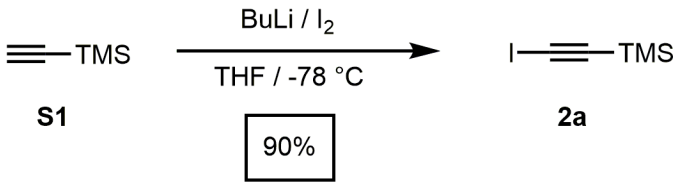

Synthesis of 2a: To a flame dried flask, **S2** (2.9 g, 4.3 mL, 30 mmol) was dissolved in 50 mL of THF and placed in a -78 °C dry ice/acetone bath. To this solution, 24.5 mL of *n*-butyl lithium (2.5 M in THF) was added dropwise and allowed to stir for 15 minutes before a solution of I_2 (8.625 g, 33.98 mmol) in 50 mL of THF was added dropwise. The reaction was let to stir for another 15 minutes at -78 °C before washing with 50 mL of a saturated aqueous solution of $Na_2S_2O_3$. The reaction mixture was extracted with ethyl ether (50 mL 3x), before being dried with sodium sulfate and filtered. The solvent was removed under reduced pressure to give compound **2a** (6.384 g, 90 % yield). Its ^1H and ^{13}C NMR specta match previously reported data.[2]

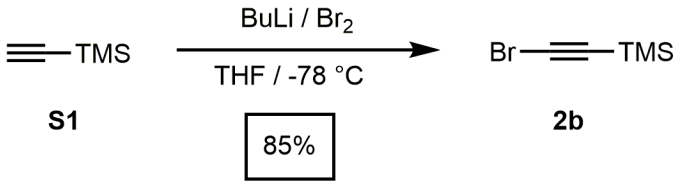

Synthesis of 2b: To a flame dried flask, **S3** (4.992 g, 50.94 mmol) was dissolved in 50 mL of THF and placed in a -78 °C dry ice/acetone bath. To this solution, 24.5 mL of *n*-butyl lithium (2.5 M in THF) was added dropwise and allowed to stir for 15 minutes before Br_2 (11.443 g, 71.60 mmol) was added dropwise. The reaction was let to stir for another 15 minutes at -78 °C before washing with 50 mL of a saturated aqueous solution

of $Na_2S_2O_3$. The reaction mixture was extracted with ethyl ether (50 mL 3x), before being dried with sodium sulfate and filtered. The solvent was removed under reduced pressure to give compound **2b** (7.719 g, 85 % yield). The ^{1}H and ^{13}C NMR agree with literature values.[3]

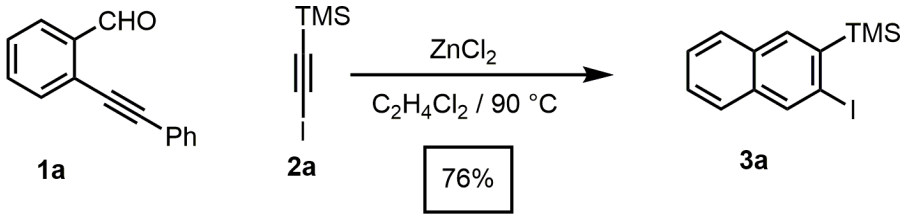

Synthesis of 3a: 2a (0.503 g, 2.24 mmol) and **1a** (0.946 g, 4.59 mmol) are dissolved in $C_2H_4Cl_2$. To this solution, 2.6 mL of $ZnCl_2$ (0.2 eq, 1 M in ethyl ether) was added via syringe. The reaction mixture turned a light yellow color and the reaction was placed in a 90 °C oil bath for 12 hours. The reaction was then poured into hexanes and passed through a silica plug using hexanes as the eluent. The solvent was removed under reduced pressure to yield compound **3a** (0.558 g, 76 % yield). ^{1}H NMR (300 MHz, $CDCl_3$): δ 8.39 (s, 1 H), 7.88 (s, 1 H), 7.79 (m, 1 H), 7.68 (m, 1 H), 7.49 (m, 2 H), 0.52 (s, 9H) ppm, ^{13}C NMR (175 MHz, $CDCl_3$) δ 142.2, 138.6, 136.7, 135.2, 131.8, 128.2, 127.2, 126.6, 126.4, 99.7, 0.1 ppm. IR (solid, ATR) 3050, 2951, 2891, 1620, 1567, 1482, 1405, 1288, 1246, 1196, 1137, 1091, 1017, 950, 871, 831, 742, 688 cm^{-1}. HRMS (EI-TOF) calcd for $[C_{13}H_{15}ISi]^{+}$, 325.9988 found 325.9981.

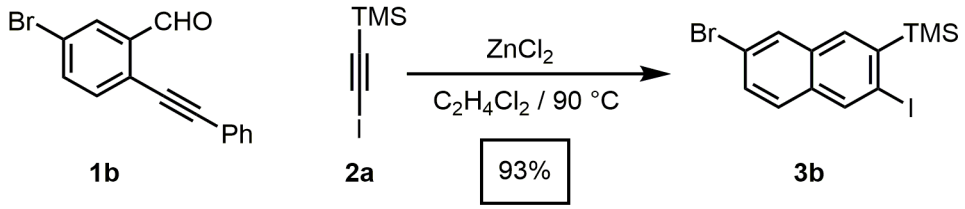

Synthesis of 3b: 2a (0.104 g, 0.464 mmol) and **1b** (0.181 g, 0.635 mmol) are dissolved in $C_2H_4Cl_2$. To this solution, 0.09 mL of $ZnCl_2$ (0.2 eq, 1 M in ethyl ether) was added via syringe. The reaction mixture turned a light yellow color and the reaction was placed in an 90 °C oil bath for 12 hours. The reaction was then poured into hexanes and passed through a silica plug using hexanes as the eluent. The solvent was removed under reduced pressure to yield compound **3b** (0.169 g, 93 % yield). ^{1}H NMR (600 MHz, $CDCl_3$): δ 8.30 (s, 1 H), 7.92 (s, 1 H), 7.74 (s, 1 H), 7.51 (dd, *J* = 1.9 Hz, *J* = 8.7 Hz, 1 H), 7.48 (d, *J* = 8.7 Hz, 1 H), 0.51 (s, 9 H) ppm, ^{13}C NMR (150 MHz, $CDCl_3$) δ 143.6, 138.2, 135.4, 133.3, 130.4, 130.1, 127.9, 120.2, 99.8, -0.1. ppm. IR (solid, ATR) 2950, 1562, 1550, 1473, 1407, 1376, 1247, 1175, 1141, 1094, 1062,952, 887, 834, 798, 750, 689 cm^{-1}. HRMS (EI-TOF) calcd for $[C_{13}H_{14}SiBrI]^+$, 403.9093 found 403.9116.

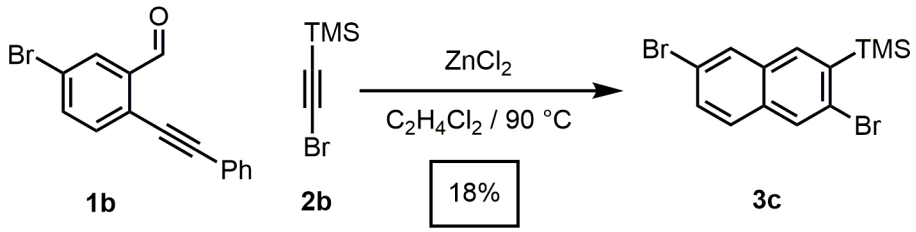

Synthesis of 3c: 2b (0.255 g, 1.44 mmol) and **1b** (0.565 g, 1.98 mmol) are dissolved in $C_2H_4Cl_2$. To this solution, 0.15 mL of $ZnCl_2$ (0.2 eq, 1 M in ethyl ether) was added via syringe. The reaction mixture turned a light yellow color and the reaction was placed in an 80 °C oil bath for 12 hours. The reaction was then poured into hexanes and passed

through a silica plug using hexanes as the eluent plug and eluted with hexanes. The solvent was removed under reduced pressure to yield compound **3c** (0.091 g, 18 % yield). ^{1}H NMR (400 MHz, $CDCl_3$): 7.97 (s, 1 H), 7.96 (s, 1 H), 7.80 (s, 1 H), 7.55 (s, 2 H), 0.48 (s, 9H) ppm, ^{13}C NMR (100 MHz, $CDCl_3$) δ 140.52, 135.72, 135.70, 133.21, 132.52, 130.66, 130.22, 128.21, 127.27, 120.04, -0.19. IR (solid, ATR)2953, 2896, 1567, 1551, 1472, 1409, 1378, 1336, 1282, 1248, 1242, 1174, 1142, 1102, 1062, 959, 907, 893, 879, 834, 800, 759, 750, 689 cm^{-1}. HRMS (EI-TOF) calcd for $[C_{13}H_{14}SiBr_2]^+$, 355.9232 found 355.9247.

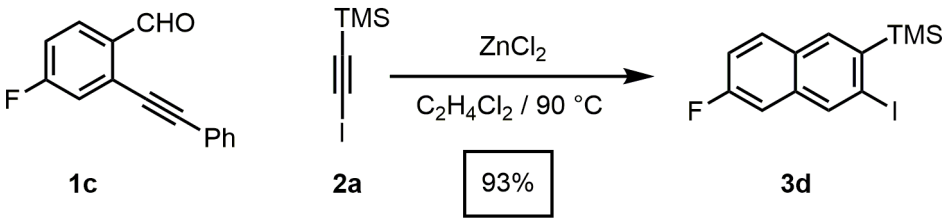

Synthesis of 3d: 2a (0.105 g, 0.471 mmol) and **1c** (0.146 g, 0.651 mmol) are dissolved in $C_2H_4Cl_2$. To this solution, 0.09 mL of $ZnCl_2$ (0.2 eq, 1 M in ethyl ether) was added via syringe. The reaction mixture turned a light yellow color and the reaction was placed in a 90 °C oil bath for 12 hours. The reaction was then poured into hexanes and passed through a silica plug using hexanes as the eluent. The solvent was removed under reduced pressure to yield compound **3d** (0.144 g, 93 % yield). ^{1}H NMR (400 MHz, $CDCl_3$): δ 8.32 (s, 1 H), 7.86 (s, 1 H), 7.77 (dd, *J* = 5.3 Hz, 8.5 Hz, 1 H), 7.29-7.23 (m, 2 H), 0.54 (s, 9 H) ppm, ^{13}C NMR (100 MHz, CDCl3) δ 161.07 (*J* = 248.8 Hz), 141.5 (*J* = 2.6 Hz), 137.9 (*J* = 5.3 Hz), 136.4 (*J* = 1.2 Hz), 135.9 (*J* = 9.8 Hz), 130.8 (*J* = 9.3 Hz), 128.9 (*J* = 0.9 Hz), 117.0 (*J* = 25.3 Hz), 109.5 (*J* = 20.93 Hz), 101.2, 0.02 ppm.

^{19}F NMR (375 MHz, CDCl3) δ -112.01 (td, *J* = 6.1 Hz, 9.0 Hz, 1 F) ppm IR (solid, ATR) 2951, 1627, 1563, 1484, 1433, 1379, 1332, 1276, 1246, 1229, 1204, 1146, 1122, 1091, 970, 950, 931, 893, 881, 836, 801, 757, 746, 689 cm^{-1}. HRMS (EI-TOF) calcd for $[C_{13}H_{14}SiFI]^+$, 343.9894 found 343.9897.

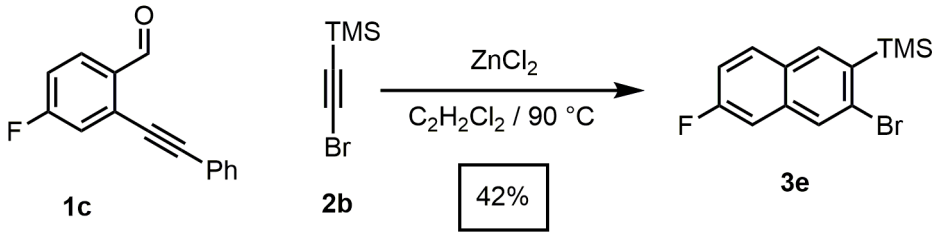

Synthesis of 3e: 2a (0.247 g, 1.39 mmol) and **1c** (0.465 g, 1.56 mmol) are dissolved in 14 mL of $C_2H_4Cl_2$. To this solution, 0.2 mL of $ZnCl_2$ (0.2 eq, 1 M in ethyl ether) was added via syringe. The reaction mixture turned a light yellow color and the reaction was placed in a 90 °C oil bath for 12 hours. The reaction was then poured into hexanes and passed through a silica plug using hexanes as the eluent plug and eluted with hexanes. The solvent was removed under reduced pressure to yield compound **3e** (0.173 g, 42 % yield). ^{1}H NMR (400 MHz, $CDCl_3$): δ 7.93 (s, 1H) , 7.86 (s, 1H), 7.75 (dd, *J* = 5.7 Hz, *J* = 8.7 Hz, 1 H), 7.27 (dd, *J* = 2.3 Hz, *J* = 9.6 Hz, 1 H), 7.21 (dt, *J* = 2.3 Hz, 8.7 Hz, 1 H), 0.46 (s, 9 H) ppm, ^{13}C NMR (100 MHz, $CDCl_3$) δ 161.4 (*J* = 248.6 Hz), 138.3 (*J* = 2.8 Hz), 136.6, 135.7 (*J* = 10.3 Hz), 130.7 (*J* = 9.3 Hz), 130.1 (*J* = 5.7 Hz), 128.7, 128.3f, 116.7 (*J* = 25.6 Hz), 109.8 (*J* = 21.2 Hz) , -0.15 ppm. ^{19}F NMR (375 MHz, $CDCl_3$) δ -112.3 (dt, *J* = 5.6 Hz, 8.9 Hz, 1 F) ppm. IR (solid, ATR) 2954, 1627, 1564, 1486, 1438, 1381, 1336, 1280, 1247, 1231, 1205, 1145, 1123, 1096, 972, 947, 882, 836,

804, 755, 690 cm^{-1}. HRMS (EI-TOF) calcd for $[C_{13}H_{14}FSiBr]^+$, 296.0032 found 296.0039.

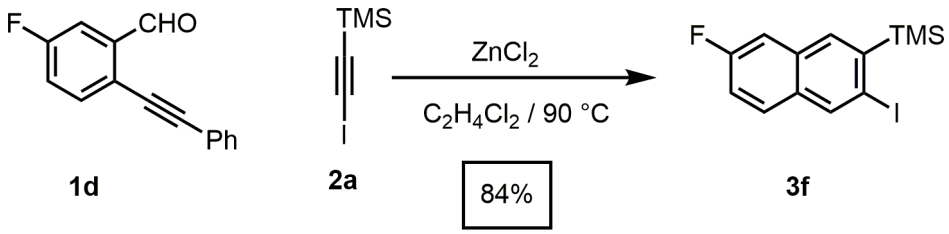

Synthesis of 3f: 2a (0.103 g, 0.461 mmol) and **1d** (0.144 g, 0.642 mmol) are dissolved in $C_2H_4Cl_2$. To this solution, 0.09 mL of $ZnCl_2$ (0.2 eq, 1 M in ethyl ether) was added via syringe. The reaction mixture turned a light yellow color and the reaction was placed in a 90 °C oil bath for 12 hours. The reaction was then poured into hexanes and passed through a silica plug using hexanes as the eluent. The solvent was removed under reduced pressure to yield compound **3f** (0.131 g, 84 % yield). ^{1}H NMR (400 MHz, $CDCl_3$): δ 8.36 (s, 1 H), 7.82 (s, 1 H), 7.65 (dd, *J* = 5.6 Hz, *J* = 9.0 Hz,1 H), 7.40 (dd, *J* = 2.2 Hz, *J* = 9.7 Hz, 1 H), 7.26 (td, *J* = 2.2 Hz, *J* = 9.0 Hz, 1 H) 0.53 (s, 9 H) ppm, ^{13}C NMR (100 MHz, $CDCl_3$) δ 160.8 (*J* = 247.0 Hz), 143.5 (*J* = 0.8 Hz), 138.4 (*J* = 1.1 Hz), 135.9 (*J* = 5.5 Hz), 132.5 (*J* = 9.0 Hz), 132.2 (*J* = 0.9 Hz), 128.9 (*J* = 9.1 Hz), 117.7 (*J* = 25.6 Hz), 111.3 (*J* = 20.5 Hz), 98.4 (*J* = 3.0 Hz), 0.0 ppm. ^{19}F NMR (375 MHz, CDCl3) δ -113.0 ppm (td, *J* = 5.4 Hz, *J* = 9.1 Hz, 1 F). IR (solid, ATR) 2952, 1628, 1570, 1489, 1387, 1335, 1277, 1246, 1197, 1144, 1122, 1093, 937, 898, 878, 835, 803, 759, 739, 688 cm^{-1}. HRMS (EI-TOF) calcd for $[C_{13}H_{14}SiFI]^+$, 343.9894 found 343.9879.

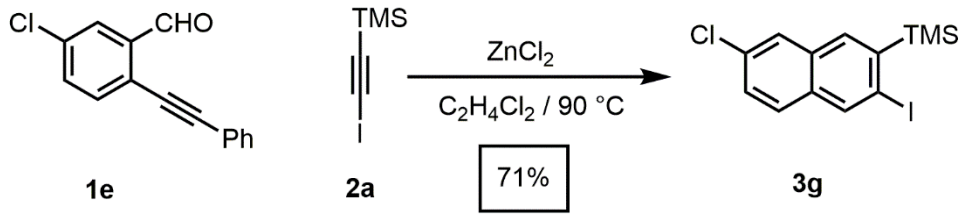

Synthesis of 3g: 2a (0.102 g, 0.450 mmol) and **1e** (0.154 g, 0.640 mmol) are dissolved in $C_2H_4Cl_2$. To this solution, 0.09 mL of $ZnCl_2$ (0.2 eq, 1 M in ethyl ether) was added via syringe. The reaction mixture turned a light yellow color and the reaction was placed in a 90 °C oil bath for 12 hours. The reaction was then poured into hexanes and passed through a silica plug using hexanes as the eluent. The solvent was removed under reduced pressure to yield compound **3g** (0.115 g, 71 % yield). ^{1}H NMR (300 MHz, $CDCl_3$): δ 8.34 (s, 1 H), 7.78 (s, 2 H), 7.59 (d, *J* = 8.9 Hz, 1 H), 7.55 (dt, *J* = 1.5, *J* = 8.7, 1 H), 0.53 (s, 9 H) ppm, ^{13}C NMR (75 MHz, $CDCl_3$) δ 143.7, 138.3, 135.6, 133.2, 132.3, 132.1, 128.1, 127.9, 126.9, 99.8, -0.0 ppm. IR (solid, ATR) 2951, 1566, 1553, 1474, 1409, 1382, 1246, 1175, 1139, 1097, 1080, 953, 953, 900, 879, 833, 800, 751, 733, 688, 667 cm^{-1}. HRMS (EI-TOF) calcd for $[C_{13}H_{14}SiClI]^+$, 359.9598 found 359.9569.

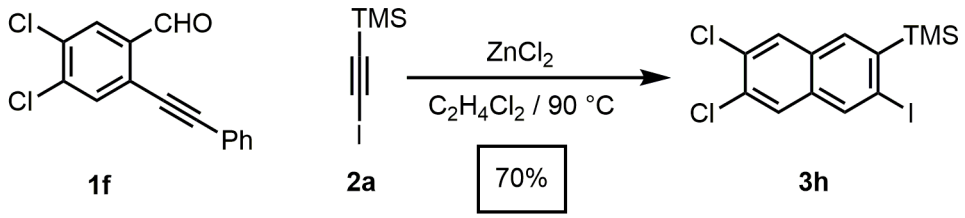

Synthesis of 3h: 2a (0.307 g, 1.37 mmol) and **1f** (0.507 g, 1.84 mmol) were dissolved in $C_2H_4Cl_2$. To this solution, 0.54 eq of $ZnCl_2$ (0.4 eq, 1 M in ethyl ether) was added via

syringe. The reaction mixture turned a light yellow color and the reaction was placed in a 90 °C oil bath for 12 hours. The reaction was then poured into hexanes and passed through a silica plug using hexanes as the eluent. The solvent was removed under reduced pressure to yield compound **3h** (0.370 g, 70 % yield). ^{1}H NMR (500 MHz, $CDCl_3$): δ 8.28 (s, 1 H), 7.90 (s, 1 H), 7.78 (s, 1 H), 7.75 (s, 1 H), 0.49 (s, 9 H) ppm, ^{13}C NMR (125 MHz, $CDCl_3$) 144.3, 137.4, 135.3, 133.8, 131.6, 130.8, 130.7, 129.2, 127.3, 100.9, -0.07 ppm. IR (solid, ATR) 2954, 1548, 1460, 1407, 1352, 1243, 1175, 1118, 1093, 981, 972, 931, 903, 885, 825, 752, 679 cm^{-1}. HRMS (EI-TOF) calcd for $[C_{13}H_{13}SiCl_2]^+$, 393.9208 found 393.9211.

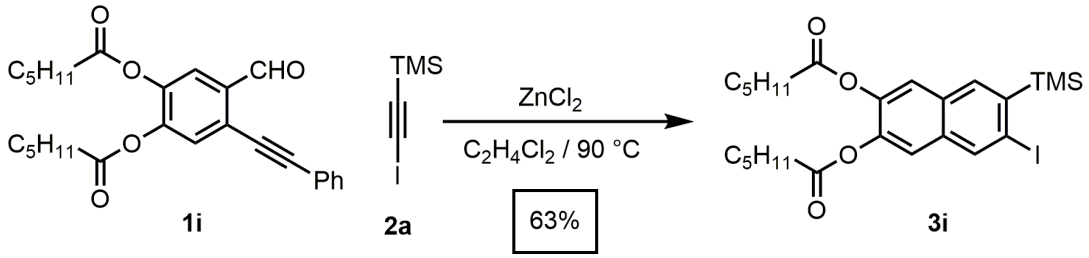

Synthesis of 3i: 2a (0.105 g, 0.470 mmol) and **1i** (0.263 g, 0.605 mmol) were transferred to a 100 mL round bottom flask with 5 mL of $C_2H_4Cl_2$. This reaction flask was then placed into an 90 °C oil bath and allowed to stir for 2 hours. When the reaction was complete, the solvent was removed under reduced pressure and product was purified by column chromatography (1:1 Hexanes/CH_2Cl_2). Compound **3i** was isolated as a colorless oil (0.1557 g, 63 %). ^{1}H NMR (500 MHz, $CDCl_3$): 8.33, (s, 1H), 7.81 (s, 1H), 7.61 (s, 1H) 7.48 (s, 1H), 2.57 (dt, *J* = 2.5, 7.6 Hz, 4H), 1.81-1.74 (m, 4H), 1.46-1.36 (m, 8H), 0.94 (t, *J* = 6.9 Hz, 6H), 0.48, (s, 9H) ppm, ^{13}C NMR (125 MHz, $CDCl_3$) δ 171.3, 171.3, 143.0, 142.2, 141.7, 137.9, 136.1, 133.2, 130.0, 121.4, 119.5, 100.0, 34.3,

31.5, 24.8, 22.5, 14.1, -0.03 ppm. IR (solid, ATR) 2955, 2929, 2859, 1766, 1629, 1667, 1488, 1466, 1425, 1377, 1340, 1246, 1226, 1159, 1137, 1095, 949, 917, 837, 760, 689 cm^{-1}. HRMS (ESI) calcd for $[C_{25}H_{35}O_4ISi]Na^+$, 577.1242 found 577.1243.

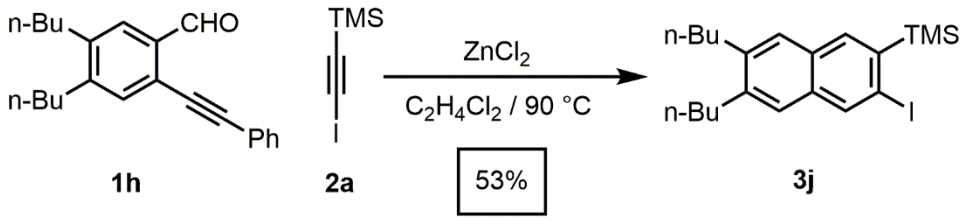

Synthesis of 3j: 2a (0.300 g, 1.34 mmol) and **1h** (0.568 g, 1.78 mmol) were transferred to a 100 mL round bottom flask with 30 mL of $C_2H_4Cl_2$. To this solution, 0.3 mL of $ZnCl_2$ (0.2 eq, 1M in ethyl ether) were added and the reaction was placed into a 90 °C oil bath and allowed to stir for 2 hours. When the reaction was complete, the solvent was removed under reduced pressure and product was purified by column chromatography with hexanes as the eluent. Compound **3j** was isolated as a colorless oil (0.347 g, 59%). ^{1}H NMR (500 MHz, $CDCl_3$): δ 8.28 (s, 1H), 7.78 (s, 1H), 7.54 (s, 1H), 7.43 (s, 1H), 2.78-2.73 (m, 4H), 1.71-1.60 (m, 4H), 1.50-1.37 (m, 4H), 1.00-0.95 (dt, *J* = 2.8, 7.2 Hz, 6H) ppm, ^{13}C NMR (125 MHz, $CDCl_3$) δ 141.3, 140.9, 140.6, 137.8, 136.0, 134.2, 130.6, 127.2, 125.5, 98.5, 33.3, 33.3, 32.7, 23.0, 22.9, 14.2, 14.2, 0.1 ppm. IR (solid, ATR) 2954, 2928, 2869, 2857, 1570, 1464, 1376, 1247, 1098, 949, 909, 835, 758, 687 cm^{-1}. HRMS (EI-TOF) calcd for $[C_{21}H_{31}SiI]^+$,438.1240 found 438.1250.

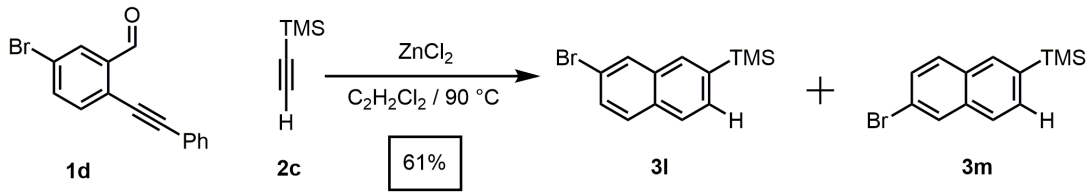

Synthesis of 3l and 3m: 2c (0.109 g, 1.11 mmol) and **1d** (0.386 g, 1.35 mmol) were dissolved in 10 mL of $C_2H_4Cl_2$. To this solution, 0.2 mL of ZnCl2 (0.2 eq, 1 M in ethyl ether) was added via syringe. The reaction mixture turned a light yellow color and it was placed in a 90 °C oil bath for 12 hours. After cooling to rt, the solvent was removed under vacuum and the product was purified by silica gel chromatography using hexanes as the eluent. The products were isolated as a 1:1 inseparable mixture to give **3l** and **3m** as a white solid (0.172 g, 61 % yield). ^{1}H NMR of **3l** (400 MHz, $CDCl_3$): δ 8.03 (d, *J* = 1.6 Hz, 1H), 7.92 (s, 1H), 7.79 (d, *J* = 8.2 Hz, 1H), 7.69 (d, *J* =8.4 Hz, 1H), 7.62 (dd, *J* = 8.2, 1.1 Hz, 1H), 7.55 (d, *J* = 8.4 Hz, 1H) ppm. ^{13}C NMR of **3l** (100 MHz, $CDCl_3$): δ 139.6, 143.1, 132.9, 132.1, 130.4, 130.2, 129.7, 129.5, 126.9, 119.8 ppm. ^{1}H NMR of **3m** (400 MHz, $CDCl_3$): δ 7.99 (d, *J* = 1.7 1H), 7.98 (s, 1H), 7.73 (d, *J* = 8.0 Hz, 1H), 7.72 (d, *J* = 9.4 Hz, 1H), 7.63 (dd, *J* = 8.0, 0.9 Hz, 1H), 7.55 (dd, *J* = 9.0, 1.7 Hz, 1H) ppm, ^{13}C NMR of **3m** (100 MHz, $CDCl_3$): δ 138.8, 134.8, 133.7, 131.4, 131.4, 131.0, 129.8, 129.4, 126.1, 120.3 ppm, IR (solid, ATR) 3042, 2956, 2894, 1616, 1576, 1493, 1450, 1407, 1310, 1247, 1180, 1139, 1087, 1059, 949, 882, 829, 751, 694, 652 cm^{-1}. HRMS (EI-TOF) calcd for $[C_{13}H_{15}SiBr]^+$, 278.0126 found 278.0139.

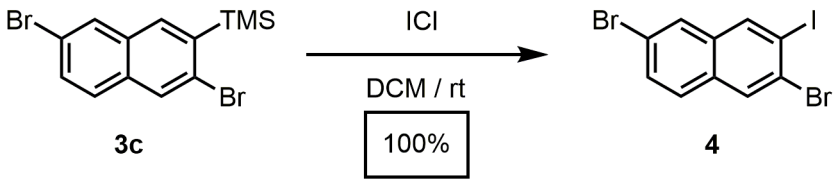

Synthesis of 4: 3c (0.050 g, 0.140 mmol) and ICl (0.025 g, 0.140 mmol) were dissolved in separate CH_2Cl_2 solutions (1 mL and 0.5 mL respectively), which were combined. The resulting reaction mixture was stirred for 5 min, after which the solution was washed with saturated $Na_2S_2O_3$ (1 mL) and extracted with CH_2Cl_2 (3 x 3 mL). The organic fractions were combined, dried ($MgSO_4$), and filtered to provide a light yellow solution. The solvent was removed, and **4** was purified using column chromatography (SiO_2, hexanes) to provide a white solid in quantitative yield (0.057 g, 100 %). **4:** ^{1}H NMR (400 MHz, $CDCl_3$): δ 8.29 (s, 1H), 8.08 (s, 1H), 7.85 (1, 1H) 7.57 (d, 2H) ppm, ^{13}C NMR (100 MHz, $CDCl_3$) δ 138.6, 134.1, 132.1, 130.9, 130.9, 128.8, 128.6, 126.9, 121.1, 99.9 ppm. IR (solid, ATR) 2956, 1693, 1609, 1560, 1475, 1413, 1375, 1331, 1284, 1263, 1175, 1142, 1088, 1059, 943, 889, 872, 803, 795 cm^{-1}. HRMS (DART) calcd for [$C_{10}H_5Br_2I^+$] 409.7797, found 409.7789.

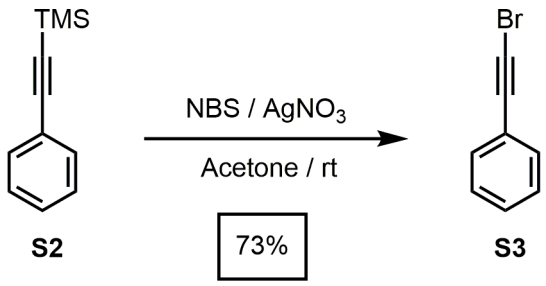

Synthesis of S3: S2 (0.598 g, 2.87 mmol), N-Bromosuccinimide (0.589 g, 3.31 mmol), and $AgNO_3$ (0.499 g, 2.98 mmol) was dissolved in 15 mL of acetone and stirred at rt for 12 h. The solvent was removed under vacuum and the crude reaction mixture was purified by silica gel chromatography using hexanes as the eluent. The solvent was removed under reduced pressure to afford **S3** as a clear liquid (0.3776 g, 73 % yield). Its ^{1}H and ^{13}C NMR specta match previously reported data.[4]

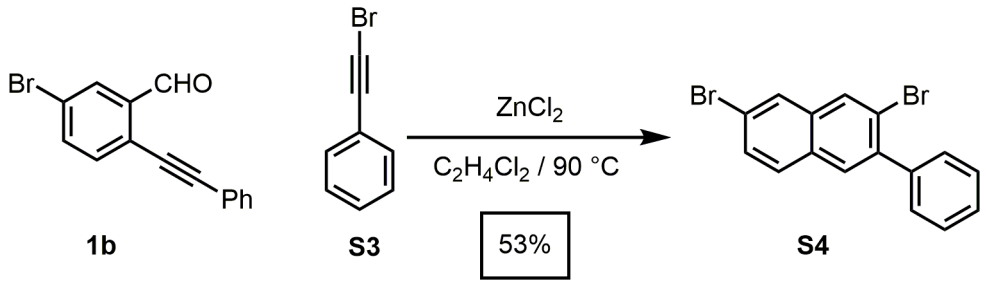

Synthesis of S4: S**3** (0.101 g, 0.553 mmol) and **1b** (0.210 g, 0.720 mmol) were dissolved in 3 mL of $C_2H_4Cl_2$. To this solution, 0.1 mL of ZnCl2 (0.2 eq, 1 M in ethyl ether) was added via syringe. The reaction mixture turned a light yellow color and it was placed in a 90 °C oil bath for 12 hours. After cooling to rt, the solvent was removed under vacuum and the product was purified by silica gel chromatography using hexanes as the eluent. The products were isolated as a 1:1 inseparable mixture to give **S4** as a light yellow solid (0.107 g, 53 % yield). ^{1}H NMR (400 MHz, $CDCl_3$): δ 1H NMR (400 MHz, Chloroform-d) δ 8.08 (S, 1H), 7.93 (d, *J* = 2.0 Hz, 1H), 7.75 (s, 1H), 7.66 (d, *J* = 8.75 Hz, 1H), 7.58 (dd, *J* = 2.0 Hz, *J* = 8.75 Hz, 1H), 7.51-7.44 (m, 5H) ppm. ^{13}C NMR (100 MHz, $CDCl_3$): δ 140.7, 140.7, 134.4, 130.7, 130.7, 130.1, 129.9, 129.7, 129.5, 128.7, 128.1, 127.9, 122.2, 121.0 ppm. IR (solid, ATR) 3056, 1618, 1576, 1557, 1496, 1473, 1442, 1372, 1341, 1302, 1266, 1219, 1170, 1140, 1061, 1027, 952, 836, 802, 760 cm^{-1}. HRMS ($C_{16}H_{10}Br_2$) calcd for $[C_{16}H_{10}Br_2]^+$ 359.9149, found 359.9158.

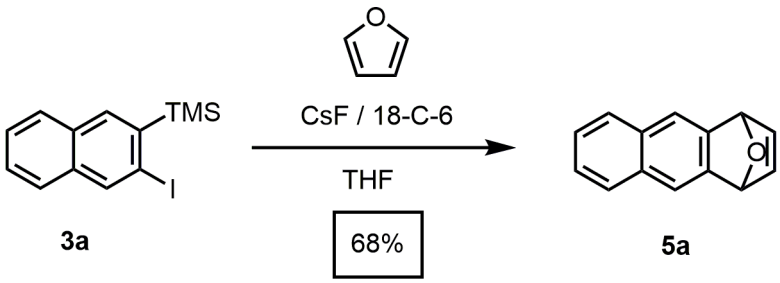

3a **5a**

Synthesis of 5a: Cesium fluoride (0.052 g, 0.342 mmol) and 18 Crown 6 (0.107g, 0.406 mmol) were placed in a flame dried round bottom flask which was evacuated and backfilled with nitrogen. Compound **3a** (0.055 g, 0.169 mmol) and furan were then dissolved into anhydrous THF and this solution was added to the reaction flask and let to stir at rt for 12 hours. When the reaction was finished, 2 mL of water was added and it was extracted with CH_2Cl_2 (3 x 3 mL). The organic fractions were collected and dried using $MgSO_4$ before being purified by column chromatography using CH_2Cl_2 as the eluent. Compound **5a** was isolated as a white solid (0.022 g, 68 % Yield). The ^{1}H and ^{13}C NMR agreed with literature values.[5]

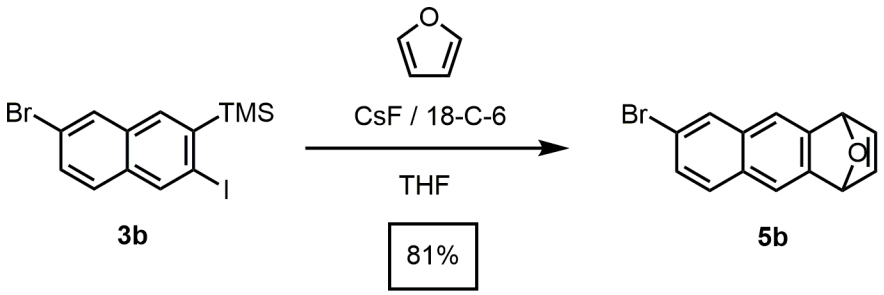

3b **5b**

Synthesis of 5b: Cesium fluoride (0.018 g, 0.12 mmol) and 18 Crown 6 (0.058 g, 0.22 mmol) were placed in a flame dried round bottom flask which was evacuated and backfilled with nitrogen. Compound **3b** (0.022 g, 0.054 mmol) and furan (0.05 mL, 0.7 mmol) were then dissolved into anhydrous acetonitrile and this solution was added to

the reaction flask. The reaction was stirred for 24 hours and monitored by TLC. When the reaction was finished, 2 mL of water was added and it was extracted with CH_2Cl_2 (3 x 3 mL). The organic fractions were collected, dried using $MgSO_4$, and filtered before being purified by silica gel column chromatography (70% Hexanes : 30 % CH_2Cl_2). **5b** was isolated as a white solid (0.011 g, 81 % Yield). ^{1}H NMR (500 MHz, $CDCl_3$): δ 7.49 (s, 2H), 7.37 (s, 2H), 6.94 (s, 2H), 5.77 (s, 2H), 2.73 (t, *J* = 7.64, 4H), 1.66-1.59, (m, 4H), 1.48-1.40 (m, 4 H), 0.97 (t, *J* = 8.01 Hz, 6H) ppm, ^{13}C NMR (125 MHz, $CDCl_3$) δ 143.3, 141.7, 139.8, 130.5, 127.7, 118.1, 82.0, 33.6, 32.7, 23.0, 14.2 ppm. IR (solid, ATR) 3018, 1593, 1495, 1424, 1305, 1285, 1224, 1197, 1147, 1068, 986, 907, 83, 846, 809, 731 cm^{-1}. HRMS (ESI) calcd for $[C_{14}H_{10}BrO]H^+$, 272.9910 found 272.9905.

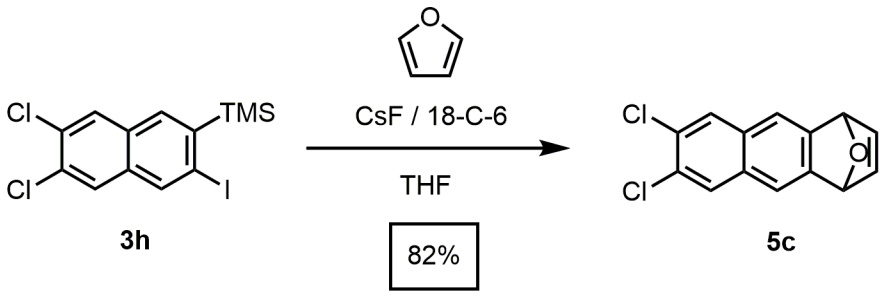

3h **5c**

Synthesis of 5c: Cesium fluoride (0.019 g, 0.13 mmol) and 18 Crown 6 (0.057 g, 0.22 mmol) were placed in a flame dried round bottom flask which was evacuated and backfilled with nitrogen. Compound **3h** (0.020 g, 0.051 mmol) and furan (0.05 mL, 0.7 mmol) were then dissolved into anhydrous acetonitrile and this solution was added to the reaction flask. The reaction was stirred for 24 hours and monitored by TLC. When the reaction was finished, 2 mL of water was added and it was extracted with CH_2Cl_2 (3 x 3 mL). The organic fractions were collected, dried using $MgSO_4$, and filtered before

being purified by silica gel column chromatography (70% Hexanes : 30 % CH_2Cl_2). **5c** was isolated as a white solid (0.011 g, 82 % Yield). ^{1}H NMR (500 MHz, $CDCl_3$): δ 7.49 (s, 2H), 7.37 (s, 2H), 6.94 (s, 2H), 5.77 (s, 2H), 2.73 (t, *J* = 7.64, 4H), 1.66-1.59, (m, 4H), 1.48-1.40 (m, 4 H), 0.97 (t, *J* = 8.01 Hz, 6H) ppm, ^{13}C NMR (125 MHz, $CDCl_3$) δ 143.3, 141.7, 139.8, 130.5, 127.7, 118.1, 82.0, 33.6, 32.7, 23.0, 14.2 ppm. IR (solid, ATR) 3037, 2928, 2857, 1589, 1475, 1426, 1413, 1399, 1280, 1197, 1176, 1124, 1069, 1059, 981, 965, 910, 877, 861, 847, 737, 705, 661 cm^{-1}. HRMS (APPI) calcd for $[C_{14}H_7Cl_2O]^-$, 260.9879 found 260.9891.

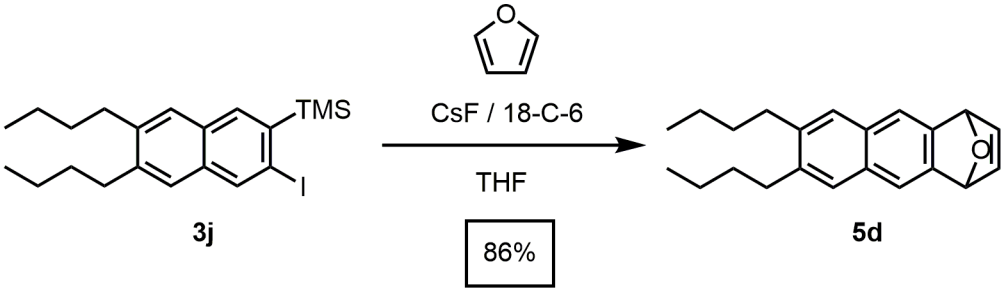

Synthesis of 5d: Cesium Fluoride (0.023 g, 0.151 mmol) and 18 Crown 6 (0.0508 g, 0.192 mmol) were placed in a flame dried round bottom flask which was evacuated and backfilled with nitrogen. Compound **3j** (0.021 g, 0.084 mmol) and furan (0.05 mL, 0.7 mmol) were then dissolved into anhydrous acetonitrile and this solution was added to the reaction flask. The reaction was stirred for 24 hours and monitored by TLC. When the reaction was finished, 2 mL of water was added and it was extracted with CH_2Cl_2 (3 x 3 mL). The organic fractions were collected, dried using $MgSO_4$, and filtered before being purified by silica gel column chromatography (70% Hexanes : 30 % CH_2Cl_2). **5d** was isolated as a white solid (0.012 g, 86 % Yield). ^{1}H NMR (500 MHz, $CDCl_3$): δ 7.49

(s, 2H), 7.37 (s, 2H), 6.94 (s, 2H), 5.77 (s, 2H), 2.73 (t, J = 7.64, 4H), 1.66-1.59, (m, 4H), 1.48-1.40 (m, 4 H), 0.97 (t, J = 8.01 Hz, 6H) ppm, ^{13}C NMR (125 MHz, $CDCl_3$) δ 143.3, 141.7, 139.8, 130.5, 127.7, 118.1, 82.0, 33.6, 32.7, 23.0, 14.2 ppm. IR (solid, ATR) 29.54, 2930, 2868, 1497, 1464, 1377, 1279, 1194, 1148, 1103, 1060, 984, 913, 877, 865, 847, 828, 734, 697 cm^{-1}. HRMS (ESI) calcd for $[C_{22}H_{26}O]H^+$, 307.2065 found 307.2056.

General Procedure for Copper Catalyst:

Copper Cyanide (19.9 mg, x mmol) was transferred to a flame dried 20 mL round bottom flask, evacuated, and back filled with N_2. To this was added 20 mL of anhydrous THF and the flask was cooled to -78 °C. After *n*-BuLi (0.18 mL, 2.5 M in hexanes) was slowly added the flask was warmed to 0 °C for 30 min.

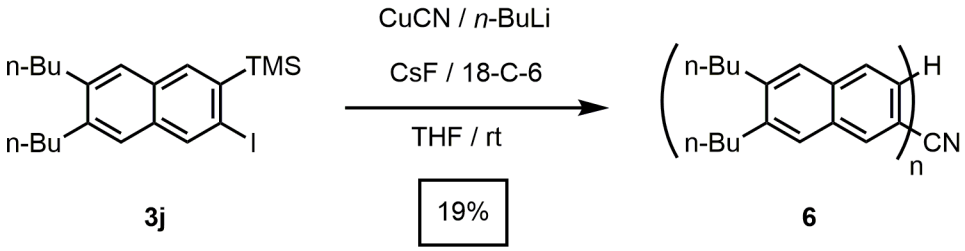

Synthesis of 6: Cesium fluoride (0.0733 g, 0.483 mmol) was transferred to a vial and flame dried under vacuum and backfilled with N_2. Once the reaction vessel was cooled to rt, anhydrous 18 Crown 6 (0.243 g, 0.920 mmol) was added to the reaction vessel which was evacuated and backfilled with N_2 before being dissolved in 3 mL of anhydrous THF. To this stirring solution, a 1 mL solution of **3j** (0.103 g, 0.235 mmol) in anhydrous THF and 0.1 mL of the previously prepared Lipshultz Cuprate is added simultaneously. The reaction was allowed to stir for 12 hours until completion. When

the reaction had finished, 5 mL of water is added and the reaction is extracted using CH_2Cl_2 (3 x 5 mL). The organic fractions were collected and dried using $MgSO_4$. This solution was concentrated under vacuum and **6** was precipitated into MeOH and isolated as a yellow solid (0.011 g, 19%). ^{1}H NMR (500 MHz, $CDCl_3$): δ 7.48 (bs, 4 H), 2.76 (br, 4 H), 1.46 (br, 8 H), 0.98 (br, 6 H) ppm, ^{13}C NMR (125 MHz, $CDCl_3$) δ 138.3, 129.8, 125.9, 32.5, 31.7, 22.0, 13.2 ppm. IR (solid, ATR) 2954, 2937, 2859, 1487, 1464, 1377, 1260, 1102, 1021, 908, 837, 804, 734 cm^{-1}.

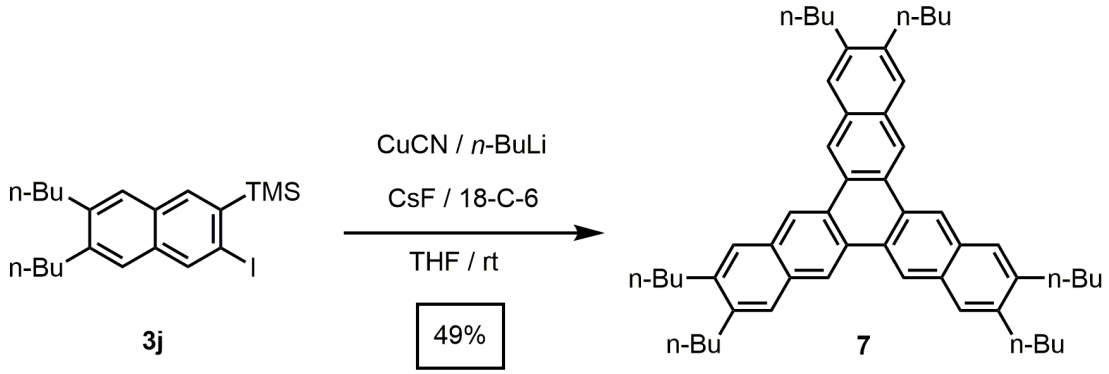

Synthesis of 7: Cesium fluoride (0.070 g, 0.461 mmol) was transferred to a vial and flame dried under vacuum and backfilled with N_2. Once the reaction vessel was cooled to rt, anhydrous 18 Crown 6 (0.255 g, 0.965 mmol) was added to the reaction vessel which was evacuated and backfilled with N_2 before being dissolved in 2 mL of anhydrous THF. To this stirring solution, a 1 mL solution of **3j** (0.107 g, 0.249 mmol) in anhydrous THF and 1 mL of the previously prepared Lipshultz Cuprate is added simultaneously. The reaction was allowed to stir for 12 hours until completion. When the reaction had finished, 5 mL of water is added and the reaction is extracted using CH_2Cl_2 (3 x 5 mL). The organic fractions were collected and dried using $MgSO_4$ before being purified by column chromatography using hexanes as the eluent. **7** was isolated

as a red solid (0.027 g, 49%). ^{1}H NMR (400 MHz, $CDCl_3$): δ 8.87 (s, 6H), 7.77 (s, 6H), 2.84 (dd, 12H) 1.82-1.72 (m, 12H), 1.60-1.49 (s, 12H), 1.06 (t, 18H) ppm, ^{13}C NMR (100 MHz, $CDCl_3$) δ 140.07, 131.70, 128.59, 126.92, 121.41, 33.25, 32.81, 23.06, 14.31 ppm. IR (solid, ATR) 29.53, 2923, 2857, 1599, 1504, 1461, 1394, 1377, 1260, 1182, 1091, 1024, 939, 892, 800, 737, 702 cm^{-1}. HRMS (APPI) calcd for $[C_{54}H_{66}]H^{+}$, 715.5237 found 715.5241.

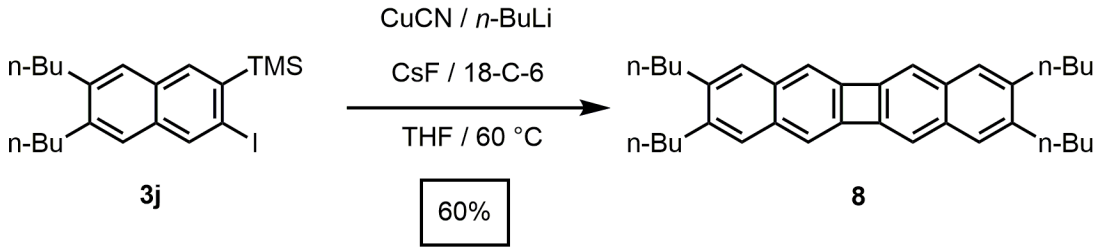

Synthesis of 8: Cesium fluoride (0.074 g, 0.487 mmol) was transferred to a vial and flame dried under vacuum and backfilled with N_2. Once the reaction vessel was cooled to rt, anhydrous 18 Crown 6 (0.254 g, 0.962 mmol) was added to the reaction vessel which was evacuated and backfilled with N_2 before being dissolved in 2 mL of anhydrous THF. To this stirring solution, a 1 mL solution of **3j** (0.106 g, 0.242 mmol) in anhydrous THF and 1 mL of the previously prepared Lipshultz Cuprate is added simultaneously. The reaction is placed in a 60 °C oil bath and allowed to stir for 12 hours to completion. After the reaction has cooled to rt 5 mL of water is added and the reaction is extracted using CH_2Cl_2 (3 x 5 mL). The organic fractions were collected and dried using $MgSO_4$ before being purified by silica gel column chromatography (100% hexanes to 70:30 Hexanes/CH_2Cl_2). **8** was isolated as a yellow solid (0.034 g, 60 %). ^{1}H NMR (400 MHz, $CDCl_3$): δ 7.35 (s, 6H), 7.15 (s, 6H), 2.69 (dd, 12H), 1.69-1.59 (m,

12H), 1.51-1.40 (m, 12H), 0.99 (t, 18H) ppm, ^{13}C NMR (100 MHz, $CDCl_3$) δ 145.93, 139.81, 133.79, 128.61, 116.15, 33.49, 32.58, 22.99, 14.21 ppm. IR (solid, ATR) 2956, 2925, 2857, 1486, 1456, 1372, 1325, 1262, 1196, 1148, 1096, 1033, 936, 900, 889, 977, 845, 802, 756, 737 cm^{-1}. HRMS (APPI) calcd for $[C_{36}H_{44}]H^+$, 476.3438 found 476.3441.

C. 1D NMR Spectroscopy

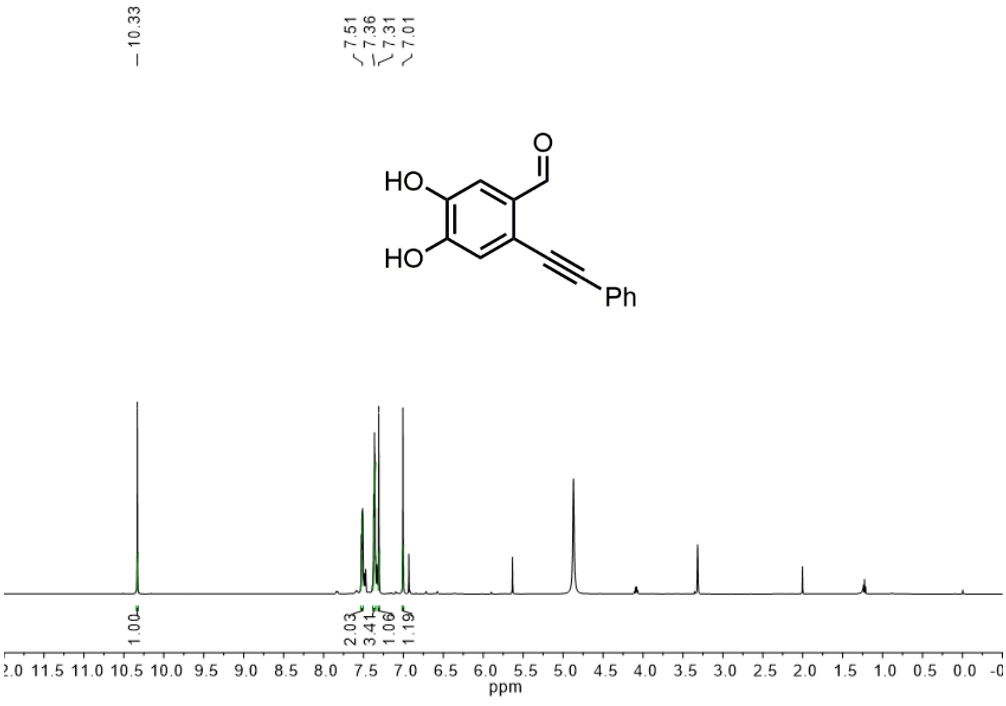

Figure S4.1. ^{1}H NMR of **S1** (500 MHz, CD_3OD, 298 K)

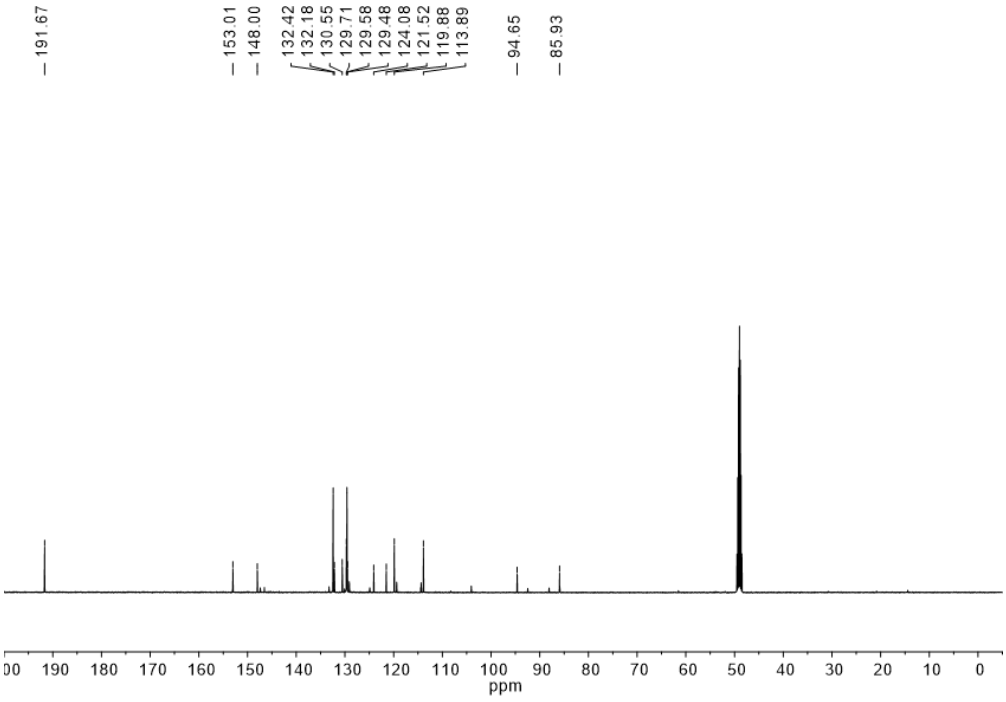

Figure S4.2. ^{13}C NMR of **S1** (125 MHz, CD_3OD, 298 K)

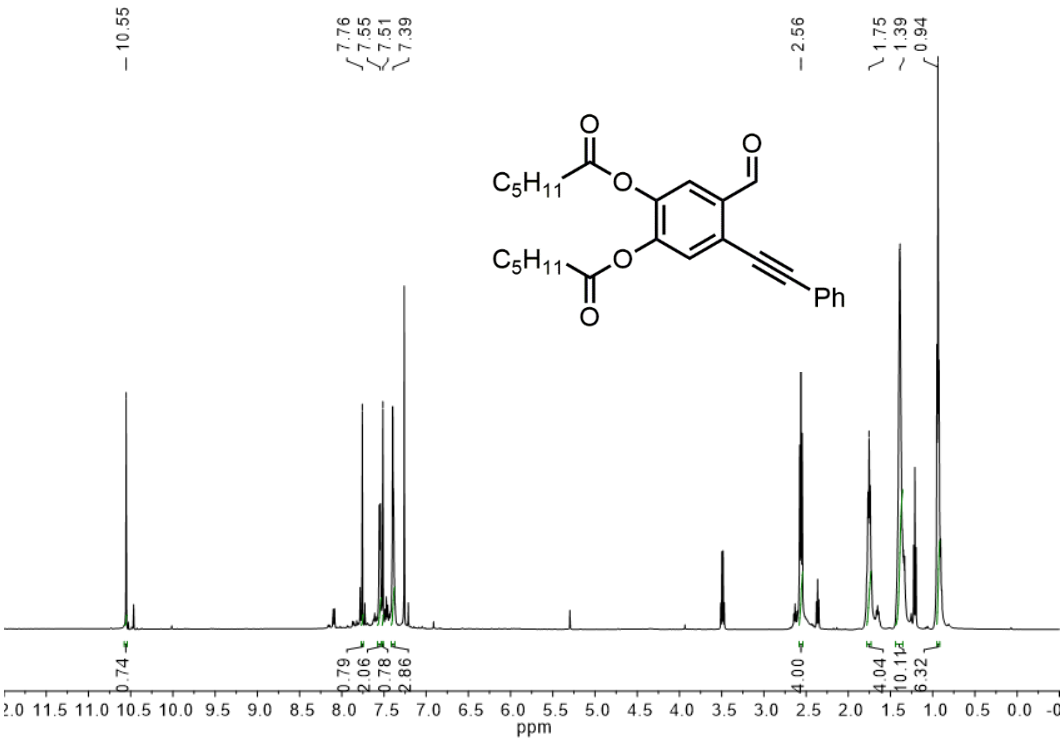

Figure S4.3. ^{1}H NMR of **1g** (500 MHz, $CDCl_3$, 298 K)

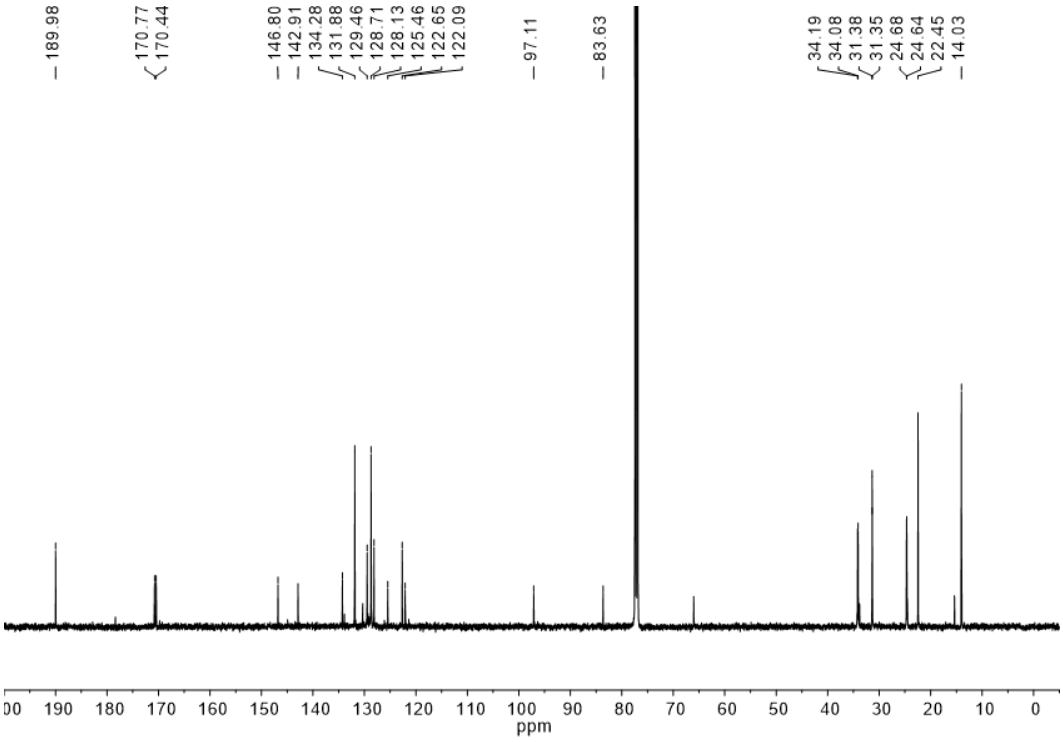

Figure S4.4. ^{13}C NMR of **1g** (125 MHz, $CDCl_3$, 298 K)

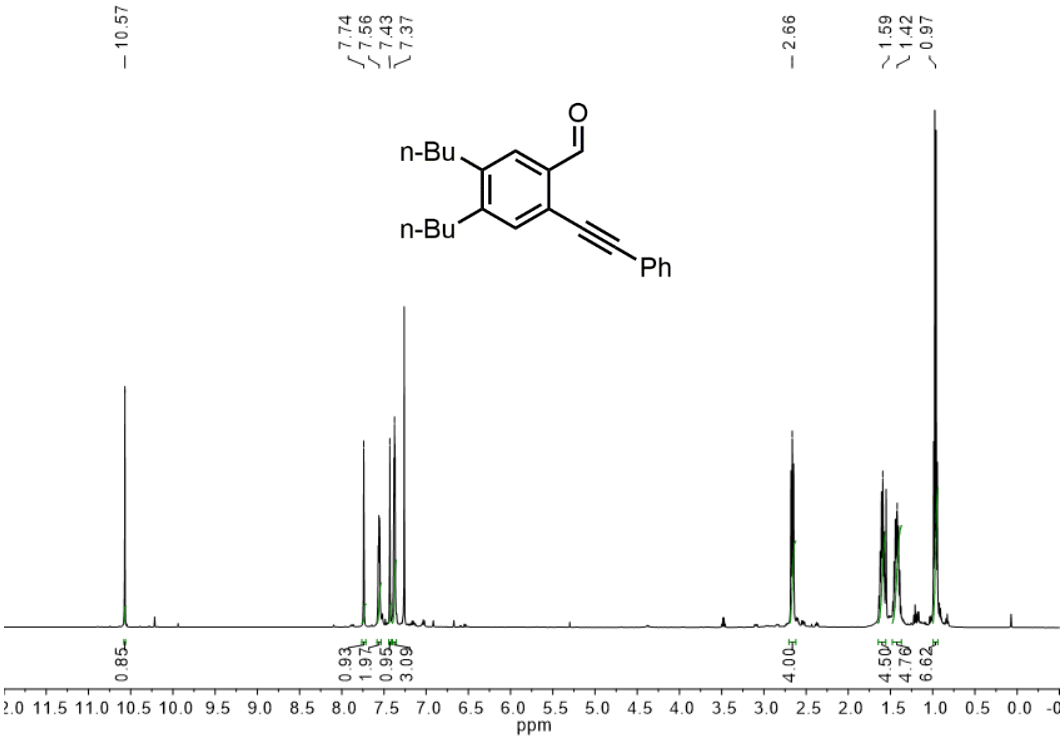

Figure S4.5. ^{1}H NMR of **1h** (500 MHz, CD_3OD, 298 K)

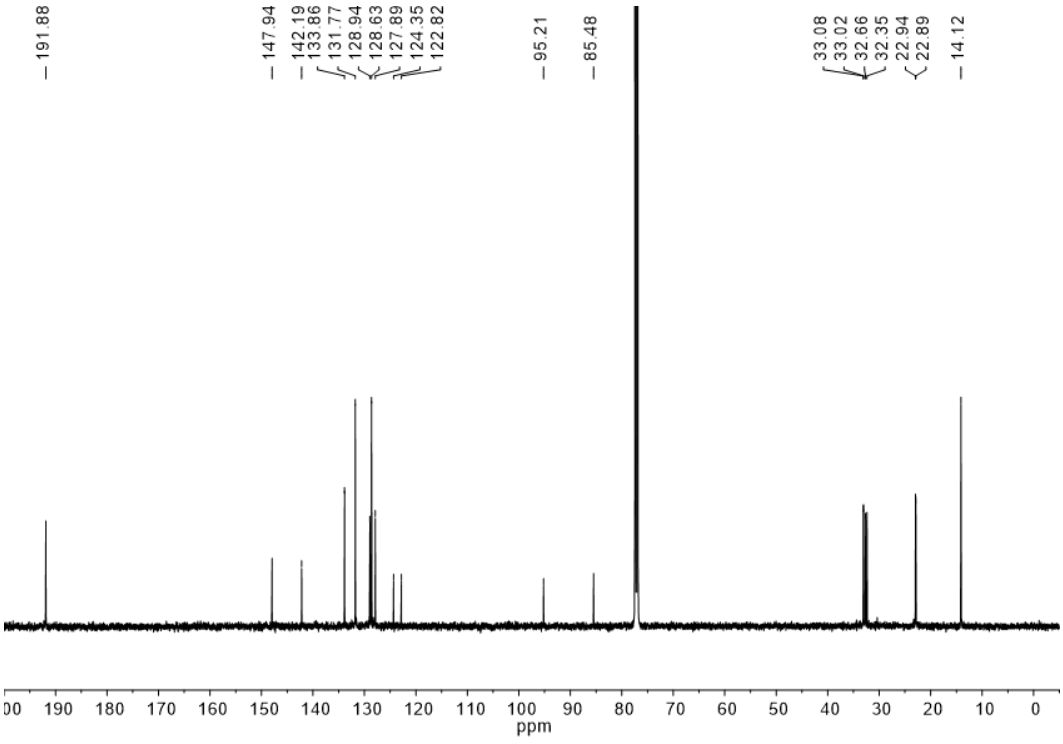

Figure S4.6 ^{13}C NMR of **1h** (125 MHz, $CDCl_3$, 298 K)

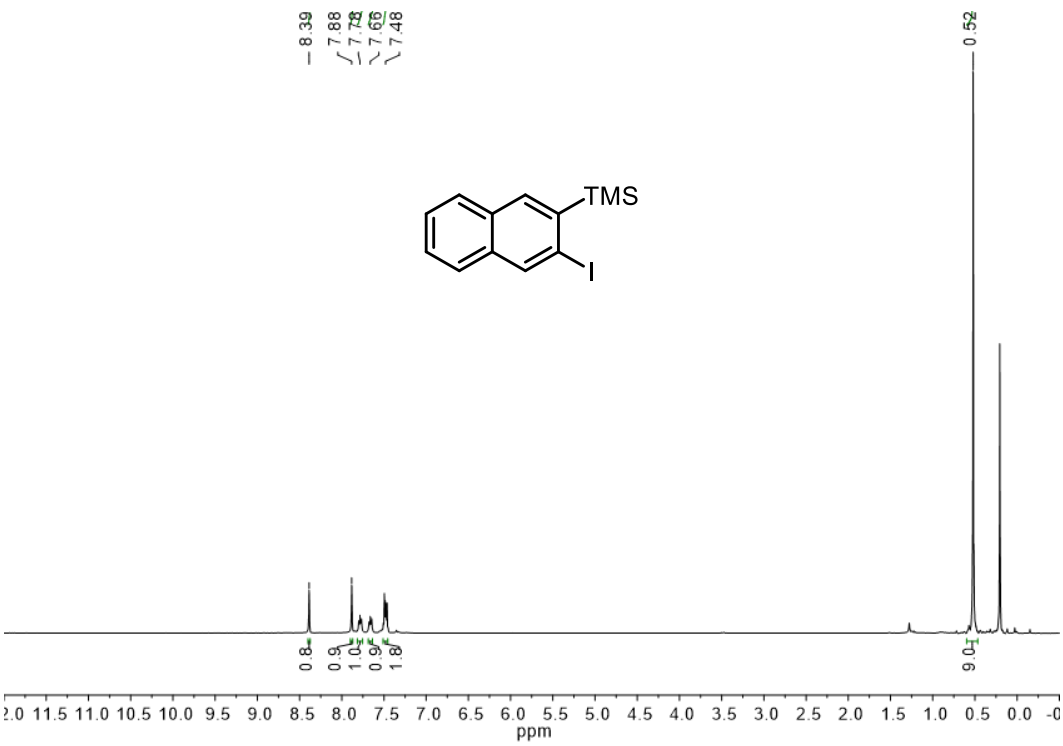

Figure S4.7. ^{1}H NMR of **3a** (400 MHz, $CDCl_3$, 298 K)

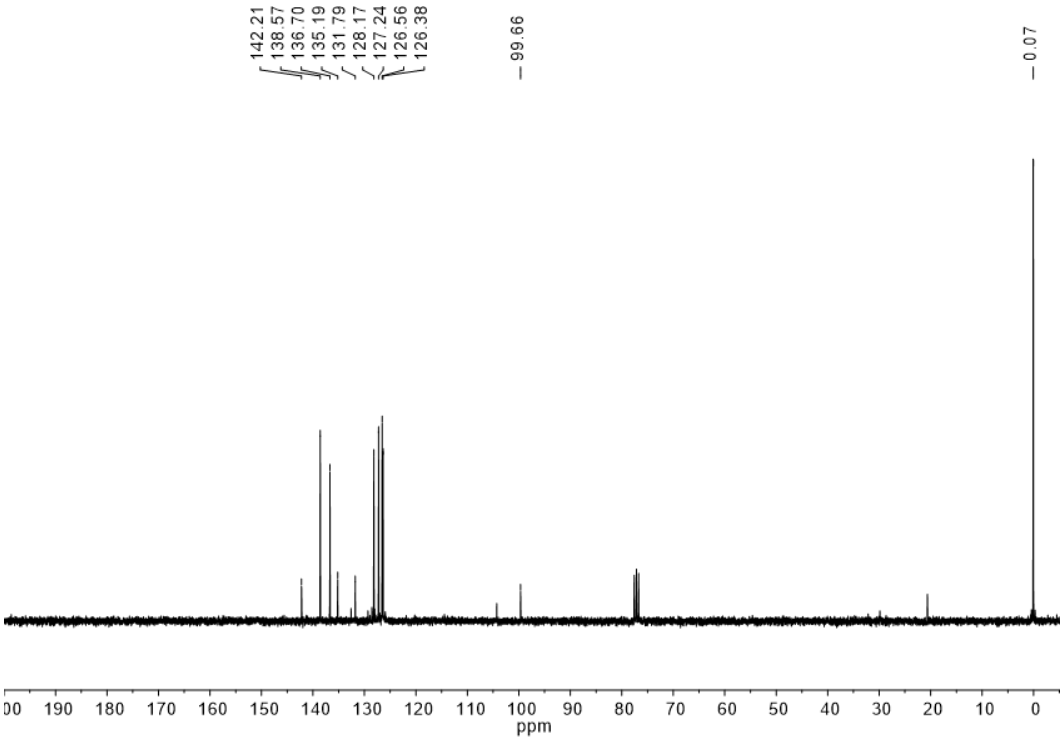

Figure S8. ^{13}C NMR of **3a** (100 MHz, $CDCl_3$, 298 K)

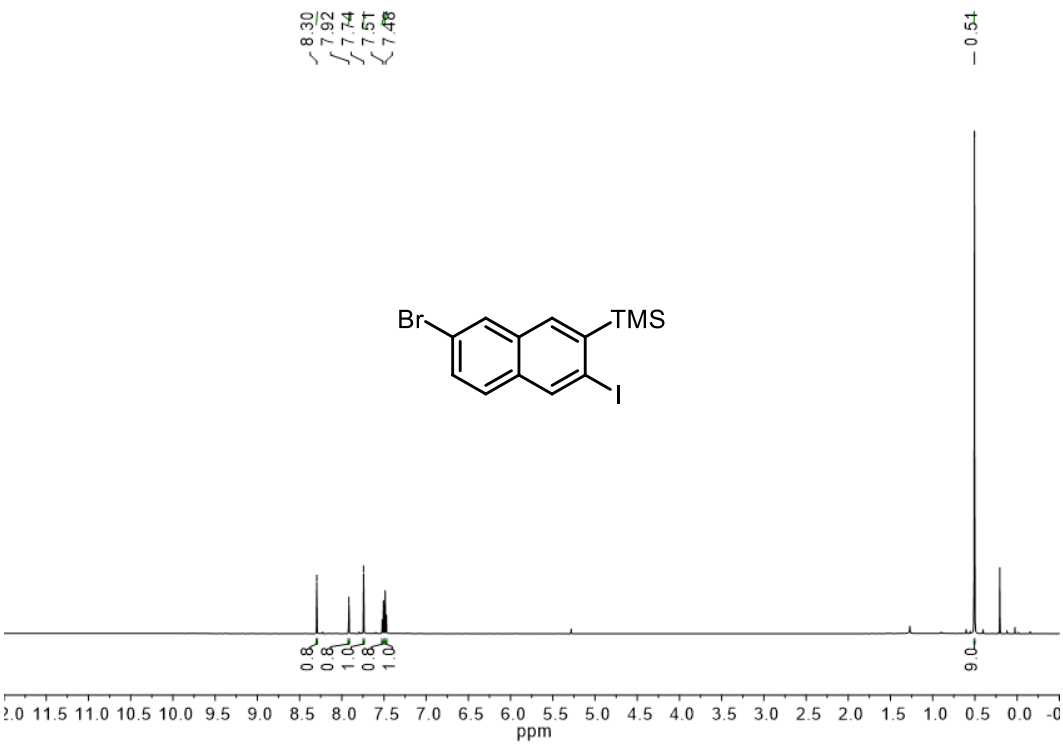

Figure S4.9. ^{1}H NMR of **3b** (600 MHz, $CDCl_3$, 298 K)

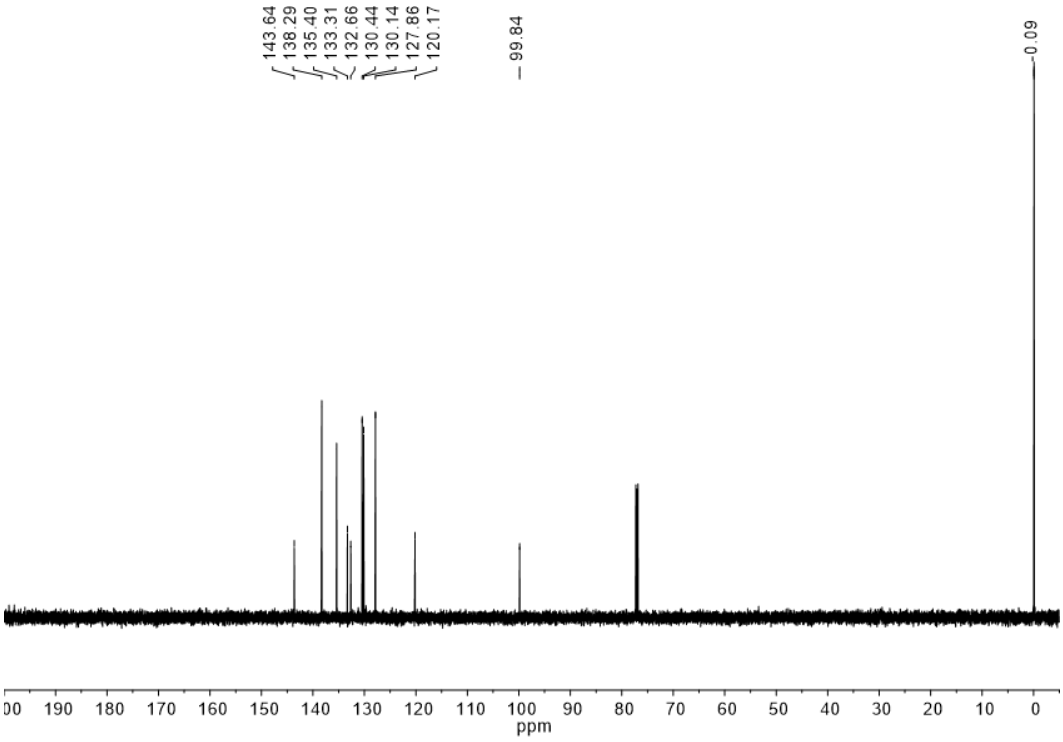

Figure S4.10. ^{13}C NMR of **3b** (150 MHz, $CDCl_3$, 298 K)

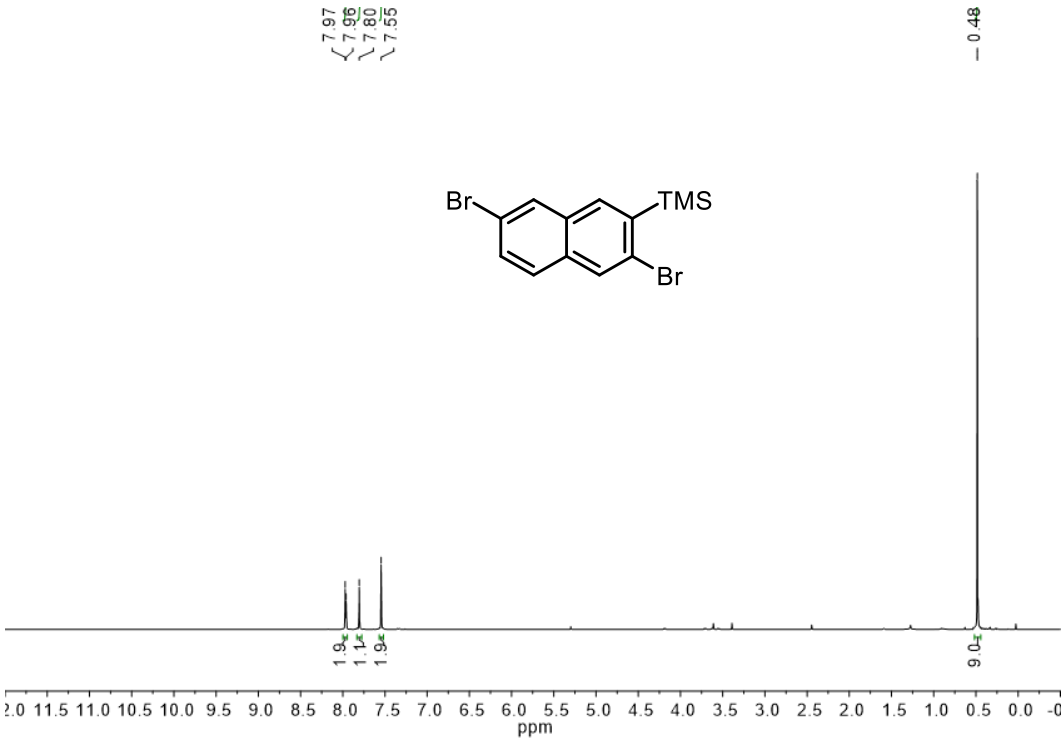

Figure S4.11. ^{1}H NMR of **3c** (400 MHz, $CDCl_3$, 298 K)

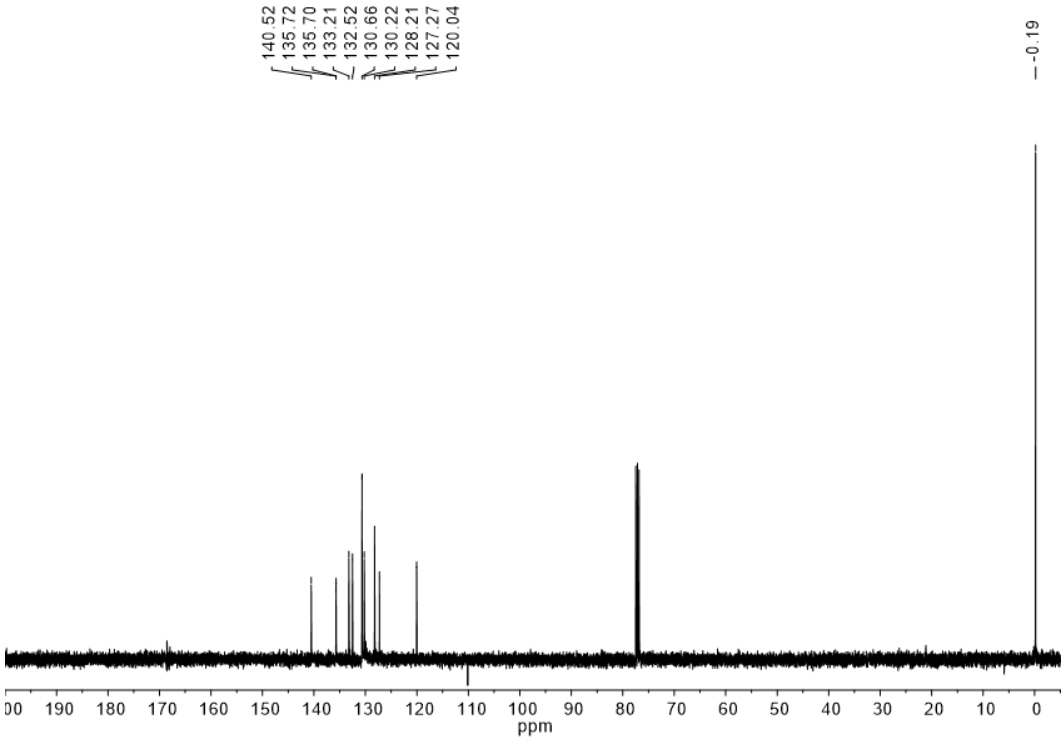

Figure S4.12. ^{1}H NMR of **3c** (100 MHz, $CDCl_3$, 298 K)

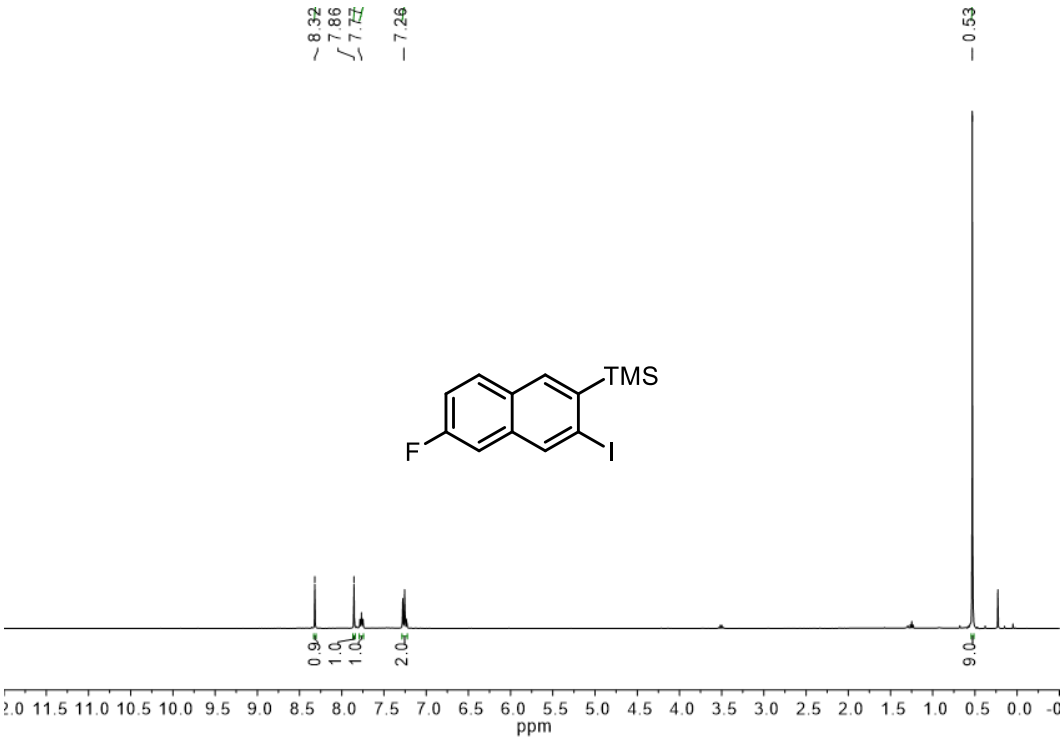

Figure S4.13. ^{1}H NMR of **3d** (100 MHz, $CDCl_3$, 298 K)

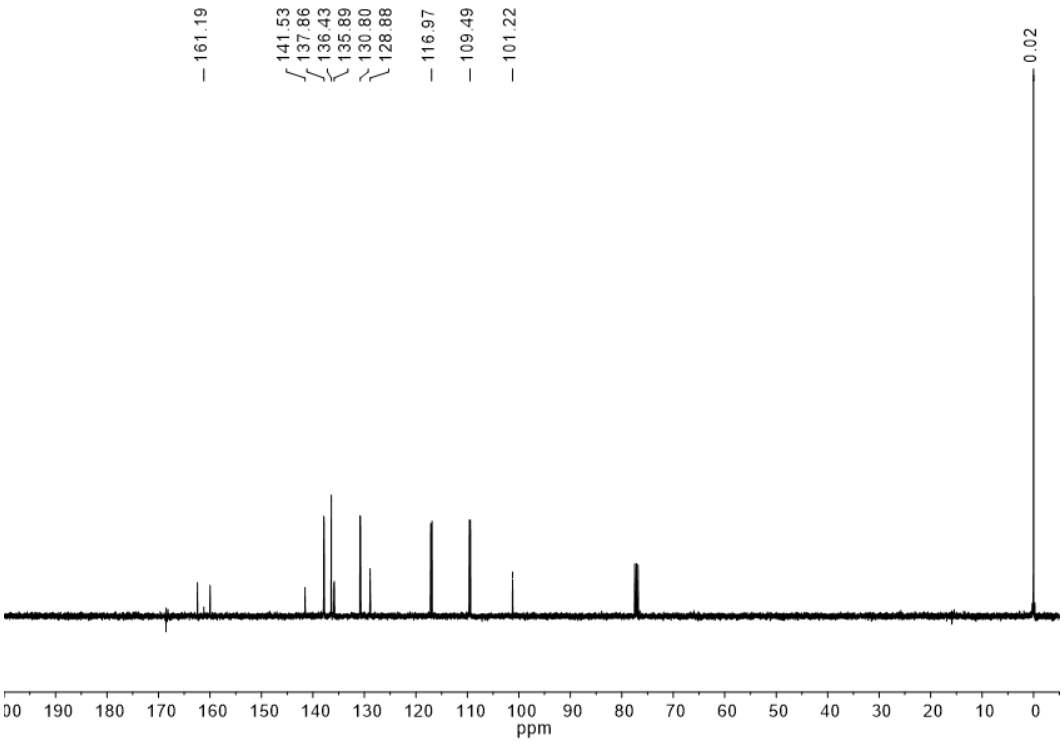

Figure S4.14. ^{13}C NMR of **3d** (100 MHz, $CDCl_3$, 298 K)

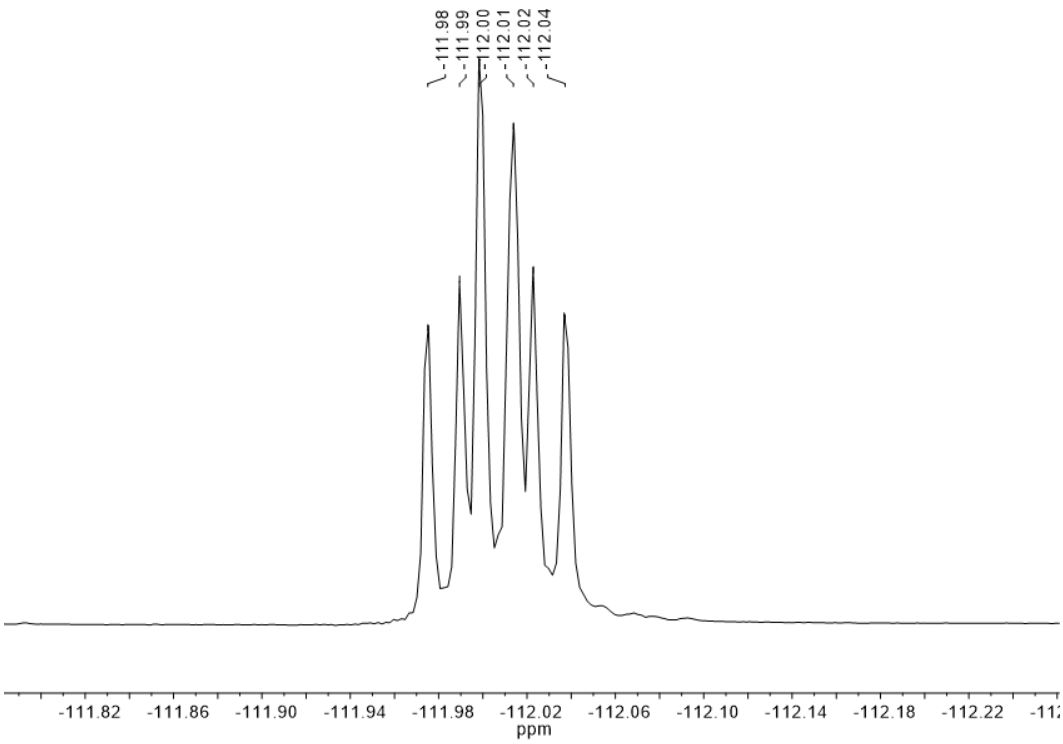

Figure S4.15. ^{19}F NMR of **3d** (375 MHz, $CDCl_3$, 298 K)

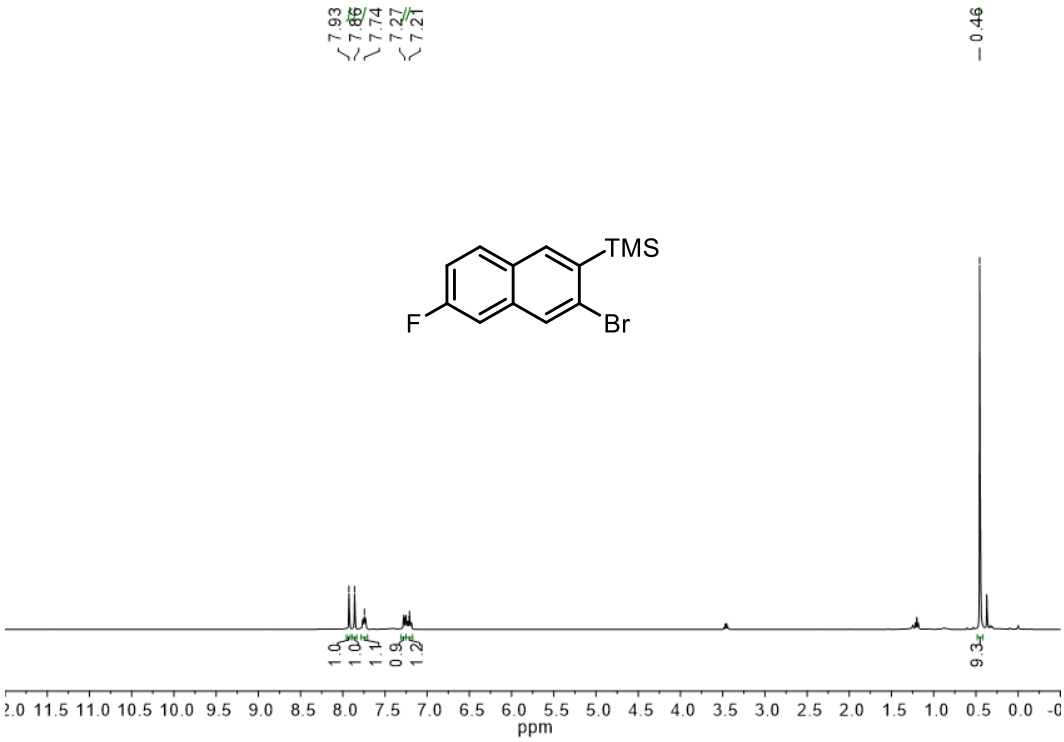

Figure S4.16. ^{1}H NMR of **3e** (400 MHz, $CDCl_3$, 298 K)

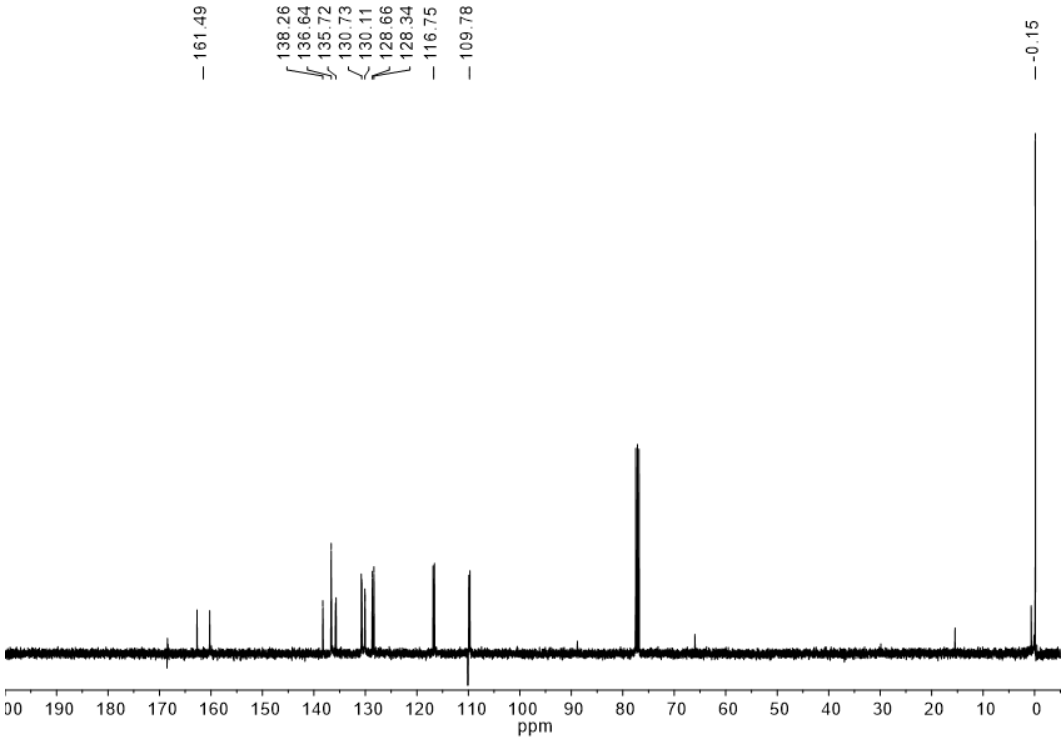

Figure S4.17. ^{13}C NMR of **3e** (100 MHz, $CDCl_3$, 298 K)

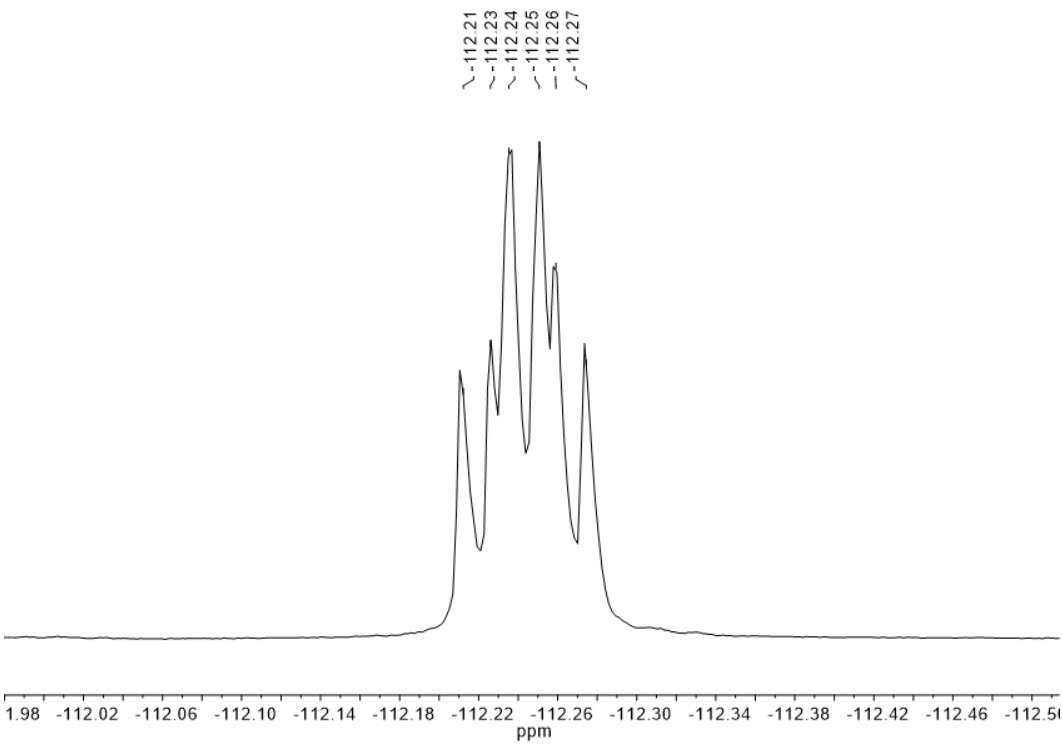

Figure S4.18. ^{19}F NMR of **3e** (376 MHz, $CDCl_3$, 298 K)

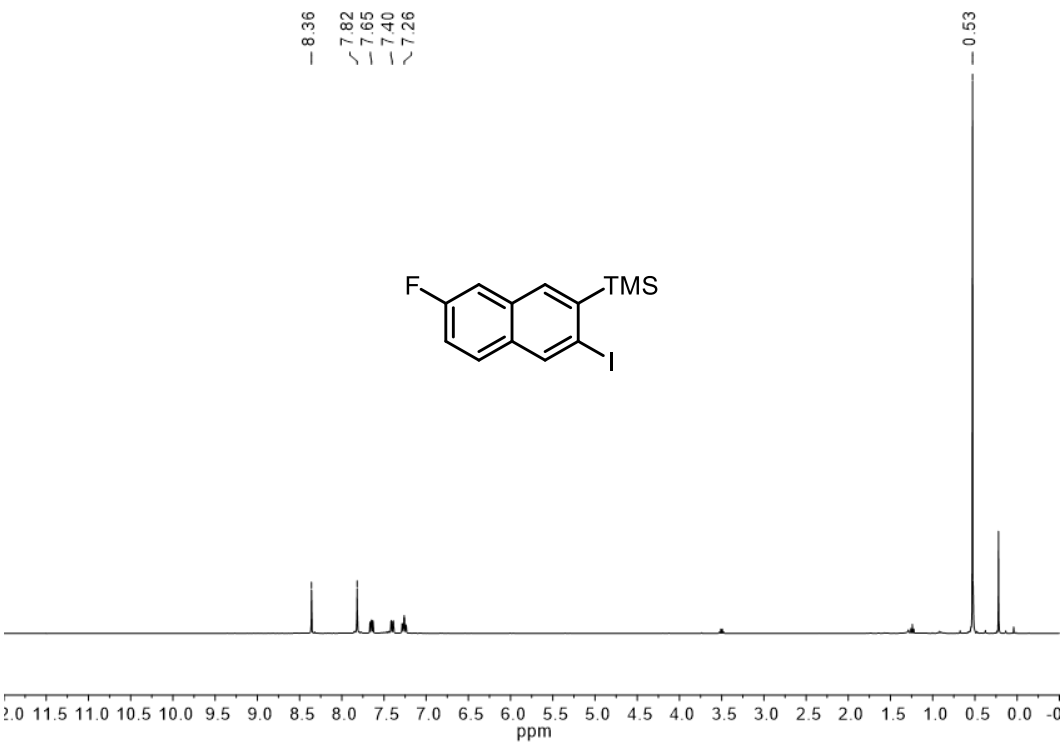

Figure S4.19. ^{1}H NMR of **3f** (400 MHz, $CDCl_3$, 298 K)

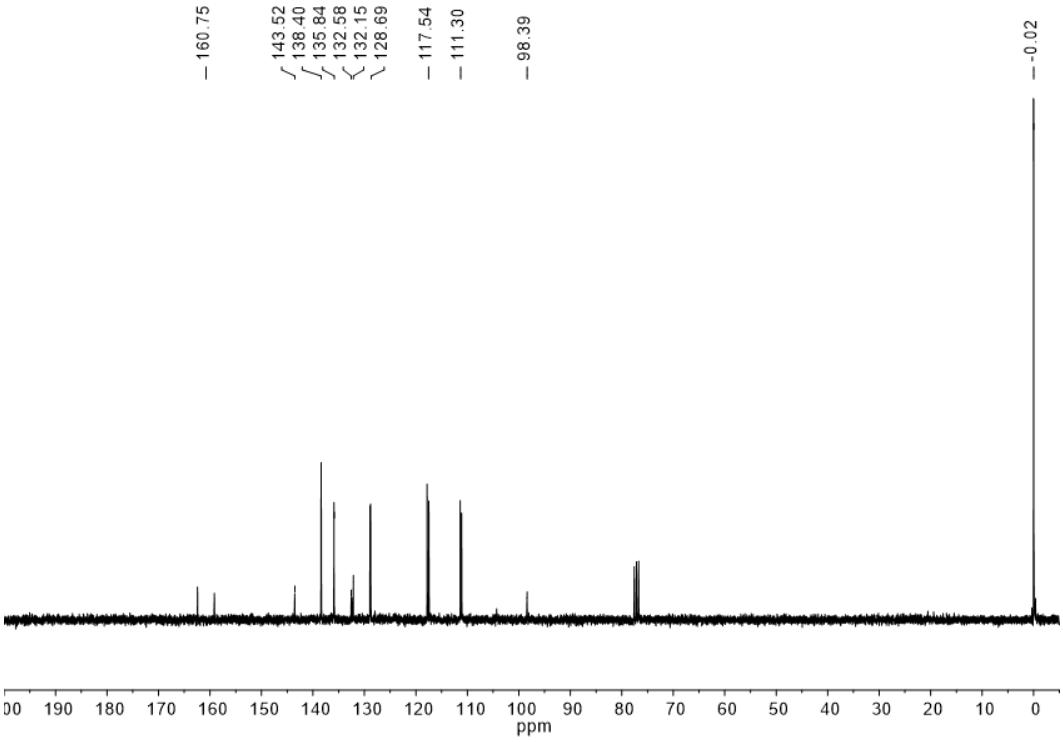

Figure S4.20. ^{13}C NMR of **3f** (100 MHz, $CDCl_3$, 298 K)

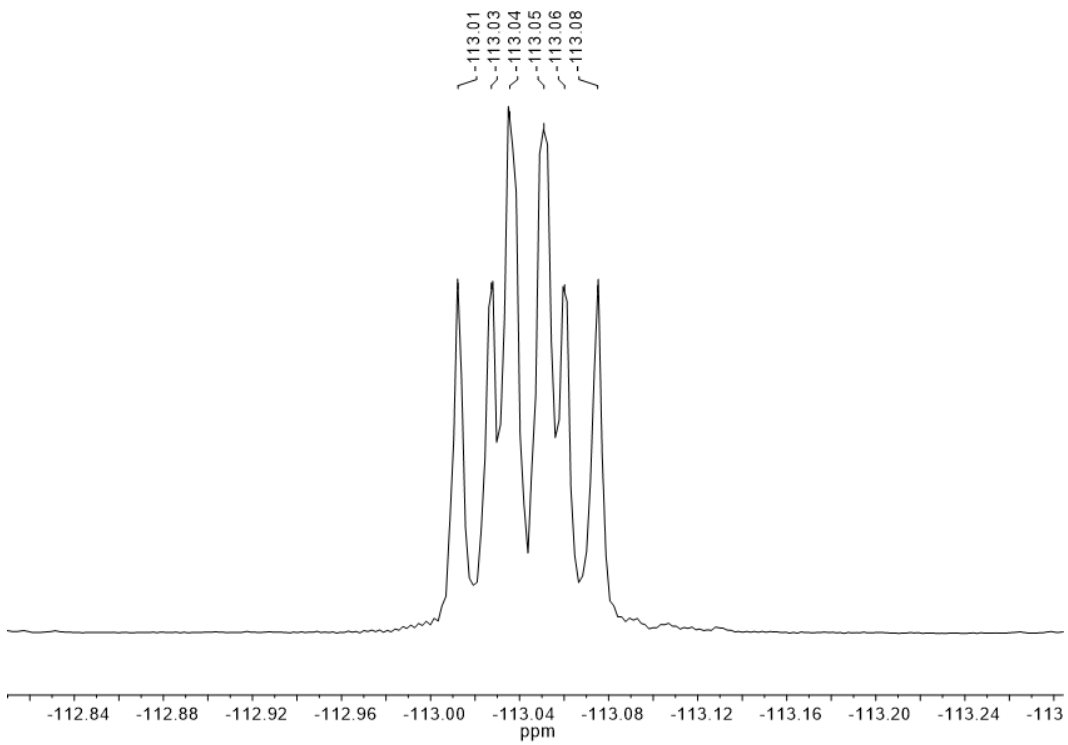

Figure S4.21. ^{19}F NMR of **3f** (375 MHz, $CDCl_3$, 298 K)

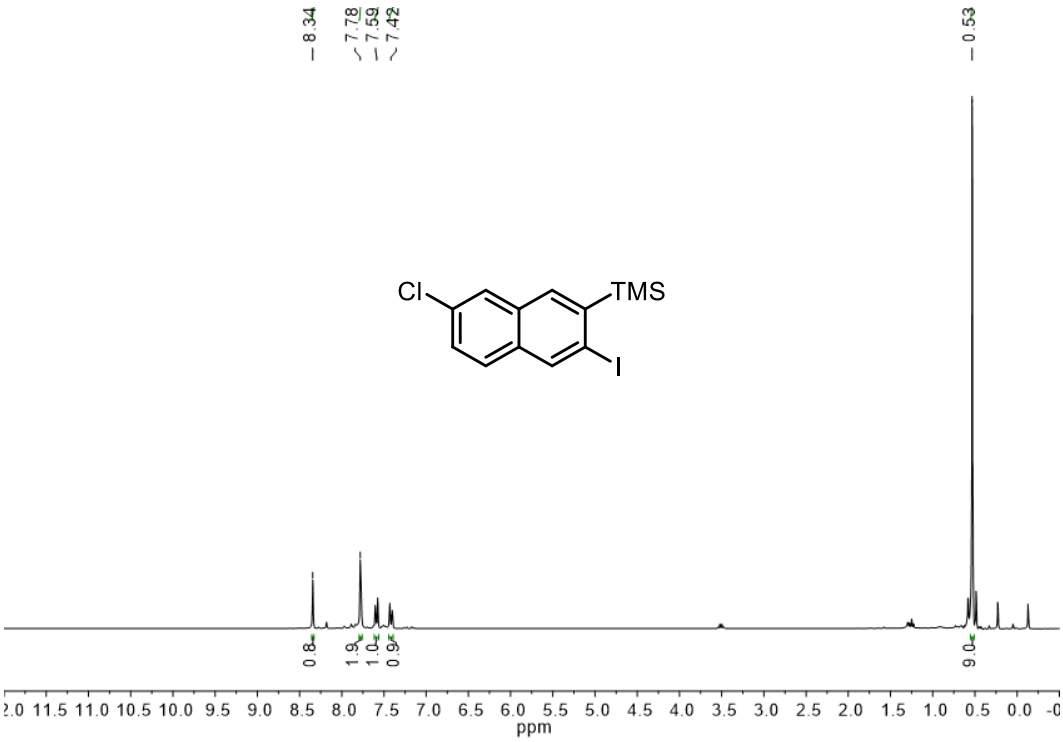

Figure S4.22. ^{1}H NMR of **3g** (300 MHz, $CDCl_3$, 298 K)

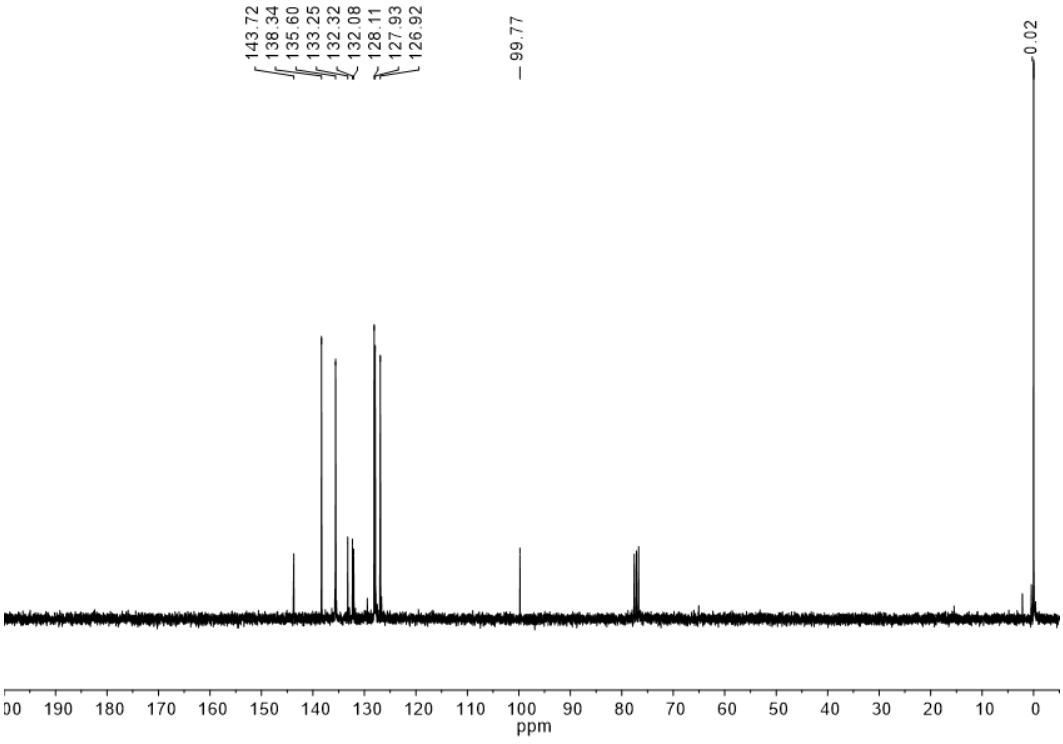

Figure S4.23. ^{13}C NMR of **3g** (75 MHz, $CDCl_3$, 298 K)

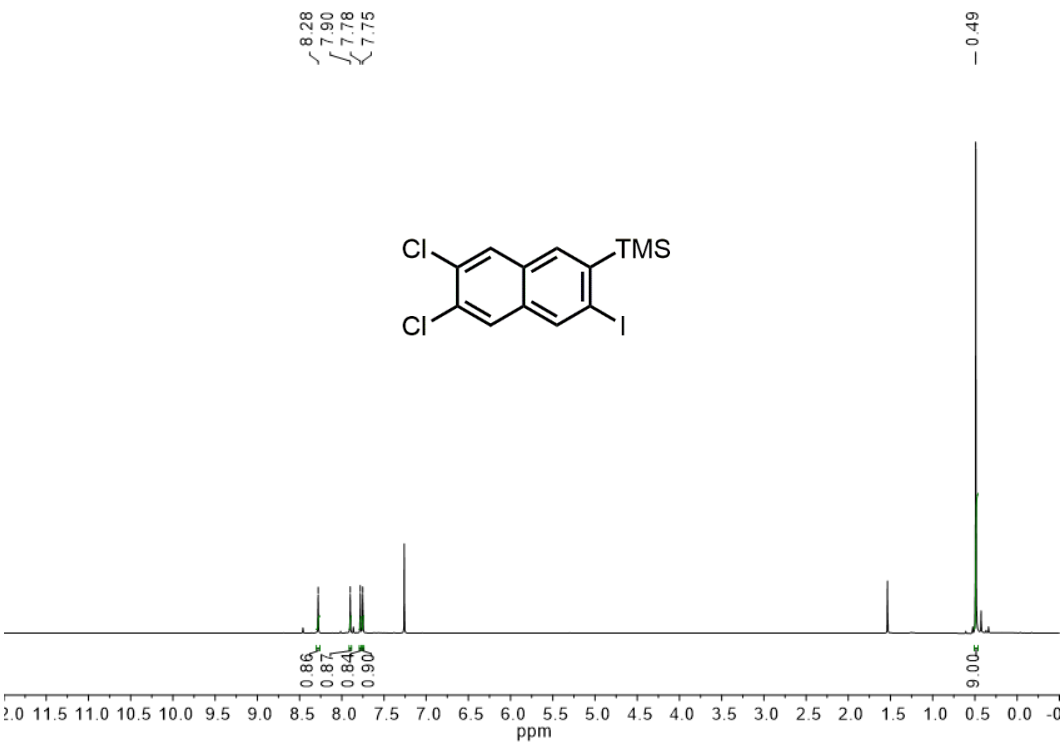

Figure S4.24. ^{1}H NMR of **3h** (500 MHz, $CDCl_3$, 298 K)

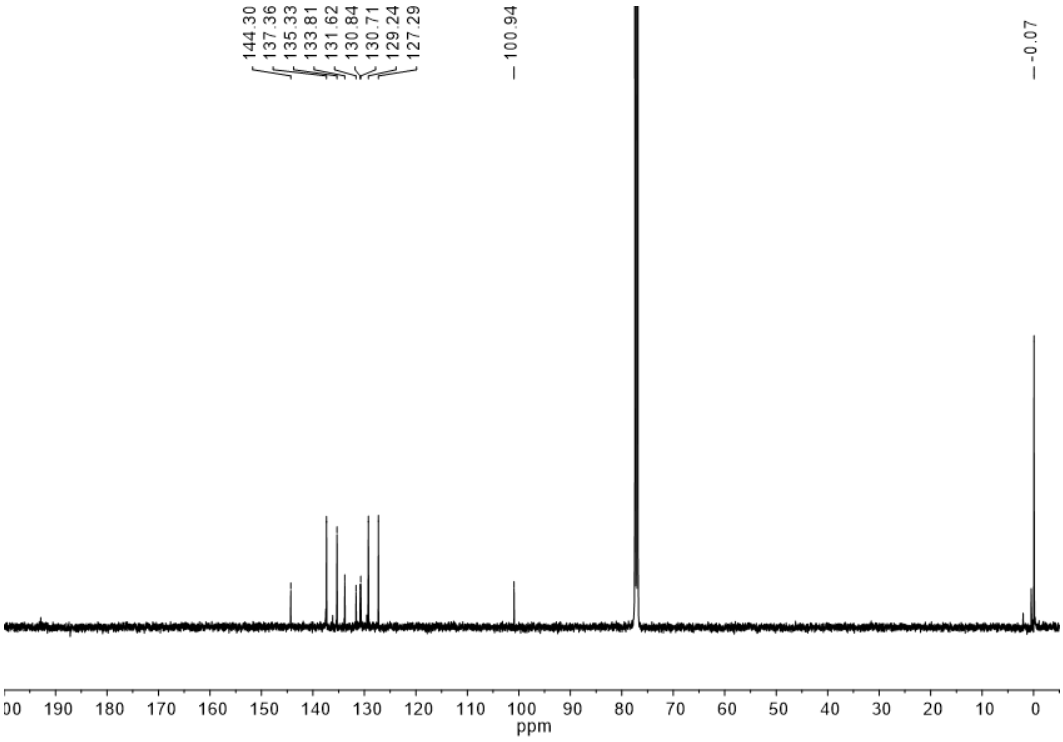

Figure S4.25. ^{13}C NMR of **3h** (125 MHz, $CDCl_3$, 298 K)

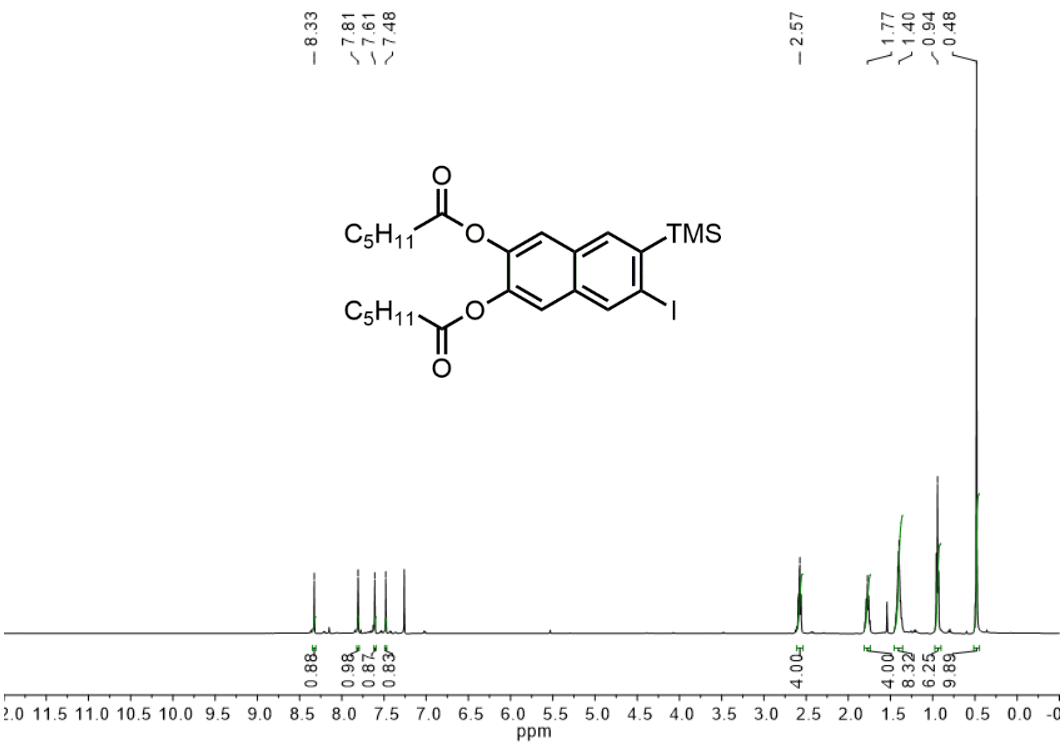

Figure S4.26. ^{1}H NMR of **3i** (500 MHz, $CDCl_3$, 298 K)

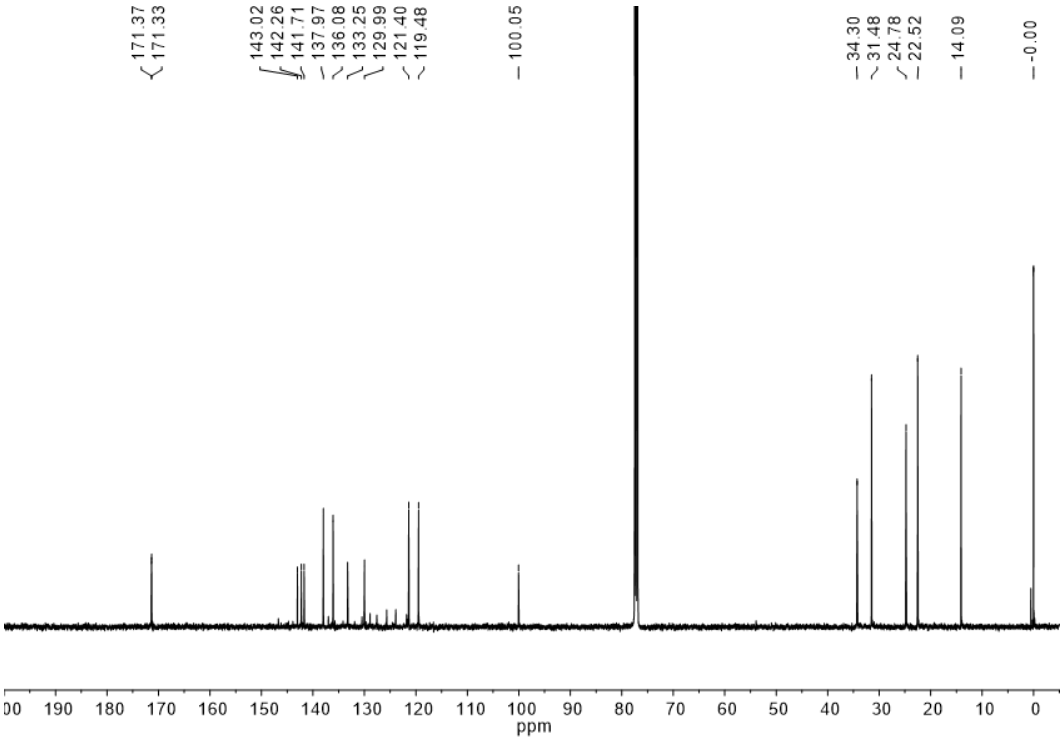

Figure S4.27. ^{13}C NMR of **3i** (125 MHz, $CDCl_3$, 298 K)

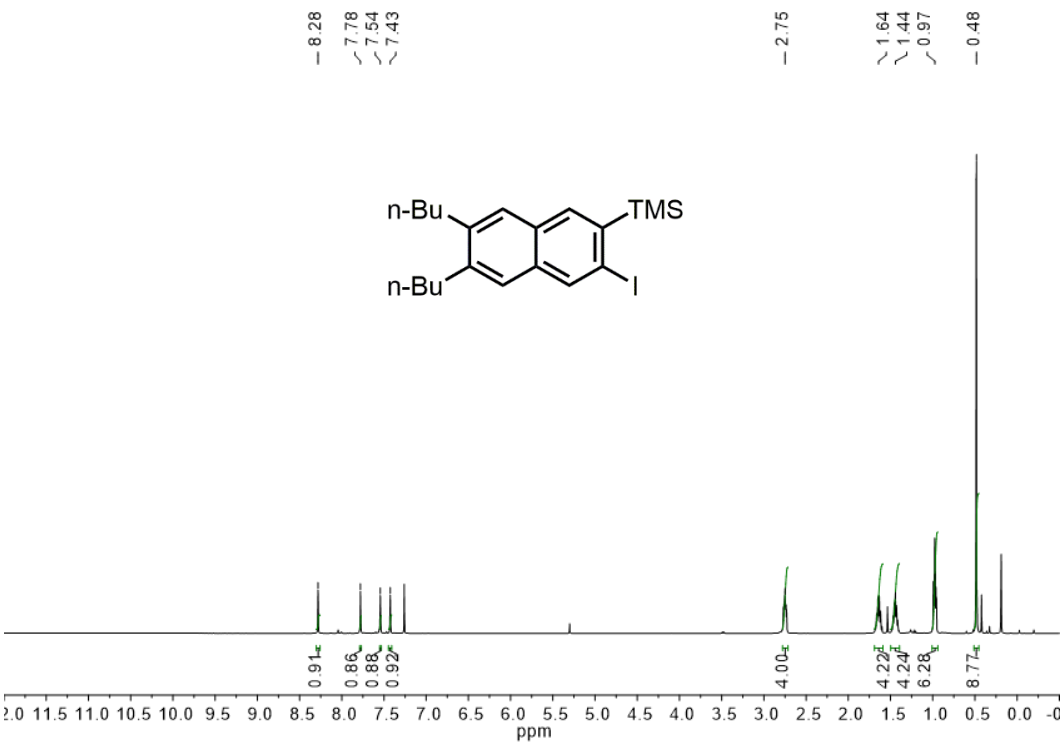

Figure S4.28. ^{1}H NMR of **3j** (500 MHz, $CDCl_3$, 298 K)

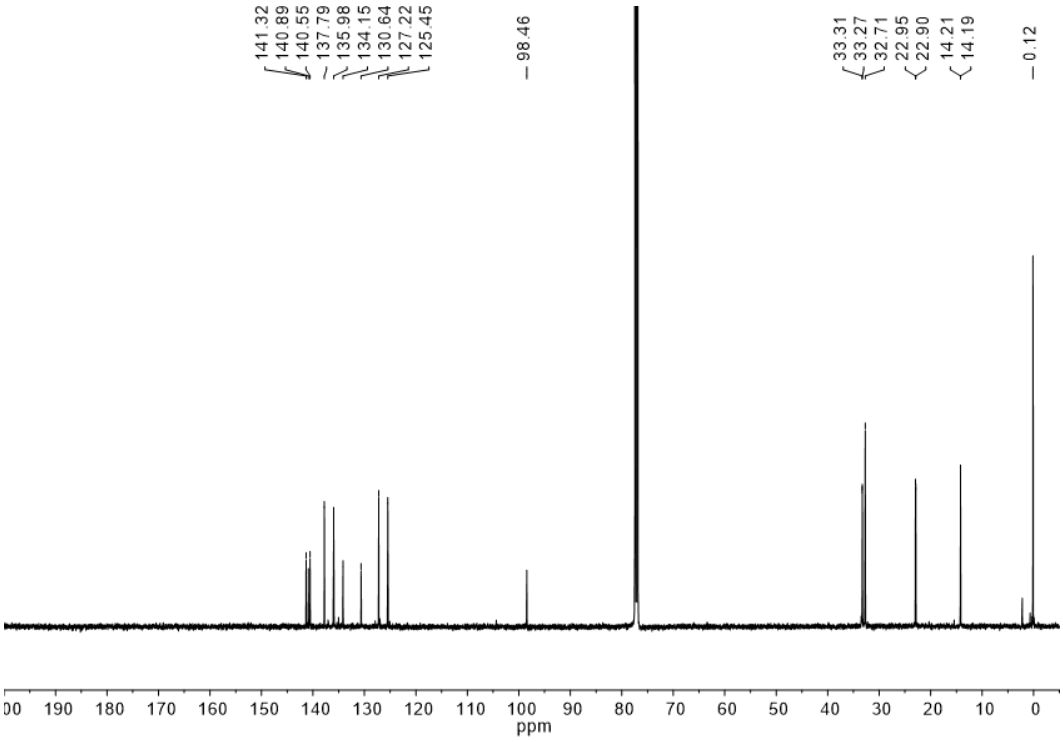

Figure S4.29. ^{13}C NMR of **3j** (125 MHz, $CDCl_3$, 298 K)

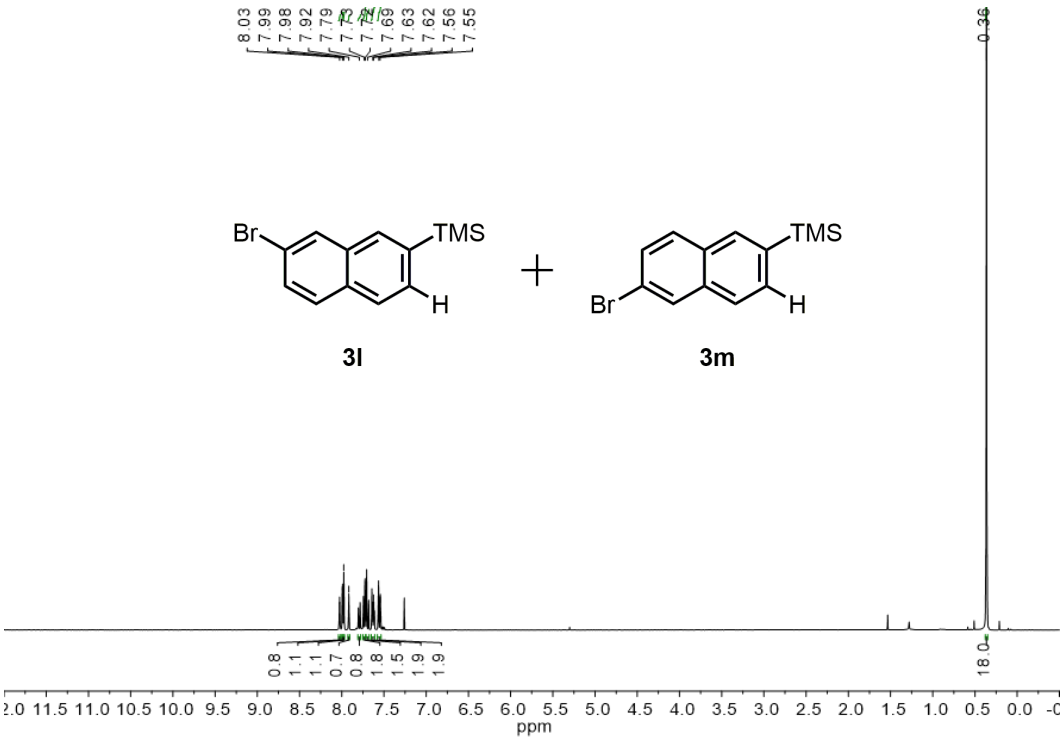

Figure S4.30. ^{1}H NMR of **3l and 3m** (400 MHz, $CDCl_3$, 298 K)

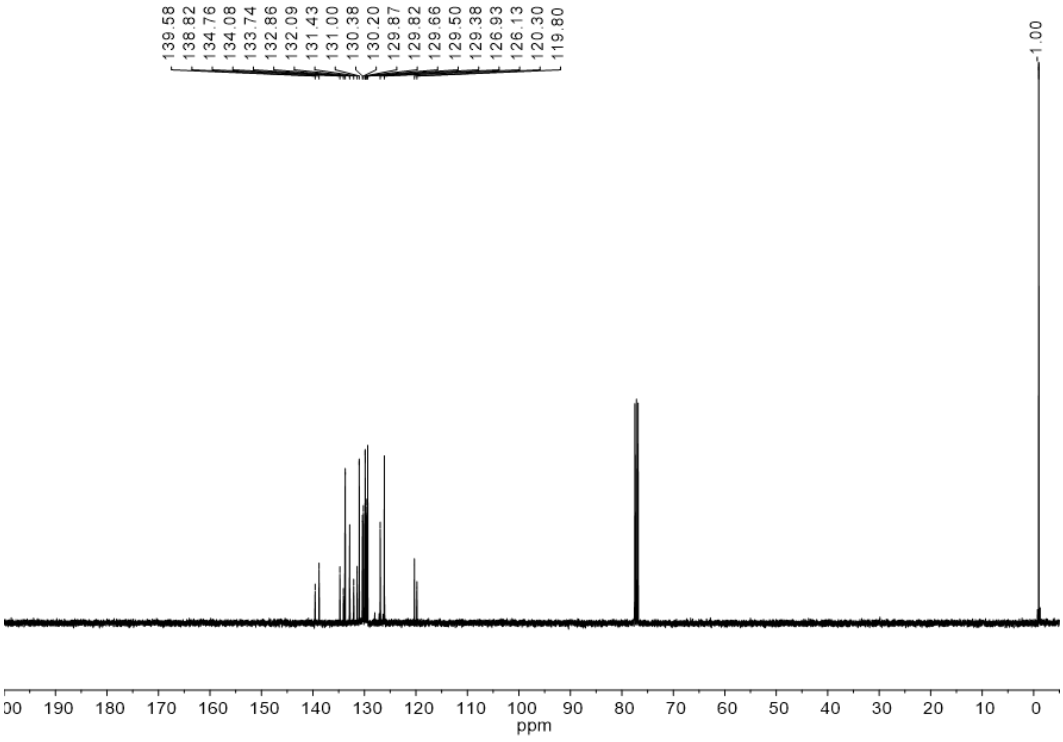

Figure S4.31. ^{13}C NMR of **3l and 3m** (100 MHz, $CDCl_3$, 298 K)

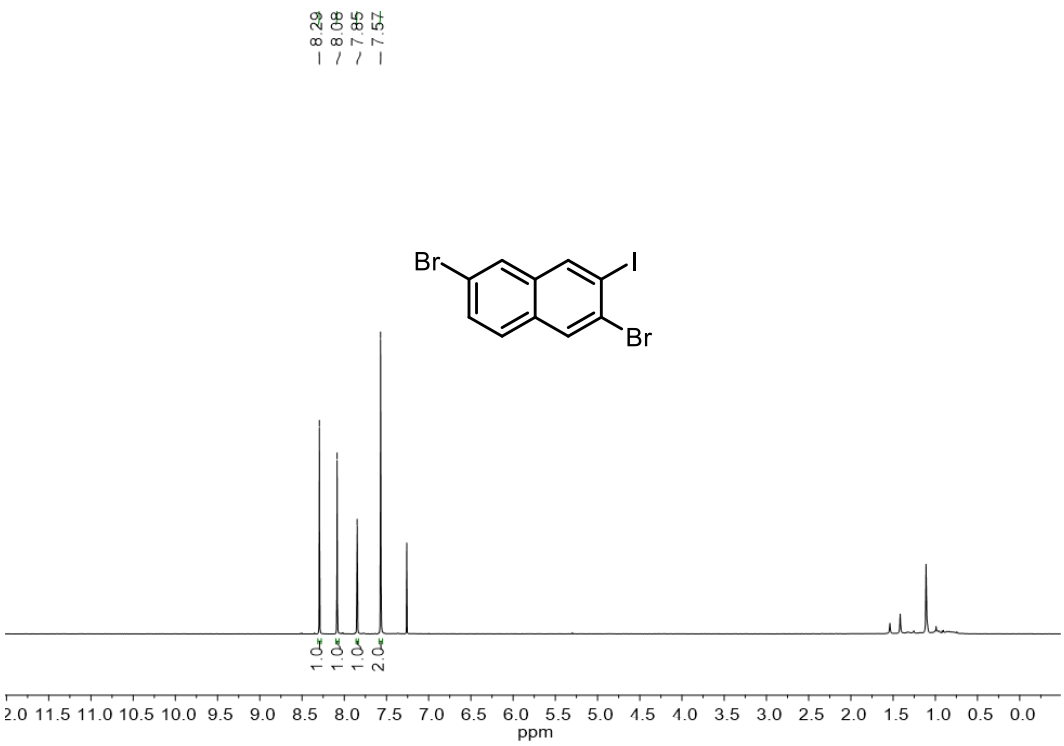

Figure S4.31. ^{1}H NMR of **4** (400 MHz, $CDCl_3$, 298 K)

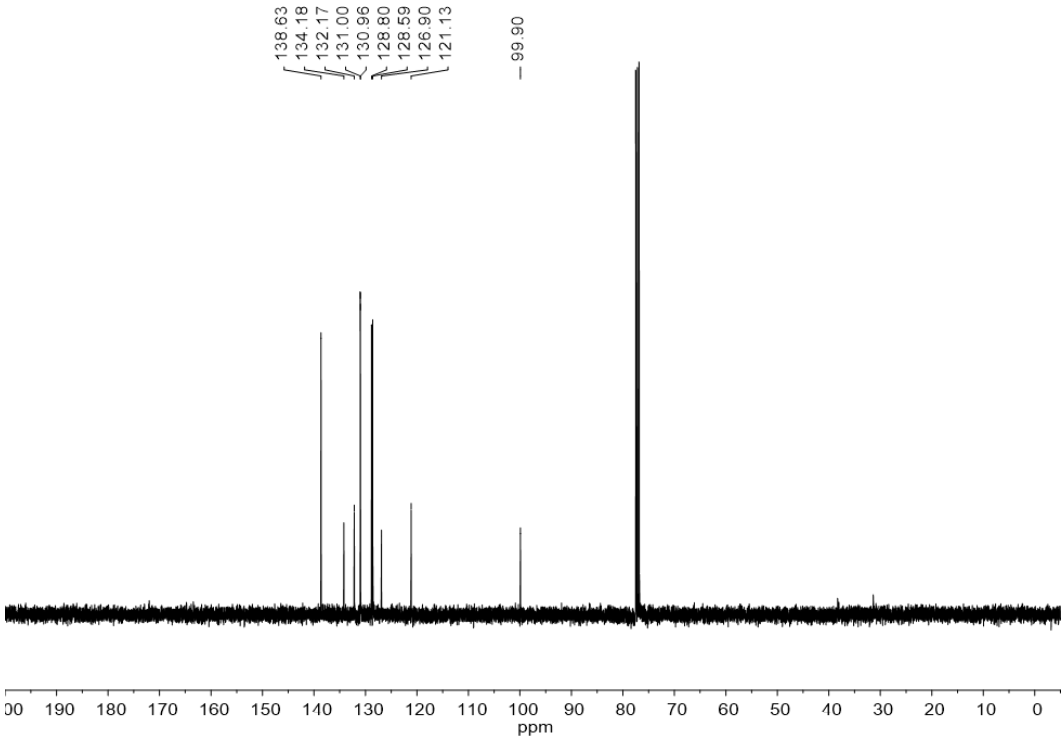

Figure S4.32. ^{13}C NMR of **4** (100 MHz, $CDCl_3$, 298 K)

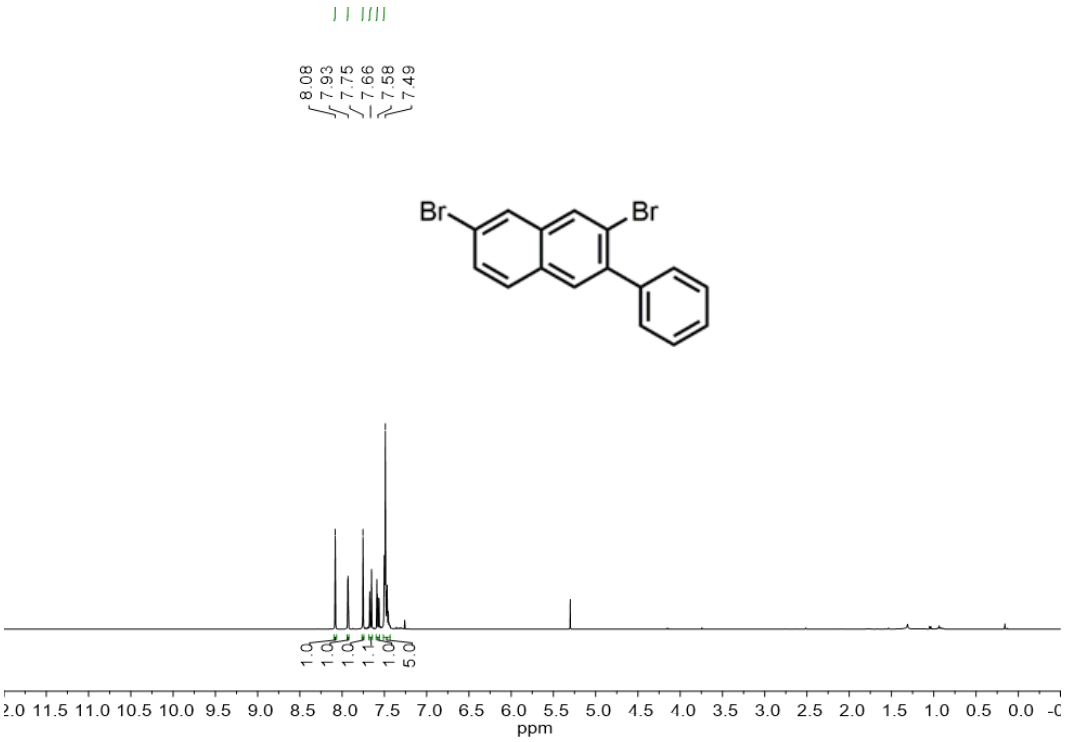

Figure S4.33. ^{13}C NMR of **4** (100 MHz, $CDCl_3$, 298 K)

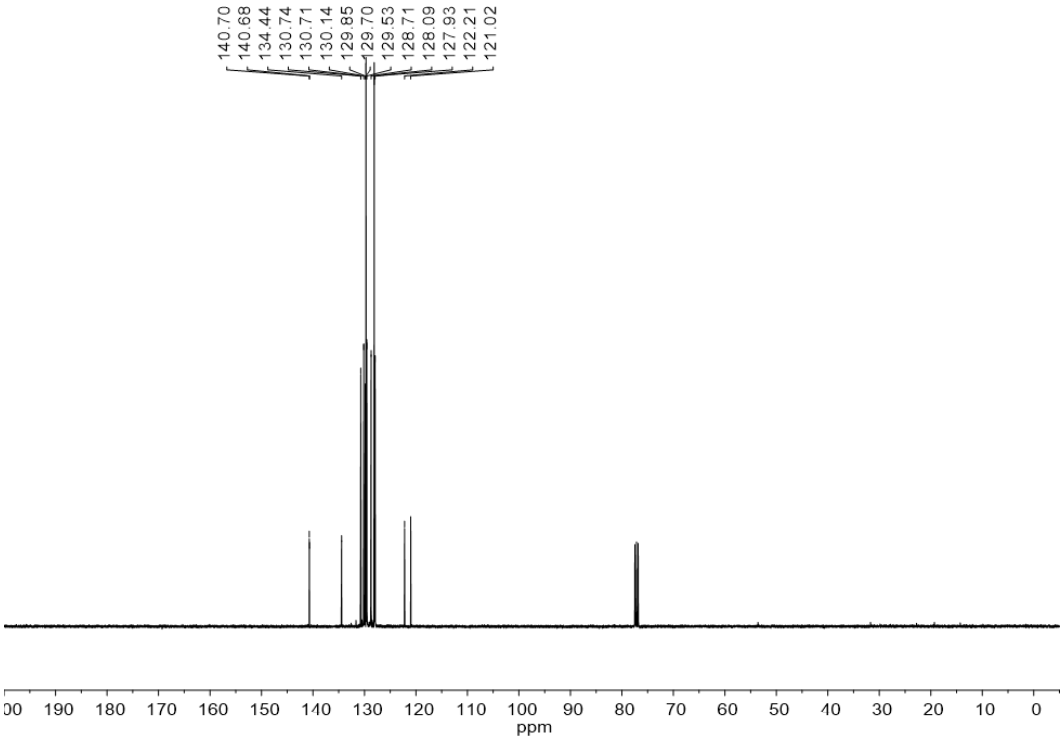

Figure S4.34. ^{13}C NMR of **4** (100 MHz, $CDCl_3$, 298 K)

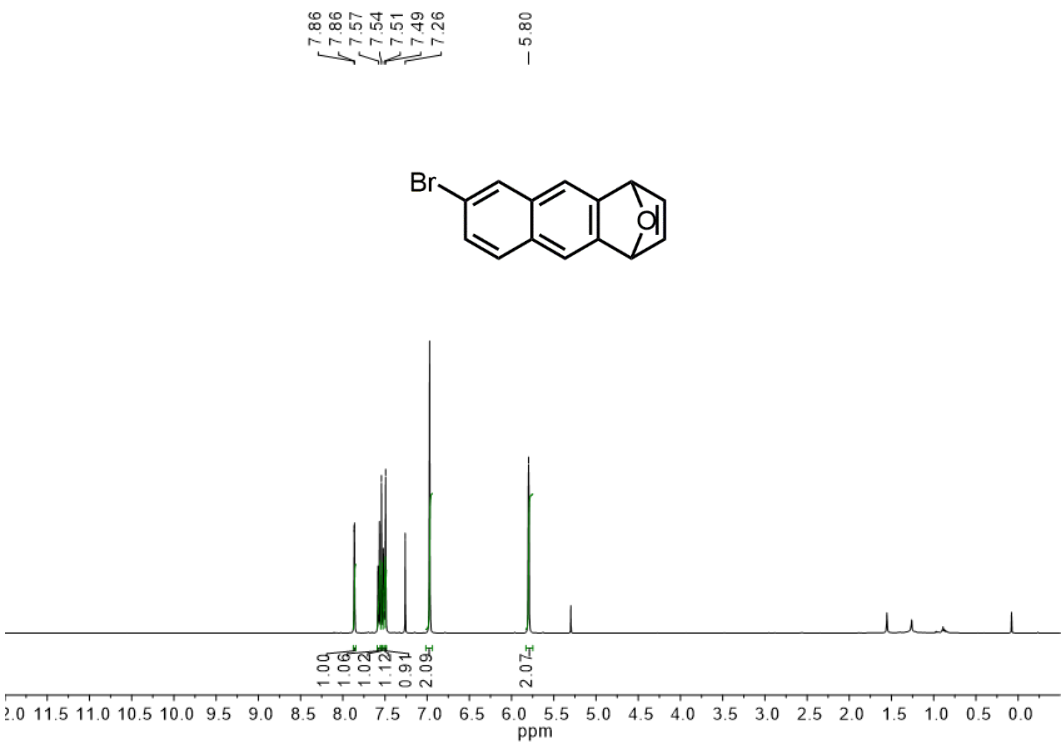

Figure S4.35. ^{1}H NMR of **5b** (500 MHz, $CDCl_3$, 298 K)

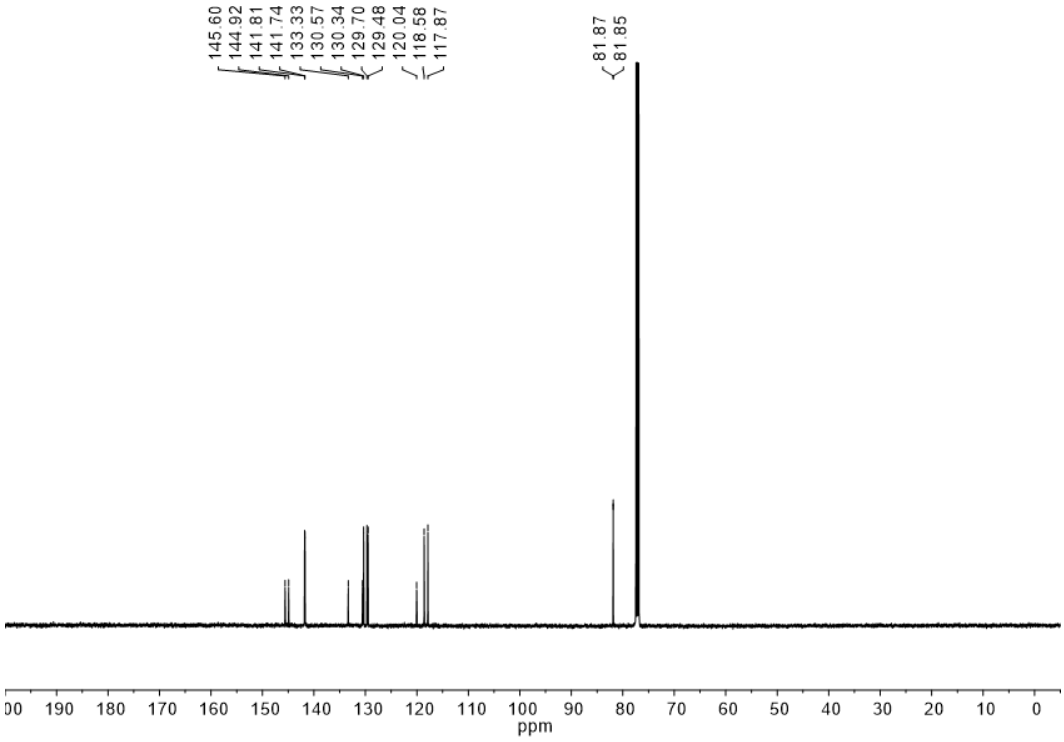

Figure S4.36. ^{13}C NMR of **5b** (125 MHz, $CDCl_3$, 298 K)

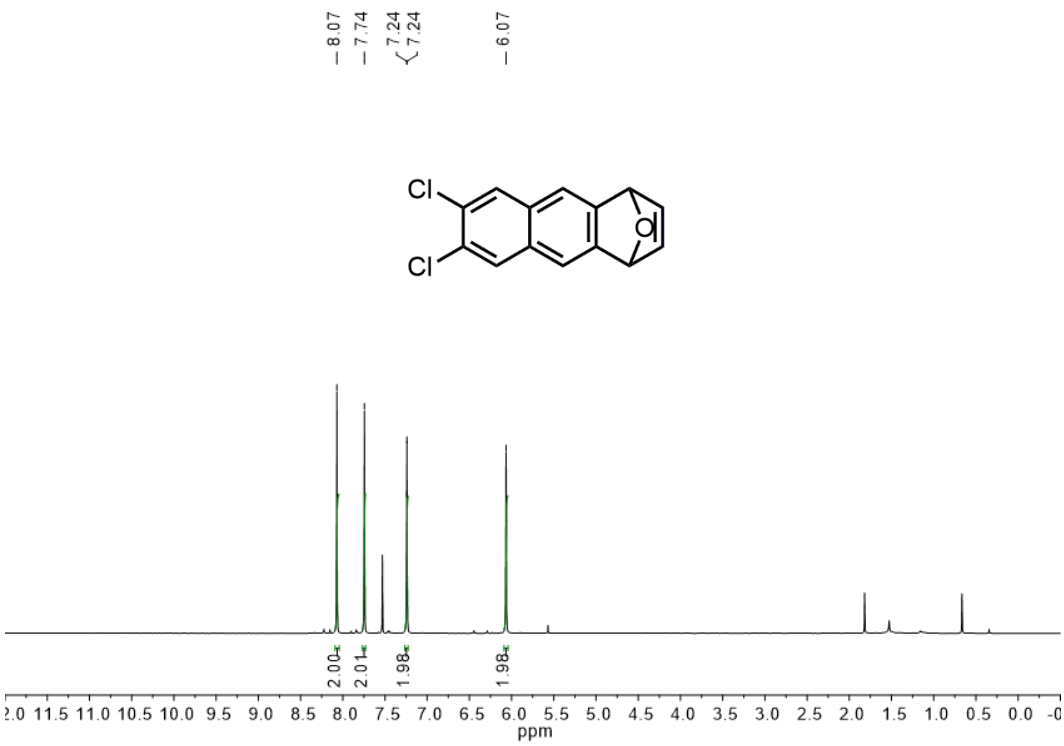

Figure S4.37. ^{1}H NMR of **5c** (500 MHz, $CDCl_3$, 298 K)

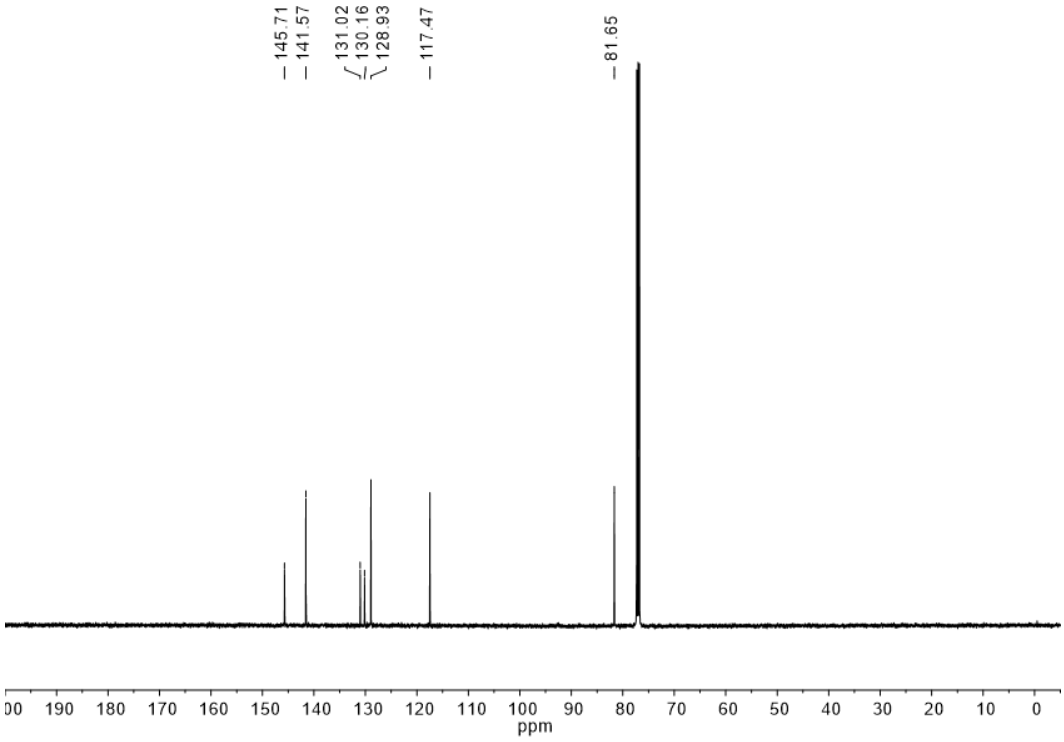

Figure S4.38. ^{13}C NMR of **5c** (125 MHz, $CDCl_3$, 298 K)

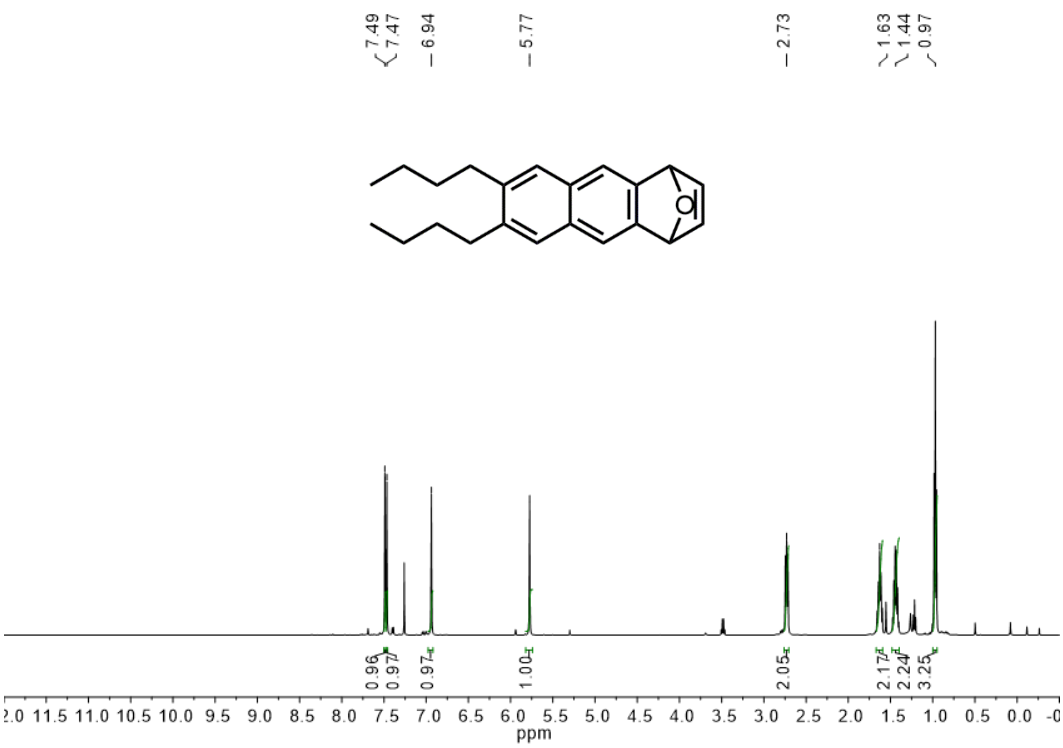

Figure S4.39. ^{1}H NMR of **5d** (500 MHz, $CDCl_3$, 298 K)

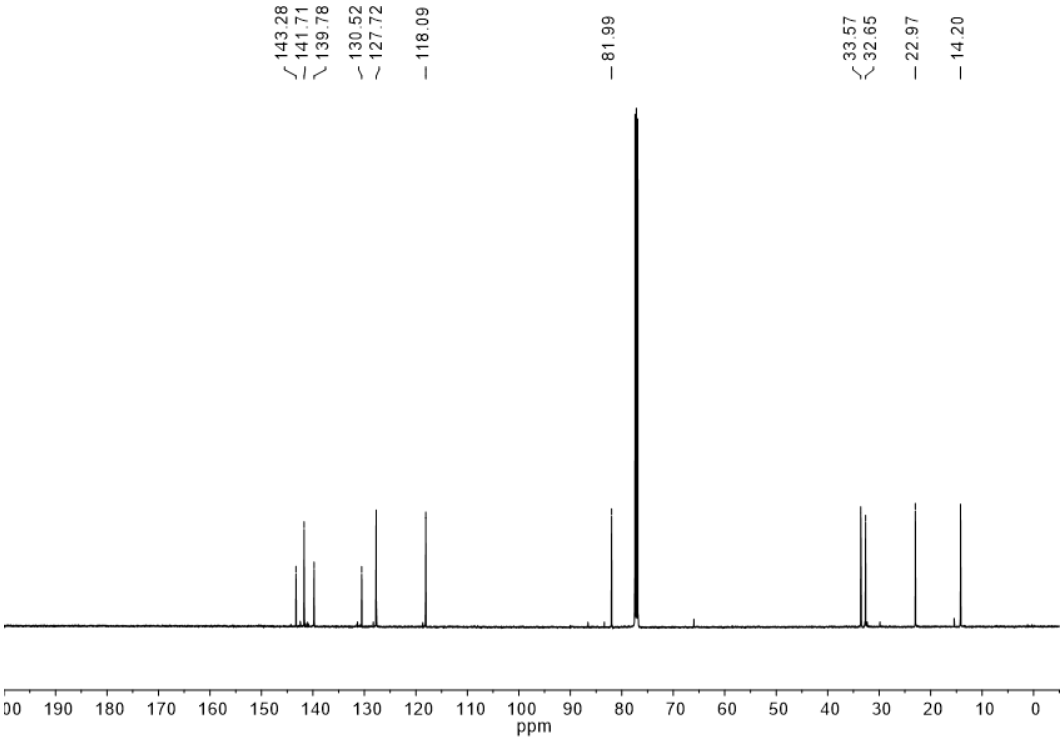

Figure S4.40. ^{13}C NMR of **5d** (500 MHz, $CDCl_3$, 298 K)

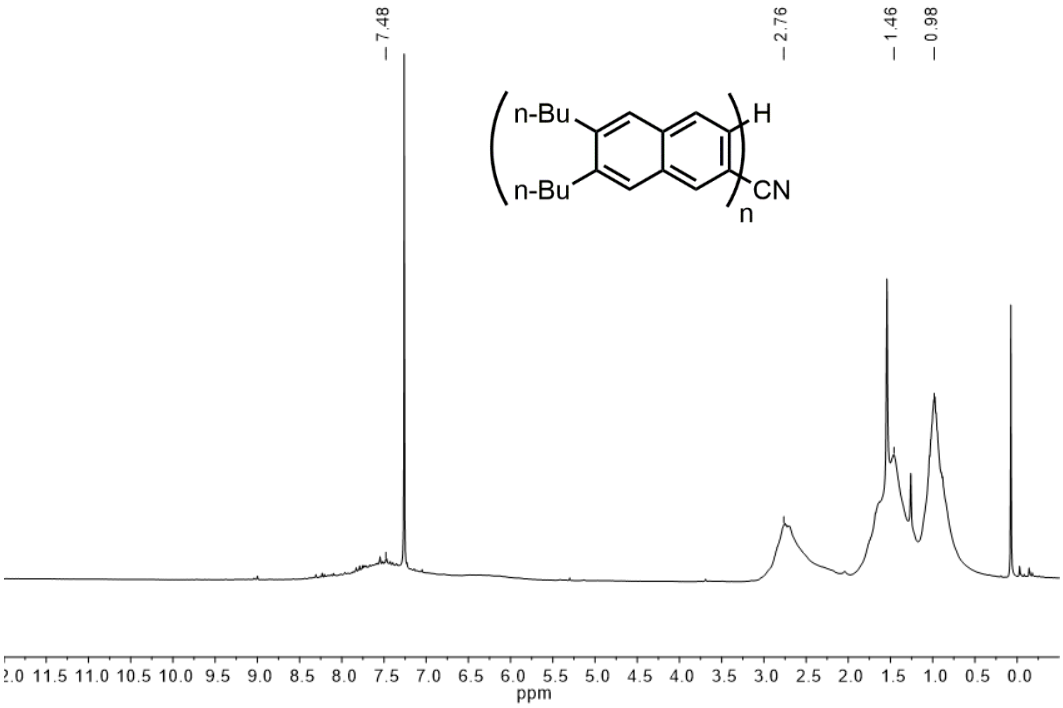

Figure S4.41. ^{1}H NMR of **6** (500 MHz, $CDCl_3$, 298 K)

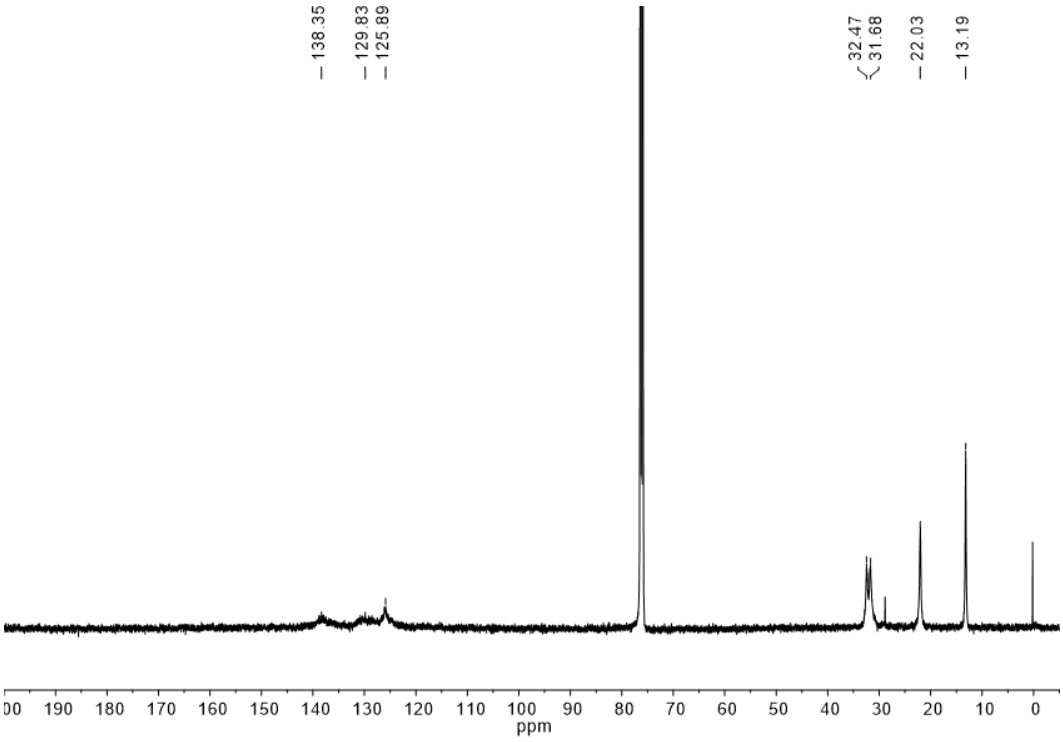

Figure S4.42. ^{13}C NMR of **6** (125 MHz, $CDCl_3$, 298 K)

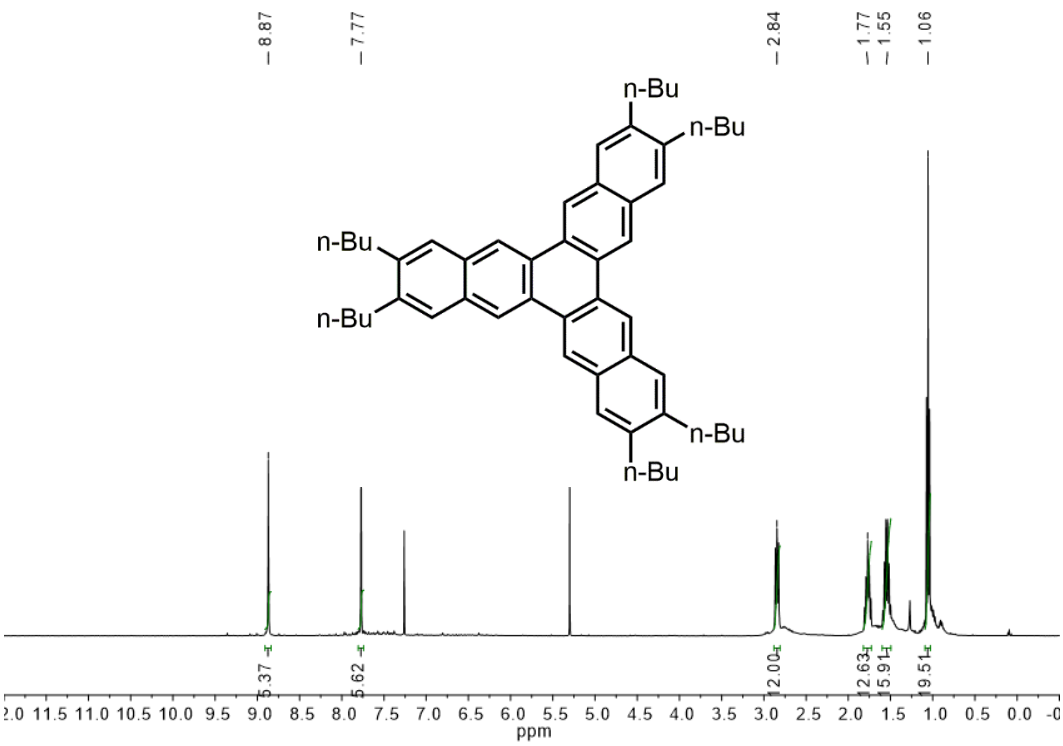

Figure S4.43. ^{1}H NMR of **7** (500 MHz, $CDCl_3$, 298 K)

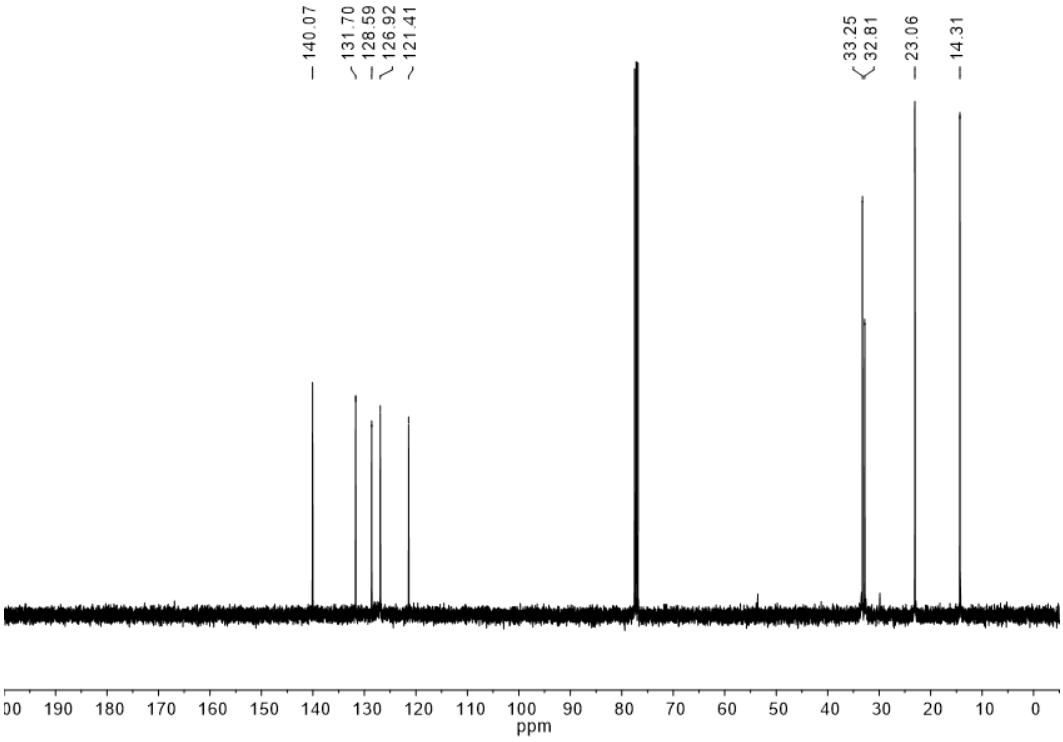

Figure S4.44. ^{13}C NMR of **7** (125 MHz, $CDCl_3$, 298 K)

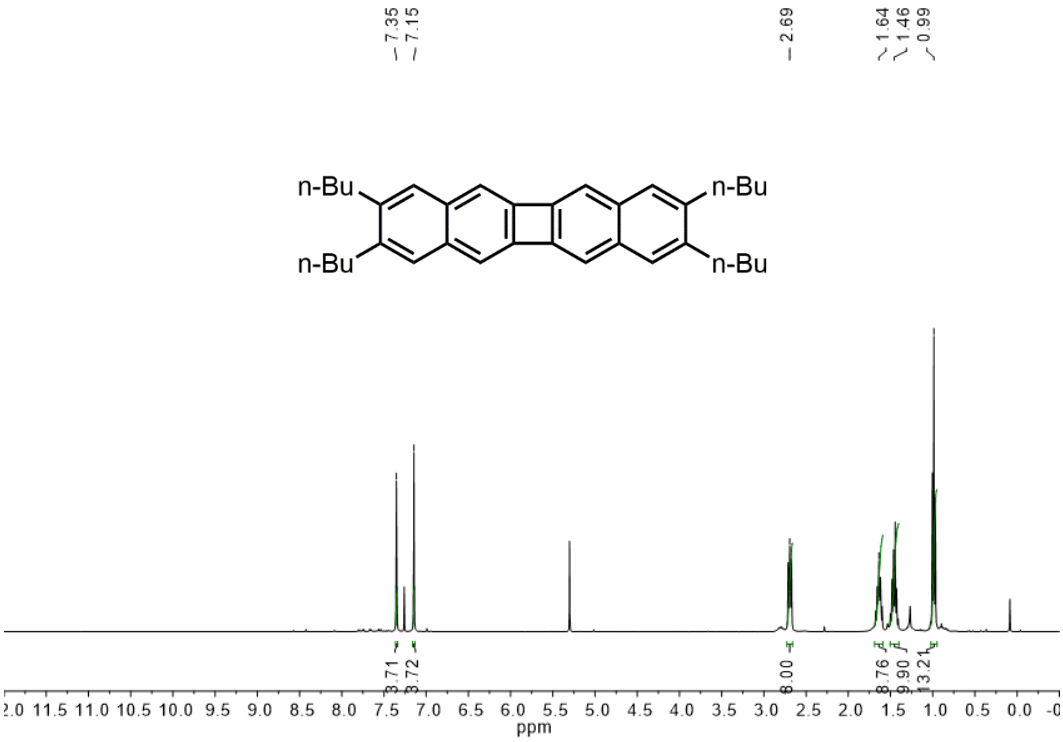

Figure S4.45. ^{1}H NMR of **8** (500 MHz, $CDCl_3$, 298 K)

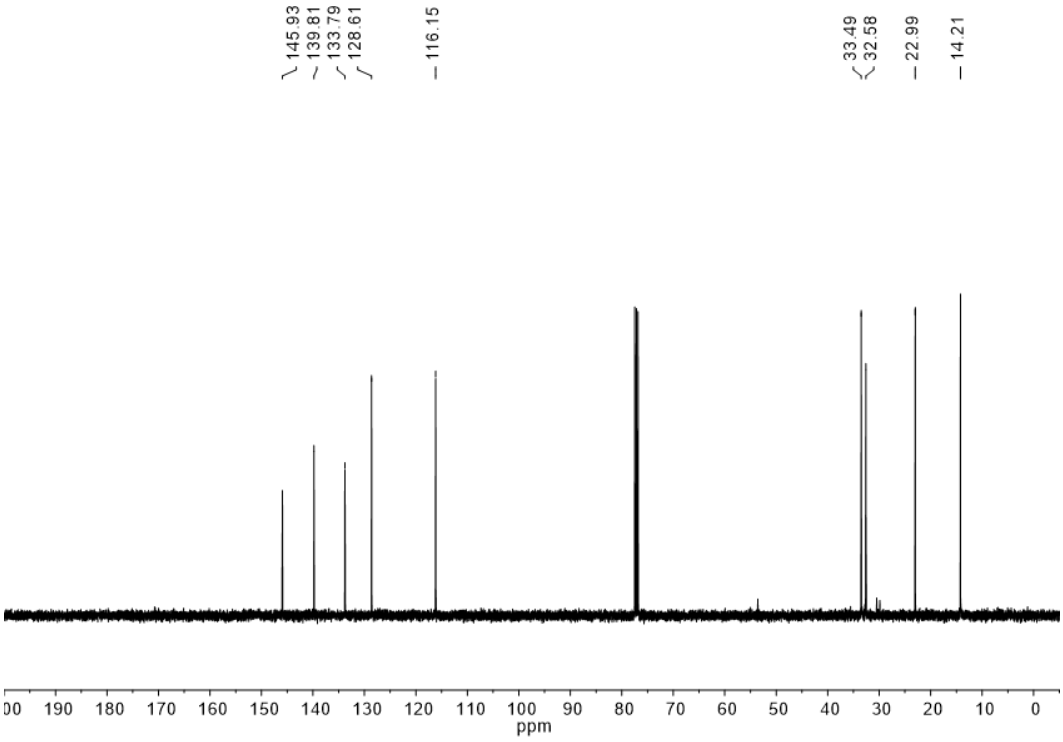

Figure S4.46. ^{13}C NMR of **8** (125 MHz, $CDCl_3$, 298 K)

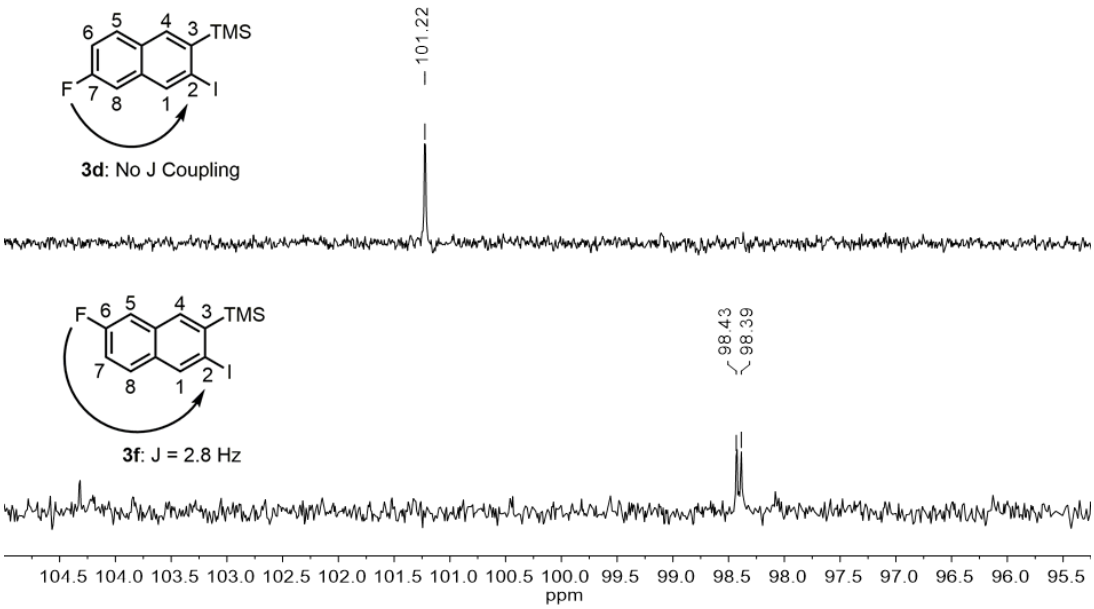

Figure S4.47. Partial ^{13}C NMR of **3d** and **3f** showing the long range ^{19}F-^{13}C coupling between fluorine on C7 and C6 with iodo-carbon C2. The weak *J* coupling present for **3f** indicates the observed regioisomer was formed.[6]

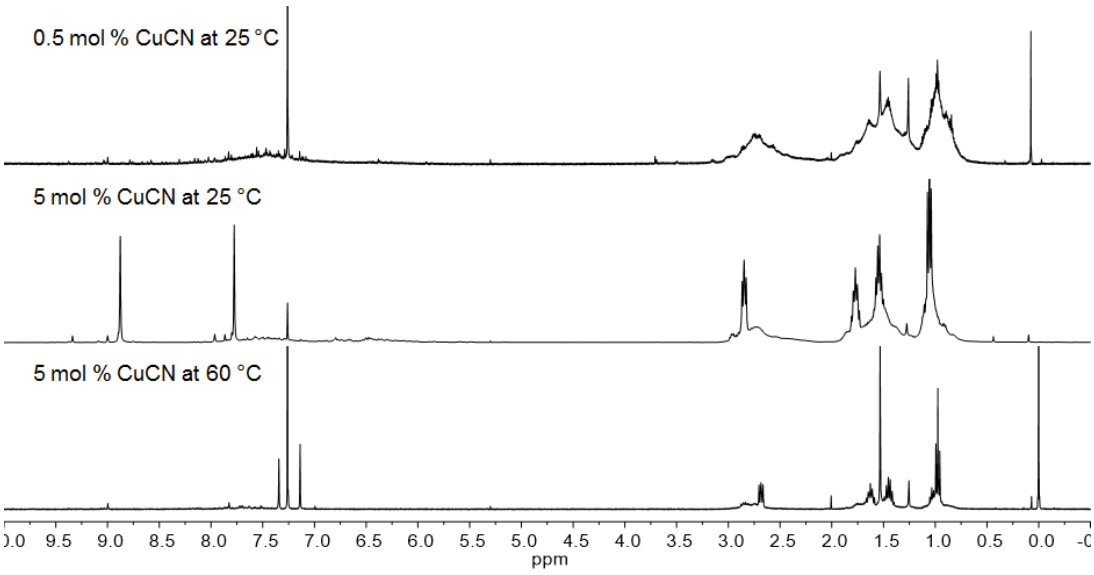

Figure S4.48. Crude ^{1}H NMR (400 MHz, $CDCl_3$, 298 K) of **6**, **7**, **8** after precipitation into methanol showing the selective formation of each product.

D. 2D NMR Spectroscopy

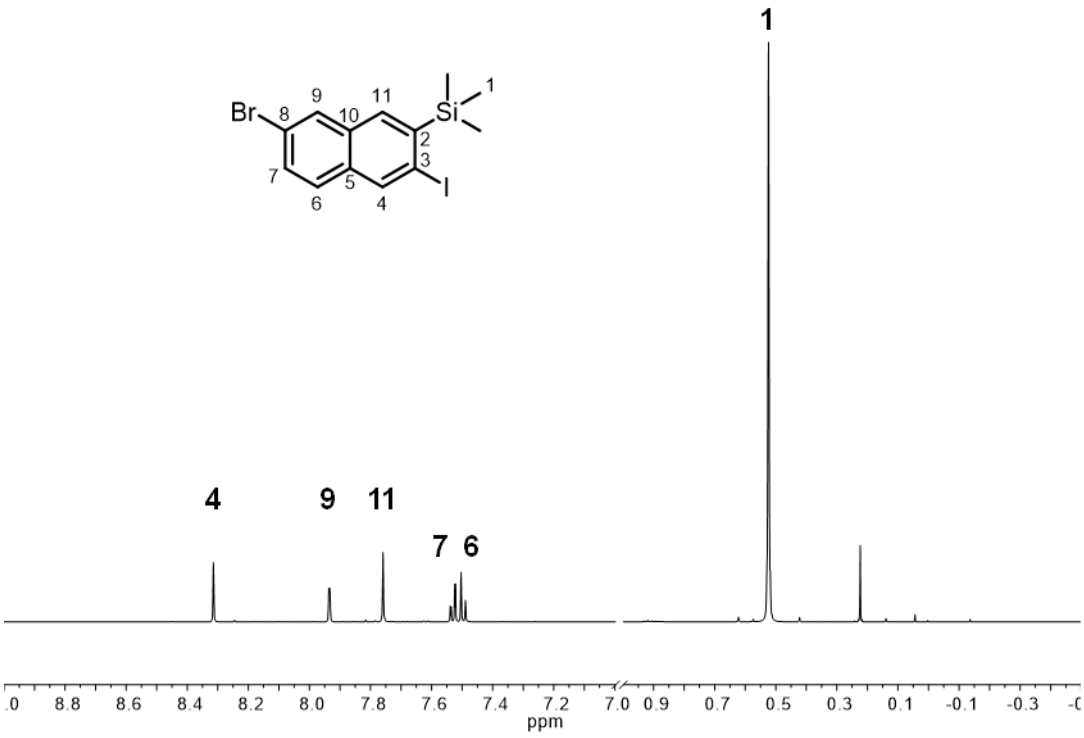

Figure S4.49: Full ^{1}H NMR spectrum (600 MHz, $CDCl_3$, 295K) of **3b**, including assignments derived from HSQC and HMBC 2D NMR experiments (see below). Chemical shift range 7.0-1.0 ppm were removed to clearly show assignments.

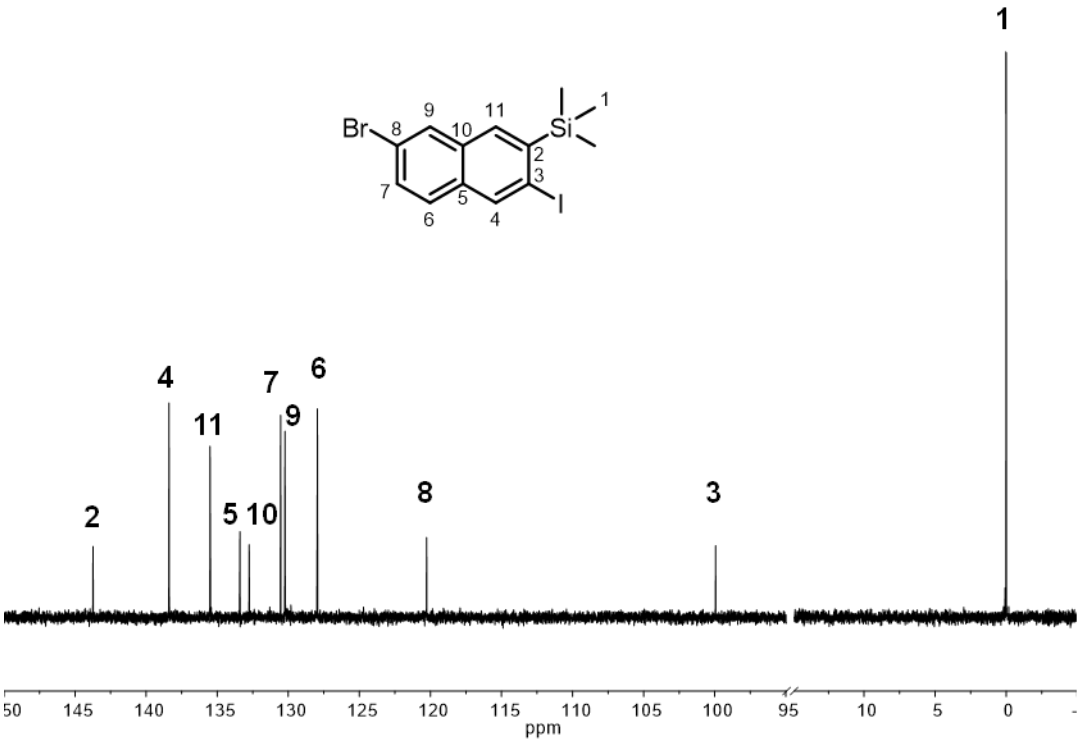

Figure S4.50: Full ^{13}C NMR spectrum (600 MHz, $CDCl_3$, 295K) of **3b**, including assignments derived from HSQC and HMBC 2D NMR experiments (see below). Chemical shift range 95-15 ppm were removed to clearly show assignments.

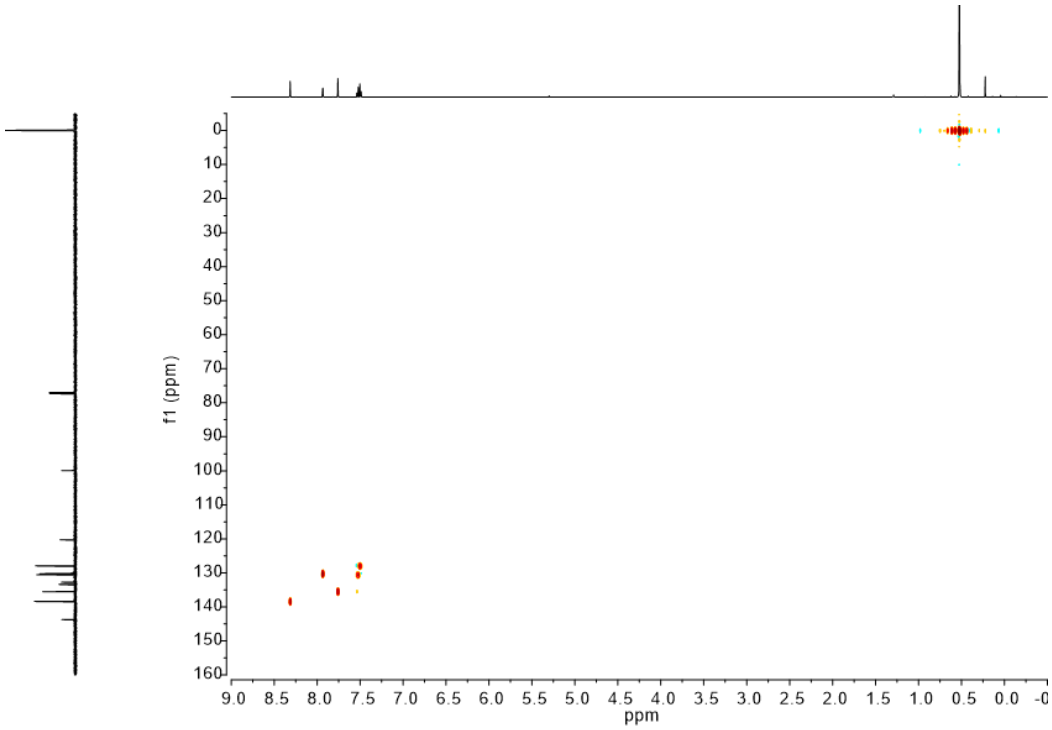

Figure S4.51. Full HSQC of **3b** (600 MHz, $CDCl_3$, 298 K)

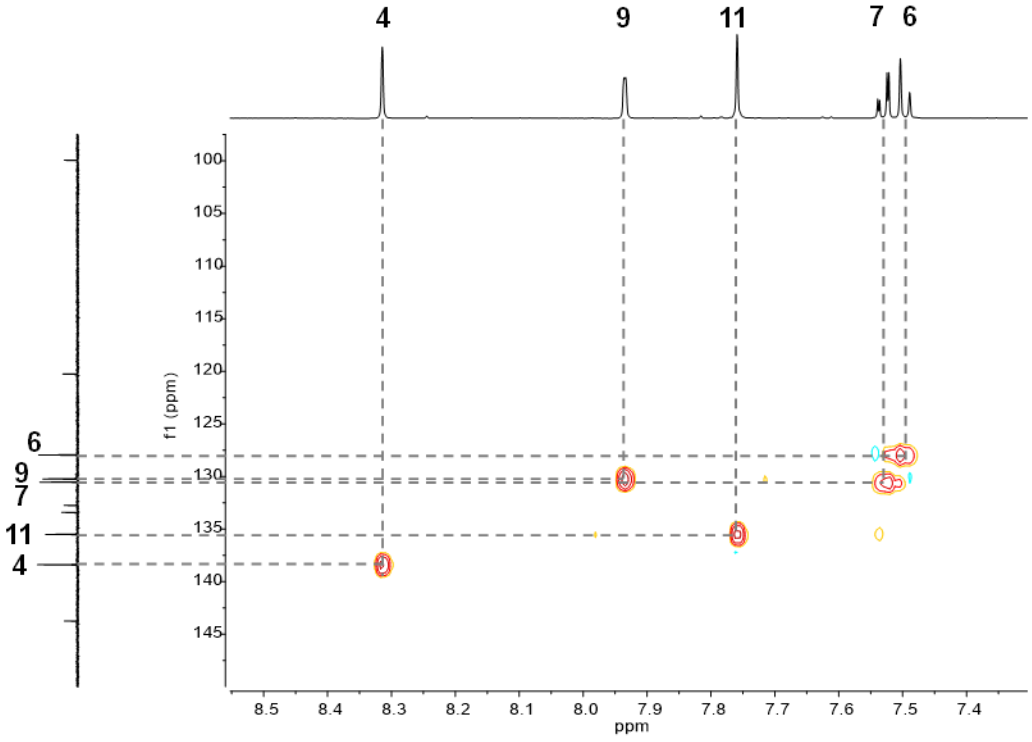

Figure S4.52. Partial HSQC of the aromatic region of **3b** (600 MHz, $CDCl_3$, 298 K)

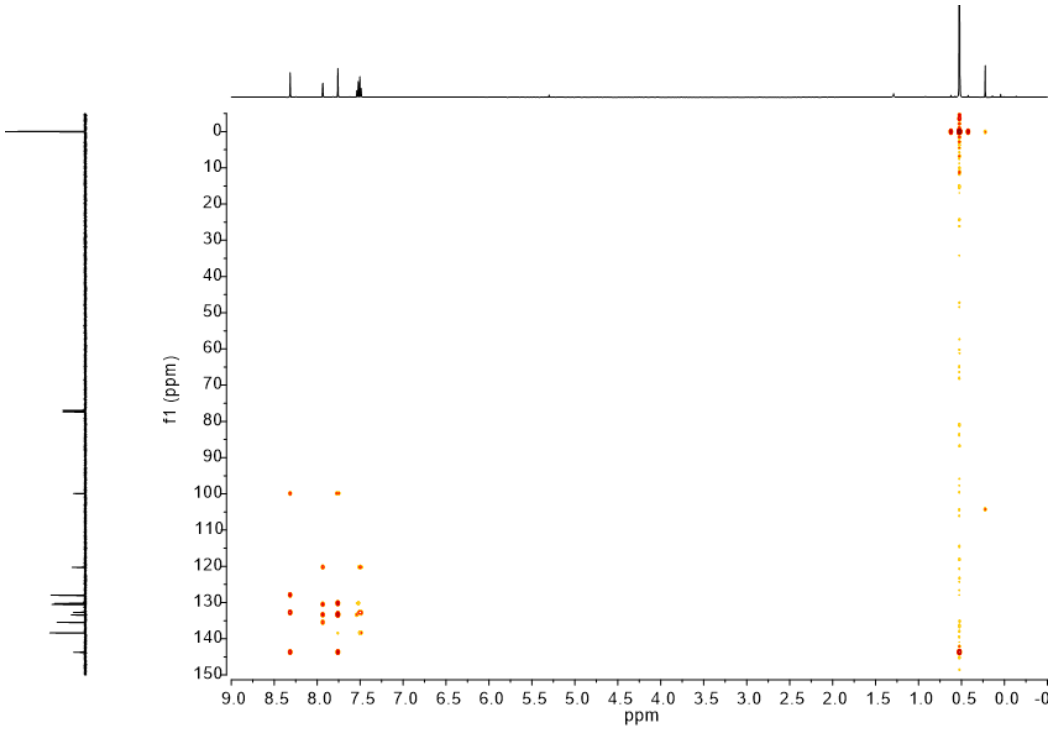

Figure S4.53. Full HMBC of **3b** (600 MHz, $CDCl_3$, 298 K)

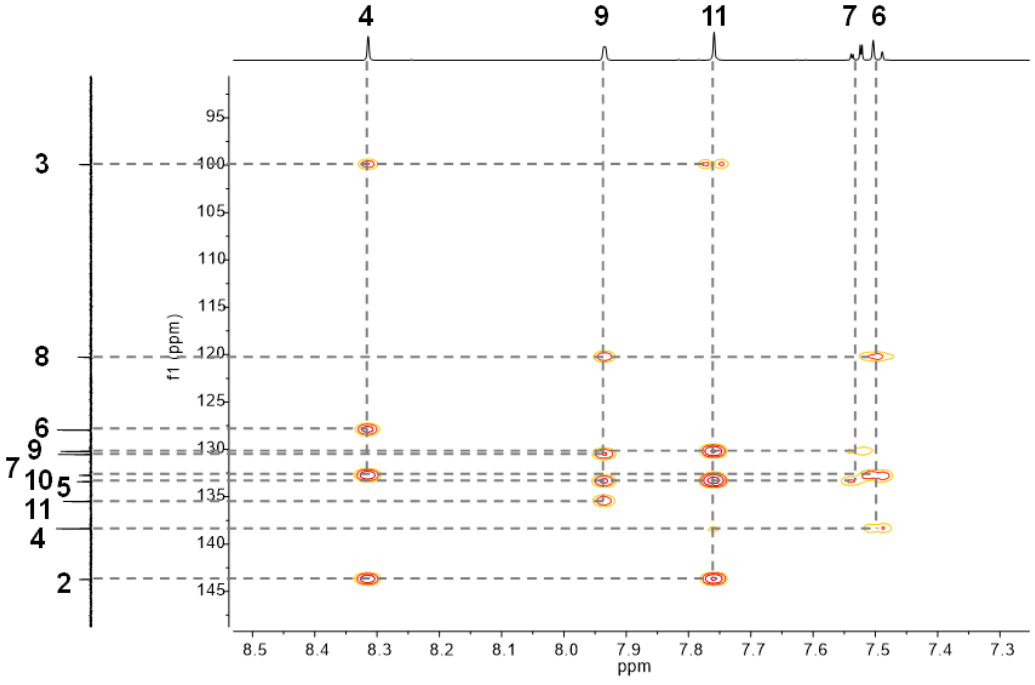

Figure S4.54. Partial HMBC of the aromatic region of 3b (600 MHz, $CDCl_3$, 298 K)

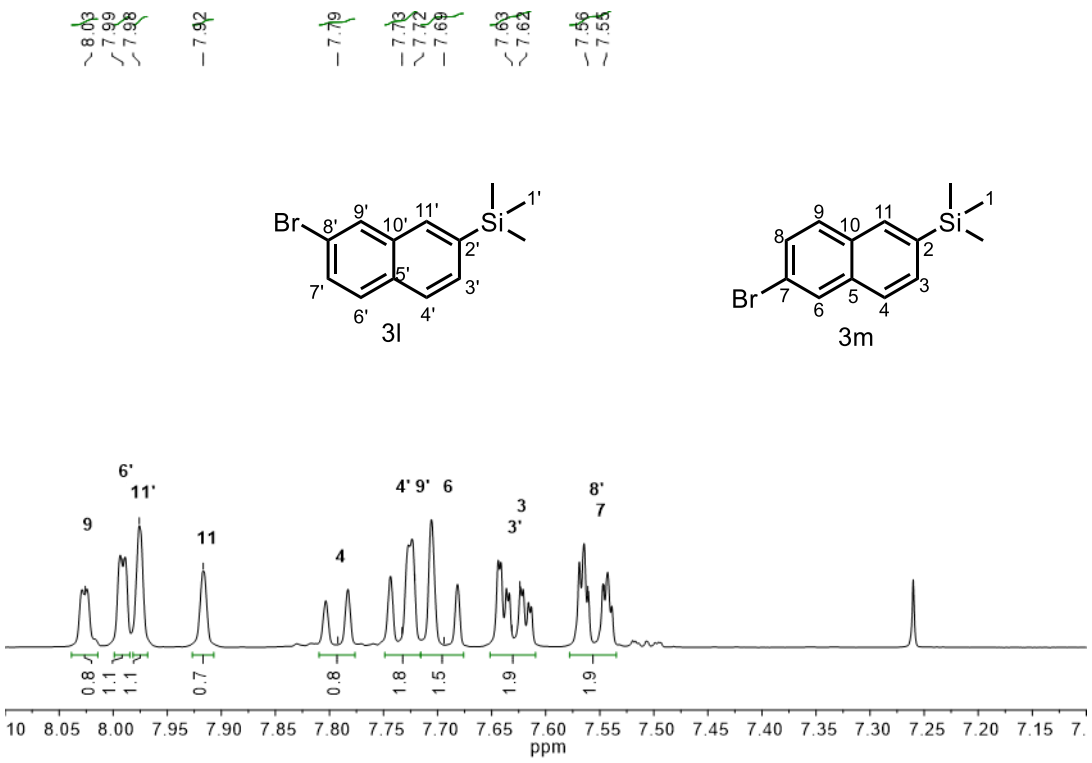

Figure S4.55: Partial ^{1}H NMR spectrum (400 MHz, $CDCl_3$, 295K) of **3l** and **3m**, including assignments derived from HSQC and HMBC 2D NMR experiments (see below).

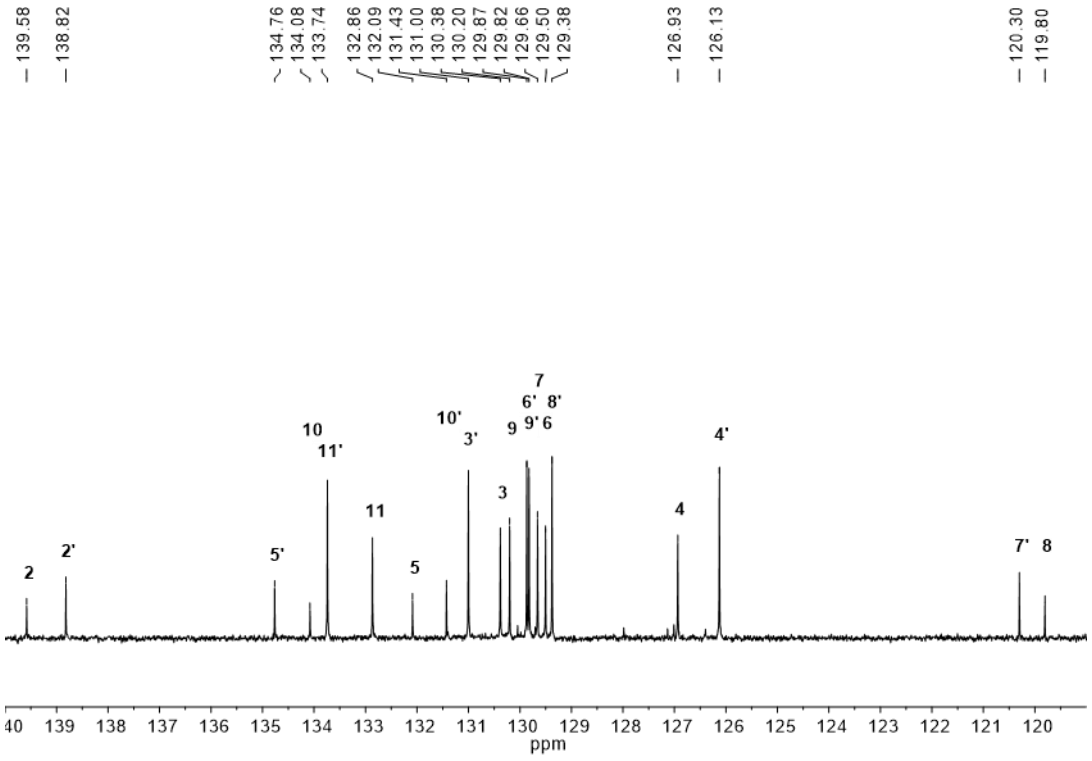

Figure S4.56: Partial ^{13}C NMR spectrum (100 MHz, $CDCl_3$, 295K) of **3l** and **3m**, including assignments derived from HSQC and HMBC 2D NMR experiments (see below).

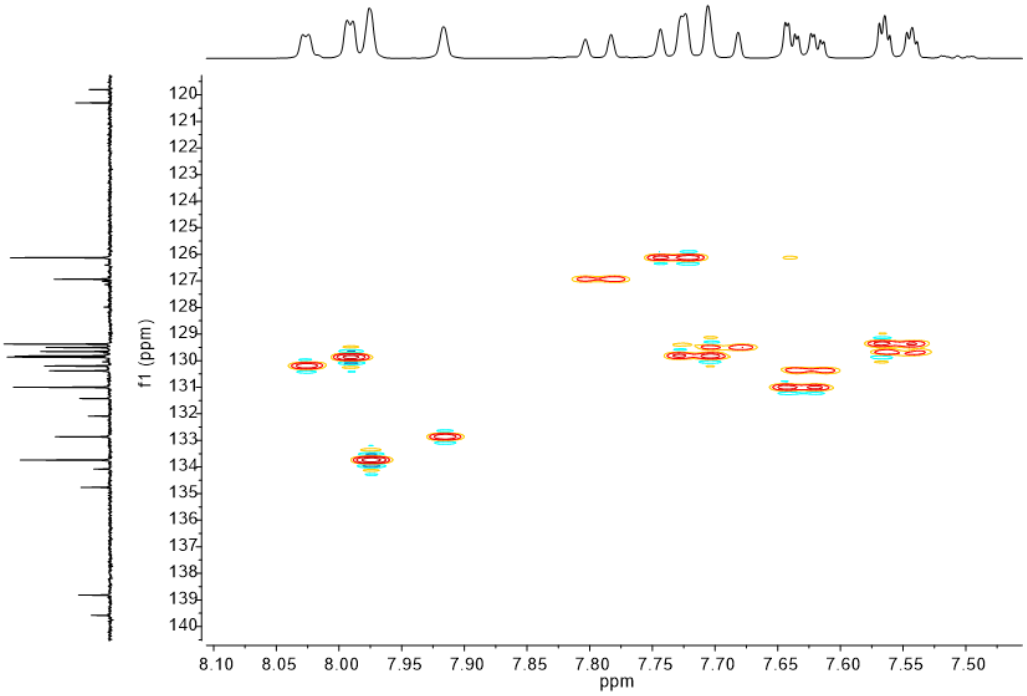

Figure S4.57: Partial bandselective HSQC spectrum of the aromatic region of **3l** and **3m** (100 MHz, $CDCl_3$, 295K).

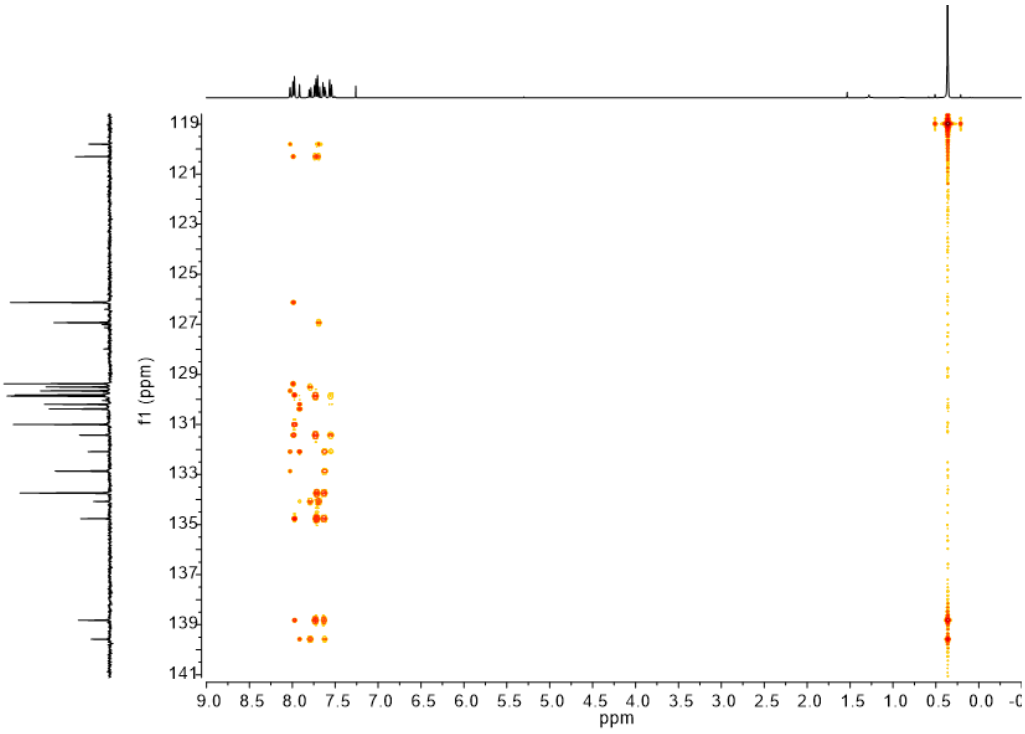

Figure S4.58: Bandselective HMBC spectrum of **3l** and **3m** (100 MHz, $CDCl_3$, 295K).

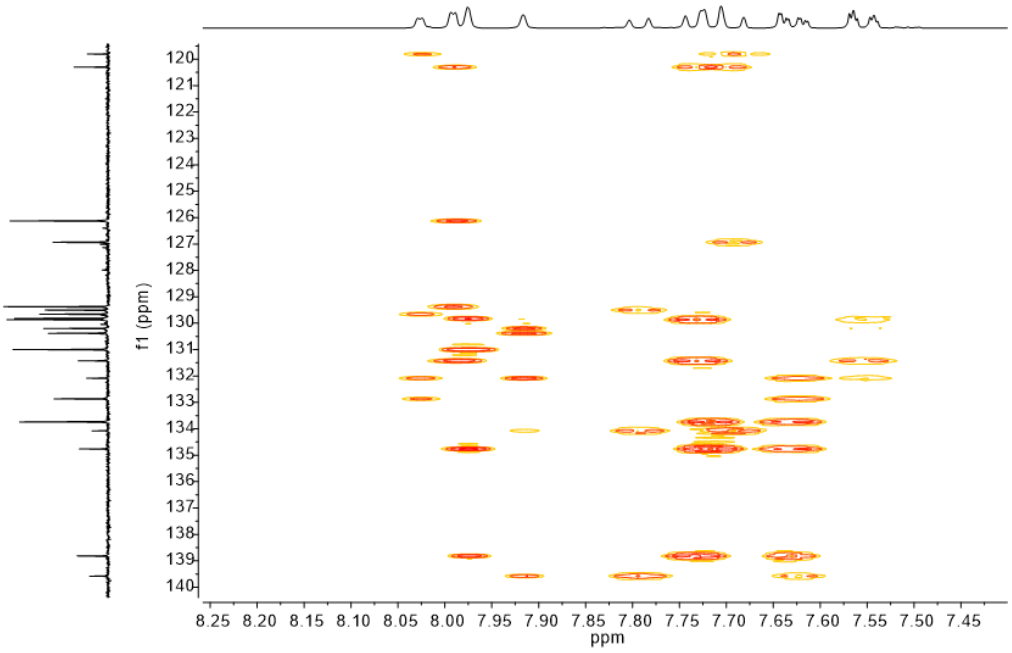

Figure S4.59: Partial bandselective HMBC spectrum of the aromatic region of **3l** and **3m** (100 MHz, $CDCl_3$, 295K).

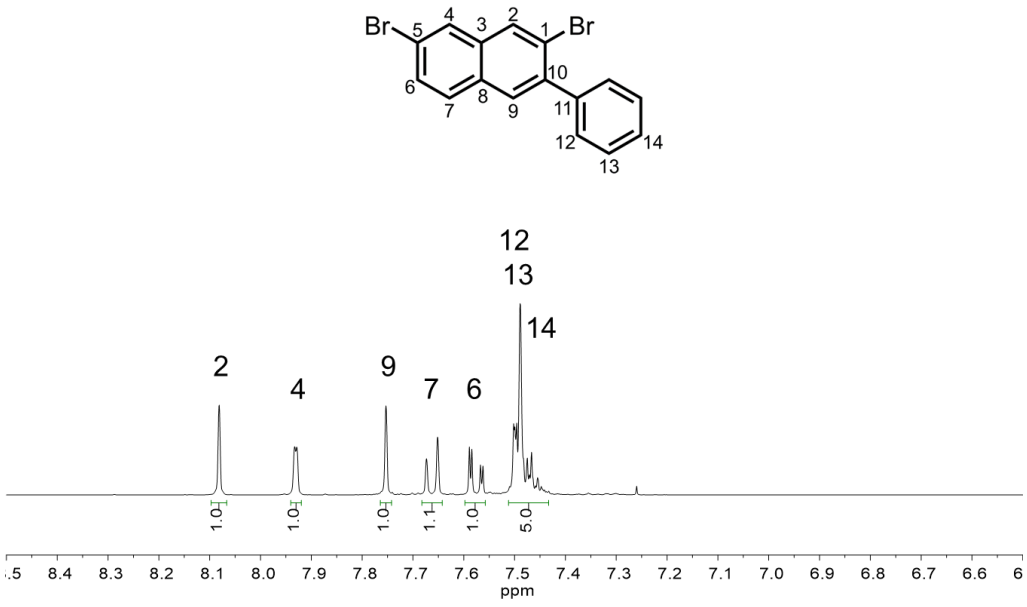

Figure S4.60: Partial ^{1}H NMR spectrum (400 MHz, $CDCl_3$, 295K) of **S4**, including assignments derived from HSQC and HMBC 2D NMR experiments (see below).

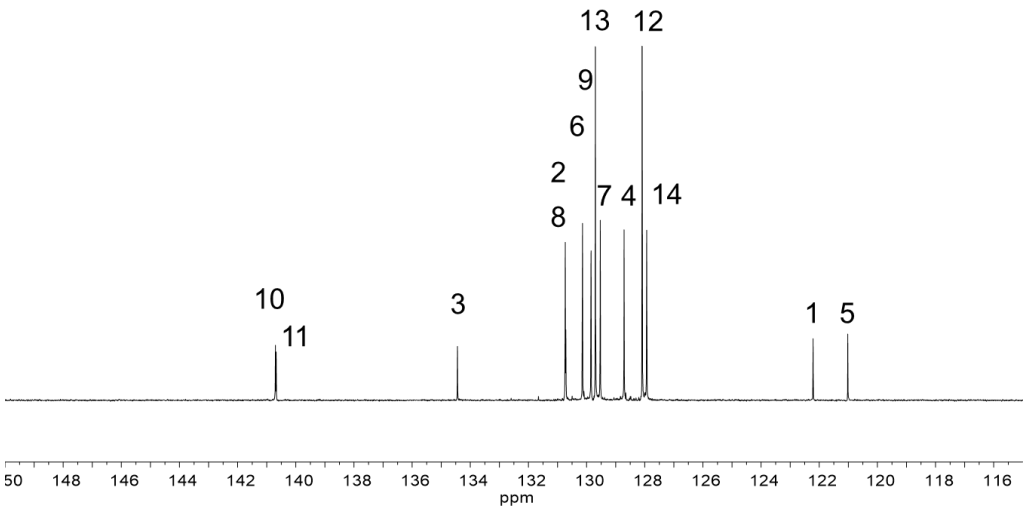

Figure S4.61: Partial ^{13}C NMR spectrum (100 MHz, $CDCl_3$, 295K) of **S4**, including assignments derived from HSQC and HMBC 2D NMR experiments (see below).

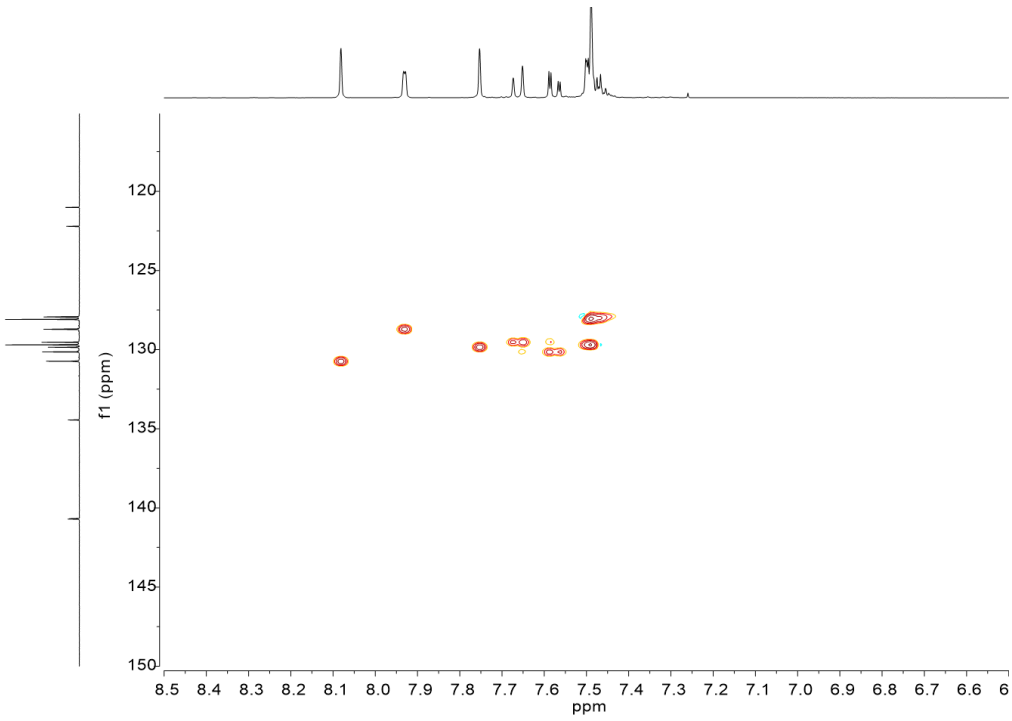

Figure S4.62: Partial bandselective HSQC spectrum of the aromatic region of **S4** (100 MHz, $CDCl_3$, 295K).

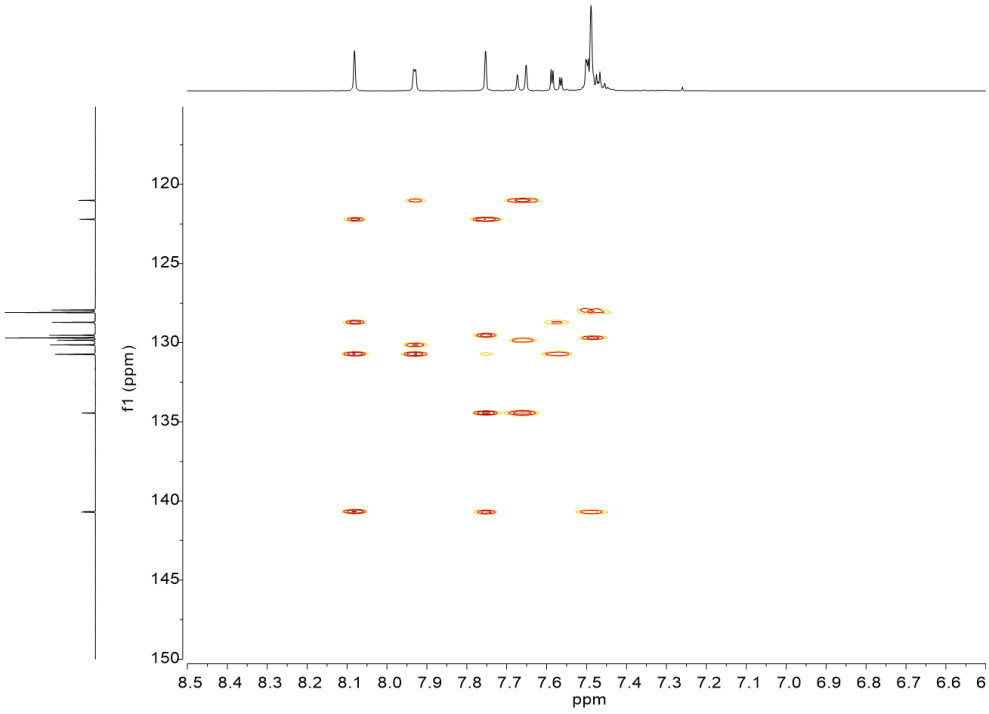

Figure S4.63: Partial bandselective HMBC spectrum of the aromatic region of **S4** (100 MHz, $CDCl_3$, 295K).

E. DFT Calculations

Discussion of Proposed Reaction Mechanism Associated Regiochemical Outcomes

Mechanistic aspects of the $Cu(OTf)_2$ catalyzed benzannulation of arylhaloalkynes was reported in by Dichtel and coworkers in *Chem. Eur. J.* **2015**, *21*, 18122. A comprehensive discussion of experimental and computational studies related to the mechanism and evidence for route 2 can be found therein.

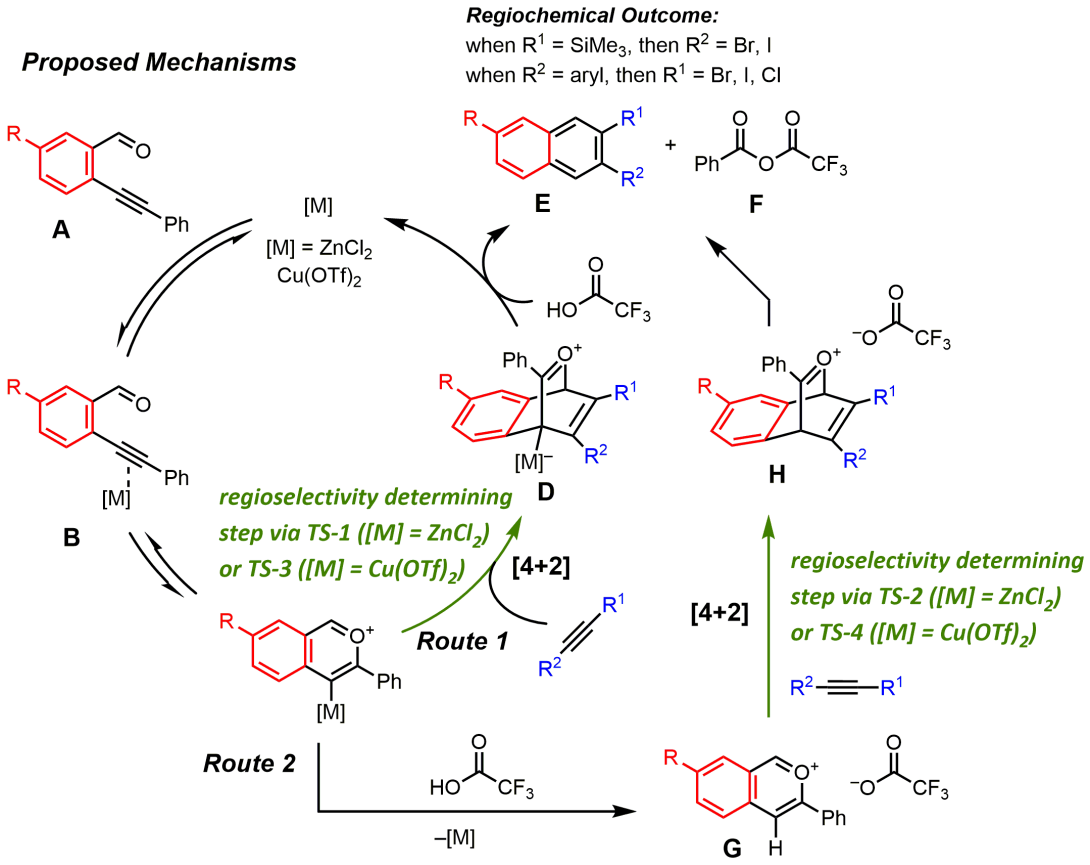

Figure S4.64 Proposed mechanism based on reported mechanistic studies of the $Cu(OTf)_2$ catalyzed benzannulation of arylhaloalkynes (see reference 1 in the Appendix).

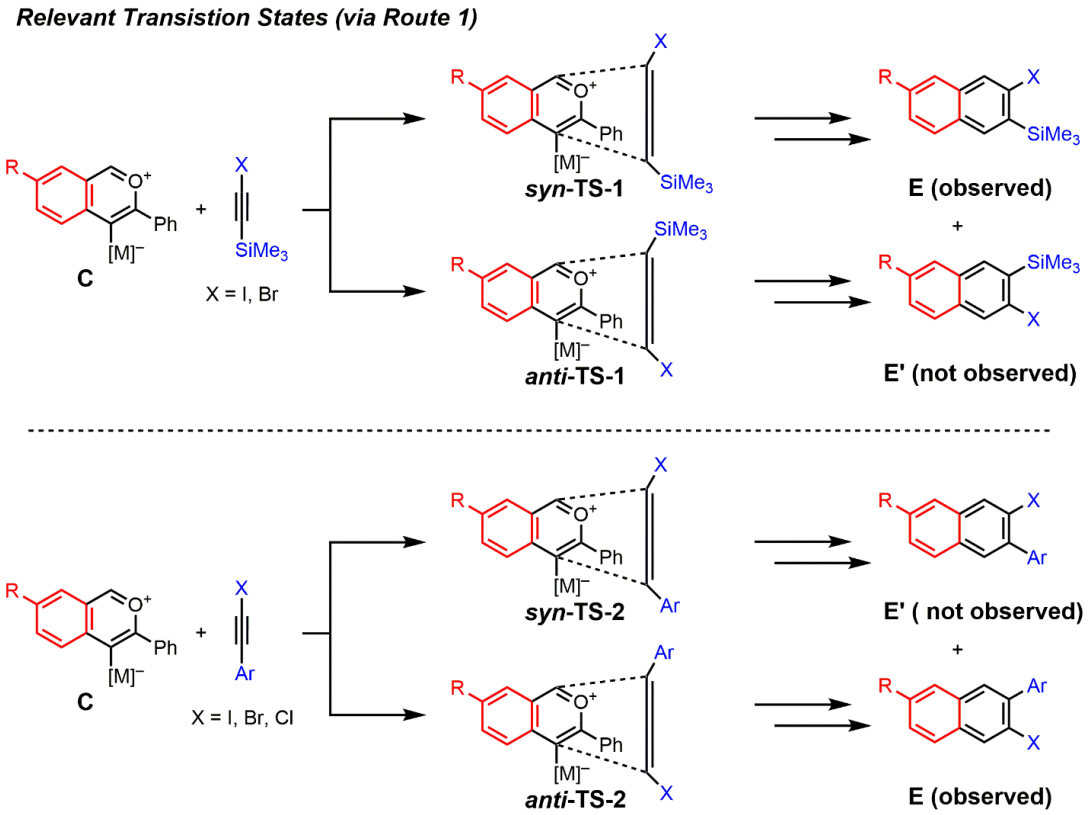

Figure S4.65. Regioselectivity determining transition state relevant to route 1 of mechanism proposed in **Figure S57**. [M] = $ZnCl_2$ or $Cu(OTf)_2$.

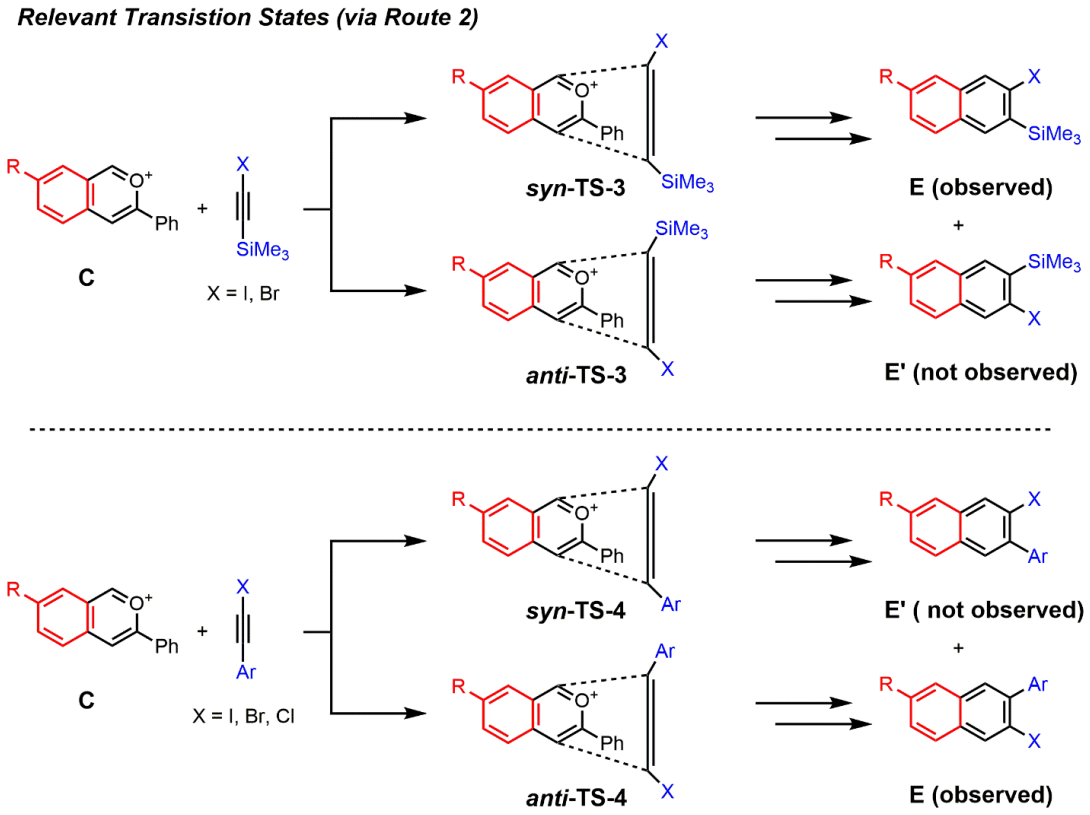

Figure S4.66. Regioselectivity determining transition state relevant to route 2 of mechanism proposed in **Figure S57**. The trifluoroacetate counter-anion has been omitted from C, TS-3, TS-4 for computational simplification.

Computational Method and Graphical Representation. Calculations were performed using the Gaussian 09 program.[7] Default geometric and SCF convergence criteria were used. Stationary points were characterized by the presence of all positive eigenvalues of the Hessian for minima or a single negative eigenvalue of the Hessian for transition states. All DFT methods were used as their default implementations in Gaussian 09. All electronic energies reported are corrected energies with regards to zero point energy (ZPE) corrections. Cartesian coordinates for **TS-2** and **TS-4** were previously reported.[1] All molecular structures were rendered in CYLView.[8]

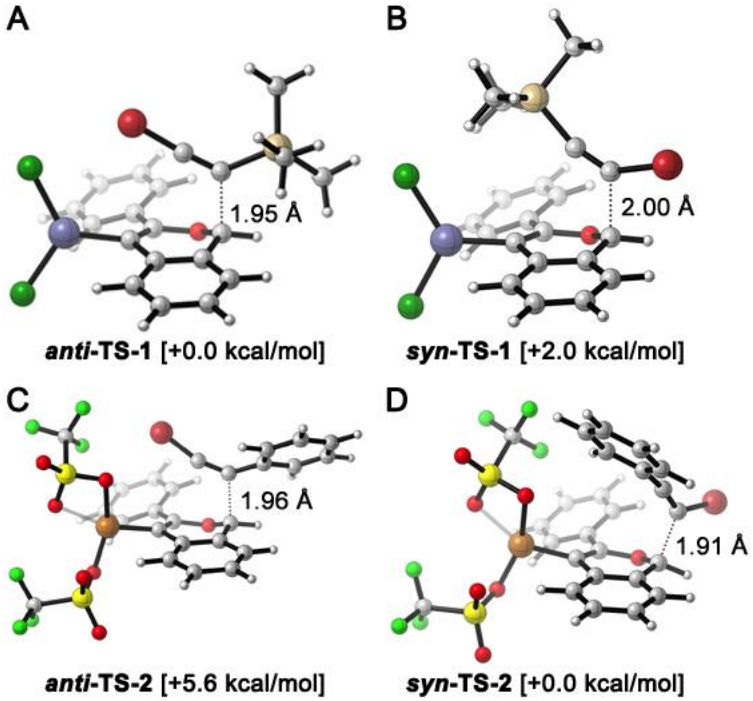

Figure S4.67. DFT calculated transition-states using B3LYP/6-31G(d) potentially responsible for the regioselectivity outcome in the benzannulation of: (A,B) silylhaloalkynes & (C,D) arylhaloalkynes, along with their relative electronic energies and bond forming interatomic distances. Element coloring scheme: C = silver, H = white, O = light red, Zn = blue, Cl = dark green, F = light green, S = yellow, Br = dark red, Cu = bronze.

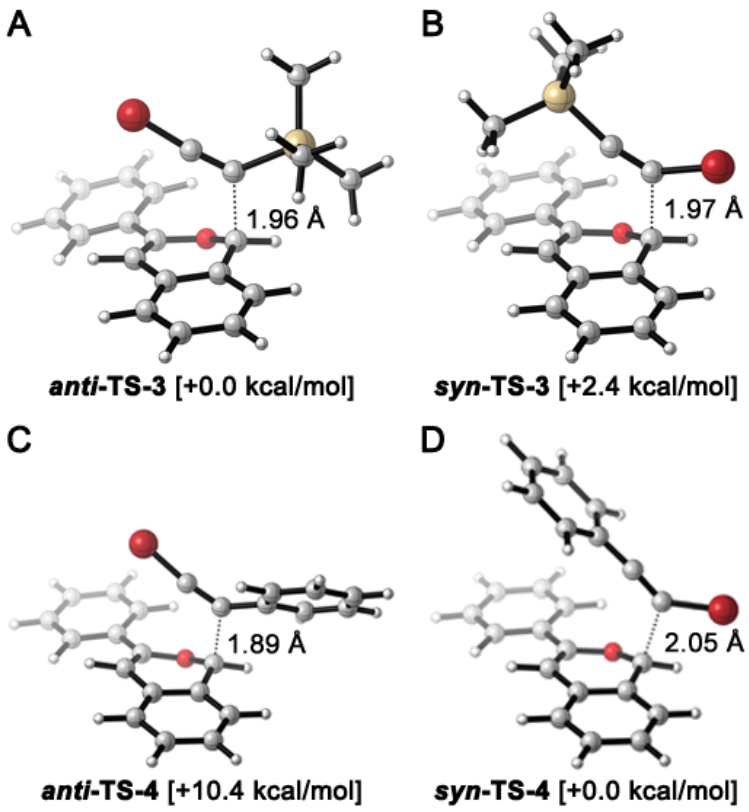

Figure S4.68. DFT calculated transition-states TS-3 and TS-4 using B3LYP/6-31G(d) potentially responsible for the regioselectivity outcome in the benzannulation of: (A,B) silylhaloalkynes & (C,D) arylhaloalkynes, along with their relative electronic energies and bond forming interatomic distances. Element coloring scheme: C = silver, H = white, O = light red, Br = dark red.

Cartesian Coordinates of DFT Optimized Structures

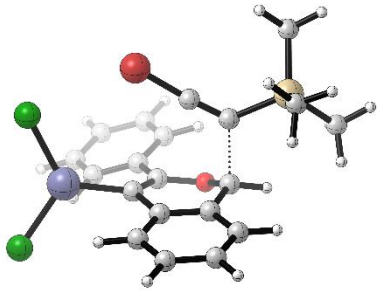

Structure: ***anti*-TS-1** (TMS-CC-Br Zn-major TS)

Charge: 0

Spin Multiplicity: 1

Computational Method/Basis Set: B3LYP/6-31G(d)

Solvation: gas phase

Number of Imaginary Frequencies: 1 (Freq. = –302.30)

Electronic Energy (AU): -6409.54186819

Gibbs Free Energy at 298.150 K (AU): -6409.275230

C	0.328283	3.192460	-0.363978
C	-0.059991	1.886692	-0.743299
C	-1.360461	1.713337	-1.285198
C	-2.242944	2.798186	-1.432926
C	-1.829113	4.066618	-1.061650
C	-0.538739	4.259183	-0.527115
H	1.331176	3.349286	0.023775

H	-3.231576	2.641238	-1.858556
H	-2.494409	4.915498	-1.188905
H	-0.220215	5.258028	-0.243211
C	0.811018	0.746165	-0.591548
C	0.462086	-0.391190	-1.281983
O	-0.737389	-0.487346	-1.967615
C	-1.729155	0.356454	-1.616174
H	-2.598158	0.191426	-2.244796
C	1.278354	-1.601023	-1.460269
C	0.676454	-2.846309	-1.718636
C	2.680591	-1.534244	-1.371747
C	1.455131	-3.991631	-1.858107
H	-0.403565	-2.911871	-1.794479
C	3.455220	-2.682957	-1.508883
H	3.175894	-0.574816	-1.252720
C	2.845893	-3.915893	-1.747846
H	0.975137	-4.947894	-2.047440
H	4.536245	-2.608180	-1.440237
H	3.451104	-4.811729	-1.854839
C	-2.382302	-0.423060	0.046077
C	-1.501307	-0.709206	0.892356
Br	-0.366782	-1.114657	2.190584
Zn	2.492573	0.888633	0.469968

Cl	2.767386	-0.012348	2.491202
Cl	4.132428	2.138341	-0.351323
Si	-4.271559	-0.593386	0.168220
C	-4.629482	-2.096026	1.246477
H	-4.172409	-1.994984	2.237114
H	-5.710207	-2.218950	1.388396
H	-4.245796	-3.016547	0.792624
C	-4.923404	0.990371	0.957139
H	-4.623244	1.881137	0.394750
H	-6.019534	0.972905	1.001529
H	-4.547667	1.102377	1.980161
C	-4.999501	-0.837975	-1.557654
H	-4.523356	-1.667626	-2.092985
H	-6.066002	-1.079186	-1.467429
H	-4.928930	0.058490	-2.184547

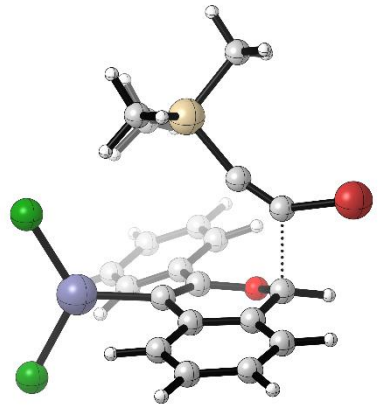

Structure: ***syn*-TS-1** (TMS-CC-Br Zn-minor TS)

Charge: 0

Spin Multiplicity: 1

Computational Method/Basis Set: B3LYP/6-31G(d)

Solvation: gas phase

Number of Imaginary Frequencies: 1 (Freq. = –414.29)

Electronic Energy (AU): -6409.53866341

Gibbs Free Energy at 298.150 K (AU): -6409.270880

C	-0.098379	-3.199821	0.282906
C	0.183740	-1.990045	-0.400039
C	1.431658	-1.888600	-1.080169
C	2.374327	-2.936095	-1.044972
C	2.061852	-4.100438	-0.370528
C	0.817960	-4.232241	0.288985
H	-1.060703	-3.312831	0.773974
H	3.327570	-2.822684	-1.552683

H	2.770266	-4.923276	-0.351229
H	0.582902	-5.157461	0.806706
C	-0.736016	-0.889955	-0.412327
C	-0.482753	0.119226	-1.332255
O	0.652352	0.121346	-2.101132
C	1.695008	-0.636234	-1.723249
H	2.511324	-0.546317	-2.433281
C	-1.393966	1.201532	-1.729529
C	-0.891321	2.385279	-2.302630
C	-2.783770	1.064745	-1.564809
C	-1.755250	3.412269	-2.669252
H	0.178420	2.499146	-2.441226
C	-3.643982	2.095955	-1.933225
H	-3.204517	0.131844	-1.202244
C	-3.133540	3.274074	-2.480209
H	-1.353134	4.325133	-3.099678
H	-4.714262	1.968869	-1.802558
H	-3.805704	4.078309	-2.765735
C	1.778424	1.025325	0.535367
C	2.542139	0.420070	-0.253116
Br	4.369635	0.111686	-0.473662
Zn	-2.396041	-0.990078	0.696262
Cl	-2.652679	0.104571	2.599518

Cl	-3.968885	-2.391450	0.004853
Si	1.137681	2.111892	1.928610
C	-0.430773	3.024962	1.450832
H	-0.639959	3.787160	2.212178
H	-0.343925	3.531106	0.484036
H	-1.288774	2.346673	1.423821
C	2.571844	3.331133	2.161951
H	2.349275	3.993696	3.008337
H	3.516091	2.819447	2.376887
H	2.717440	3.957356	1.275000
C	0.925511	1.022842	3.444821
H	0.741555	1.651259	4.325431
H	0.062957	0.358426	3.333382
H	1.821140	0.423273	3.642083

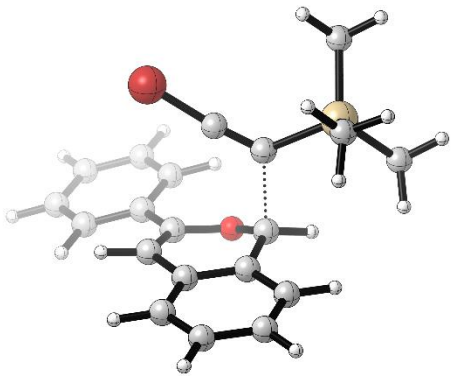

Structure: ***anti*-TS-3** (TMS-CC-Br metal-free major TS)

Charge: 1

Spin Multiplicity: 1

Computational Method/Basis Set: B3LYP/6-31G(d)

Solvation: gas phase

Number of Imaginary Frequencies: 1 (Freq. = –280.33)

Electronic Energy (AU): -3710.31570935

Gibbs Free Energy at 298.150 K (AU): -3710.031910

C	-0.821001	3.522740	1.107783
C	-0.380391	2.432932	0.328445
C	-1.282769	1.838778	-0.592670
C	-2.589853	2.337343	-0.740588
C	-2.993883	3.422435	0.019531
C	-2.108533	4.007574	0.949063
H	-0.140889	3.984304	1.817662
H	-3.266592	1.885644	-1.460628

H	-3.993465	3.827845	-0.100392
H	-2.441381	4.853480	1.542790
C	0.937374	1.882020	0.406821
C	1.399843	1.009610	-0.544942
O	0.535193	0.574280	-1.515378
C	-0.799057	0.678620	-1.304081
H	-1.334420	0.340633	-2.184084
C	2.760236	0.491678	-0.692928
C	3.002575	-0.658914	-1.467082
C	3.844009	1.132784	-0.062513
C	4.295106	-1.158480	-1.595785
H	2.176829	-1.159177	-1.960535
C	5.132286	0.624768	-0.191690
H	3.687779	2.045192	0.504412
C	5.361903	-0.521810	-0.957280
H	4.470269	-2.047226	-2.194381
H	5.960797	1.132045	0.292982
H	6.369674	-0.912662	-1.061012
C	-0.368604	-1.071754	0.762514
C	-1.195244	-0.847936	-0.148178
H	1.609406	2.212461	1.190075
Br	0.753711	-1.531636	2.056338
Si	-2.819045	-1.798222	-0.594665

C	-4.168210	-1.073521	0.497265
H	-5.127339	-1.553778	0.266547
H	-3.956607	-1.246616	1.557954
H	-4.292028	0.004573	0.350453
C	-2.483226	-3.607208	-0.215199
H	-3.378311	-4.205022	-0.426398
H	-1.667686	-4.006610	-0.827983
H	-2.224557	-3.761609	0.838073
C	-3.178812	-1.549365	-2.427624
H	-2.336964	-1.845485	-3.064331
H	-4.026009	-2.190000	-2.703207
H	-3.465794	-0.523649	-2.686654

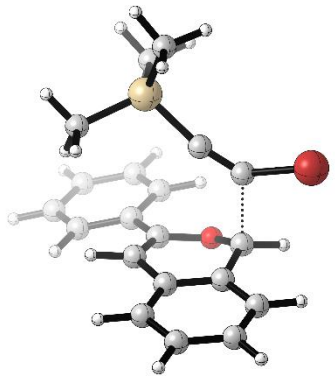

Structure: ***anti*-TS-3** (TMS-CC-Br metal-free minor TS)

Charge: 1

Spin Multiplicity: 1

Computational Method/Basis Set: B3LYP/6-31G(d)

Solvation: gas phase

Number of Imaginary Frequencies: 1 (Freq. = –391.07)

Electronic Energy (AU): -3710.31184235

Gibbs Free Energy at 298.150 K (AU): -3710.027611

C	1.528769	-2.802645	1.873005
C	0.907542	-2.088784	0.824802
C	1.687364	-1.700938	-0.302358
C	3.057828	-2.017040	-0.373148
C	3.636987	-2.734203	0.658135
C	2.871087	-3.122380	1.781246
H	0.944769	-3.105227	2.737101
H	3.642885	-1.705670	-1.232463

H	4.687372	-3.002614	0.608038
H	3.346971	-3.680177	2.581974
C	-0.467243	-1.718241	0.826901
C	-1.087421	-1.264223	-0.321063
O	-0.323802	-1.025098	-1.420525
C	1.016219	-0.889578	-1.280384
H	1.474275	-0.717927	-2.249638
C	-2.522443	-1.094821	-0.546899
C	-2.984520	-0.377977	-1.668374
C	-3.461193	-1.656743	0.341167
C	-4.350108	-0.218633	-1.883951
H	-2.272448	0.053009	-2.363042
C	-4.824189	-1.488299	0.121259
H	-3.132462	-2.251593	1.187244
C	-5.272579	-0.768607	-0.989708
H	-4.695562	0.335700	-2.751127
H	-5.537957	-1.931525	0.808644
H	-6.337367	-0.643740	-1.161893
C	0.422911	1.342677	0.234021
C	1.292950	0.928410	-0.572081
Br	2.906013	1.492855	-1.301208
H	-1.063509	-1.888351	1.714987
Si	-0.737320	2.321623	1.346373

C	-2.110010	3.024529	0.271652
H	-2.768618	3.656597	0.879968
H	-1.706076	3.646693	-0.534277
H	-2.726748	2.239468	-0.178269
C	0.404226	3.670060	2.015499
H	-0.183960	4.347936	2.647263
H	1.210504	3.254159	2.628254
H	0.852191	4.266091	1.214019
C	-1.396746	1.230965	2.730524
H	-0.591041	0.721421	3.269808
H	-1.937345	1.851769	3.455271
H	-2.100028	0.480956	2.353937

F. MALDI-TOF Mass Spectra

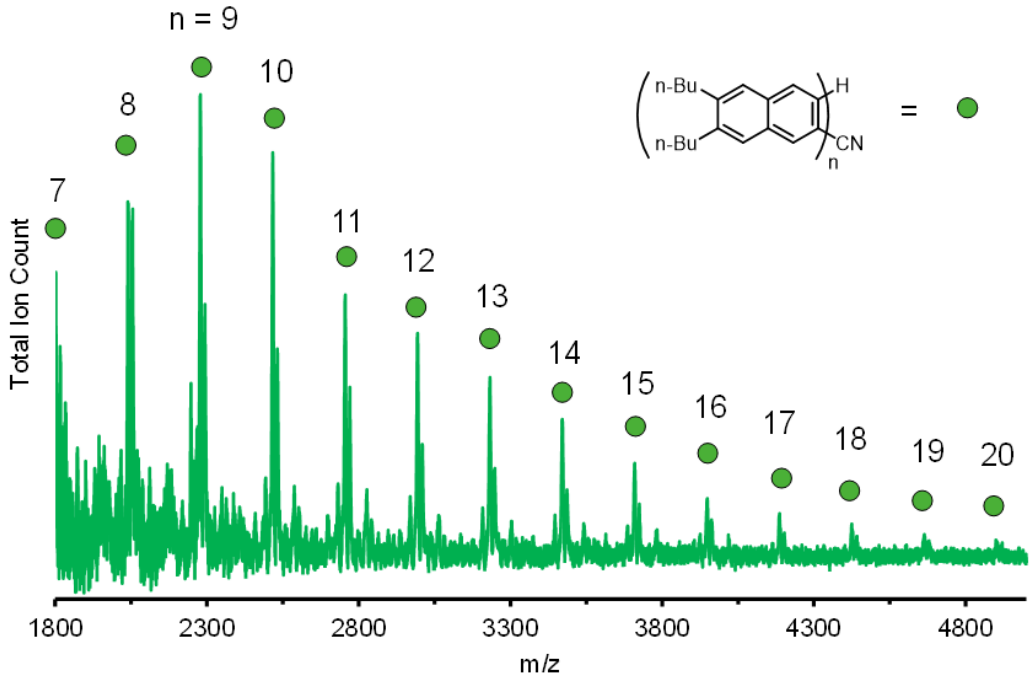

Figure S4.69: MALDI-TOF-MS of **8** using a matrix of 2,5-dihydroxybenzoic acid and Ag($OCOCF_3$) additive.

G. Single Crystal X-Ray Structure

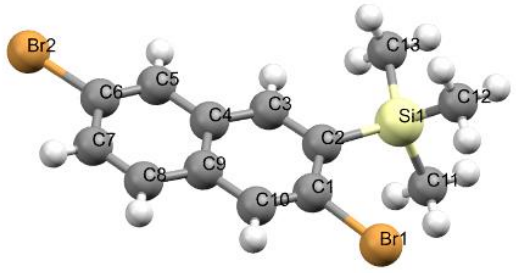

Figure S4.70: Single crystal X-ray structure of **3c** taken at 100 K.

Table S4.1: Crystal data and structure refinement for CCDC 1539451

Empirical formula	$C_{13}H_{14}SiBr_2$
Formula weight	358.15
Temperature / K	100.0
Crystal system	monoclinic
Space group	$P2_1/n$
a / Å, b / Å, c / Å	7.1961(4), 7.4763(4), 26.1123(14)
α/°, β/°, γ/°	90, 95.1754(14), 90
Volume / $Å^3$	1399.12(13)
Z	4
ρ_{calc} / mg mm^{-3}	1.700
μ / mm^{-1}	5.852

F(000)	704
Crystal size / mm^3	0.193 × 0.06 × 0.033
2Θ range for data collection	3.132 to 60.396°
Index ranges	$-10 \leq h \leq 9$, $-10 \leq k \leq 10$, $-36 \leq l \leq 36$
Reflections collected	48708
Independent reflections	4154[R(int) = 0.0365]
Data/restraints/parameters	4154/0/148
Goodness-of-fit on F^2	1.036
Final R indexes [I>2σ (I)]	R_1 = 0.0193, wR_2 = 0.0416
Final R indexes [all data]	R_1 = 0.0256, wR_2 = 0.0431
Largest diff. peak/hole / e $Å^{-3}$	0.435/-0.450

Table S4.2 Fractional Atomic Coordinates (×10^4) and Equivalent Isotropic Displacement Parameters (Å^2×10^3) for CCDC 1539451. U_{eq} is defined as 1/3 of of the trace of the orthogonalised U_{IJ} tensor.

Atom	*x*	*y*	*z*	U(eq)
Br1	-290.5(2)	5554.7(2)	6333.1(2)	22.81(4)
Br2	9648.2(2)	7293.9(2)	8442.8(2)	20.57(4)
Si1	3325.1(5)	7401.5(6)	5713.7(2)	18.60(8)
C1	2086.7(18)	6049.6(18)	6691.0(6)	17.3(3)
C2	3511.0(18)	6853.5(18)	6423.5(5)	15.6(3)
C3	5161.6(18)	7211.1(17)	6718.0(5)	14.8(2)

C4	5460.2(18)	6784.8(17)	7247.7(5)	14.5(2)
C5	7176.8(18)	7171.1(17)	7538.1(6)	16.0(3)
C6	7381.7(19)	6731.2(18)	8047.6(6)	16.6(3)
C7	5952(2)	5897.2(18)	8296.1(6)	18.7(3)
C8	4292(2)	5519.8(18)	8021.9(6)	18.4(3)
C9	3995.6(18)	5957.4(17)	7492.3(5)	15.6(3)
C10	2284.4(19)	5608.7(18)	7199.4(6)	18.0(3)
C11	1567(2)	9198(3)	5562.6(7)	30.4(4)
C12	2749(2)	5350(3)	5323.9(7)	35.8(4)
C13	5641(2)	8246(2)	5549.0(6)	20.7(3)

Table S4.3 Anisotropic Displacement Parameters ($Å^2×10^3$) for CCDC 1539451. The Anisotropic displacement factor exponent takes the form: $-2\pi^2[h^2a^{*2}U_{11}+2hka^*b^*U_{12}+\ldots]$.

Atom	U_{11}	U_{22}	U_{33}	U_{23}	U_{13}	U_{12}
Br1	12.27(6)	23.85(8)	32.01(9)	3.09(6)	0.34(5)	-1.88(5)
Br2	20.93(7)	17.95(7)	22.24(8)	2.78(5)	-1.33(5)	-3.52(5)
Si1	13.76(17)	23.9(2)	18.22(19)	-2.09(15)	1.88(14)	1.78(14)
C1	11.9(6)	12.6(6)	27.3(7)	-0.7(5)	1.5(5)	1.5(5)
C2	14.3(6)	11.8(6)	21.2(7)	0.1(5)	3.7(5)	2.9(5)
C3	13.8(6)	11.9(6)	19.5(6)	0.3(5)	5.7(5)	1.3(5)
C4	14.4(6)	9.5(5)	20.3(7)	0.2(5)	4.6(5)	1.1(4)

C5	14.8(6)	12.1(6)	21.5(7)	0.6(5)	4.6(5)	-0.7(5)
C6	16.4(6)	11.5(6)	22.1(7)	-0.9(5)	2.3(5)	0.3(5)
C7	22.1(7)	15.7(6)	19.1(7)	2.6(5)	6.3(5)	0.9(5)
C8	17.4(6)	14.8(6)	24.3(7)	3.3(5)	8.6(5)	-0.2(5)
C9	15.4(6)	11.3(6)	20.9(7)	1.1(5)	5.5(5)	1.6(5)
C10	13.7(6)	14.1(6)	26.9(7)	2.4(5)	6.5(5)	0.2(5)
C11	21.7(7)	45(1)	24.6(8)	12.1(7)	3.3(6)	11.0(7)
C12	26.3(8)	46.7(11)	35.3(10)	-18.9(8)	7.7(7)	-9.5(8)
C13	18.0(6)	26.5(7)	18.0(7)	0.0(6)	3.1(5)	1.3(6)

Table S4.4 Bond Lengths for CCDC 1539451.

Atom	Atom	Length/Å	Atom	Atom	Length/Å
Br1	C1	1.9101(14)	C3	C4	1.417(2)
Br2	C6	1.8969(14)	C4	C5	1.4196(19)
Si1	C2	1.8911(15)	C4	C9	1.4224(19)
Si1	C11	1.8632(17)	C5	C6	1.366(2)
Si1	C12	1.8664(18)	C6	C7	1.4105(19)
Si1	C13	1.8683(15)	C7	C8	1.365(2)
C1	C2	1.4244(19)	C8	C9	1.418(2)
C1	C10	1.363(2)	C9	C10	1.414(2)
C2	C3	1.3816(19)			

Table S4.5 Bond Angles for CCDC 1539451.

Atom	Atom	Atom	Angle/°	Atom	Atom	Atom	Angle/°
C11	Si1	C2	110.51(7)	C3	C4	C5	121.58(12)
C11	Si1	C12	111.33(9)	C3	C4	C9	118.88(13)
C11	Si1	C13	108.08(8)	C5	C4	C9	119.53(13)
C12	Si1	C2	110.44(8)	C6	C5	C4	118.93(12)
C12	Si1	C13	108.12(7)	C5	C6	Br2	119.25(10)
C13	Si1	C2	108.25(6)	C5	C6	C7	122.39(13)
C2	C1	Br1	119.61(11)	C7	C6	Br2	118.35(11)
C10	C1	Br1	116.11(10)	C8	C7	C6	119.33(14)
C10	C1	C2	124.28(13)	C7	C8	C9	120.77(13)
C1	C2	Si1	125.57(11)	C8	C9	C4	119.05(13)
C3	C2	Si1	119.00(10)	C10	C9	C4	118.80(13)
C3	C2	C1	115.42(13)	C10	C9	C8	122.15(13)
C2	C3	C4	123.16(12)	C1	C10	C9	119.45(13)

Table S4.6 Hydrogen Atom Coordinates (Å×10^4) and Isotropic Displacement Parameters (Å^2×10^3) for CCDC 1539451.

Atom	*x*	*y*	*z*	U(eq)
H3	6143	7770	6558	18
H5	8167	7727	7380	19

H7	6141	5601	8651	22
H8	3326	4958	8188	22
H10	1281	5072	7356	22
H11A	329	8763	5631	46
H11B	1557	9531	5199	46
H11C	1890	10246	5778	46
H12A	3669	4416	5421	54
H12B	2773	5631	4958	54
H12C	1502	4928	5388	54
H13A	5936	9366	5734	31
H13B	5598	8460	5178	31
H13C	6605	7355	5649	31

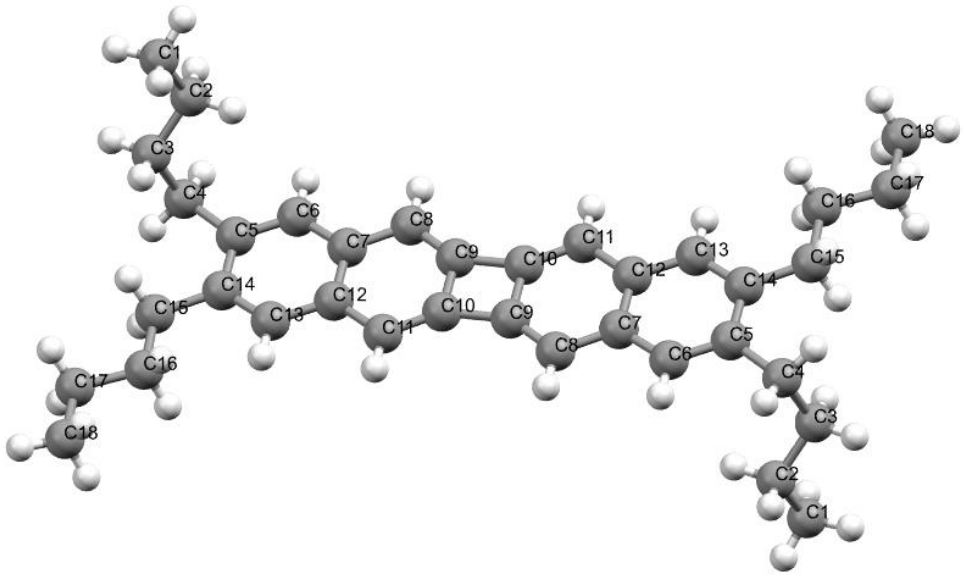

Figure S4.71: Single crystal X-ray structure of **8** taken at 100 K.

Table S4.7: Crystal data and structure refinement for CCDC 1539450

Empirical formula	$C_{36}H_{44}$
Formula weight	476.71
Temperature / K	100.0
Crystal system	triclinic
Space group	P-1
a / Å, b / Å, c / Å	8.2828(4), 8.9132(4), 9.1524(4)
α/°, β/°, γ/°	88.129(2), 79.474(2), 86.662(2)
Volume / $Å^3$	663.02(5)
Z	1
ρ_{calc} / mg mm^{-3}	1.194
μ / mm^{-1}	0.067

F(000)	260
Crystal size / mm^3	0.486 × 0.281 × 0.09
2Θ range for data collection	4.578 to 51.55°
Index ranges	$-10 \leq h \leq 10$, $-10 \leq k \leq 10$, $-11 \leq l \leq 11$
Reflections collected	14580
Independent reflections	2529[R(int) = 0.0545]
Data/restraints/parameters	2529/0/165
Goodness-of-fit on F^2	1.075
Final R indexes [I>2σ (I)]	R_1 = 0.0481, wR_2 = 0.1353
Final R indexes [all data]	R_1 = 0.0495, wR_2 = 0.1367
Largest diff. peak/hole / e $Å^{-3}$	0.350/-0.223

Table S4.8 Fractional Atomic Coordinates (×10^4) and Equivalent Isotropic Displacement Parameters (Å^2×10^3) for CCDC 1539450. U_{eq} is defined as 1/3 of of the trace of the orthogonalised U_{IJ} tensor.

Atom	*x*	*y*	*z*	U(eq)
C1	7242.7(18)	5871.2(15)	10336.7(16)	21.2(3)
C2	5985.0(17)	6981.8(15)	9815.8(15)	19.6(3)
C3	6797.0(16)	8102.7(15)	8660.3(15)	17.0(3)
C4	5584.0(16)	9125.1(14)	7947.3(14)	15.2(3)
C5	4811.2(16)	8307.1(14)	6852.6(15)	13.7(3)

C6	3272.2(16)	7752.9(14)	7295.0(14)	13.8(3)
C7	2508.4(16)	6919.6(14)	6358.8(14)	13.7(3)
C8	897.1(15)	6369.8(14)	6870.9(14)	13.9(3)
C9	263.7(15)	5580.9(14)	5889.4(15)	13.8(3)
C10	1150.3(16)	5270.4(14)	4411.9(15)	13.9(3)
C11	2673.6(16)	5754.6(14)	3894.2(14)	14.4(3)
C12	3378.5(15)	6625.1(14)	4893.2(14)	13.7(3)
C13	4946.7(16)	7220.3(14)	4450.1(14)	14.1(3)
C14	5670.3(15)	8048.0(13)	5378.6(14)	13.5(3)
C15	7339.1(15)	8697.4(14)	4859.1(14)	14.8(3)
C16	8206.6(16)	8294.8(14)	3299.7(15)	15.1(3)
C17	9920.3(16)	8907.7(14)	2906.3(15)	17.1(3)
C18	10833.4(17)	8353.3(16)	1404.9(16)	21.0(3)

Table S4.9 Anisotropic Displacement Parameters ($Å^2×10^3$) for CCDC 1539450. The Anisotropic displacement factor exponent takes the form: $-2\pi^2[h^2a^{*2}U_{11}+2hka^*b^*U_{12}+\ldots]$.

Atom	U_{11}	U_{22}	U_{33}	U_{23}	U_{13}	U_{12}
C1	27.0(7)	15.0(7)	23.2(7)	0.3(5)	-7.8(6)	-4.1(5)
C2	20.8(7)	16.2(7)	21.5(7)	1.7(5)	-2.5(5)	-4.0(5)
C3	17.6(6)	15.6(6)	18.1(6)	-0.7(5)	-3.1(5)	-4.8(5)
C4	17.4(6)	11.8(6)	16.1(6)	-2.1(5)	-0.9(5)	-3.2(5)

C5	15.9(6)	7.5(6)	18.0(6)	0.2(5)	-4.0(5)	0.4(5)
C6	15.6(6)	10.5(6)	14.6(6)	-0.8(5)	-0.8(5)	0.3(5)
C7	14.6(6)	8.6(6)	17.3(6)	1.0(5)	-2.1(5)	0.5(5)
C8	14.8(6)	10.9(6)	15.1(6)	-0.2(5)	-0.3(5)	-0.6(5)
C9	13.0(6)	9.1(6)	18.6(6)	1.4(5)	-1.2(5)	-0.9(5)
C10	16.2(6)	9.0(6)	16.9(6)	-1.4(5)	-3.8(5)	-0.5(5)
C11	16.0(6)	11.0(6)	15.4(6)	-1.1(5)	-0.7(5)	-0.9(5)
C12	15.2(6)	8.1(6)	17.5(7)	0.5(5)	-2.3(5)	-0.3(5)
C13	14.9(6)	10.6(6)	15.8(6)	-0.5(5)	-0.4(5)	-0.6(5)
C14	13.4(6)	8.4(6)	18.1(7)	0.8(5)	-1.7(5)	0.0(5)
C15	15.1(6)	11.0(6)	18.2(7)	-0.8(5)	-2.2(5)	-2.9(5)
C16	15.1(6)	10.8(6)	19.0(7)	-1.2(5)	-1.5(5)	-3.2(5)
C17	16.5(7)	11.8(6)	22.2(7)	-2.4(5)	0.0(5)	-3.4(5)
C18	18.9(7)	17.9(7)	24.2(7)	-3.6(5)	3.2(5)	-4.5(5)

Table S4.10 Bond Lengths for CCDC 1539450.

Atom	Atom	Length/Å	Atom	Atom	Length/Å
C1	C2	1.5242(19)	C9	$C10^{1}$	1.5028(18)
C2	C3	1.5226(18)	C10	$C9^{1}$	1.5029(18)
C3	C4	1.5362(18)	C10	C11	1.3544(18)
C4	C5	1.5104(18)	C11	C12	1.4398(18)

C5	C6	1.3801(18)	C12	C13	1.4166(18)
C5	C14	1.4248(18)	C13	C14	1.3799(18)
C6	C7	1.4073(18)	C14	C15	1.5189(17)
C7	C8	1.4400(17)	C15	C16	1.5201(18)
C7	C12	1.4266(18)	C16	C17	1.5276(17)
C8	C9	1.3539(19)	C17	C18	1.5250(18)
C9	C10	1.4431(18)			

$1^{-X},1^{-Y},1^{-Z}$

Table S4.11 Bond Angles for CCDC 1539450.

Atom	Atom	Atom	Angle/°	Atom	Atom	Atom	Angle/°
C3	C2	C1	111.85(11)	C9	C10	$C9^1$	89.93(11)
C2	C3	C4	114.32(11)	C11	C10	$C9^1$	147.36(13)
C5	C4	C3	112.48(10)	C11	C10	C9	122.70(12)
C6	C5	C4	119.78(12)	C10	C11	C12	116.53(12)
C6	C5	C14	119.12(12)	C7	C12	C11	120.75(12)
C14	C5	C4	121.05(11)	C13	C12	C7	118.10(12)
C5	C6	C7	122.95(12)	C13	C12	C11	121.15(12)
C6	C7	C8	120.86(12)	C14	C13	C12	122.90(12)
C6	C7	C12	118.21(12)	C5	C14	C15	119.71(11)
C12	C7	C8	120.93(12)	C13	C14	C5	118.69(12)

C9	C8	C7	116.54(12)	C13	C14	C15	121.60(11)
C8	C9	$C10^{1}$	147.39(12)	C14	C15	C16	116.08(11)
C8	C9	C10	122.53(12)	C15	C16	C17	112.60(11)
C10	C9	$C10^{1}$	90.07(11)	C18	C17	C16	111.58(11)

$1^{-X},1^{-Y},1^{-Z}$

Table S4.12 Torsion Angles for CCDC 1539450.

A	B	C	D	Angle/°	A	B	C	D	Angle/°
C1	C2	C3	C4	172.70(11)	C8	C7	C12	C11	-0.72(18)
C2	C3	C4	C5	-73.99(14)	C8	C7	C12	C13	178.92(11)
C3	C4	C5	C6	97.61(14)	C8	C9	C10	$C9^{1}$	179.23(15)
C3	C4	C5	C14	-80.10(14)	C8	C9	C10	C11	-0.5(2)
C4	C5	C6	C7	-176.95(11)	$C9^{1}$	C10	C11	C12	179.69(17)
C4	C5	C14	C13	176.33(11)	C9	C10	C11	C12	-0.74(19)
C4	C5	C14	C15	-4.39(18)	$C10^{1}$	C9	C10	$C9^{1}$	0.000(1)
C5	C6	C7	C8	-179.77(11)	$C10^{1}$	C9	C10	C11	-179.77(15)
C5	C6	C7	C12	0.68(19)	C10	C11	C12	C7	1.33(18)
C5	C14	C15	C16	176.84(11)	C10	C11	C12	C13	-178.31(11)
C6	C5	C14	C13	-1.40(18)	C11	C12	C13	C14	-179.39(11)
C6	C5	C14	C15	177.88(11)	C12	C7	C8	C9	-0.53(18)
C6	C7	C8	C9	179.94(11)	C12	C13	C14	C5	0.51(19)

C6	C7	C12	C11	178.82(11)	C12	C13	C14	C15	-178.75(11)
C6	C7	C12	C13	-1.53(18)	C13	C14	C15	C16	-3.91(18)
C7	C8	C9	C10	1.16(18)	C14	C5	C6	C7	0.81(19)
C7	C8	C9	$C10^{1}$	179.73(17)	C14	C15	C16	C17	-176.24(10)
C7	C12	C13	C14	0.96(19)	C15	C16	C17	C18	174.05(11)

$1^{-X},1^{-Y},1^{-Z}$

Table S4.13 Hydrogen Atom Coordinates (Å×10^4) and Isotropic Displacement Parameters (Å^2×10^3) for CCDC 1539450.

Atom	*x*	*y*	*z*	U(eq)
H1A	7742	5218	9516	32
H1B	6696	5258	11169	32
H1C	8100	6424	10660	32
H2A	5193	6422	9384	24
H2B	5364	7534	10681	24
H3A	7537	7541	7866	20
H3B	7483	8740	9136	20
H4A	4706	9534	8739	18
H4B	6170	9983	7429	18
H6	2703	7943	8276	17
H8	309	6551	7847	17
H11	3247	5531	2922	17

H13	5526	7042	3470	17
H15A	8065	8356	5565	18
H15B	7198	9806	4910	18
H16A	7532	8702	2575	18
H16B	8301	7187	3217	18
H17A	9821	10020	2879	21
H17B	10561	8587	3686	21
H18A	10243	8732	621	32
H18B	10897	7252	1416	32
H18C	11947	8720	1212	32

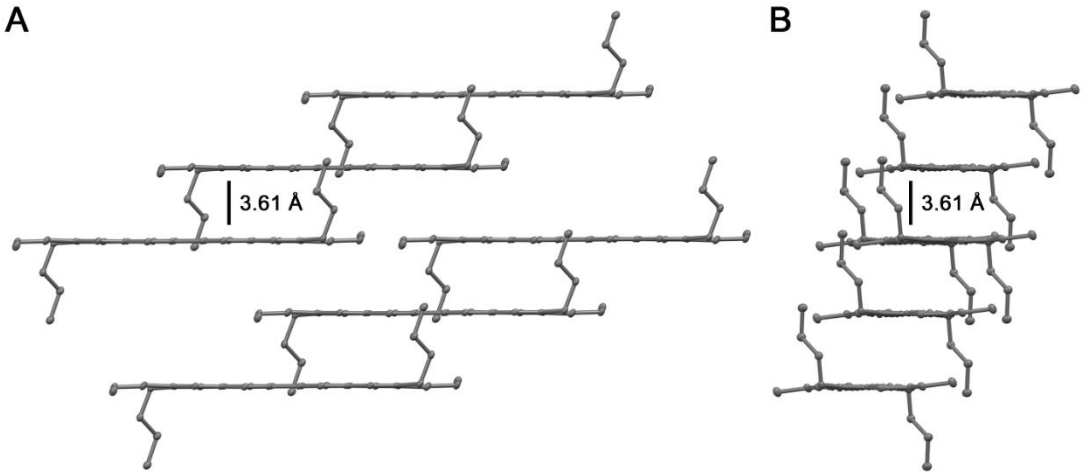

Figure S4.72. (A) Solid-state packing of compound **8** viewed down the short molecular axis and (B) viewed down the long molecular axis. Hydrogens are omitted for clarity, thermal ellipsoids shown at the 50% probability level.

H. UV/Vis and Fluorescence Spectroscopy

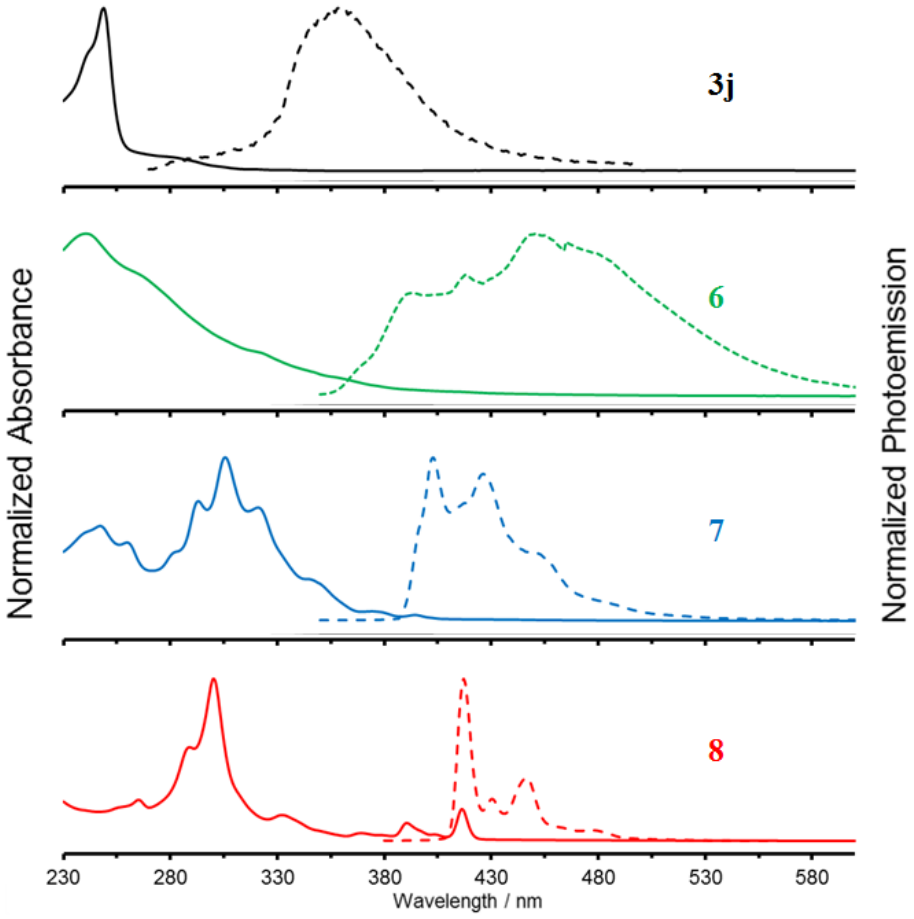

Figure S4.73. UV/Vis absorption (solid) and photoemission (dashed) of **3j** (black), **6** (green), **7** (blue), and **8** (red) at 5.0 μg/mL in CH_2Cl_2. The spectra are normalized to the λ_{max} of each compound (λ_{max} = 249 nm and ε = 1.0 x 10^5 $M^{-1}cm^{-1}$ for **3j**; λ_{max} = 240 nm and ε = 3.0 x 10^4 $M^{-1}cm^{-1}$ for **6**; λ_{max} = 306 nm and ε = 9.7 x 10^4 $M^{-1}cm^{-1}$ for **7**; λ_{max} = 301 nm and ε = 1.3 x 10^5 $M^{-1}cm^{-1}$ for **8**). Photoemission spectrum for each compound is normalized to the λ_{em} of each compound (λ_{ex} = 260 nm for **3j**; λ_{ex} = 340 nm for **6**; λ_{ex} = 330 nm for **7**; λ_{ex} = 370 nm for **8**).

I. References for Supporting Information

1. D. Lehnerr, J.M. Alzola, E.B. Lobkovsky, W.R. Dichtel, *Chem. Eur. J.* **2015**, *21*, 18122 –18127
2. *C. Amatore, E. Blart, J. P. Genet, A. Jutand, S. Lemaire-Audoire, M Savignac, J. Org. Chem.*, **1995**, *60*, 6829–6839
3. X. Zhang, Y. Zhang, J. Huang, R. P. Hsung, K. C. M. Kurtz, J. Oppenheimer, M. E. Petersen, I. K. Sagamanova, L. Shen, M. R. Tracey, *J. Org. Chem*. **2006**, *71*, 4170.
4. Chen, X. Y.; Wang, L.; Frings, M.; Bolm, C. *Org. Lett.* **2014**, *16*, 3796–3799.
5. *T. Kitamura, N. Fukatzu, Y. Fujiwara, J. Org. Chem.*, **1998**, *63*, 8579–8581
6. Doddrell, D.; Barfield, M.; Adcock, W.; Aurangzeb, M.; Jordan, D. *J. Chem. Soc., Perkin Trans.* **1976**, *4*, 402–412.
7. Gaussian 09, Revision D.01, M. J. Frisch, G. W. Trucks, H. B. Schlegel, G. E. Scuseria, M. A. Robb, J. R. Cheeseman, G. Scalmani, V. Barone, B. Mennucci, G. A. Petersson, H. Nakatsuji, M. Caricato, X. Li, H. P. Hratchian, A. F. Izmaylov, J. Bloino, G. Zheng, J. L. Sonnenberg, M. Hada, M. Ehara, K. Toyota, R. Fukuda, J. Hasegawa, M. Ishida, T. Nakajima, Y. Honda, O. Kitao, H. Nakai, T. Vreven, J. A. Montgomery, Jr., J. E. Peralta, F. Ogliaro, M. Bearpark, J. J. Heyd, E. Brothers, K. N. Kudin, V. N. Staroverov, T. Keith, R. Kobayashi, J. Normand, K. Raghavachari, A. Rendell, J. C. Burant, S. S. Iyengar, J. Tomasi, M. Cossi, N. Rega, J. M. Millam, M. Klene, J. E. Knox, J. B. Cross, V. Bakken, C. Adamo, J. Jaramillo, R. Gomperts, R. E. Stratmann, O. Yazyev, A. J. Austin, R. Cammi, C. Pomelli, J. W. Ochterski, R. L. Martin, K. Morokuma, V. G.

Zakrzewski, G. A. Voth, P. Salvador, J. J. Dannenberg, S. Dapprich, A. D. Daniels, O. Farkas, J. B. Foresman, J. V. Ortiz, J. Cioslowski, and D. J. Fox, Gaussian, Inc., Wallingford CT, **2013**.

8. CYLview, 1.0b; Legault, C. Y., Université de Sherbrooke, **2009** (http://www.cylview.org).